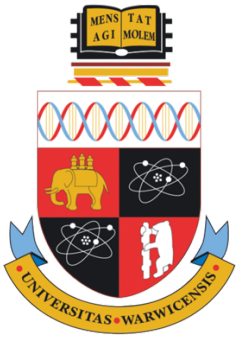

FOOD OR JUST A FREE RIDE? EXPLORING MARINE MICROBIAL COMMUNITY DYNAMICS ON NATURAL AND SYNTHETIC POLYMERS

Robyn Joanna Wright

A thesis submitted for the degree of Doctor of Philosophy

School of Life Sciences

University of Warwick

August 2019

MIBTP
Midlands Integrative Biosciences Training Partnership

Contents

List of figures

List of tables

List of appendices

Acknowledgements

I would like to thank, first of all, my supervisors Dr. Joseph Christie-Oleza and Prof. Matt Gibson, for their kind help and advice throughout the PhD, and in particular Joseph for his endless enthusiasm and for being so supportive and easy to work with. Thanks also go to my advisory panel, Dr. Guy Barker and Prof. Gary Bending, for useful discussions as well as to the teaching staff at Plymouth University (especially Colin and Richard), for giving me the opportunities and encouragement to go for a PhD and inspiring me to want to do so.

I would also like to thank all members of C126 and everyone in the Christie-Oleza and Gibson groups, but in particular Vinko and Gabriel, the 'plastics gang' – both for help in the lab and when support was needed in the form of wine and cheese evenings out of the lab – as well as Audam and Mar for their help and support. Thanks also go to all of the micro group at SLS for the supportive environment that they've provided and for all of the helpful and thought-provoking conversations, as well as the friendships, that have helped keep me pointing forwards.

I'd also like to thank my friends and particularly my family, for reminding me that there is a life outside of the PhD and for always supporting and believing in me. Finally, I'd like to thank my little dog, Bolt, who unfortunately didn't make it to the end with me, but who definitely helped to keep me sane by forcing me out of the house for walks and of course Andy – for putting up with living in Coventry for the last 3 and a half years and for always listening to me talk about my experiments, even when neither of us really knew what I was talking about.

Declaration

This thesis is submitted to the University of Warwick in support of my application for the degree of Doctor of Philosophy. It has been composed by myself and has not been submitted in any previous application for any degree. The work presented (including data generated and data analysis) was carried out by the author except in the cases outlined below:

- Illumina MiSeq sequencing shown in Chapter 2 was carried out by the University of Warwick Genomics Facility.
- Whole genome sequencing and assembly of microbial isolates in Chapters 3 and 4 was performed by MicrobesNG, Birmingham.
- Metabolomic analyses in Chapter 4 were carried out by Rafael Bosch at the University of the Balearic Islands, Palma, Spain.

Parts of this thesis have been published by the author:

Wright, R., Gibson, M.I. and Christie-Oleza, J. (2019) Understanding microbial community dynamics to improve optimal microbiome selection. *Microbiome*. **7** (85). 1-14. (Appendix 1)

Summary

Recalcitrant polymers are widely distributed in the marine environment. This includes natural polymers, such as chitin, but also synthetic polymers such as plastics, which are becoming increasingly abundant and for which biodegradation is uncertain. Distribution of labour in microbial communities commonly evolves in nature, particularly for arduous processes, suggesting that a community may be better at degrading recalcitrant compounds than individual microorganisms. Microbial communities that colonise surfaces and polymers in the marine environment are also known to go through distinct stages of community succession, generally characterised as: i) the attachment phase, defined by an abundance of organisms that are good at colonising; ii) the selection phase, which sees an increase in the abundance of organisms that are good at degrading that substrate; and iii) the succession phase, where efficient degraders are overtaken by cheaters and grazers.

Here, it was hypothesised that the general principles of microbial community succession also apply to the colonisation of and growth on, plastics. The majority of studies that investigate the "Plastisphere" – the microorganisms found colonising plastics – examine these at only one time point and the incubation time is often not known, nor whether these communities are degrading the plastics, their associated additives and contaminants, or neither. First, the method of artificial selection was applied to whole microbial communities in order to improve the ability of a microbial community to degrade the natural polymer chitin. It was shown that only when the incubation time was continuously optimised was there an increase in chitinase activity and therefore chitin degradation and this was predominantly due to a shift in the microbial community from the *Gammaproteobacteria* – active chitin degraders in this case – to the *Alphaproteobacteria*, which merely possessed the ability to utilise the sub-products of chitin degradation. Application of the artificial selection method requires knowledge of the enzymes used for the process of interest, a high-throughput test for relevant enzymatic activity, knowledge of approximate appropriate incubation times and, as was shown here, constant optimisation of incubation times between selections.

Little is currently known about the microbial degradation of plastics in the marine environment, including how long degradation may take and when typical stages of biofilm development occur. Microbial community succession was therefore characterised across six weeks of incubation with different types of polyethylene terephthalate (PET), with the aim of identifying the key stages of microbial community succession. This showed that the communities were more distinct and also enriched with potential PET-degraders, at earlier stages of incubation and had converged by the end of the incubation period, as found in environmental Plastisphere studies when time is examined as a factor. Also, the ability of two marine isolates to degrade PET was characterised using a combined proteogenomic approach and the enzymes used by one of these bacteria to degrade PET were tentatively identified, although the pathway used by the second bacterium was not clear. Finally, the ability of marine bacteria to degrade three common plastic additives, *i.e.* plasticizers, was also investigated. A proteogenomic approach was again used to characterise the ability of two marine isolates to degrade two phthalic acid ester plasticizers and one citrate plasticizer and this degradation was confirmed by metabolomics. This revealed different mechanisms for the degradation of the two phthalic acid ester plasticizers and also identified tentative mechanisms for degradation of the citrate plasticizer for the first time.

This thesis represents a significant step forwards in our understanding of the pathways used for the degradation of recalcitrant compounds by several bacterial isolates, as well as a deeper understanding of the microbial processes and colonisation dynamics that govern the degradation of these compounds in the marine environment.

Abbreviations

A	Adenine
AFM	Atomic Force Microscopy
ANOSIM	Analysis of similarities
ARISA	Automated ribosomal intergenic spacer analysis
ASV	Amplicon sequence variant
ATBC	Acetyl tributyl citrate
BHET	Bis(2-hydroxy ethyl) terephthalate
BLAST	Basic Local Alignment Search Tool
bp	Base pairs
BPA	Bisphenol A
C	Cytosine
c	centi
Ca	Calcium
CARD-FISH	Catalysed reporter deposition-Fluorescence *in situ* hybridisation
CFU	Colony forming units
Cl	Chlorine
CLSM	Confocal laser scanning microscopy
Co	Cobalt
CO_2	Carbon dioxide
CoA	Coenzyme A
Cu	Copper
DADA2	Divisive Amplicon Denoising Algorithm 2
DBP	Dibutyl phthalate
DDT	Dichlorodiphenyltrichloroethane
DEHP	Bis(2-ethyl hexyl) phthalate
DGGE	Denaturing gradient gel electrophoresis
DINP	Diisononyl phthalate
DIDP	Diisodecyl phthalate
DNA	Deoxyribose nucleic acid
DOC	Dissolved organic carbon
DOM	Dissolved organic matter
EDTA	Ethylenediaminetetraacetic acid
e.g.	*exempli gratia*

EG	Ethylene glycol
et al.	et alli
EPS	Extracellular polymeric substances
F	Forward (when describing primers)
Fe	Iron
FIO	Faecal indicator organisms
FTIR	Fourier Transform Infrared Spectroscopy
G	Guanine
g	gram(s) (when describing mass)
g	gravity (when describing centrifugation)
GC	Gas Chromatography
GlcNAc	N-acetyl-D-glucosamine
H	Hydrogen
h	hours
GPC	Gas Permeation Chromatography
HCH	Hexachlorocyclohexane
HDPE	High Density Polyethylene
HMM	Hidden Markov Model
HS	High sensitivity
Hz	Hertz
I	Iodine
i.e.	*id est*
ITS	Internal Transcribed Spacer
K	Potassium
KEGG	Kyoto Encyclopedia of Genes and Genomes
KO	KEGG ortholog
K_{OW}	n-Octanol/Water Partition Coefficient
LC	Liquid chromatography
LC-ESI-MS/MS	Liquid chromatography-electrospray ionisation-tandem mass spectrometry
LDPE	Low Density Polyethylene
LLDPE	Linear Low Density Polyethylene
LDS	Lithium dodecyl sulphate
m	metre (when describing distance)

m	milli (when describing magnitude)
M	molar
Mb	Megabase
MHET	Mono(hydroxy ethyl) terephthalate
MHETase	MHET hydrolase
Mg	Magnesium
mL	milliliter
Mn	Manganese
Mo	Molybdenum
MP	Microplastic
MS	Mass spectrometry
MUF	Methylumbelliferyl
N	Nitrogen
n	nano
Na	Sodium
NCBI	National Centre for Biotechnology Information
NGS	Next Generation Sequencing
nMDS	Non-metric multidimensional scaling
NMR	Nuclear Magnetic Resonance
NP	Nanoplastic
NSTI	Nearest Sequenced Taxon Index
O	Oxygen
OTU	Operational Taxonomic Unit
P	Phosphate
p	Probability value
PA	Phthalic acid (Phthalate)
PAE	Phthalic acid ester
PAHs	Polyaromatic hydrocarbons
PBDE	Polybrominated diphenyl ether
PCBs	Polychlorinated biphenyls
PCL	Polycaprolactone
PCR	Polymerase chain reaction
PE	Polyethylene
PEG	Polyethylene Glycol

PES	Polyethylene Succinate
PerMANOVA	Permutational multivariate analysis of variance
PerMDISP	Permutational analysis of multivariate dispersions
PESTUR	Polyesterurethane
PET	Polyethylene terephthalate
PETase	PET hydrolase
PHA	Polyhydroxyalkanoate
PHB	Polyhydroxybutyrate
PHBV	Poly(3-hydroxybutyrate-co-3-hydroxyvalerate)
PICRUSt	Phylogenetic Investigation of Communities by Reconstruction of Unobserved States
PLA	Polylactic acid
POC	Particulate organic carbon
POM	Particulate organic matter
POPs	Persistent Organic Pollutants
PP	Polypropylene
ppb	parts per billion
PRC	Principal Response Curve
PS	Polystyrene
PUR	Polyurethane
PVA	Polyvinyl alcohol
PVC	Polyvinyl chloride
QIIME	Quantitative Insights Into Microbial Ecology
qPCR	quantitative PCR
R	Reverse (when describing primers)
RNA	Ribonucleic acid
rRNA	ribosomal RNA
rpm	revolutions per minute
S	Sulphur
s	second(s)
SAN	Styrene acrylonitrile resin
SDS-PAGE	Sodium dodecyl sulphate-Polyacrylamide gel electrophoresis
SEC	Size exclusion chromatography
SEM	Scanning electron microscopy

SIMPER	Similarity percentages
sp.	species (singular)
spp.	species (plural)
T	Thymine
TAE	Tris base, acetic acid and EDTA
TCA	Tricarboxylic acid cycle
TEM	Transmission electron microscopy
TOTM	Trioctyl trimellitate
TPA	Terephthalic acid
UV	Ultraviolet
v	volume
w	weight
WWTP	Wastewater treatment plant
Zn	Zinc
µ	micro
˚C	Degrees Celsius

Chapter 1

Introduction

1.1 Oil derived plastics in the environment

Recalcitrant compounds are widely distributed in the marine environment (Barnes et al., 2009; Cózar et al., 2014; Derraik, 2002; Souza et al., 2011; Thompson et al., 2009; Wenning and Martello, 2014). These include natural polymers, that are challenging to degrade due to their insolubility and crystalline structures, such as cellulose (Opsahl and Benner, 1997) and chitin (Souza et al., 2011) and, more recently, xenobiotic compounds like pesticides, detergents (Johnston et al., 2015) and plastics (Barnes et al., 2009; Browne et al., 2010; Cózar et al., 2014; Derraik, 2002). The European plastic industry is worth over €350 billion a year, with plastic production increasing year-on-year (PlasticsEurope, 2018). It was predicted that between 4.8 and 12.7 million tons of plastics enter the oceans annually, which is likely to continue to increase, possibly even by an order of magnitude (Jambeck et al., 2015). Marine plastic pollution has received increasing attention over the last several decades (Figure 1.1) because plastics are now known to cause a range of problems in the environment: direct, through entanglement (Carr, 1987; Fowler, 1987; Gregory, 2009) or ingestion (Boerger et al., 2010; Browne et al., 2008; Colabuono et al., 2010; Graham and Thompson, 2009; Ryan et al., 1988; Vered et al., 2019; Ward and Kach, 2009) or indirect, through the transfer of toxic chemicals to marine life (González-Soto et al., 2019; Rochman et al., 2013; Teuten et al., 2009; Vered et al., 2019) and there are numerous factors that can affect the fate, transport and impacts of plastics (Figure 1.2).

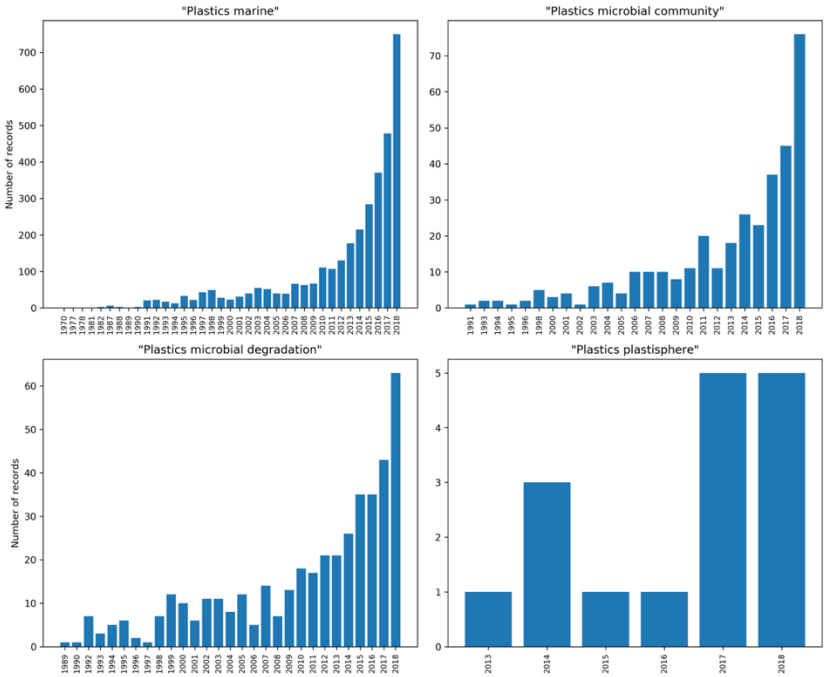

Figure 1.1. Number of records added per year on web of knowledge for four search terms: “Plastics marine”, “Plastics microbial community”, “Plastics microbial degradation” and “Plastics plastisphere”.

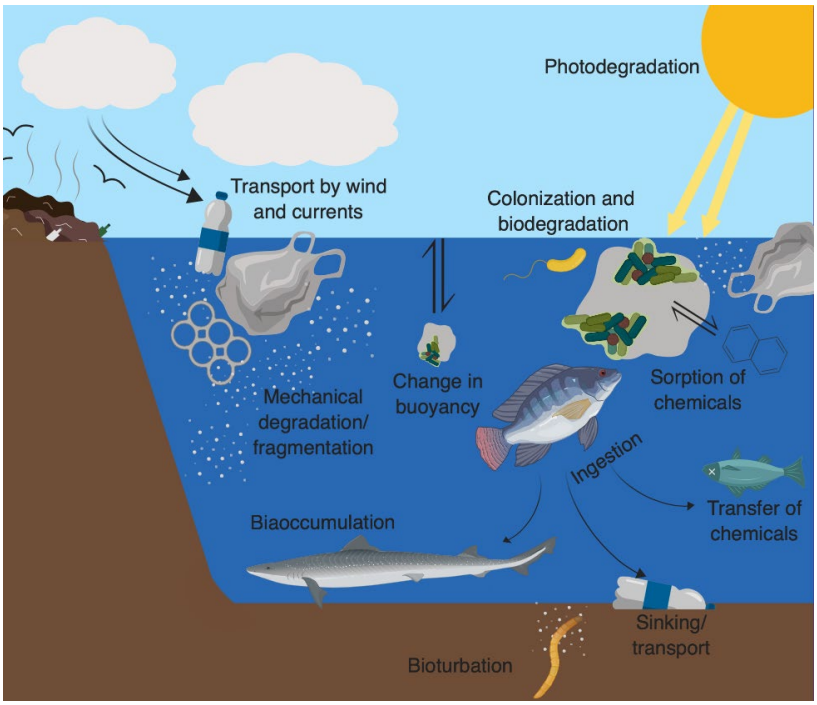

Figure 1.2. Factors and processes affecting the fate, transport and biodegradation of plastics in the marine environment. Diagram created with Biorender.com.

It is now well known that plastic pieces carry not only the additives from manufacturing, but also that hydrophobic chemicals may sorb to their surfaces (Groh et al., 2019) in concentrations significantly higher than in the surrounding seawater (Mato et al., 2001).

These pollutants may subsequently desorb, either in areas with lower environmental concentrations (Teuten et al., 2009), or when the plastics are ingested (Besseling et al., 2013; González-Soto et al., 2019; Rochman et al., 2013). These pollutants include pesticides (e.g. Dichlorodiphenyltrichloroethane; DDTs), plasticizers (*e.g.* Bisphenol-A; BPA) (Teuten et al., 2009) and flame retardants (e.g. Polybrominated diphenyl ethers; PBDEs) (Hahladakis et al., 2018) and many are carcinogenic or endocrine-disrupting (Mathieu-Denoncourt et al., 2015; Turusov et al., 2002), even at concentrations much lower than those found in the environment. For example, for DDTs, typical environmental values may still be above 100 ppb (Barakat et al., 2013), while exposure to just 0.05 ppb led to reduced survivability and hatchability in zebrafish (Njiwa et al., 2004). For some of these pollutants, biodegradation is possible, either by microbial communities and consortia or isolated organisms (Ahuactzin-Pérez et al., 2016; Hesselsoe et al., 2005; Stanislauskienė et al., 2011), but the extent to which this occurs in the marine environment is largely unknown (Liang et al., 2008; Paluselli et al., 2019; Yang et al., 2018).

Whilst processes to degrade natural compounds have had time to evolve and adapt, these processes may still require the participation of a consortia of organisms, each specialised in one of the multiple steps involved in the breakdown of the compound (Beier and Bertilsson, 2013; Ruiz-Dueñas and Martínez, 2009). Laborious biodegradation processes are therefore rarely carried out entirely by a single microorganism in nature and it is now well documented that a distribution of labour is favoured in natural microbial communities (Cavaliere et al., 2017; Delgado-Baquerizo et al., 2017; Hug and Co, 2018; Ponomarova and Patil, 2015; Zhang et al., 2016). Whilst the ability to degrade plastics has now been demonstrated by a number of isolated microorganisms (Jeon and Kim, 2016; Roy et al., 2008; Wei and Zimmermann, 2017; Yoshida et al., 2016a), it has also been suggested that microbial consortia or communities may be faster and more efficient at the degradation of recalcitrant compounds than individuals (Abraham et al., 2002; Cavaliere et al., 2017; Hesselsoe et al., 2005) and there are still relatively few studies that show plastic degradation by marine organisms (Devi et al., 2019; Harshvardhan and Jha, 2013; Kathiresan, 2003; Kumar et al., 2016, 2007; Mohanrasu et al., 2018; Paço et al., 2017; Sudhakar et al., 2008) or try to study this *in-situ* in the marine environment (Muthukrishnan et al., 2018).

The specific microbial communities colonising plastics have only been investigated more recently (Dang et al., 2008; Harrison et al., 2011; Figure 1.1), although it has long been known that plastics offer the potential to transport invasive species across ocean basins (Derraik,

2002; Gregory, 2009, 1978). The microorganisms that are found colonising plastics – termed the "Plastisphere" by Zettler et al. (2013) (Figure 1.3) – are distinct from those found in the surrounding seawater or on natural surfaces (Bryant et al., 2016a; Oberbeckmann et al., 2018) and several studies have suggested that some community members may be capable of plastic degradation (Muthukrishnan et al., 2018; Syranidou et al., 2019, 2017b, 2017a), although it is thought that this degradation could take hundreds of years (Avio et al., 2016). There are many properties that contribute to the recalcitrance of plastics and these include, but are not limited to, their chemical structure, high molecular weight, high crystallinity and hydrophobicity (Tokiwa et al., 2009).

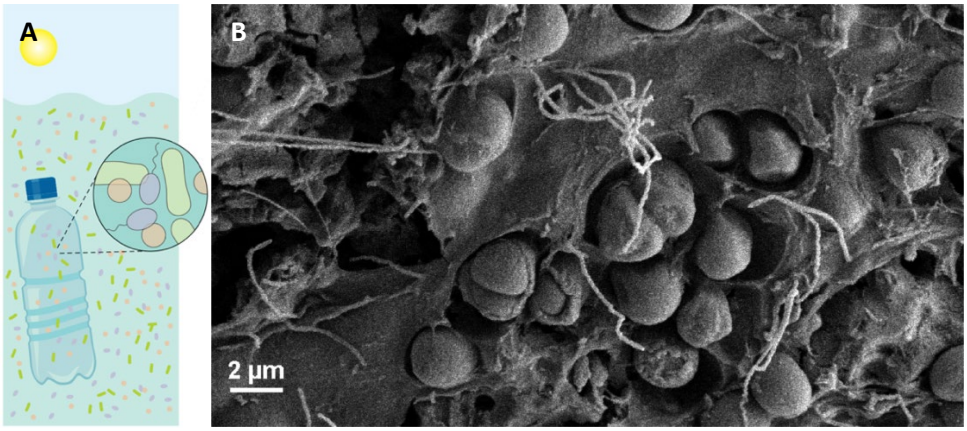

Figure 1.3. Plastics in the environment are colonised by microorganisms. **(A)** is modified from Wright (2019) and **(B)** is taken from Zettler et al. (2013), who suggest that the presence of bacteria in pits on the surface of plastics is potential evidence of plastic degradation.

Any potential biodegradation of plastics could be drastically affected by plastic size, shape or other physicochemical properties, the effects of which should be elucidated in order to determine the environmental fate of plastics. Plastics, in the context of environmental pollution, are broadly split into four categories (nanoplastics, 1-1000 nm – potentially further divided into nanoplastics of 1-100 nm and submicron-plastics of 100-1000 nm; microplastics, 1-1000 µm; mesoplastics, 1-10 mm; and macroplastics, > 1 cm), however, other factors to consider when classifying plastics include chemical composition, solid state, solubility, size, shape, structure, colour and origin (Hartmann et al., 2019). All of these criteria contribute towards the behaviour of the plastic when it reaches the environment, thereby determining its geographic location as well as its vertical location within the water column, which will in turn not only impact the extent to which abiotic degradation may occur, but also the microorganisms that it comes into contact with and therefore have the opportunity to degrade it.

1.2 Plastic physicochemical properties and abiotic factors influencing degradation

Plastics are produced using a range of different polymers (Figure 1.4) in a large variety of sizes and shapes and may have vastly differing physical properties depending on their intended use (Andrady and Neal, 2009). Microplastics (MPs) – previously defined as <5 mm (Koelmans et al., 2017; Moore, 2008; Wagner et al., 2014) and more recently to <1 mm (Hartmann et al., 2019) in size – are a category that has received increasing attention, particularly because they are within the size range ingested as food by a number of organisms (Cole et al., 2011) and 557 marine species are now known to be impacted by marine plastic pollution, for example through entanglement, consumption and smothering (Kühn et al., 2015). MPs can be defined as primary or secondary; primary are those which are specifically manufactured for their small size, for example those used in personal care products (Napper et al., 2015), in sand-blasting media (Heskett et al., 2012) or as virgin plastic pellets, intended for use as a raw material (Moore et al., 2005), while secondary are those which are produced by the fragmentation of larger plastic pieces (Barnes et al., 2009). The fragmentation of larger plastics, leading to the generation of MPs, is usually induced by abiotic weathering, although the rate at which this occurs depends upon a number of different factors, both environmental and intrinsic to the plastic polymer itself (Andrady, 2011).

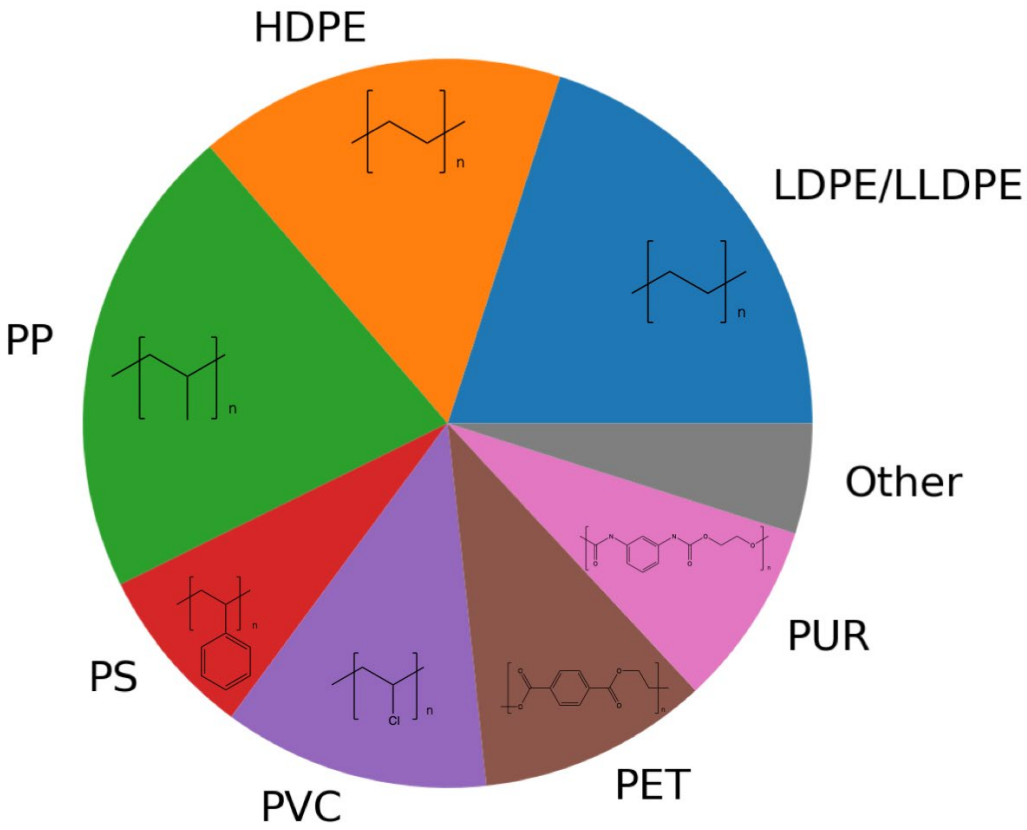

Figure 1.4. Share of total polymer production for Europe, USA, China and India for 2002-2014. Adapted from Geyer et al. (2017). Showing HDPE (high-density polyethylene), LDPE/LLDPE (low-density polyethylene/linear low-density polyethylene), PET (polyethylene terephthalate), PP (polypropylene), PS (polystyrene), PUR (polyurethane) and PVC (polyvinyl chloride) alongside chemical structures of these polymers. HDPE, LDPE and LLDPE differ in regards to the extent to which the polymer chains are branched, which subsequently affects their density and crystallinity; HDPE has minimal branching of its chains and is therefore highest in crystallinity and density (0.941-0.95 g cm^{-3}), LDPE has the most branching and therefore the lowest crystallinity and density (density 0.91-0.925 g cm^{-3}) and LLDPE (density 0.92-0.93 g cm^{-3}) has a larger number of short chains and a narrower molecular weight distribution (Andrady, 2017; Zhang et al., 2004).

There are five main types of plastic degradation: biodegradation – with the action of microorganisms; photodegradation – with the action of light; thermooxidative degradation – slow, oxidative breakdown; thermal degradation – action of high temperatures (Andrady, 2011); and mechanical – with the action of waves or abrasion *e.g.* with sand (Andrady, 2017). Abiotic degradation in the marine environment is usually initiated by UV-B photodegradation (Andrady, 2011; Figure 1.2), which only penetrates the ocean to a depth of approximately 0-15 m (Tedetti and Semperv, 2006), although beached plastics are frequently reported to have become yellowed and brittle (Heskett et al., 2012), indicative that photodegradation has occurred (Andrady, 2017). When plastics become more brittle, this is due to an increase in their crystallinity, which refers to the extent to which the polymer chains are ordered into

parallel bundles, while the rest of the chains are randomly oriented and amorphous. An increase in crystallinity could also lead to the desorption of persistent organic pollutants (POPs), as these are only able to be absorbed by the amorphous fraction of the plastic (Andrady, 2017). On the other hand, a low degree of crystallinity increases the durability of the plastic, but it also makes the ends of the polymer chains more accessible for microbial attack (Yoshida et al., 2016a).

Photo- or thermal degradation of plastics has been used in order to make them more accessible for microbial metabolisation (Sudhakar et al., 2008). Depending on the polymer type, these have both been shown to add functional groups to the plastics (Gewert et al., 2015; Jahnke et al., 2017) and a recent study was also able to identify over 20 low molecular weight polymer fragments with oxidised end groups in water after laboratory exposure of a range of plastics to UV radiation (Gewert et al., 2018). Alkanes are very structurally similar to PE, with PE essentially being an alkane with much higher molecular weight and, as is the case for the degradation of alkanes, it is the presence of these oxidised end groups and a subsequent reduction in molecular weight which are likely a necessary precursor for the biodegradation of plastics (Albertsson et al., 1995; Jeon and Kim, 2016) and is the only way for complete mineralisation of plastics to CO_2 and H_2O to occur (Andrady, 2011). One can see from this how it is the properties of plastics that make them so widely used – light weight, flexible, strong and durable – that also underlie the reasons that they are so difficult to degrade.

1.3 Plastic-associated toxic compounds

A recent report found that there are as many as 906 potentially toxic compounds that are likely to be associated with plastic packaging and a further 3377 substances that are possibly associated (Groh et al., 2019). These are from a wide range of chemical classes and therefore have broad and far-reaching effects on biota and the environment (González-Soto et al., 2019; Rochman et al., 2013; Teuten et al., 2009; Vered et al., 2019). These chemicals can be generally split into additives – those that are added intentionally during manufacturing (Hahladakis et al., 2018) – and contaminants – those that preferentially sorb to the plastics once in the environment (Bakir et al., 2012; Teuten et al., 2009, 2007) (Table 1.1).

Table 1.1. Summary of the classes of contaminants that have been found associated with plastics. All information adapted from Groh et al. (2019) and Hahladakis et al. (2018) unless otherwise stated.

Class		**Groups**	**Typical range (%)** (where available)
Additives	Accelerator	Dithiocarbamate	
		Thiazole or thiuram	
	Antioxidants and stabilisers	Phenols	0.05-3
		Cadmium and lead compounds	
		Toluenes	
	Biocide	Carbamate	
		Phenolic	
		Metal-containing	
		Paraben	
	Colorant	Dye, azo	0.01-10
		Pigment	
	Flame retardant	Inorganic	3-25
		Organophosphate	
		Reactive (e.g. bromine, halogenated phenols)	
	Plasticizers	Chlorinated paraffin	10-70
		Phthalate	
		Adipates	
		Citrates	
		Trimellitates (“Plasticizers,” 2019)	
	Foaming	Alkane	
	Monomer or intermediate	Acrylic	
		Amine	
		Bisphenol	
		Other (e.g. naphthalene, biphenyl)	
		Zinc-containing	
	Solvent	Limonene	
		Naphthalene-related	
		Other hydrocarbon (e.g. cyclohexane, benzene)	

Class		Groups	Typical range (%) (where available)
	Fillers and reinforcements	Clay	Up to 50
		Metal powder	
		Wood powder	
		Glass	
		Carbon fivers	
Contaminants	Persistent organic pollutants (POPs)	Polychlorinated biphenyls (PCBs)	
		Polybrominated diphenyl ethers (PBDEs)	
		Polyaromatic hydrocarbons (PAHs)	
	Pesticides	Dichlorodiphenyltri-chloroethane (DDT)	
		Hexachlorocyclohexane (HCH)	
	Heavy metals	Zinc	
		Cadmium	
		Copper	
		Lead (Munier and Bendell, 2018)	

Plastic additives: Many of the plastics' properties that have led to their widespread use, such as flexibility, durability and ductility are actually given to the plastics through plasticizers and additives (Groh et al., 2019), which make up an average of 7% of non-fibre plastics by mass. Plasticizers account for approximately 35% of all plastic additive use (Geyer et al., 2017) and can represent up to 10-70% of the material's weight, mainly in plasticized or flexible polyvinyl chloride (PVC), a material which comprises 80% of the global use of these chemicals (Hahladakis et al., 2018). Importantly, plasticizers are not covalently bound to the plastic and are therefore likely to leach out of the plastic into the environment or in the tissues of organisms that ingest the plastics (Paluselli et al., 2019). Dibutyl phthalate (DBP) and bis(2-ethyl hexyl) phthalate (DEHP) are currently the two most widely used plasticizers ("Plasticizers," 2019), however, there is now a push to replace these traditional plasticizers with less toxic alternatives, such as acetyl tributyl citrate (ATBC) (Erceg et al., 2005; Van Vliet et al., 2011), although the extent to which biodegradation of these alternatives occurs is still unknown.

Environmental sorbed chemicals

Plastics have been reported to harbour toxic POPs at up to 10^6 times the concentration of the surrounding water (Mato et al., 2001) and have even been used as a monitoring tool for POPs (Takada, 2006). Many of these pollutants have been banned from production for decades (*e.g.* DDT), yet they are still found in concentrations exceeding safe levels on plastics (Hirai et al., 2011; Ogata et al., 2009) and some POPs preferentially sorb to plastics rather than natural sediments (Teuten et al., 2007) and onto some polymers as opposed

to others (Bakir et al., 2012; Napper et al., 2015; Teuten et al., 2009). Many plastics have porous or heterogeneous surfaces, allowing greater sorption of POPs (Hirai et al., 2011) and sorption in the water column is regarded as the primary route of exposure (Endo et al., 2005; Mato et al., 2001), although the pathway by which the plastic enters the environment may also play a role. Plastics with higher concentrations of polyaromatic hydrocarbons (PAHs) and PCBs are likely to have accumulated these from transport by the drainage systems of roads, while plastics with higher concentrations of other POPs such as DDTs are likely to have sorbed these from the water column (Moore et al., 2005). Many POPs, however, have been found in concentrations that are correlated with the ambient POP concentrations in the environments in which they are found, for example, concentrations of PCBs have been found to be up to 20 orders of magnitude higher at a polluted than an unpolluted beach (Karapanagioti et al., 2011).

Toxic and persistent heavy metals are also frequently encountered in the marine environment, for example as antifouling paint on ships (Turner, 2010). There have been recent moves to classify some surface coatings and paints with plastics (Hartmann et al., 2019), however, regardless of their classification, they are likely to co-occur with plastics due to the relatively higher occurrences of both surface coatings or paints (Muller-Karanassos et al., 2019) and plastics (Claessens et al., 2011) in areas of intense boating and many discarded electronic items may contain both plastics and toxic heavy metals (Li et al., 2011). Copper and zinc have both been found to be able to leach from an antifouling paint to either PS or PVC fragments in seawater and the extent to which this occurred was largely dependent upon the surface properties of the plastic (Brennecke et al., 2016) as well as the pH and salinity of the surrounding environment (Holmes et al., 2014). Furthermore, plastics that have been collected from the environment have been found to harbour heavy metals such as copper, lead, zinc and cadmium (Munier and Bendell, 2018). These paints are generally produced with the aim of preventing colonisation by microorganisms and are therefore toxic to a wide variety of marine organisms (Turner, 2010). There are also microorganisms that are capable of detoxifying heavy metals by converting them to less toxic forms, for example in the methylation of mercury (Lloyd and Lovley, 2001), although it is interesting to note that a recent study found no correlation between the microbial communities colonising plastics or living in seawater and the presence of metal resistance genes (Yang et al., 2019).

Microbial degradation of plastic-associated toxic compounds

The microbial degradation of plastic-associated chemicals such as plasticizers has been reported since the 1950s (Stahl and Pessen, 1952). There are numerous studies on the terrestrial degradation of plasticizers (*e.g.* Ahuactzin-Pérez et al., 2016; Feng et al., 2018; Hesselsoe et al., 2005; Kumar et al., 2017; Kumar and Maitra, 2016; Liang et al., 2008; Park et al., 2009, 2008; Xie et al., 2010; Yuan et al., 2002), but this has been less extensively investigated in the marine environment. To our knowledge, there are only four studies to date that investigate plasticizer degradation in the marine environment (Paluselli et al., 2019; Wang and Gu, 2006a; Yang et al., 2018). The degradation intermediates of phthalate acid ester plasticizer degradation by *Rhodococcus ruber* YC-YT1 (*Actinobacteria*; Yang et al., 2018), *Sphingomonas yanoikuyae* DOS01 (*Alphaproteobacteria*; Wang and Gu, 2006b) and *Variovorax parodoxus* strain T4 (*Betaproteobacteria*; Wang and Gu, 2006a) have been identified, although the enzymes used for this degradation remain unknown and Paluselli et al. (2019) suggested that the presence of light and bacterial activity may lead to an increase in the concentration of phthalate plasticizers released from plastics. The leaching or degradation of these plasticizers can lead to a deterioration in the mechanical properties of the plastic (Wei et al., 2019), although no studies on the degradation of plasticizers when attached to plastics could be found. Many other plastic-associated chemicals are also known to be biodegraded in the marine environment, for example, naphthalene, phenanthrene (Wang and Tam, 2019), anthracene (Lai et al., 2014), DDT and PCBs (Lu et al., 2019). Due to the presence of these more readily biodegradable compounds on marine plastics – the additives as well as residual monomers (Groh et al., 2019) and the sub-products of UV degradation being present (Gewert et al., 2018, 2015) – it is perhaps more likely that the additives of plastics are being degraded rather than the plastics themselves.

1.4 Literature review on plastic colonisation and degradation

Marine microbial communities are known to rapidly colonise natural organic matter, or surfaces, when they are introduced to the environment and it is well known that they go through distinct stages of community succession. For example, for the abundant marine polymer chitin there are three main stages in community succession: a) colonisation, where the most abundant organisms are just good at colonising; b) selection, where chitin degraders become enriched; and c) succession, where chitin degraders are overtaken by "cheaters", cross-feeders, grazers and viruses (Datta et al., 2016). In this case, degraders are able to produce chitinases – enzymes that break down the chitin polymer to monomers and oligomers – "cheaters" are able to use the chitin monomers and other small sugar molecules, but are not able to produce chitinases (Enke et al., 2019, 2018) and cross-feeders are not able to produce chitinases or use chitin monomers but benefit from the production of public goods by others (Beier and Bertilsson, 2011; Cordero et al., 2012; Keyhani and Roseman, 1999). Whilst many of the studies that have looked at microbial communities colonising plastics have characterised them at only one time point (*e.g.* Kettner et al., 2017; Kirstein et al., 2018) and it is often unknown how long these plastics have been in the water (*e.g.* Zettler et al., 2013), several have identified successional stages on plastics that are common to microbial communities colonising natural marine surfaces or particles (*e.g.* Dang et al., 2008; De Tender et al., 2017).

In order to ascertain the current state of knowledge regarding the microbial colonisation of plastics in the marine environment, a thorough literature search was carried out. This was conducted using the Web of Science core collections, with the phrases "Plastics plastisphere" (22 results), "Plastics microbial community" (358 results) and "Plastics microbial degradation" (318 results). This search was carried out on 12 March 2019 and yielded a total of 728 results, which was supplemented by any relevant papers held personally. The abstracts of all studies were obtained and any studies not mentioning oil-based plastics or the marine environment, or with experimental results not involving the interactions between microbes and plastics, were removed, leaving 52 studies. The details of these studies, including experimental setup, incubation period, plastic type and identification method used, community characterisation method, degradation determination method and key findings, are summarised in Table 1.2. The colonisation and degradation of plastics by both microbial communities (Section 1.5) and isolates (Section 1.6) is discussed in detail below.

Table 1.2. Table summarising the studies identified by the literature review that report on colonisation or degradation of plastics in the marine environment.

Study	Aims and basic experimental setup	Polymer type	Community determination	Degradation	Key findings
Amaral-Zettler *et al.* (2015a)	• Determine whether composition of plastisphere communities reflects biogeographic origins • Collection of water and plastic samples from North Pacific and North Atlantic subtropical gyres	PE, PP, PS Raman and FTIR	16S rRNA gene Primers as in (Eren et al., 2013) Illumina HiSeq QIIME	Not tested	• Free-living different than plastic-associated and coastal *vs* open ocean plastic-colonisers are also different • PS different from PE and PP • Communities differed more by geography than polymer type
Antonio *et al.* (2019)	• Investigate MP concentration in benthic estuarine sediment • Collection of plastics from Vitória Bay, SE Brazil	Not tested	SEM	Not tested	• Bacteria were main colonisers, but fungal filaments and spores were also present
Bryant *et al.* (2016)	• Investigate plastic concentration and metabolic activity of plastic colonisers within the "great Pacific garbage patch" • Collection of plastics and water from North Pacific gyre	PE, PP FTIR	SEM Metagenomic shotgun sequencing Illumina MiSeq and NextSeq500 PANDAseq	Not tested	• Dominance of a few metazoan taxa and diverse photoautotrophic and heterotrophic protists and bacteria • Plastic-associated bacteria distinct from surrounding free-living bacteria and had significantly higher abundances of *che*, secretion system and *nifH* genes • Net community oxygen production on PMD was positive • *Bryozoa*, *Cyanobacteria*, *Alphaproteobacteria* and *Bacteroidetes* dominated all plastic particles (regardless of size)
Carson *et al.* (2013)	• Investigate the relationship between plastic-associated communities and physico-chemical properties • Collection of plastics from North Pacific gyre	PE, PP, PS FTIR	SEM	Not tested	• *Bacillus* bacteria and pennate diatoms most abundant attached microorganisms • Density of *Bacillus* was related to plastic type, with more on PS than PE or PP • Diatom density was significantly related to trawl site and higher on rough surfaces • Richness was correlated with plastic size and collection site
Curren and Leong (2019)	• Profile microbial communities on plastics from populated and pristine beaches	Not tested	16S rRNA gene 515F-806R	Not tested	• Populated: *Erythrobacter* (21%), *Cohaesibacter* (12%) and *Hyphomonas* (10%) • Moderate: *Arcobacter* (6%), *Albimonas* (5%), *Bacteroides* (4%)

Study	Aims and basic experimental setup	Polymer type	Community determination	Degradation	Key findings
	• Collection of plastics from three beaches in Singapore		Amplicon sequencing QIIME, UCHIME, UPARSE, Mothur		• Pristine: *Brachymonas* (5%), *Pseudomonas* (5%), *Sphingobium* (4%)
Dang *et al.* (2008)	• Assess early microbial community succession on inert materials • Incubated materials for 24 or 72 h off Qingdao Coast, China	Glass, plexiglass, PVC	16S rRNA gene 27F and 1387R and reamplified with RV-M and M13-D Clone libraries	Not tested	• *Alphaproteobacteria* (*Rhodobacterales*) increased in abundance between 24 and 72 h, while *Gammaproteobacteria* (*Oceanospirillales*) decreased • Assemblage was similar regardless of surface type
De Tender *et al.* (2017)	• Explore the processes underlying biofilm formation on marine plastics by bacteria and fungi • Incubate plastic sheets and ropes for 1, 2, 3, 4, 9, 14, 18, 22, 27, 31, 35, 40 and 44 weeks in a Belgian harbor and for 4, 14, 18 or 22 weeks offshore (Belgian North Sea) and compare these with water and sediment samples	PE sheets or rope	16S rRNA gene 341F and 805R ITS2 rRNA gene Adapted fITS7bis and ITS4NGSr Illumina MiSeq v3 QIIME	Not tested	• *Alpha-* and *Betaproteobacteria* and *Flavobacteria* increase in relative abundance over time while *Gammaproteobacteria* decrease – clearer pattern for sheets than ropes • Majority of fungal reads couldn't be assigned, but *Ascomycota* and *Basidiomycota* were most abundant • Fungal communities much more variable than bacterial, even between replicates • Intermediate or late stage biofilm formation was not observed offshore • Seawater and sediment communities were similar to each other, but distinct from those inhabiting plastics • Three fungal OTUs present that were previously found to degrade plastics, but no bacteria
De Tender *et al.* (2015)	• Study plastic colonisation and factors influencing it • Collection of plastics, sediment and seawater in the Belgian North Sea	PE Raman	16S rRNA gene S-D-Bact-0341-b-S-17 and S-D-Bact-0785-a-A-21 Illumina MiSeq v3 QIIME	Not tested	• *Actinobacteria* high in abundance on beached pellets, while *Proteobacteria* dominate on other sample types • *Vibrionaceae* and *Pseudoalteromonadaceae* higher in abundance on plastics • Primary colonisers are *Alpha-* and *Gammaproteobacteria* and secondary are *Bacteroidetes*

Study	Aims and basic experimental setup	Polymer type	Community determination	Degradation	Key findings
					• Suggest that *Mycobacteria* (high in abundance on coloured pellets) are degrading dyes and that the presence of chemicals influences the community
Didier, Anne and Alexandra (2017)	• Define a core microbiome on the surface of plastics • Collection of plastics and wood from the North Atlantic sea surface	PET, PE, PS, wood FTIR	16S rRNA gene 515F and 806R 18S rRNA gene 960F and NSRI1438 Illimina MiSeq v2 Vsearch	Not tested	• Mesoplastics are enriched in *Planctomycetes*, *Alphaproteobacteria*, *Bacteroidetes*, *Cyanobacteria* and *Chloroplexi* while MPs enriched in *Beta-* and *Gammaproteobacteria* • *Rhodobacteraceae* most widespread on plastics • OTUs associated with plastics: *Ralstonia*, unclassified *Gammaproteobacteria*, *Thiotrichiales*, *Muricauda*, *Pelomonas*, *Sphingomonas*, *Acinetobacter*, *Staphylococcus epidermis*, *Thalassospira* • Enrichment in KEGG pathways (PICRUSt) related to xenobiotics biodegradation (particularly PAH, nitrotoluene, chlorocyclohexane and chlorobenzene)
Devi *et al.* (2019)	• Isolate bacteria capable of HDPE degradation • Collected plastics from beaches and mangrove forests of India, isolated and identified potential HDPE degrading bacteria	HDPE	16S rRNA gene 27F and 1522R Sanger	Weight loss, cell viability and FTIR after 30 days incubation	• Most isolates *Pseudomonas* or *Bacillus* • Up to 23% weight loss of HDPE in 30 days by 10 most potent HDPE degraders
Dussud, Meistertzheim, *et al.* (2018)	• Compare free-living, particle associated and plastic-colonising bacteria • Collection of plastics from the *Tara*-Mediterranean expedition	PE, PP, PS, composites FTIR	16S rRNA gene 515FY and 926R Illumina MiSeq QIIME SEM, AFM	Not tested	• PMD dominated by *Cyanobacteria* (40%, *Pleurocapsa*) and *Alphaproteobacteria* (32%, *Roseobacter*) • *Pleurocapsa* sp., *Calothrix* sp., *Scytonema* sp. and *Oscillatoriales* sp. significantly more abundant on PMD • Find the hydrocarbonoclastic *Erythrobacter*, *Hyphomonas* and *Phormidium*

Study	Aims and basic experimental setup	Polymer type	Community determination	Degradation	Key findings
					• Enrichment in KEGG pathways (PICRUSt) related to membrane transport, cell motility and xenobiotics biodegradation (benzoate)
Dussud, Hudec, *et al.* (2018)	• Investigate the steps of plastic colonisation in traditional and biodegradable plastics • Incubate materials for 7, 15, 22, 30 and 45 days in a lab mesocosm with natural seawater flow-through in the dark	LDPE, OXO (PE with pro-oxidant), AA-OXO (artificially aged OXO), PHBV	16S rRNA gene 515FY and 926R Illumina MiSeq Mothur AFM, fluorescence microscopy, flow cytometry, bacterial production	Not tested	• First colonisers on plastics are *Gammaproteobacteria*, which decrease over time as *Alphaproteobacteria* increase • PE, OXO and AA-OXO: *Alcanivorax*, *Aestuariicella hydrocarbonica*, *Alteromonas*, *Thalassolituus*, *Marinobacter*, *Maricurvus* • On PHBV *Neptiniibacter* 30% of relative abundance • Growing (days 7-22) and maturation (days 22-45) phases on PE and OXO had few changes, where AA-OXO and PHBV had large differences between incubation times
Frere *et al.* (2018)	• Investigate the effect of size and polymer type on microbial community composition • Collected plastics from the Bay of Brest, France	PE, PP, PS Raman	16S rRNA gene 518F and 926R Illumina MiSeq v2 FROGS, Galaxy, UCHIME, SWARM qPCR for *Vibrio* spp.	Not tested	• High proportions of shared OTUs between MP and SW • No effect of MP size on community composition • PS assemblages distinct from PE and PP – suggest additive is related to bacterial colonisation • *Vibrio splendidus* detected on MP but not in SW • PE: *Pseudomonadales*, *Oceanospirillales*, *Propionispira* • PP: *Alphaproteobacteria*, *Holophagae* • PS: *Rhodospirillaceae*, *Roseovarius*, *Nitrosomonas*
Harrison *et al.* (2014)	• Investigate microbial colonisation of plastics in a benthic habitat • Incubation in microcosm with three coastal marine sediments from Humber Estuary, UK for 2 mins, 6 h, 1, 2, 4, 7 or 14 days	LDPE	16S rRNA gene qPCR (EUB338 and EUB518) T-RFLP (FAM-63 F and 1389R) Sequencing of cloned genes (27F and 1492R) SEM, CARD-FISH	Not tested	• Colonisation (qPCR) increased up to 1 week – no difference between 1 and 2 weeks incubation • At 2 days communities are sediment-specific, but these converge by 7 and 14 days and become less diverse • *Arcobacter* and *Colwellia* dominate LDPE bacterial assemblages

Study	Aims and basic experimental setup	Polymer type	Community determination	Degradation	Key findings
Harshvardhan and Jha (2013)	• Isolate marine bacteria capable of degrading LDPE • Collected seawater from the Arabian Sea, India and screened for LDPE degradation	LDPE	16S rRNA gene 27F and 1495R	Weight loss, cell viability, FTIR, SEM	• Three of 60 isolates capable of LDPE degradation: *Kocuria palustric*, *Bacillus pumilus* and *Bacillus subtilis* showing 1, 1.5 and 1.75% weight loss of LDPE after 30 days incubation • SEM and FTIR confirm the results
Jiang *et al.* (2018)	• Investigate the plastic-associated microbial community in the intertidal zone • Collected MPs from three intertidal locations of the Yangtze Estuary, China	PE, PP, PS FTIR	16S rRNA gene 319F and 806R Illumina MiSeq v3 Mothur	Not tested	• Microbial community clustered by sedimentary or aquatic origin and clustered by location rather than plastic type • Keystone genera: *Rhodobacterales*, *Sphingomonadales*, *Rhizobiales* • Enrichment in KEGG pathways (PICRUSt) related to xenobiotics degradation and metabolism and decrease in cell motility
Kathiresan (2003)	• Determine whether plastic bags are degraded in mangrove soil and identify predominant microbial species • Incubate plastic bags and cups for 2, 4, 6 and 9 months in mangrove soil in Vellar Estuary, India. Isolates used for 1 month degradation tests	PE bags and plastic cups	Isolations and morphological identification	Weight loss	• PE bags were degraded after 6 and plastic cups after 9 months • PE 3.77 and 4.21% weight loss after 9 months under *Rhizophora* sp. or *Avicennia* sp. zones, respectively • Those degrading plastic bags were much more diverse with many *Aspergillus* species • Plastic bags maximum degradation in the lab of 20.54 and 8.16% weight loss with *Pseudomonas* and *Moraxella* (1 month) • PE maximum degradation of 28.8 and 7.26% weight loss with *Aspergillus glaucus* and *A. niger* (1 month)
Kesy *et al.* (2016)	• Investigate whether microbial assemblages on PS are modified during passage through lugworm gut • *Arenicola marina* collected from Germany, fed pre-incubated plastics (7 days) and egested particles incubated in SW	PS (250-400 µm), glass	16S rRNA gene 519-536F and 907-925R Single-strand conformation polymorphism gel electrophoresis, bands re-amplified and sequenced	Not tested	• Prior to ingestion, PS and glass differed from sediment assemblage, but most abundant OTUs were the same • After ingestion, differences between faeces, PS and glass not significant • *A. atlantica* (potential symbiont) was enriched exclusively in PS • *Lentisphaera marina* enriched in PS samples but also present in others

Study	Aims and basic experimental setup	Polymer type	Community determination	Degradation	Key findings
			qPCR on *Amphritea atlantica*		
Kettner *et al.* (2017)	• Explore the diversity of plastic-attached fungi in marine, freshwater and WWTP • Incubate plastics for two weeks at 5 locations in NE Germany (Baltic Sea, River Warnow and WWTP)	PS, PE, wood	18S rRNA gene Eu565F and Eu981R Illumina MiSeq Mothur	Not tested	• Only 4% of the reads were fungi • Substrate type as well as location had an effect, except for between PE and PS • In WWTP substrate had a weak effect • *Chytridium* was significantly associated with MP while lots of OTUs were associated with water or wood
Kirstein *et al.* (2019)	• Identify plastic-specific microorganisms closely attached to the surface • Three phase incubation (21 month incubation, removal of upper biofilm layers and then 5 month enrichment) using seawater flow-through system in Helgoland, Germany	HDPE, LDPE, PP, PS, PET, PLA, SAN, PVC, PESTUR, glass	16S rRNA gene 341F and 785R Illumina MiSeq v3 SILVAngs pipeline SEM	Not tested	• Attachment occurs most strongly on PP and least on glass (least of plastics on PET) • Short-term richness is higher than long-term on plastics • PS, HDPE, LDPE short and long cluster together • Identified plastic-specific OTUs: *Aquibacter* (PET), *Oceanococcus* (PET), *Parvularcula* (PET, HDPE), *Nannocystaceae* (HDPE), *Polycyclovorans* (HDPE), *Ulvibacter* (HDPE), *Phyllobacteriaceae* (PP, LDPE, HDPE), *Labrenzia* (PP), *Maricaulis* (PP, HDPE, SAN), *Planctomycetes* OM190 (LDPE, HDPE, SAN, PS), *Simiduia* (all but PS, PLA, PVC), *Planctomycetes* BD7-11 (LDPE, PS), *Winogradskyella* (LDPE), *Dokdonia* (LDPE, PP), *Spongiibacter* (SAN, PS, PLA), *Roseovarius* (SAN, PVC), *Rhizobiales* OCS116 (SAN, PS), *Congregibacter* (SAN, PS), *Saprospiraceae* (PS), *Planctomycetes* SPG12-401-411-B72 (PS), *Hirschia* (PESTUR), *Erythrobacter* (PESTUR), *Flexithris* (PVC) • Discriminating OTUs indicate closeness of HDPE and LDPE and PP, PS and SAN
Kirstein *et al.* (2018)	• Identify microbes that preferentially colonise and interact with plastics and determine how biofilm varies between substrates	HDPE, LDPE, PP, PS, PET, PLA, SAN,	16S rRNA gene 341F and 785R 18S rRNA gene Eu565F and Eu981R	Not tested	• Glass grouped away from all other substrates for 16S rRNA gene but there was no clear difference for 18S rRNA gene, suggesting it is unaffected by surface properties

Study	Aims and basic experimental setup	Polymer type	Community determination	Degradation	Key findings
	• Incubate polymers for 9 months using seawater flow-through system in Helgoland, Germany	PVC, PESTUR, glass	Illumina MiSeq v3 SILVAngs pipeline SEM		• *Halophagae* Sva0725 and *Gilvibacter* were characteristic for synthetic communities while *Acidobacteria* AT-s3-28 was characteristic of glass • *Leptobacterium* was characteristic for PLA communities
Kirstein *et al.* (2016)	• Determine whether MPs act as vectors for the dispersal of pathogens • Collect MP and water samples from North and Baltic Sea and isolate *Vibrio* spp.	PE, PP, PS most abundant (others also found)	Enrichment for *Vibrio* spp. and identification using MALDI-TOF MS followed by PCR of *Vibrio* AMR genes	Not tested	• 38% of all water isolates were potentially pathogenic *V. parahaemolyticus*, *V. cholerae* or *V. vulnificus* – one had virulence associated *tdh* gene • 12 MPs (13%) had cultivable *V. parahaemolyticus* – none had *V. cholerae* or *V. vulnificus* • No *Vibrio* spp. had *tdh* or *ctxA* genes
Kumar, Hatha and Christi (2007)	• Determine the ability of bacteria and fungi to degrade PE • Incubate plastics with mangrove soil (Fiji) for 8 weeks	HDPE, LDPE	Isolation and characterisation of lipase, amylase and gelatinase activity	Weight loss	• Higher bacterial load and lipolytic activity on HDPE than LDPE • *Bacillus*, *Listeria* and *Staphylococcus* attached to plastics • ~1% weight loss at week 4 and 2-3% weight loss at week 8
Kumar, Xie and Curley (2016)	• Study the biodegradation products of PET MPs in the marine environment • Incubate isolates (*Shewanella putrefaciens* and *Aureobasidium pullulans*) with PET for 2 weeks	PET (UV-A treated for 96 h)	Not tested	Weight loss, FTIR of water content and lysed microorgansisms	• Degradation did not release plastic by-products to the surrounding environment • Fragments of PET not found in the media
Lacerda *et al.* (2019)	• Quantify and characterize plastic debris in surface water • Plastics collected from Antarctic surface waters	PUR, polyacrylamide, PE, PS, PP	SEM	Not tested	• Diatoms and bacteria were the most abundant fouling organisms, but microalgae and invertebrates were also found • Coccoid and filamentous bacteria were found on MPs and coccoid and elongated cells on paint particles

Study	Aims and basic experimental setup	Polymer type	Community determination	Degradation	Key findings
Laganà *et al.* (2019)	• Investigate bacteria isolated from plastic debris for their resistance to antibiotics • Collection of plastics from King George Island (Antarctica) and isolation and resistance testing of bacteria	FTIR PS FTIR	16S rRNA gene 27F and 1492R Biochemical characterisation	Not tested	• Seven biofilm-forming strains selected: *Alteromonas hispanica*, *Pseudomonas balearica*, *Thalassospira lohafexi*, *Shewanella* sp., *Halomonas* sp., *Pseudoalteromonas* sp., *Pseudomonas balearica* • Resistance against beta-lactams, cephalosporins and quinolones • Plastics act as potential reservoirs of resistance traits
Lobelle and Cunliffe (2011)	• Investigate early biofilm formation on plastics and the effect that this has on buoyancy • Incubate plastics in Plymouth Sound, UK, for 1, 2 or 3 weeks	PE	Biofilm quantification Buoyancy determination	Clearance zones	• Firmly attached biofilm and surface hydrophilicity increased during the experiment • After 2 weeks plastic still floated but below air-SW interface, at 3 weeks it started to sink. After removing the biofilm it remained buoyant • Number of cells colonising increased from 10^4 at week 1 to 10^5 at week 3 • No PE clearance zones were formed after 3 weeks – no indication of degradative ability of biofilm
Michels *et al.* (2018)	• Investigate interactions of MPs with biogenic particles • Incubate MPs with biogenic particles/phytoplankton for 8 or 12 days in a roller tank with unfiltered seawater from the Bay of Kiel, Baltic Sea	PS (only neutrally buoyant)	Buoyancy determination	Not tested	• MPs that were clean or had a biofilm interacted with biogenic particles resulting in large aggregates • MPs increase natural particle aggregation rates • Colonisation and biofilm formation on MPs can be rapid
Mohanrasu *et al.* (2018)	• Determine HDPE and PAH degradation alongside PHB production in marine microbes • Isolates taken from marine soil sediments, marine water and oil spilled marine water and screened	PAH, HDPE	TTC (metabolic activity) assays	PAH – HPLC, CLSM, SEM HDPE – CLSM, FTIR,	• Best PAH-degrading: *Klebsiella pneumonia* • *K. pneumonia* degraded PAHs better individually than when mixed with other PAHs • Best HDPE-degrading: *Brevibacillus borstelensis* • Increase in protein content on day 10 and 11.4% weight loss of HDPE on day 30 – new peaks were shown with FTIR and pits and cavities on HDPE were visualised with SEM

Study	Aims and basic experimental setup	Polymer type	Community determination	Degradation	Key findings
	for degrading/producing activity in 10-30 days			SEM, weight loss	
Muthukrishnan, Khaburi and Abed (2018)	• Investigate substrate- and location-specific effects on colonising microbial communities • Incubate materials at two locations in the Sea of Oman for 30 days	PET, PE, steel, wood	16S rRNA gene 341F and 805R Illumina MiSeq MR DNA analysis pipeline	SEM, FTIR	• Biomass on PET and PE was less than on steel and wood • Grouped by location and then substrate within location • *Actinobacteria* higher in abundance on PET • Steel had lots of *Deltaproteobacteria* • Most differences in communities between plastic and non-plastics were related to low abundance (<3%) OTUs • *Microcyctis* PET-specific and *Hydrogenophaga, Sphingomonas* and *Laceyella* PE-specific • SEM revealed fissures on both PE and PET and FTIR showed increase in hydroxyl groups on PE and carboxyl groups on PET
Nauendorf *et al.* (2016)	• Compare biodegradation of plastic bags by aerobic and anaerobic benthic sediment microbes • Incubate plastics in Baltic Sea sediments in lab mesocosms for ~7, 21, 50 and 99 days	PE, biodegradable bags (COMP)	Cell density Live/dead staining SEM	Raman, weight loss, wettability	• Higher biofilm in oxic than anoxic and on COMP than PE • COMP lost more mass than PE, but they lost weight in inactive sediments, too • Slight decrease in amorphous regions of PE after incubation • Both bags more hydrophilic after incubation • No signs of biodegradation for PE or COMP and plastic waste is therefore likely to accumulate in sediments
Oberbeckmann, Kreikemeyer and Labrenz (2018)	• Investigate how different *in situ* conditions contribute to the composition and specificity of MP- and natural particle associated communities • Incubate materials for 2 weeks along an environmental gradient (coastal Baltic Sea to freshwater WWTP)	PS, PE, wood	16S rRNA gene 515F and 806R (nested PCR with 27F and 1492R) Illumina MiSeq Mothur qPCR for *Vibrio* spp. 567F and 680R	Not tested	• Plastic-specific communities only under low nutrient and high salinity conditions • Both environment and substrate differentiates communities significantly • Associated with plastics: *Hyphomonas*, *Erythrobacter*, *Blastopirellula*, *Sphingopyxis* (all high abundance), *Phyllobacteriaceae* and *Tenacibaculum* (low abundance) • More differential taxa for PS (34) than PE (12 • *Erythrobacteraceae* higher in PE and *Verrucomicrobiaceae* in PS

Study	Aims and basic experimental setup	Polymer type	Community determination	Degradation	Key findings
					• No increased abundance in potential pathogens – *Vibrio* spp. higher on wood than plastics
Oberbeckmann, Osborn and Duhaime (2016)	• Characterise microbial biofilm communities on single-use drinking bottles • Incubate materials for 5-6 weeks in the North Sea and compare these with the free-living (FL) and particle-associated (PA) communities	PET, glass	16S rRNA gene 515F and 806R 18S rRNA gene 1391F and 1795R Illumina MiSeq v2 Mothur	Not tested	• Differences between PET and FL but not PA or glass communities • *Tenacibaculum*, *Crocinitomix* and *Owenweeksia* abundant on PET • *Crocinitomix*, *Owekweeksia*, *Fluviicola*, *Acinetobacter*, *Persicirhabdus*, *Cryomorphaceae* and *Alcanivoraceae* were all discriminative of PET as opposed to glass • Abundant eukaryotes were diatoms, *Phaeophyceae*, ciliates and *Chlorophyta* and fungi were more prevalent on plastic and glass than in SW • Communities varied with season and station
Oberbeckmann *et al.* (2014)	• Investigate how the structure of plastisphere communities varies with season, location and plastic type • Incubate materials for 6 weeks in the North Sea, UK (repeated winter, spring and summer) and collect plastics in Northern European waters and compare with FL and PA communities	PET, glass (incubation), HDPE, LDPE, PP, PS FTIR	16S rRNA gene 341F and 534R DGGE and sequencing SEM	Not tested	• Site-specific and seasonal variability between biofilms • Communities in SW (FL and PA) significantly different from PET • In spring, PET and glass showed clear differences, PET-attached: *Thiotrichales*, *Alteromonodales*, *Flavobacteria*, *Stanieria*, *Pseudophormidium*, *Bacillariophyceae*, *Phaeophyceae* • In winter, PET dominated by *Synedra* sp. at Dowsing station, *Tenacibaculum* at Warp and *Thiomicrospira* at both. West Gabbard had *Shewanella*, *Bowanella* and *Algibacter* • *Bacteroidetes* and *Cyanobacteria* dominate on plastic samples • *Alphaproteobacteria* weren't really found on PET, but were most abundant on surface waters
Ogonowski *et al.* (2018)	• Examine the effects of substrate type on microbial community assembly • Incubate materials for 2 weeks in a 16:8 light:dark cycle in Baltic seawater (with grazers removed)	PE, PP, PS, cellulose, glass	16S rRNA gene 341F and 805R Illumina MiSeq v3 UPARSE qPCR for 16S rRNA gene abundance	Not tested	• Highest biofilm density on cellulose • *Bacteroidetes*, *Actinobacteria* and *Cytophagales* more common on glass and cellulose while *Burkholderiales* were overrepresented on plastics • PE and PP were more similar than PS – PS more diverse with OTUs in multiple phyla more abundant • Not many *Gammaproteobacteria* because this is Brackish

Study	Aims and basic experimental setup	Polymer type	Community determination	Degradation	Key findings
					• Higher on plastics: *Hyphomonas, Hydrogenophaga, Aquabacterium, Loktanella, Lewinella, Perellula* • PE and PP more *Sphingobium* and *Saparospiraceae*
Paço *et al.* (2017)	• Determine plastic degradation response of marine fungus *Zalerion maritimum* • Incubate fungus for 7, 14, 21 and 28 days with plastics in laboratory conditions	PE	Not tested	Weight loss, FTIR, NMR	• High removal of MPs between 7 and 14 days, but no difference in growth • Suggest that initial growth (<7 days) is using nutrients in the media and growth thereafter is reliant upon MPs • Decrease in both mass and size of PE pellets • Approximately 70% of PE pellets removed by day 28
Pollet *et al.* (2018)	• Investigate microbial community composition and succession on plastics • Materials incubated for 1, 4, 8, 12, 28 and 75 days in Toulon Bay, France	PVC	16S rRNA gene 515F and 926R Illumina MiSeq v2 MiSeq SOP (Kozich et al., 2013), UCHIME	Not tested	• Suggest use of 515F and 926R based in *in silico* analyses • *Gammaproteobacteria* were initially dominant (60% on day 1) and dropped from day 4 (12-19%), but *Alphaproteobacteria* increased in abundance from 10% on day 1 to 21-44% on day 4 • *Bacteroidetes* had no clear temporal pattern and *Flavobacteria* were constantly dominant • Samples cluster by time period and most abundant (>2%) OTUs were intermittent (61% at 25-75% of time points) • From day 12 the community dynamics slowed and three of the four most dominant OTUs remained as the most abundant
Quilliam, Jamieson and Oliver (2014)	• Assess whether seaweed or plastic helps survival of faecal indicator organisms (FIOs) • Collect seaweed (*Fucus spiralis*) and plastic debris from Bracken Bay, Scotland and determine *E. coli* persistence in lab environment	Plastic debris	FIO isolated and *E. coli*, *Vibrio* spp. and *Enterococci* quantified	Not tested	• Loosely attached *Vibrio* spp. but not *E. coli* or *Enterococcus* were isolated from plastic rubbish • Seaweed enhanced *E. coli* persistence compared with plastic • Similar number of potentially pathogenic bacteria on seaweed and plastic
Raghul *et al.* (2014)	• Determine the ability of a marine consortia to degrade blended plastic films	PVA-LLDPE (different % composit	Isolation of PVA-degrading microorganisms	Tensile strengt h, SEM, clearan	• Decline in tensile strength of plastic films after 15-week incubation • As PVA concentration increases, so does the reduction in tensile strength, indicating degradation of PVA • Cracks and grooves were visible on the surfaces of films

Study	Aims and basic experimental setup	Polymer type	Community determination	Degradation	Key findings
	• Isolation and incubation of *Vibrio alginolyticus* and *V. parahaemolyticus* with plastic films for 15 weeks in labatory conditions	ions of PVA)		ce zones	
Reisser *et al.* (2014)	• Characterise the biodiversity of organisms on floating plastics • Collection of plastics from coastal and oceanic, tropical to temperate Australia	Multiple FTIR	SEM	Not tested	• Diatoms were most abundant, with many morphologies • *Nitzschia* were most frequent, followed by *Amphora*, *Licmophora*, *Navicula*, *Microtabella*, *Cocconeis*, *Thalassionema* and *Minidiscus* • Several unidentified organisms resembling bacterial, cyanobacterial and fungal cells – rounded/oval cells most frequent, followed by elongated and spiral • Several pits and grooves contained bacteria-like cells
Rodrigues *et al.* (2019)	• Map the spatial distribution of beach-cast pellets and quantify their colonisation by faecal indicator organisms (FIOs) • Collect plastics from Forth Estuary, Scotland	Not tested	Isolation of either *Vibrio* spp. *or E. coli* using selective agar	Not tested	• Each of five beaches contained nurdles colonised by *E. coli* and *Vibrio* spp. with 9-43% and >75% colonisation, respectively
Romera-castillo *et al.* (2018)	• Determine whether plastics release dissolved organic carbon (DOC) and whether this stimulates the activity of microbes • Incubate plastics for 6 or 30 days with UV radiation in laboratory conditions and then use this water for microbial growth	HDPE, LDPE, PP	Flow cytometry	Not tested	• About 60% of leached DOC is available to microorganisms within 5 days, but it is less labile if exposed to solar radiation • No significant differences in bacterial abundance between plastic treatments and controls, but bacterial leucine incorporation higher in plastic than non-plastic treatments
Sudhakar *et al.* (2008)	• Determine if two marine bacteria can degrade plastics • Incubate *Bacillus sphericus* GC subgroup IV and *Bacillus cererus* subgroup A with plastics for 1, 3, 6, 8 or 12 months	HDPE, LDPE (thermally pre-treated or not),	CFU counts every 15 days for first 6 months AFM	FTIR, weight loss, crystallinity, tensile	• Growth higher for *B. sphericus* than *B. cereus* and higher with the thermal pre-treatment (80˚C for 10 days) • Rate of decrease in carbonyl index is lower in HDPE than LDPE, indicating less biodegradation in HDPE • Starch-blended LDPE had highest biodegradation

Study	Aims and basic experimental setup	Polymer type	Community determination	Degradation	Key findings
		unpre-treated starch blended LDPE		strength, contact angle	• Weight loss of pre-treated LDPE and HDPE were ~19 and 9% respectively and unpre-treated 10 and 3.5%, respectively, for *B. sphericus* • Weight loss of starch-blended LDPE was 25% with *B. cereus* • Surface morphological changes observed in biologically treated samples and they were more hydrophilic
Summers, Henry and Gutierrez (2018)	• Examine the interaction of EPS with NPs and MPs in forming agglomerates • Incubate EPS of *Halomonas* sp. TGOS-10 with NPs and MPs for 24 h	PS NPs and MPs (50 nm, 1 µm and 10 µm)	Assessment of agglomeration using flow cytometry and sediment velocity	Not tested	• Formation of agglomerates occurred within 24 h in all treatments • Agglomerates containing larger plastics were not significantly different from those in control conditions • Presence of 50 nm PS promoted the formation of larger agglomerates • EPS contributes to the formation and abundance of plastic agglomerates
Syranidou *et al.* (2019)	• Investigate the ability of indigenous of bioaugmented consortia to degrade weathered PE and PS • Incubate naturally weathered plastic pieces for 10 months (two phases, 5 months, biofilm removed and used to inoculate new plastics for a further 5 months) with a microbial community from Chania, Greece, with (BIOG) or without (INDG) strains known to degrade plastics, under laboratory conditions	PE, PS	16S rRNA gene 515F and 806R Illumina MiSeq v3 QIIME	FTIR, SEC, sinking velocity	• FTIR showed additional peaks for PE and PS after weathering and these were further altered with the microbial community • M_w of PE increased with incubation time, but was stable for PS • INDG showed more weight loss than BIOG and higher weight loss in phase 2 (7 and 11% for PE and PS, respectively) than phase 1 (1 and 2% for PE and PS, respectively) and PS sinking velocities increased after exposure • PE and PS communities were pooled for analyses • *Alcanivorax* and *Ochrobactrum* were higher in abundance in phase 2 than phase 1 (>40% abundance) • *Bacillus* and *Pseudonocardia* discriminate the acclimated communities from planktonic • Relative abundance of KEGG orthologs (PICRUSt) for xenobiotics degradation was higher in INDG than BIOG or planktonic and styrene, chloroalkane and chloroalkene degradation were higher in phase 2 than phase 1

Study	Aims and basic experimental setup	Polymer type	Community determination	Degradation	Key findings
Syranidou, Karkanorachaki, Amorotti, Franchini, *et al.* (2017)	• Investigate the ability of indigenous of bioaugmented consortia to degrade weathered PS • As in (Syranidou et al., 2019) but each phase was 6 months, with (BIOG) or without (INDG) strains known to grow with PS	PS	16S rRNA gene 515F and 806R Illumina MiSeq v3 QIIME ITS rRNA gene ITSF and ITSReub ARISA qPCR for alkB alkB-f and alkB-r SEM	Weight loss, FTIR, GPC	• BIOG showed the same weight loss in phases 1 and 2 (4.7%) • INDG showed 0.19% weight loss in phase 1 and 2.3% in phase 2 • Alterations in structure depending on treatment detected by FTIR and GPC • Clustering of biofilm communities by successional stage – *Alpha-* and *Gammaproteobacteria* increased by the end of phase 2 • Inoculated genera (BIOG) in similar abundances in all samples • Initial communities were distinct from final communities • alkB abundance showed non-significant variation • 32 OTUs enriched in INDG community: *Kiloniellaceae, Alcanivoraceae, Brucellaceae, Flavobacteriaceae, Pseudomonadaceae, Bacillaceae* and *Pseudonocardiaceae* • Xenobiotics and styrene KEGG orthologs (PICRUSt) increased in abundance by the end of phase 2
Syranidou, Karkanorachaki, Amorotti, Repouskou, *et al.* (2017)	• Investigate the ability of indigenous of bioaugmented consortia to degrade weathered PE • As in (Syranidou et al., 2017a) but with PE	PE	16S rRNA gene 515F and 806R Illumina MiSeq v3 QIIME ITS rRNA gene ITSF and ITSReub ARISA qPCR for alkB alkB-f and alkB-r SEM CFU	Weight loss, FTIR, rheology	• PE attachment and colonisation was faster in phase 2 (acclimated) than phase 1 (non-acclimated) • BIOG had a higher ability to attach compared with INDG • Phase 1 0.4 and 0.3% weight loss for BIOG and INDG, respectively and phase 2 19 and 4.2% for BIOG and INDG, respectively • SEM and FTIR showed changes in surfaces before and after incubation • Initial community did not affect final community structure – inoculated strains not detected at the end of phase 1 • *Alpha-* and *Gammaproteobacteria* were most abundant in biofilm samples • alkB abundance showed a significant effect of month and treatment • *Pseudonocardia* and *Bacillus* increased in abundance in PE-associated biofilms • *Cellulosimicrobium* and *Ochrobactrum* discriminant of BIOG

Study	Aims and basic experimental setup	Polymer type	Community determination	Degradation	Key findings
Tsiota *et al.* (2018)	• Determine whether secondary MPs can be degraded my microbial communities • Incubate PE developed consortia (Agios) or indigenous microbial community from Chania, Greece (Souda), with secondary MPs (produced by UV radiation and fragmentation) for 4 months	HDPE	Viable cell counts EPS measurement qPCR for alkB alkB-f and alkB-r	Weight loss	• Souda community decreased the weight of HDPE fragments by 18% and Agios by 8% by the end of the second month • The weight loss had occurred by 1 month and then nothing further • Abundances of cells and alkB increased over time • Protein content decreased between months 1 and 2 whereas carbohydrate increased
Webb *et al.* (2009)	• Investigate ability of marine bacteria to attach to and survive on plastic pieces • Incubate Melbourne, Australia, seawater with plastics for 3 or 6 months	PET	CFU counts	Surface wettability, roughness	• After exposure water contact angle didn't change, but formamide and diidomethane contact angles increased • Surfaces were rougher after bacterial attachment • Attachment occurred to varying degrees and bacteria were recoverable after 6 months from mesocosms with PET, but not from those without PET
Woodall *et al.* (2018)	• Characterise bacterial and archaeal communities colonising deep sea plastics • Collect plastics from the equatorial Atlantic Ocean deep sea	Plastic, rubber, glass, sediment FTIR	16S rRNA gene 515F and 806R Illumina MiSeq v3 QIIME and UCLUST	Not tested	• Only 20% of OTUs could be assigned to genera • Sediment and glass communities were most similar with the highest abundance of *Crenarchaeota* • *Bacteroidetes* were more abundant on litter than in sediment and *Actinobacteria* were an order of magnitude higher in abundance on one rubber sample than all others • Composition at class level of *Proteobacteria* was similar among samples, but metal had *Zetaproteobacteria* • Most OTUs were only present on a single sample type • Litter and sediment samples differ, but no obvious patterns in assemblage composition or key set of OTUs across litter types and no difference between different basins
Yang *et al.* (2019)	• Determine whether the plastisphere is a reservoir for antibiotic and metal resistance genes (ARGs and MRGs)	PE, PP FTIR	Metagenomes assembled and searched for ARGs and MRGs	Not tested	• ARGs were found in all plastic samples (13 types), but only in 4 of 17 SW samples (6 types) • No difference in ARGs between macro- and microplastics

Study	Aims and basic experimental setup	Polymer type	Community determination	Degradation	Key findings
	• Uses metagenomic dataset collected from North Pacific gyre plastics by (Bryant et al., 2016a)				• Diversity and richness of MRGs greater for plastics than SW, but no difference in relative abundance • Multi-metal resistance genes highest in abundance • No correlation between abundance of ARGs and MRGs on plastics, but multi-drug and multi-metal resistance genes tended to co-occur • Congruence between community and ARG but not MRG profiles
Zettler, Mincer and Amaral-Zettler (2013)	• Characterise microbial diversity on plastic marine debris (PMD) • Collected plastic from multiple locations in the North Atlantic	PE, PP Raman	16S rRNA gene 518F and 1046R 18S rRNA gene 1380F and 1510R 454 genome sequencer UCLUST	Not tested	• Coined the term "plastisphere" • Plastics showed signs of degradation (cracks and pitting with round cells of ~2 µm) • Communities were consistently distinct between plastics and surrounding SW • *Navicula, Nitzschia*, *Sellaphora*, *Stauroneis* and *Chaetoceros* were abundant • SW dominated by *Pelagibacter* and one plastic sample contained 24% *Vibrio* • Harmful dinoflagellate *Alexandrium* was also found on plastics • Community richness was greater in SW, but evenness greater on plastics • 350 OTUs were shared between PE and PP (30-40% abundance) and 1789 OTUs were unique to SW • PE and PP: *Phormidium*, *Pseudoalteromonas*, *Hyphomonadaceae* • Some putative hydrocarbon degrading bacteria co-occur in close proximity to each other in network analysis

1.5 Microbial communities on marine plastics

When the results of the literature review (Table 1.2) are taken together, they suggest that the largest differences in community structure when comparing plastics between different locations or polymer types are at specific time points (De Tender et al., 2017; Dussud et al., 2018a; Harrison et al., 2014; Kesy et al., 2016; Pollet et al., 2018; Syranidou et al., 2019). These time points have differed between studies, likely due to varying stochastic factors driving community assembly (Enke et al., 2019; Ortiz-Álvarez et al., 2018; Zhou and Ning, 2017), but generally, the microbial community colonising plastics follows the distinct phases often observed on natural marine particles and surfaces: initially, *Gammaproteobacteria* – that may be specialised in degrading that substrate – dominate microbial communities (often in excess of 40% relative abundance) and then there is a subsequent shift to a dominance of *Alphaproteobacteria* (again, often in excess of 40%; Pollet et al., 2018). Many of these studies have also observed that while these communities may be specific to a particular polymer type (Carson et al., 2013; Frere et al., 2018; Kirstein et al., 2019, 2018), they are also location- (Amaral-Zettler et al., 2015; Carson et al., 2013; Jiang et al., 2018; Kettner et al., 2017; Muthukrishnan et al., 2018; Oberbeckmann et al., 2018, 2016, 2014) or season- specific (Oberbeckmann et al., 2016, 2014) and these differences in community structure may be driven by environmental gradients such as salinity or nutrient availability (Oberbeckmann et al., 2018). In order to determine the fate of plastics in the oceans, it is important to understand the microbial community dynamics that may be driving the degradation of plastics, however, there are currently many more studies that have characterised the microbial communities colonising plastics compared with those looking at plastic degradation in the marine environment (50 as opposed to 16 of 52; Table 1.2).

Several studies have been able to identify a plastic-specific prokaryotic community on one or more polymer types. Recently, Kirstein et al. (2019) identified the substrate-specific communities on a wide range of synthetic materials (HDPE, LDPE, PP, PS, PET, PLA, SAN, PVC, PESTUR and glass), by removing the top layers of the biofilm and enriching those organisms that were tightly-attached. They were able to identify 23 operational taxonomic units (OTUs) that were discriminatory of different treatments and these indicated the closeness of the Plastispheres of similar polymer types (*i.e.* HDPE and LDPE as well as PP, PS and SAN; see Figure 1.4 for chemical structures of different plastic types). This has been further confirmed by a number of other studies that found that PE and PP communities were generally similar (Amaral-Zettler et al., 2015; Carson et al., 2013; Ogonowski et al., 2018; Zettler et al., 2013),

while PE and PP communities were generally different from those colonising PS (Amaral-Zettler et al., 2015; Frere et al., 2018) or PET (Muthukrishnan et al., 2018). There are some taxonomic groups of bacteria that have been identified as abundant colonisers of plastics in more than one study, for example, *Alcanivoraceae* (Dussud et al., 2018a; Oberbeckmann et al., 2016; Syranidou et al., 2019, 2017a), *Bacillaceae* (Arutchelvi et al., 2008; Carson et al., 2013; Devi et al., 2019; Harshvardhan and Jha, 2013; Kumar et al., 2007; Syranidou et al., 2019, 2017b, 2017a), *Alteromonodales* (De Tender et al., 2015; Dussud et al., 2018a; Oberbeckmann et al., 2014; Zettler et al., 2013) and *Erythrobacteraceae* (Curren and Leong, 2019; Dussud et al., 2018b; Kirstein et al., 2019; Oberbeckmann et al., 2018). Several of the studies have also characterised the eukaryotic communities colonising plastics and found an abundance of diatoms (Carson et al., 2013; Lacerda et al., 2019; Oberbeckmann et al., 2016), particularly *Nitzschia* sp. (Reisser et al., 2014; Zettler et al., 2013), which are not likely to be contributing to the degradation of plastics, however, those that also identify fungi (De Tender et al., 2017; Kettner et al., 2017; Oberbeckmann et al., 2016) have suggested that these could be contributing to plastic biodegradation (De Tender et al., 2017).

The majority of studies that characterise the Plastisphere employ next generation, culture-independent sequencing technologies (*e.g.* Illumina MiSeq amplicon sequencing), however, there is little consensus between the primers and the bioinformatic analyses used. The use of different primers can lead to the introduction of different bias as well as an under-representation of different taxonomic groups, for example the hydrocarbonoclastic or phototrophic bacteria (Berry et al., 2017; Pollet et al., 2018), which complicates comparisons made between studies. The use of data processing pipelines that cluster taxa into operational taxonomic units (OTUs) rather than amplicon sequence variants (ASVs) – where OTUs are clusters of sequences that differ by less than a dissimilarity threshold (usually 97%) and ASVs are exact sequence variants that have been corrected for errors (Callahan et al., 2017) – further compounds the problems with direct comparisons between studies sequenced at different times and using different primers (Callahan et al., 2016; Hugerth and Andersson, 2017). It is likely, however, that where plastic-specific taxa are observed, these vary geographically and seasonally (*e.g.* Oberbeckmann et al., 2018), but while these are distinct, they may originate from common genera or families, which would be elucidated if the methods employed were harmonised. It is therefore suggested that future studies employing amplicon sequencing technologies to characterise the Plastisphere use the 16S rRNA gene primer pair 515F and 926R (Parada et al., 2016; Pollet et al., 2018) and a pipeline that retains

unique sequence information, such as DADA2 (Callahan et al., 2016; Hugerth and Andersson, 2017), which is easily implemented in R (R Core Team, 2017).

Microbes do not appear in the environment as isolates and it is therefore far more realistic to study the colonisation and degradation of plastics by microbial communities and consortia. However, it is likely that processes such as microbial community succession will slow down any degradation in nature (Enke et al., 2018) and may mask the occurrence of any plastic-specific communities (Dang et al., 2008; Pollet et al., 2018), as well as increasing the difficulty of identifying novel enzymes and pathways used for plastic degradation. The degradation of plastics by microbial communities has been shown to slow over time, even as microbial cell density continues to increase (Tsiota et al., 2018), which is to be expected if marine communities go through stages of succession, as is the case for other substrates in the marine environment (Datta et al., 2016). Interestingly, the majority of studies that have looked at plastic degradation over multiple time points by microbial communities have demonstrated that weight loss of plastics continues to increase as incubation time goes on (Kathiresan, 2003; Kumar et al., 2007; Syranidou et al., 2019, 2017b, 2017a). The studies that also characterise the microbial communities do not observe a decrease in *Gammaproteobacteria* or an increase in *Alphaproteobacteria* over time, as would be typical of a community in the succession phase and rather see that both of these classes remain abundant and dominant throughout the incubation (Syranidou et al., 2019, 2017b, 2017a). This suggests that some microbial communities are somehow able to overcome the succession, or that plastic degradation may be carried out by a rare but active fraction of the Plastisphere, which fits with the hypothesis of Kirstein et al. (2019), that plastic-specific colonisers are generally rare members of the Plastisphere. This finding – that plastic degraders are rare members of the Plastisphere – could, however, be an artefact of the long incubation times of months to years used by these studies, as a recent study found that bacteria that were potentially able to degrade plastics were only enriched on the second day of incubation in coastal marine waters and had declined to <1% relative abundance by the ninth day of incubation (Erni-Cassola et al., 2019).

Whilst several of the above studies have looked at the early colonisation of plastics, none of them have looked at this on PET (Table 1.2), which is widely stated to be likely to be more degradable than other plastics such as PE and PP due to the presence of an ester bond linking together monomeric subunits (Webb et al., 2013; Figure 1.4). As with other marine polymers, such as chitin, it is likely that the microbial members of these early colonisation stages are

the ones that are able to degrade the polymer (Datta et al., 2016) and it has been suggested that the colonising communities of plastics are degrading the contaminants and additives of plastics (De Tender et al., 2015). Biofilms have also been found to inhibit abiotic weathering, for example by shielding the plastic from UV light (Rummel et al., 2017), which, as discussed in Section 1.2, is a necessary prerequisite for biotic degradation of most polymers (Albertsson et al., 1995; Jeon and Kim, 2016). Because these biofilms form very rapidly when plastics reach the environment, as demonstrated above, it is therefore likely that the majority of abiotic plastic degradation must occur before plastics reach the oceans if it is to contribute towards the degradation of plastics (Andrady, 2017; Rummel et al., 2017). It is also not known to what extent other polymer properties such as crystallinity, degree of abiotic weathering or additive content will affect the degradation of polymers that are otherwise similar, although this has been investigated to some extent in the terrestrial environment (Yoshida et al., 2016a). As such, if we wish to study microbial communities that are capable of the degradation of plastics, or plastic contaminants, then it is important that we gain a fundamental understanding of the degradability of these plastics and the plastic-associated chemicals, in the marine environment. These early successional stages must also be studied in more detail, particularly with regards to the oil-derived plastics that are potentially more degradable, such as PET.

1.6 Potentially plastic-degrading marine microbial isolates

In 2016, a terrestrial bacterium that could completely mineralise PET, *Ideonella sakaiensis* (*Betaproteobacteria*), was described and the enzymes and pathways that it uses to do this were characterised (Yoshida et al., 2016a). The bacterium initially uses an extracellular PET hydrolase (PETase) to break the PET down to mono(2-hydroxy ethyl) terephthalate (MHET) and terephthalic acid (TPA) – as well as small amounts of bis(2-hydroxy ethyl) terephthalate (BHET) – and the MHET is subsequently also broken down to TPA, as well as ethylene glycol, using a MHET-hydrolysing enzyme (MHETase). The TPA then enters the protocatechuate degradation pathway (also known as the protocatechuate branch of the β-ketoadipate degradation pathway), which is already well characterised (Liang et al., 2008; Vamsee-Krishna and Phale, 2008). This enzyme was different from previous enzymes that have been found to degrade plastics in that it appeared to exhibit higher activity with PET than with any other substrate that was tested and was active at lower temperatures, suggesting that it had actually adapted to become better at PET degradation. This was an important discovery, as, while bacteria do not occur in the environment as isolates, if we wish to gain a full, mechanistic understanding of plastic degradation (with the methods currently available), then it is necessary to obtain plastic-degrading isolates. The isolation of *I. sakaiensis* and its PETase allowed for the characterisation (Han et al., 2017; Joo et al., 2018) and engineering (Austin et al., 2018) of the enzyme and for homologs to be searched for in environmental metagenomes (Danso et al., 2018), thus gaining a broader understanding of how widespread the ability to degrade PET is. Danso et al. (2018) was also successful in expressing a PETase originating from a marine metagenome in the laboratory, although, to our knowledge, currently no marine microbes with this ability have been isolated, so the conditions necessary for their growth are not yet known.

Several studies to date have identified marine microbial isolates that are capable of plastic degradation (Devi et al., 2019; Harshvardhan and Jha, 2013; Kathiresan, 2003; Kumar et al., 2016, 2007; Mohanrasu et al., 2018; Paço et al., 2017; Raghul et al., 2014; Sudhakar et al., 2008), although the enzymes and pathways used to do this have not yet been characterised. These have been isolated from a wide range of marine environments, *e.g.* mangrove soil (Kathiresan, 2003; Kumar et al., 2007) or marine sediments (Mohanrasu et al., 2018), but are from only a few bacterial taxonomic classes; *Bacilli* (Devi et al., 2019; Harshvardhan and Jha, 2013; Kumar et al., 2007; Mohanrasu et al., 2018; Sudhakar et al., 2008), *Gammaproteobacteria* (Devi et al., 2019; Kathiresan, 2003; Kumar et al., 2016; Raghul et al.,

2014) and *Actinobacteria* (Harshvardhan and Jha, 2013), or are fungal species (Kathiresan, 2003; Kumar et al., 2016; Paço et al., 2017), although fungi are relatively rare in the natural marine environment (De Tender et al., 2017). It is also evident from the metagenomic PETase search by Danso et al. (2018) that whilst the majority of terrestrial PETases that were found originated from the *Actinobacteria*, in the marine environment these came mainly from the *Bacteroidetes*.

It is encouraging that marine bacteria have been found that apparently possess the potential for plastic degradation, however, as mentioned above, because bacteria do not occur in the environment as isolates, the extent to which they are able to degrade plastics is therefore not clear. It is possible that microbial communities are more efficient at degradation than isolates, as suggested by Syranidou et al. (2019, 2017b, 2017a), however, Kathiresan (2003) showed that the rates of degradation of PE were much lower in the environment and therefore with microbial communities, than under laboratory conditions with isolates (~4% weight loss in 9 months in the environment, compared with ~30% weight loss in 1 month in the laboratory). This clearly indicates that results obtained in the laboratory are not necessarily true of what may be achieved in the environment, as the interactions between community members may be complex and difficult to predict (Großkopf and Soyer, 2014; Ponomarova and Patil, 2015), although these studies are an important step in the right direction. Further to this, when Yoshida et al. (2016a) published their study on PET degradation, they received criticism that the evidence that they provided for PET degradation was not strong enough (Yang et al., 2016), although Yoshida et al. (2016a) evidenced the PET degradation through an array of techniques; metabolomic analyses, scanning electron microscopy, weight loss measurements, gas permeation chromatography, RNA sequencing and various enzymatic activity assays. Many of the studies on marine plastic degradation by isolates show far less convincing evidence than Yoshida et al. (2016a), for example the growth of biomass in a rich medium alongside weight loss measurements of the plastics without filtration of the medium (Paço et al., 2017) or degradation assessed only through weight loss measurements (Kathiresan, 2003; Kumar et al., 2007), as well as the lack of identification of plastic-degrading enzymes and this is something that should be addressed in future studies.

1.7 Aims and objectives

The aims of this thesis are to:

1. Evaluate the state of current knowledge on the colonisation and degradation of plastics in the marine environment (Chapter 1).
2. Gain a fundamental understanding of microbial community succession and how this impacts the degradation of recalcitrant polymers in the marine environment, using the natural polymer chitin as a case study. It was hypothesised that the method of artificial selection can be used on the naturally occurring microbial community from coastal seawater in order to achieve higher rates of chitin degradation. In order to do this, chitinase activity of microbial communities growing with chitin as the sole source of carbon and nitrogen was measured and the three best communities at each generation were selected to inoculate the next generation of microcosms. MiSeq amplicon sequencing of the 16S and 18S rRNA genes was then used to characterise the response of the microbial community to this selection and to optimise this process (Chapter 2).
3. Determine whether the general principles of microbial community succession also apply to the colonisation of and growth on the common packaging plastic polyethylene terephthalate (PET). Through MiSeq amplicon sequencing of the 16S rRNA gene the prokaryotic communities growing with several different types of PET, as well as the PET precursor, BHET, were characterised, with the aim of describing the successional stages within the community (Chapter 3).
4. Isolate marine bacteria that are capable of degrading PET. Two marine bacteria that were potentially capable of degrading PET were isolated and cellular- and exo-proteomics were performed alongside a detailed analysis of their genomes to determine the enzymes and pathways used for this degradation (Chapter 3). These genes were then searched for in the microbial communities growing with PET.
5. Determine whether plastic additives, *i.e.* plasticizers, are also degraded in the marine environment. A range of isolates were obtained from plasticizer enrichment cultures for the ability to degrade six common plasticizers; dibutyl phthalate (DBP), bis(2-ethyl hexyl) phthalate (DEHP), diisononyl phthalate (DINP), diisodecyl phthalate (DIDP), acetyl tributyl citrate (ATBC) and trioctyl trimellitate (TOTM). Two isolates that were capable of growth on all six plasticizers were chosen, their genomes were sequenced and cellular- and exo-proteomics and metabolomics were performed when they were growing with DBP, DEHP and ATBC. This was in order to

determine whether the mechanisms used for degradation were the same for two phthalic acid ester plasticizers (DBP and DEHP) and to elucidate the pathway used for ATBC degradation for the first time (Chapter 4).

Chapter 2

Understanding microbial community dynamics to improve optimal microbiome selection

2.1 Introduction

Evolution is able to act upon multiple levels of biological organisation (Goodnight, 2005, 2000; Johnson and Boerlijst, 2002; Swenson et al., 2000b; Williams and Lenton, 2007a). It had previously been contested that a whole microbial community may be used as a unit of selection – artificial microbiome selection – and that a community may become progressively better at a selective process over successive transfers (Blouin et al., 2015; Swenson et al., 2000b, 2000a; Williams and Lenton, 2007b). The artificial selection of a measurable and desirable trait is thought to outperform traditional enrichment experiments, as it bypasses community bottlenecks and reduces stochasticity (Blouin et al., 2015). Artificial selection has been shown to induce statistically significant responses in both microcosm (Blouin et al., 2015; Swenson et al., 2000b) and computational ecosystems (Williams and Lenton, 2007a). While microbial communities with desirable phenotypes have been achieved, the results of these experiments have been limited and the composition of these communities has not generally been determined. The underlying mechanisms and key players in this selection have therefore not been identified, nor have the growth parameters involved (*e.g.* incubation time) been systematically optimised (Penn and Harvey, 2004).

Microbial communities (*i.e.* bacteria, archaea and eukaryotic microorganisms) are known to go through distinct stages of community succession, where they may see large enrichments of different groups of organisms (Dang and Lovell, 2000; Datta et al., 2016; Kiørboe et al., 2003, 2002; Ortiz-Álvarez et al., 2018; Simon et al., 2002; Wu et al., 2018). During the colonisation and degradation of the abundant marine polymer, chitin, three phases of bacterial community succession were previously observed: 1) selection of colonising organisms; 2) selection of chitin degraders; and 3) chitin degraders are overtaken by "cheaters" (Datta et al., 2016). "Cheaters", often called cross-feeders, are organisms that are not metabolically capable of carrying out a particular process themselves, but are able to benefit from the public goods generated by others (Beier and Bertilsson, 2011; Cordero et al., 2012; Keyhani and Roseman, 1999). For example, in the environment, it has been shown that the number of organisms capable of taking up the by-products of chitin hydrolysis is far higher than the number that encode for chitinases (Beier and Bertilsson, 2011). Furthermore, marine microorganisms 'leak' a large diversity of organic matter which in turn may be used by the rest of the community (Christie-Oleza et al., 2017; Cordero et al., 2012) enhancing microbial interdependencies (Morris et al., 2012). Here, we define cheaters as those organisms that are able to use the chitin monomer but not produce chitinases and cross-

feeders as those that are not able to produce chitinases *or* use the chitin monomer. It has, however, also been previously observed that if the abundance of cheaters becomes sufficiently high, then access to the resource may even be blocked completely (Enke et al., 2019), leading to a loss of community function.

The undulations between cooperation and competition drive niche-specialisation and higher-level community organisation (Dang and Lovell, 2016). The structure of the microbial community has been suggested to significantly alter the observed phenotype in artificial microbiome selection experiments (Penn and Harvey, 2004) and community structure may be altered through changes in species' composition or interactions between organisms, ultimately leading to changes in the community phenotype. Computational models have shown that community structure, with (Penn, 2003) or without genetic changes (Penn and Harvey, 2004), can be responsible for differences between the phenotypes of a community subjected to a directed selection and one that is randomly selected. Hence, the understanding of microbial community ecology suggests that controlling microbial community dynamics is important for achieving a high-functioning microbial community.

The present chapter aimed to determine the mechanisms behind artificial microbiome selection and early microbial community succession in order to optimise the selection of a process *i.e.* chitin degradation. Chitin is one of the most abundant polymers on Earth (*i.e.* the most abundant polymer in marine ecosystems with a predicted production in the range of billions of tons each year) and constitutes a key component in oceanic carbon and nitrogen cycles (Souza et al., 2011). Many microorganisms are already known to degrade chitin and the enzymes and pathways used to do so are well characterised (Beier and Bertilsson, 2013). It was found that a microbiome could be artificially evolved to achieve higher chitinase activities, but there were certain methodological caveats to this selection process: the incubation time between transfers needed to be continuously optimised in order to avoid community drift and decay. Microbial community composition was evaluated, and it was confirmed that, if transfer times are not continuously optimised, efficient biodegrading communities are rapidly taken over by cheaters and predators with a subsequent loss of degrading activity.

2.2 Method

2.2.1 Microbial inoculum

The microbial community used as an inoculum for all experiments was obtained from bulk marine debris collected during boat tows from both Plymouth Sound (Devon, UK; June 2016) and Portaferry (Northern Ireland, UK; August 2016).

2.2.2 Chitinase activity measurements

Chitinase activity was measured as the liberation of the fluorogenic molecule 4-methylumbelliferyl (MUF) from three chitinase substrates, following the methods of Hood (1991), Lecleir *et al.* (2007) and Köllner *et al.* (2012). These were the chitinase substrates specific to the monomer, dimer and trimer; MUF-N-acetyl-β-D-glucosaminide, MUF-β-D-N,N'-diacetylchitobioside and MUF-β-D-N,N',N''-triacetylchitotrioside, respectively. Stock solutions of each substrate were prepared in 100% dimethyl formamide. These three MUF substrates were combined in equal concentrations so as the test substrate had a concentration of 100 µM of each. MUF hydrolysis assays were performed in black 96-well polypropylene microplates. 36 µL sample was added to 4 µL 100 µM MUF and these were incubated at room temperature (~20˚C) for 1 hour. This was performed on the total sample and not only the extracellular fraction. The reaction was stopped with 160 µL 100 mM glycine-sodium hydroxide buffer (pH 10.4). Fluorescence was measured with 362 nm excitation and 448 nm emission using a Synergy HTX microplate reader. Fluorescence measurements were converted to U mL^{-1} enzyme activity, where 1 U is the amount of enzyme required to catalyse the conversion of 1 µM of substrate to product per minute. This used standard solutions made with chitinase from *Streptomyces griseus* (~9 U mg^{-1}) dissolved in sterile phosphate buffered saline solution (pH 7.4) with a highest concentration of 0.1 U mL^{-1}. The volume of sample taken for chitinase activity measurements was the same for all experiments. Chitinase activity was calculated as a function of µmoles of chitin consumed per litre and day (µM day^{-1}).

2.2.3 Artificial selection

The process for artificial selection is depicted in Figure 2.1. Briefly, 30 individual microcosms per treatment and generation were incubated in the dark under the conditions described below. At the end of each incubation period the three microcosms with the highest chitinase activities (or three random microcosms in the case of the control) were pooled and used as the inoculum for the next generation of microcosms (*n*=30). This was repeated across

multiple transfers. Two artificial selection experiments were performed, the first to optimise the process and the second to implement optimal conditions and achieve a high-performing chitinolytic microbial community:

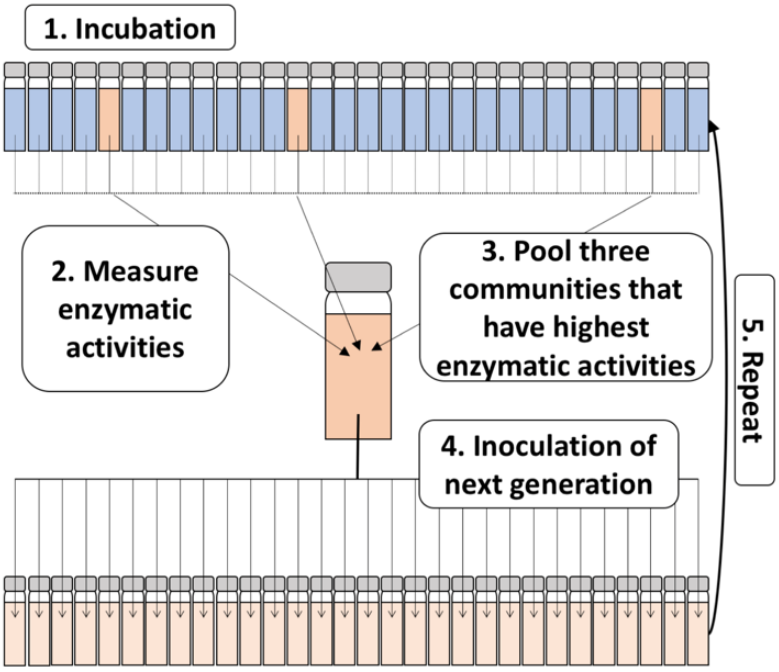

Figure 2.1. Method used for artificial selection of microbial communities. Briefly, 30 microcosms are inoculated with a natural community found in seawater (1). At the end of the incubation period, the enzymatic activity for a desired trait (e.g. chitinase activity) is measured for each microcosm (2). The three microcosms with the highest enzymatic activities are selected and pooled (3) and used to inoculate the next generation (4). This process is repeated over *n* generations (5).

First artificial selection experiment

Incubations were carried out at 23˚C in 22 mL glass vials (Sigma Aldrich), each containing 20 mL of autoclaved seawater (collected from outside Plymouth Sound, Devon, UK; June 2016) supplemented with NaH_2PO_4, F/2 trace metals (Guillard and Ryther, 1962) (Table 2.1) and 100 mg of chitin powder (from shrimp shells; Sigma Aldrich) as the sole source of carbon and nitrogen. Generation 0 was started with 200 µL of microbial inoculum. The efficiency of the selection process was assessed by comparing a 'positive selection' (where the three communities with highest activity were pooled and 200 µL was used to inoculate each one of the 30 microcosms of the next generation) against a 'random selection' (where three communities were chosen at random, using a random number generator within the Python module Random, to inoculate the following generation) to give a control against uncontrollable environmental variation (Day et al., 2011). Each treatment was repeated

across 20 generations with incubation times of nine days. In parallel, treatments where incubation times were shortened to four days were set up after generation 15. Samples were taken from each community and stored in 20% glycerol at -80˚C for further microbial isolation and pellets from 1.5 mL of culture were collected by centrifugation (14,000 *x g* for 5 mins) and stored at -20˚C for final DNA extraction and community analysis.

Table 2.1. F/2 and custom mineral media (Bushnell and Haas, 1941) nutrients and trace metals.

Media	**Nutrients**	**Final concentration (M)**
F/2	$NaH_2PO_4 \cdot 2H_2O$	3.62×10^{-5}
Custom mineral media	$MgSO_4 \cdot 5H_2O$	2×10^{-3}
	$CaCl_2 \cdot 2H_2O$	2×10^{-4}
	KH_2PO_4	7×10^{-3}
	K_2HPO_4	6×10^{-3}
	(NH_4NO_3) [1]	12.5×10^{-3}
	Trace metals	**Final concentration (M)**
F/2	$FeCl_3 \cdot 6H_2O$	1.17×10^{-5}
	$Na_2EDTA \cdot 2H_2O$	1.17×10^{-5}
	$CuSO_4 \cdot 5H_2O$	3.93×10^{-8}
	$Na_2MoO_4 \cdot 2H_2O$	2.6×10^{-8}
	$ZnSO_4 \cdot 7H_2O$	7.65×10^{-8}
	$CoCl_2 \cdot 6H_2O$	4.2×10^{-8}
	$MnCl_2 \cdot 4H_2O$	9.1×10^{-7}
Custom mineral media	H_3BO_3	4.6×10^{-4}
	$MnCl_2 \cdot 4H_2O$	1.4×10^{-4}
	$ZnSO_4 \cdot 7H_2O$	1.4×10^{-3}
	$Na_2MoO_4 \cdot 2H_2O$	1.9×10^{-6}
	$CuSO_4 \cdot 5H_2O$	5×10^{-9}
	$Co(NO_3)_2 \cdot 6H_2O$	2.7×10^{-8}
	$FeCl_3 \cdot 6H_2O$	1.8×10^{-6}
	$EDTA\ (Na_2Mg)$	7.1×10^{-6}
	Vitamins [2]	**Final concentration (M)**
	$C_{12}H_{18}Cl_2N_4OS$ (Thiamine HCl)	2.9×10^{-5}
	$C_6H_5NO_2$ (Nicotinic acid)	1.6×10^{-4}
	$C_8H_{12}ClNO_3$ (Pyridoxine HCl)	9.7×10^{-5}
	$C_7H_7NO_2$ (Para-aminobenzoic acid)	73×10^{-5}
	$C_{17}H_{20}N_4O_6$ (Riboflavin)	5.3×10^{-5}
	$C_{10}H_{16}N_2O_3S$ (Biotin)	4×10^{-6}
	$C_{63}H_{88}CoN_{14}O_{14}P$ (Cyanocobalamin vitamin B12)	7.4×10^{-7}

[1] NH_4NO_3 was not used in experiments involving chitin, but was added in all experiments in Chapters 3 and 4.
[2] In the isolate co-culture experiments 0.005% yeast extract was used in place of the vitamins.

Second artificial selection experiment

A second selection experiment was set up implementing optimal transfer incubation times. Microcosms were incubated in 2 mL 96-well plates (ABgene ™, ThermoFisher Scientific) covered by Corning® Breathable Sealing Tapes to stop evaporation and contamination while allowing gas exchange. Each well contained 1.9 mL of a custom mineral media containing

$MgSO_4$, $CaCl_2$, KH_2PO_4, K_2HPO_4, 0.52 M NaCl and artificial seawater trace metals (Table 2.1), supplemented with 10 mg of chitin powder. The microbial inoculum was 100 µL (*i.e.* initial inoculum and transfer between generations). Chitinase activity was measured daily. Transfer between generations was carried out just after the peak of chitinase activity had occurred, calculated as the mean chitinase activity across the 30 microcosms of the positive selection treatment. Plates were incubated in the dark at 30˚C with constant shaking (150 rpm). Eight days was the maximum incubation time allowed to reach maximum chitinase activity due to volume constraints.

2.2.4 DNA extraction and amplicon sequencing

DNA was extracted using the DNeasy Plant Mini Kit (Qiagen) protocol, with modifications as follows (adapted from Bryant et al., 2016): 300 µL 1 x TAE buffer was used to resuspend cell pellets and these were added to ~0.4 g of sterile 0.1 mm Biospec zirconia silica beads in 2 mL screw cap microtubes (VWR international). Bead beating was carried out for 2 x 45 s and 1 x 30 s at 30 Hz using a Qiagen Tissue Lyser. Cell lysates were then processed in accordance with the manufacturer's instructions, with an extra centrifugation step to ensure all liquid was removed (1 min, 13,000 *x g*) directly before elution of samples. A Qubit® HS DNA kit (Life Technologies Corporation) was used for DNA quantification after which they were diluted to equalise the concentrations across samples. A Q5® Hot Start High-Fidelity 2X Master Mix (New England Biolabs® inc.) was used to amplify the 16S rRNA gene v4-5 regions using primers 515F-Y and 926R and the 18S rRNA gene v8-9 regions using primers V8F and 1510R (Table 2.2). PCR products were purified using Ampliclean magnetic beads (Nimagen, The Netherlands). Index PCR was carried out using Illumina Nextera Index Kit v2 adapters. Samples were normalised using a SequelPrep™ Normalisation Plate Kit (ThermoFisher Scientific). Samples were pooled and 2 x 300 bp paired-end sequencing was carried out using the MiSeq system with v3 reagent kit (this was carried out by the University of Warwick Genomics Facility). Negative DNA extraction controls and library preparation negative controls as well as chitin-only positive controls were processed and sequenced alongside samples.

Table 2.2. Primers used in this thesis.

Target	Primers
MiSeq amplicon sequencing	
16S rRNA gene v4-5 (Parada et al., 2016) (~372 bp)	515F-Y: GTGYCAGCMGCCGCGGTAA 926R: CCGYCAATTYMTTTRAGTTT
	V8F: ATAACAGGTCTGTGATGCCCT

Target	Primers
18S rRNA gene v8-9 (Bradley et al., 2016) (~375 bp)	1510R: CCTTCYGCAGGTTCACCTAC
Sanger sequencing	27F: AGAGTTTGATCMTGGCTCAG
16S rRNA gene (Lane, 1991) (~1450 bp)	1492R: TACGGYTACCTTGTTACGACTT
qPCR with isolates	
Pseudoalteromonas shioyasakaiensis (134 bp)	F: CAACAGTTGGAAACGACTGC R: ATCGTCGCCTTGGTGAGCCA
Donghicola eburneus (122 bp)	F: AATAGTCCCGGGAAACTGGG R: ATCGTAGACTTGGTAGGCCA
Phaeobacter gallaeciensis (122 bp)	F: AATAGCCACTGGAAACGGTG R: ATCGTAGACTTGGTAGGCCG

2.2.5 Microbial community structure determination

Two different workflows were used to analyse the sequencing data: Mothur (Schloss et al., 2009) was initially used and analyses were later repeated using DADA2 (Callahan et al., 2016; Callahan et al., 2016) instead. DADA2 delivers better taxonomic resolution than other methods (*e.g.* Mothur) as it retains unique sequences and calculates sequencing error rates rather than clustering to 97% similarity (Hugerth and Andersson, 2017). The resultant taxonomic units are referred to as amplicon sequence variants (ASVs) rather than operational taxonomic units (OTUs from Mothur). For the Mothur analysis (Schloss et al., 2009), sequencing data were filtered *i.e.* adapter, barcode and primer clipped, sequence length permitted was 450 bp for the 16S rRNA gene and 400 bp for the 18S rRNA gene, maximum number of ambiguous bases per sequence = 4, maximum number of homopolymers per sequence = 8. Taxonomy assignment was performed using the SILVA reference database (Wang classification, v128) (Quast et al., 2013) and operational taxonomic units (OTUs) set at 97% similarity. For the DADA2 analysis, sequencing data were processed following the DADA2 (version 1.8.0) pipeline (Callahan et al., 2016). Briefly, the data were filtered, *i.e.* adapter, barcode and primer clipped and the ends of sequences with high numbers of errors were trimmed. The amplicons were denoised based on a model of the sequencing errors and paired end sequences were merged. Only sequences between 368 - 379 for the 16S rRNA gene and 300 – 340 bp for the 18S rRNA gene were kept and chimeras were removed. The resulting ASVs were classified using the SILVA reference database (v132) (Quast et al., 2013). For both processing workflows, chloroplasts, mitochondria and *Mammalia* were removed from the 16S rRNA gene and 18S rRNA gene datasets, eukaryotes were removed from the 16S rRNA gene dataset and bacteria and archaea from the 18S rRNA gene dataset. The average number of reads per sample was approximately 12,500 for the 16S rRNA gene and 20,000 (Mothur) or 34,000 (DADA2) for the 18S rRNA gene. Samples with fewer than 1,000

total reads were excluded from downstream analyses. Although most analyses were carried out using relative abundance, each sample was subsampled at random to normalise the number of reads per sample and the resulting average coverage was 92% (Mothur) or 94% (DADA2) for the 16S rRNA gene and 99% (Mothur and DADA2) for the 18S rRNA gene.

2.2.6 Microbial isolation and characterisation

Microbes were isolated from the final transfer of positive selection experiments by plating serial dilutions on Marine Broth 2216 (BD Difco™) and mineral medium plates (Table 2.1) supplemented with 0.1% N-acetyl-D-glucosamine (GlcNAc) and 1.5% agar. Colonies were re-streaked on fresh agar plates until pure isolates were obtained. The identification of isolates was carried out by sequencing the partial 16S rRNA gene (GATC BioTech, Germany) using primers 27F and 1492R (Lane, 1991) (Table 2.2).

Isolates were grown in mineral medium supplemented with either 0.1% chitin or 0.1% GlcNAc (w/v), as sources of carbon and nitrogen, to test for chitinase activity and chitin assimilation, respectively. Growth was monitored over 14 days by measuring: i) chitinase activity (as described above), ii) optical density at 600 nm and iii) protein content (following manufacturer's instructions; QuantiPro™ BCA Assay Kit, Sigma Aldrich, UK). Isolates were also tested on mineral medium agar plates made with the addition of 0.1% chitin and 0.8% agarose. Plates were incubated at 30˚C for 21 days to allow the formation of halos indicative of chitinase activity.

2.2.7 Co-cultures using isolates

In order to determine whether the presence of a chitin degrader could enable the growth of a cheater and a cross-feeder with chitin as the sole source of carbon and nitrogen, co-cultures were performed using the isolates: *Pseudoalteromonas shioyasakaiensis* (chitin degrader), *Donghicola eburneus* (cheater, capable of growth on GlcNAc but not chitin) and *Phaeobacter gallaeciensis* (cross-feeder, not capable of growth on either chitin or GlcNAc). Combinations of these strains were grown in 25 cm^2 tissue culture flasks with 25 mL custom mineral media (Table 2.1) supplemented with 0.1% (w/v) of chitin. Cultures were incubated at 30˚C with shaking at 200 rpm for three days. Pellets from 1.5 mL of culture on days 0 and 3 were collected by centrifugation (14,000 *x g* for 5 mins) and stored at -20˚C for DNA extraction, as above. Specific primers were designed for each of the isolates based on their 16S rRNA gene (Table 2.2) and qPCR was performed (Applied Biosystems 7500 Fast Real-Time PCR system)

using 1 µL template DNA, following the manufacturer's instructions for the GoTaq® qPCR Master Mix (Promega). Final primer concentrations were 0.5, 0.9 and 0.9 µM, for the degrader, cheater and cross-feeder, respectively. Results were normalised to standard curves that used DNA extracted from pure cultures.

2.2.8 Statistical analyses

All analyses of chitinase activity and most MiSeq data analyses were carried out using custom Python scripts (Python versions 2.7.10 and 3.6.6) using the modules: colorsys, csv, heapq, matplotlib, numpy, os, pandas, random, scipy, scikit-bio, sklearn (Pedregosa et al., 2011) and statsmodels. SIMPER analyses and plotting of phylogenetic trees were performed in R (R version 3.3.3) (R Core Team, 2017) using the following packages: ape (Paradis et al., 2004), dplyr, ggplot2, gplots, ggtree (Yu et al., 2017), lme4, phangorn (Schliep, 2011), plotly, tidyr, vegan (Dixon, 2003), phyloseq (McMurdie and Holmes, 2013). The top 5 ASVs identified in each SIMPER analyses were classified to their closest relative using a BLAST search of the GenBank database. Hypothetical community functions were obtained using PICRUSt in QIIME1 (Caporaso et al., 2010; Langille et al., 2013) by mapping ASVs to the Greengenes database (Desantis et al., 2006) (v13.5) at the default 97% similarity threshold. The PICRUSt analysis includes almost 35% of all ASVs, accounting for a mean relative abundance of 53%, 68% and 81% for the positive selection nine-day, four-day and daily analyses, respectively. The Nearest Sequenced Taxon Index (NSTI) obtained for each of the taxonomic groups is available in (Table 2.3) (a full summary for each sample can be found on Github https://github.com/R-Wright-1/ChitinSelection.git). The three groups with the highest relative abundance, *Gammaproteobacteria, Alphaproteobacteria* and *Bacteroidia* (*i.e.* 29.3%, 26.4% and 16.6%, respectively) showed NSTI values of 0.07, 0.09 and 0.18, respectively. Sequences used for phylogenetic trees were aligned using the SILVA Incremental Alignment (www.arb-silva.de) (Pruesse et al., 2012) and mid-point rooted maximum likelihood trees were constructed using QIIME1 (Caporaso et al., 2010). All scripts can be found at https://github.com/R-Wright-1/ChitinSelection.git. All sequences have been deposited in the NCBI Short Read Archive (SRA) database under Bioproject PRJNA499076. qPCR data was analysed using custom Python scripts.

Table 2.3. Summary of the information obtained from the PICRUSt analyses of all 16S rRNA gene sequences from the chitin artificial selection experiment.

Class [1]	ASVs predicted [2]	Total ASVs [3]	Relative abundance original (%) [2]	Relative abundance in PICRUSt analyses (%) [3]	Mean weighted NSTI (not including nan)
Acidimicrobiia	11	14	0.00	0.00	0.23
Actinobacteria	120	130	0.06	0.06	0.05
Alphaproteobacteria	361	1387	26.39	15.24	0.09
Anaerolineae	15	28	0.08	0.00	0.31
Babeliae	0	16	0.00	0.00	
Bacilli	94	100	0.10	0.09	0.04
Bacteroidia	504	994	16.55	14.65	0.18
Campylobacteria	15	23	0.23	0.23	0.03
Chitinivibrionia	0	12	0.92	0.00	
Chlamydiae	2	12	0.00	0.00	nan
Cloacimonadia	35	170	2.40	1.47	0.17
Clostridia	232	517	4.56	3.18	0.18
Deltaproteobacteria	163	607	6.08	3.14	0.06
Erysipelotrichia	10	13	0.02	0.02	0.06
Gammaproteobacteria	478	1280	29.28	28.18	0.07
Gracilibacteria	3	37	0.01	0.00	0.56
Ignavibacteria	3	41	0.24	0.00	0.36
Microgenomatia	10	71	0.01	0.00	0.77
Mollicutes	5	124	0.23	0.00	0.12
NA	19	440	11.64	0.22	0.36
Negativicutes	21	23	0.01	0.01	0.06
Other	0	205	0.21	0.00	

Class [1]	ASVs predicted [2]	Total ASVs [3]	Relative abundance original (%) [2]	Relative abundance in PICRUSt analyses (%) [3]	Mean weighted NSTI (not including nan)
Parcubacteria	1	119	0.02	0.00	0.81
Phycisphaerae	10	23	0.10	0.10	0.57
Planctomycetacia	12	22	0.00	0.00	0.22
Saccharimonadia	13	30	0.02	0.01	0.46
Spirochaetia	26	68	0.59	0.33	0.18
Verrucomicrobiae	34	51	0.12	0.12	0.16
Woesearchaeia	0	48	0.11	0.00	
TOTALS	**2197**	**6605**	**100.00**	**67.04**	

[1] PICRUSt was run separately for each taxonomic class.

[2] The number of ASVs and the mean relative abundance that these ASVs account for, that were able to be matched to the Greengenes reference database (v13.5) prior to running PICRUSt.

[3] The number of ASVs and the mean relative abundance that these ASVs account for, from that taxonomic class in the full MiSeq amplicon sequencing results.

2.3 Results

The experimental setup for artificially selecting microbial communities is depicted in Figure 2.1 (see Section 2.2.3 for more details). The growth of biofilms is notoriously difficult to measure (Hall-Stoodley et al., 2004) and we were therefore unable to normalise chitinase activity measurements to biomass. Attempts were made to normalise to protein content measurements (Figure 2.2), however, the standard curve was not consistent for measurements taken in seawater and no consensus could be reached for different dilutions of the same samples. The presence of chitin particles interferes with any absorbance-based method (as also noted by Datta et al., 2016) and accurate methods for the quantification of biofilms generally requires microscopy (Azeredo et al., 2017; Larimer et al., 2016), thereby making it difficult to carry out in a high throughput manner, as would have been necessary for the work presented in this chapter. Extracted DNA concentration is therefore shown along with absolute chitinase activity measurements. See Mandakhalikar et al. (2017) for a summary of current methods for biofilm quantification and Azeredo et al. (2017) for a detailed and critical overview.

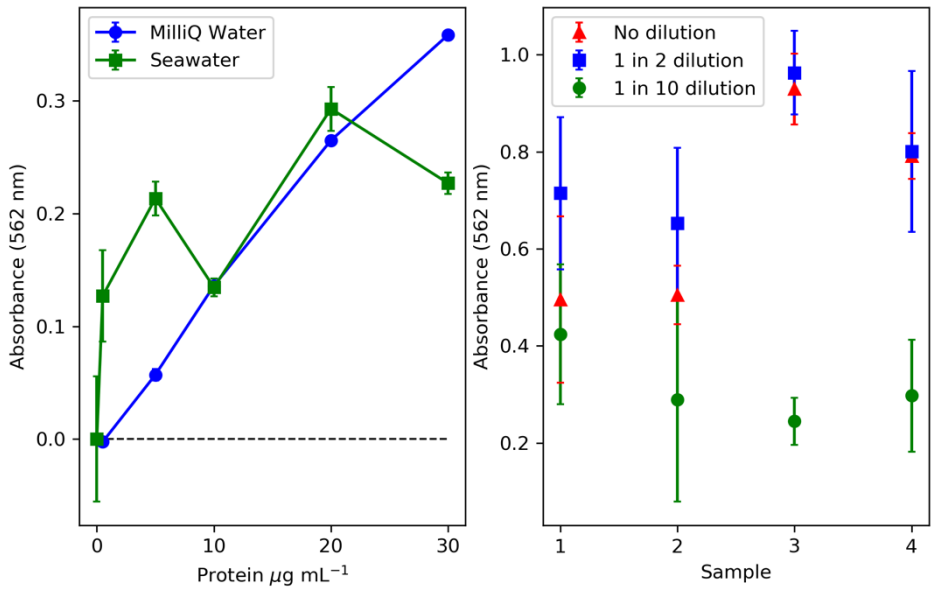

Figure 2.2. Protein content measurements using the BCA QuantiPro Assay Kit. Showing results for a standard curve using either autoclaved seawater (green) or MilliQ water (blue), where each point represents a mean of technical duplicates with standard deviation (left) and four samples at three dilutions each, where each point represents a mean of technical triplicates with standard deviation (right). Standards were prepared using the Protein Standard Solution supplied with the BCA QuantiPro Assay Kit and samples used were taken at random from transfer 14 of the first artificial selection experiment.

2.3.1 First artificial selection experiment; process optimisation

Our first artificial selection experiment highlighted the need to carry out each transfer when the desired trait (*i.e.* chitinase activity) was at its peak and not at a pre-defined incubation time, as done previously (Blouin et al., 2015; Swenson et al., 2000b, 2000a). Initially, a standardised nine-day incubation time between transfers was set, because this was the time it took for chitinase activity to peak in a preliminary enrichment experiment (data not shown). After 14 transfers a strong increase in chitinase activity was not observed (Figure 2.3A for chitinase activity in the positive selection normalised to that in the randomly selected control and Figure 2.4 for absolute chitinase activities alongside DNA concentrations) and, intriguingly, in nine out of the 14 transfers a lower activity was observed in the positive selection than in the randomly selected control (Figure 2.3), suggesting that a random selection of microcosms is more effective in enhancing chitinase activity than actively selecting for the best communities. To further investigate the reasons behind this low efficiency, regular enzymatic activity measurements were taken in the incubation period between transfers 14 and 15 (Figure 2.3). It was found that chitinase activity was peaking much earlier within the incubation, *i.e.* at day four and by the end of the nine days the chitinase activity had dropped below the activities registered for the random selection experiment (Figure 2.3B). Attending to this result, after transfer 15 an additional experiment was set up and run in parallel, where the incubation time between transfers was shortened to four days. Shortening the incubation time led to a selection of higher chitinase activities at transfers 16 and 17, but the progressive increase in activity had stalled by transfers 18 and 19 (Figure 2.3A). Chitinase activity was again measured every day within the incubation period before the final transfer, 20 and it was found that the enzymatic activity was almost nine times higher on day two than day four (Figure 2.3C), indicating that the optimal incubation time had again been reduced. Interestingly, using DNA as a proxy for biomass (see Figure 2.3C for more details), low concentrations were observed on day two *i.e.* when chitinase activity was at its peak, indicating a very high enzymatic activity amongst the existing microbial population (Figure 2.3C). Although the chitinase activity was still high on day three, there was also a considerable increase in biomass, suggesting a relatively less active chitinolytic community at this time point. Both chitinase activity and biomass had dropped at day four, presumably as a consequence of grazing (as discussed below).

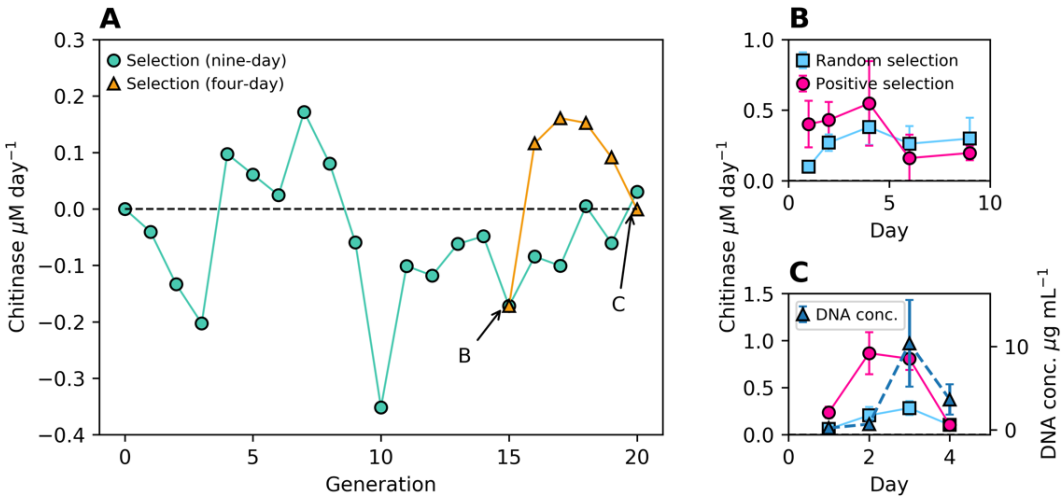

Figure 2.3. Chitinase activity in artificial selection experiment 1. **(A)** Enzymatic activity measured over 20 generations. Each point represents the mean of the positive selection communities (*n*=30) to which the mean of the randomly selected controls (*n*=30) was subtracted. The black dotted line (zero) represents where chitinase activity of the positive selection is equal to that of the random selection. **(B)** Chitinase activity measured within the incubation period of generation 15 of the nine-day incubation. **(C)** Chitinase activity and DNA concentration of the positive selection measured within the incubation period of generation 20 of the four-day incubation. Each point in panels B and C represents absolute chitinase activity measured in the positive (red) and random selection (blue). Arrows in panel A indicate the generations in which the regular monitoring of chitinase activity was performed, *i.e.* shown in panels B and C. Figure 2.4 shows absolute chitinase activities for the positive and random selections alongside the concentration of extracted DNA for the three communities that were used to inoculate the next generation.

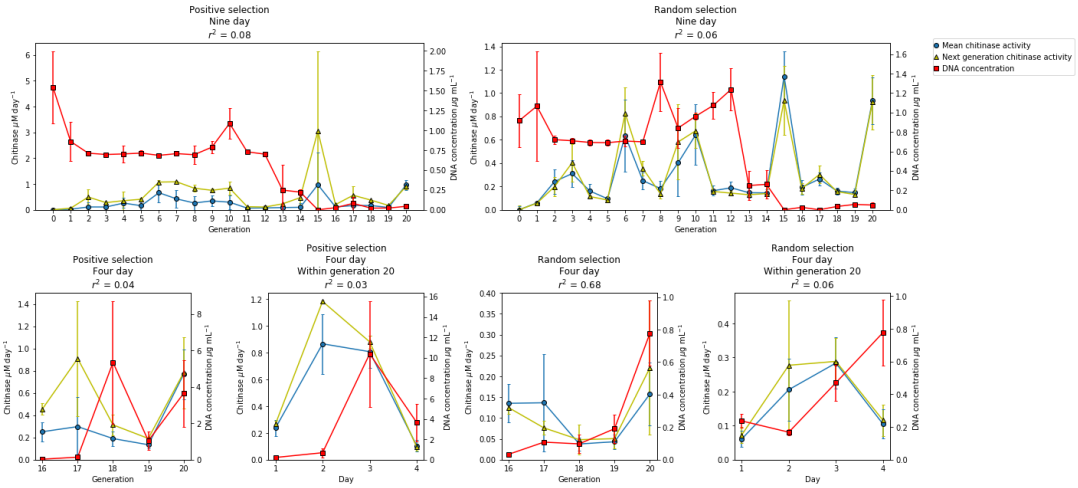

Figure 2.4. Averaged absolute chitinase activity and extracted DNA concentrations in Experiment 1. Chitinase activity measured from all communities (*n*=30; blue lines with circular markers) within each generation and from the three selected communities used to inoculate the following generation (yellow lines with triangular markers) during artificial selection experiment 1. Red lines with square markers show DNA concentrations for the three communities used to inoculate the next generation and used for 16S rRNA gene amplicon sequencing. Error bars show standard deviations. Note that scales differ between all axis. r^2 values indicate Pearson's correlation coefficients between chitinase activity (next generation) and DNA concentration.

While the nine-day incubation experiment gave an overall negative trend, shortening the incubation times to the chitinase maxima drastically increased the benefits of artificial community selection, *i.e.* initially to four days (generation 15; Figure 2.3B) and later to two days (generation 20; Figure 2.3C). This suggests that the selection of an efficient chitin degrading community shortens the time required to reach maximum chitinase activity, but also to enter decay due to community succession.

2.3.2 Microbial community succession

MiSeq amplicon sequencing was carried out on the 16S and 18S rRNA genes to characterise the microbial community succession that occurred within the first selection experiment and, by this way, gain insight into the strong variability in chitinase activity observed over time. The communities that were used as the inoculum for each of the 20 transfers, both nine and four-day long experiments, as well as the community obtained from the daily monitoring of the incubation period for transfer 20 were sequenced. This data was processed using both Mothur (Schloss et al., 2009) and DADA2 workflows (Callahan et al., 2016; Callahan et al., 2016), obtaining similar results (Figure 2.5 and Figure 2.6). DADA2 results are presented here as this workflow retains greater sequence information, better identifies sequencing errors and gives higher taxonomic resolution (Hugerth and Andersson, 2017). Unique taxa are therefore amplicon sequence variants (ASVs) rather than operational taxonomic units (OTUs).

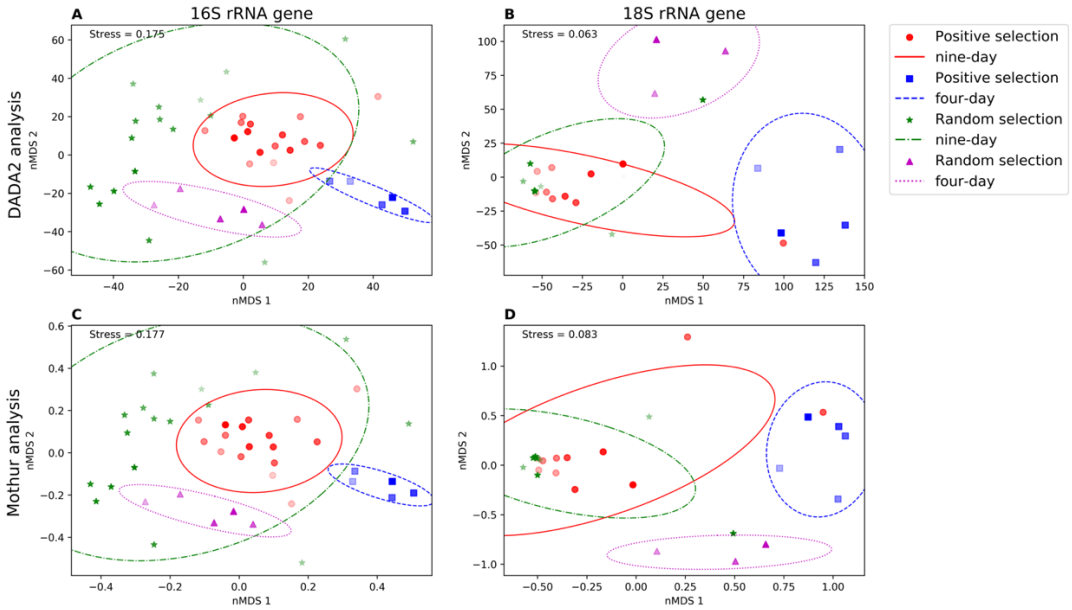

Figure 2.5. Comparison of the microbial community variation over the entre artificial evolution experiment as shown by the DADA2 and Mothur analysis pipelines. DADA2 and Mothur analyses are show in the top and bottom plots, respectively. nMDS plots showing Bray-Curtis distance of the 16S rRNA gene and 18S rRNA gene communities for the DADA2 (panels **A** and **B**) and Mothur (panels **C** and **D**) analyses. Distance between the community composition obtained from nine-day (red circles) and four-day incubations (blue squares) of the positive selection and nine-day (green stars) and four-day incubations (purple triangles) of the random controls are shown. Marker colour intensity correlates to generation number, where progressive darker colours represent later generations. Each point represents the mean of the three communities selected from one generation used to inoculate the following one. Ellipses show the mean plus the standard deviation of each group of samples.

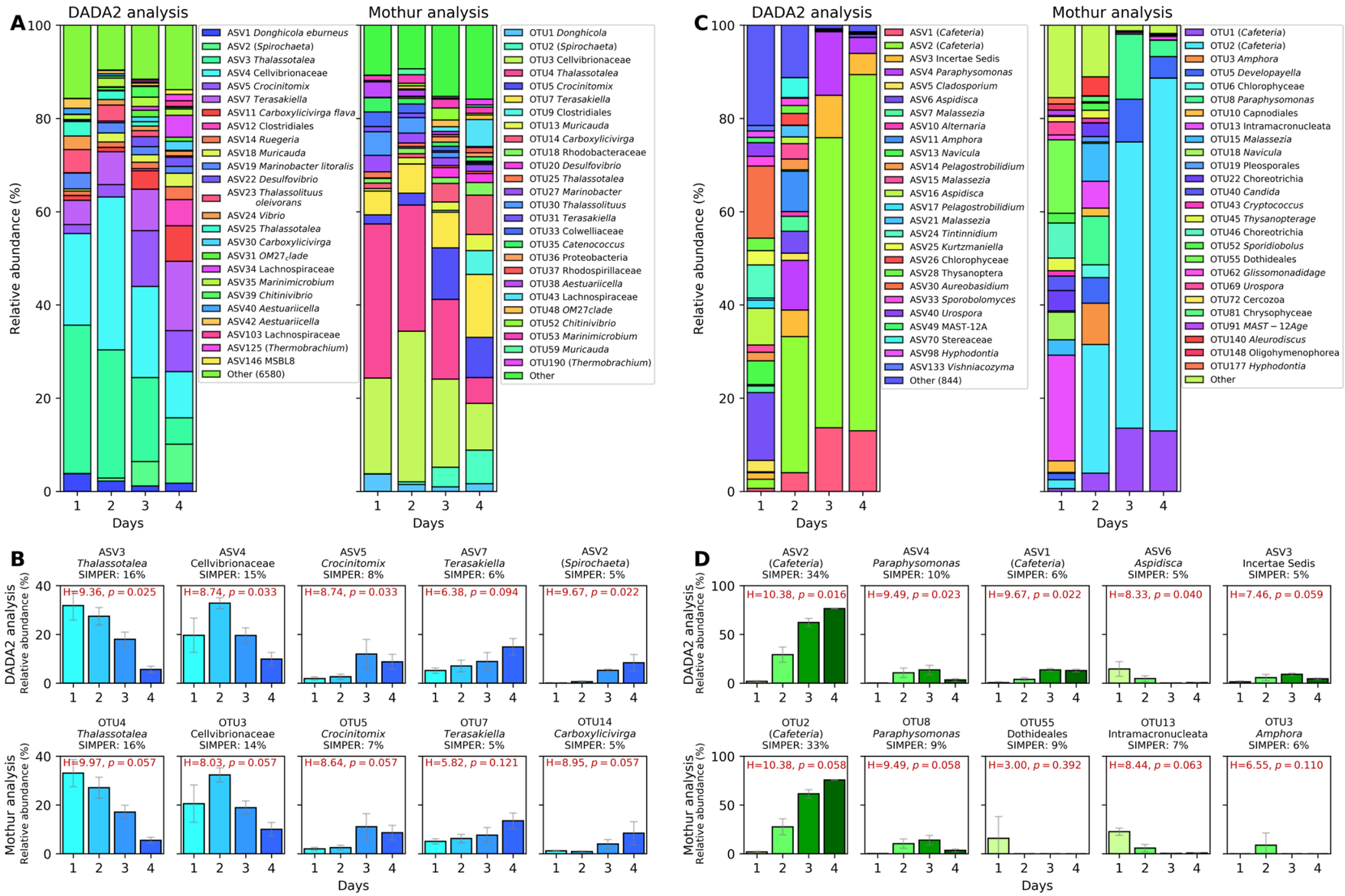

Figure 2.6. Comparison of the DADA2 and Mothur analyses for the 16S and 18S rRNA genes over the four-day incubation period within generation 20. 16S and 18S rRNA gene analyses are shown in **A** and **B** and **C** and **D**, respectively. (**A** and **C**) Community relative abundance over the four-day incubation period. Only ASVs with abundance above 1% in at least one time point are shown. The abundance for each ASV/OTU is a mean value of three communities used to inoculate the next generation. ASVs/OTUs were classified to genus level by SILVA. Names in brackets were not identifiable with the standard analysis pipeline and were identified through a BLAST search of the NCBI database. (**B** and **D**) Five ASVs/OTUs that contributed the most to the community variations over time according to a SIMPER analysis. The percentage of variation to which each ASV/OTU contributes is indicated. Error bars represent the standard deviations of three communities used to inoculate the next generation. The results obtained were very similar for both analyses, although there were fewer ASVs detected in the DADA2 analysis (6,605 16S and 870 18S) than there were OTUs in the Mothur analysis (76,395 16S and 21,159 18S).

2.3.3 Community succession over the four-day incubation period within transfer 20

The daily microbial community analysis over the four days at transfer 20 showed a progressive increase in prokaryotic diversity (from 0.83 to 0.93, according to Simpsons index of diversity) whereas a strong decrease in diversity was observed amongst the eukaryotic community (from 0.93 to 0.38; Figure 2.7A). SIMPER analyses were carried out to identify those 16S and 18S rRNA gene ASVs that were contributing most to the differences over the four successive days, observed in Figure 2.7B. The top five ASVs in these analyses were responsible for 50% and 60% of temporal variation for the 16S and 18S rRNA genes, respectively (Figure 2.7C).

For the 16S rRNA gene, the most important ASVs were: ASV3 (*Thalassotalea*, contributing to 16% of the community variation between the four days, p=0.025), ASV4 (Cellvibrionaceae, 15% variation, p=0.033), ASV5 (*Crocinitomix*, 8% variation, p=0.033), ASV7 (*Terasakiella*, 6% variation, p=0.094) and ASV2 (*Spirochaeta*, 5% variation, p=0.022) (Figure 2.7C). ASVs 3 and 4 (both *Gammaproteobacteria*) represented over 50% of the prokaryotic community abundance on day 2, when chitinase activity was highest and their abundances followed a similar pattern to the chitinase activity over the four days (Figure 2.3C), suggesting that these ASVs may be the main drivers of chitin hydrolysis. On the other hand, ASVs 7 (*Alphaproteobacteria*) and 2 (*Spirochaeta*) both showed a progressive increase over time (*i.e.* from a combined relative abundance of 5% on day 1 to 23% on day 4; Figure 2.7C), suggesting that these ASVs could be cross-feeding organisms that benefit from the primary degradation of chitin. Interestingly, the overall 16S rRNA gene analysis also showed a strong succession over time at higher taxonomic levels (Figure 2.8). While *Gammaproteobacteria* pioneered and dominated the initial colonisation and growth, presumably *via* the degradation of chitin (*i.e.* with 73% relative abundance during the first two days), all other taxonomic groups became more abundant towards the end of the incubation period (*e.g. Clostridia*, *Bacteroidia* and *Alphaproteobacteria* increased from an initial relative abundance of 0.1, 2.8 and 12% on day one to 13.5, 22 and 21% on day four, respectively; Figure 2.8). Microbial isolates confirmed *Gammaproteobacteria* as the main contributors of chitin biodegradation (as discussed below).

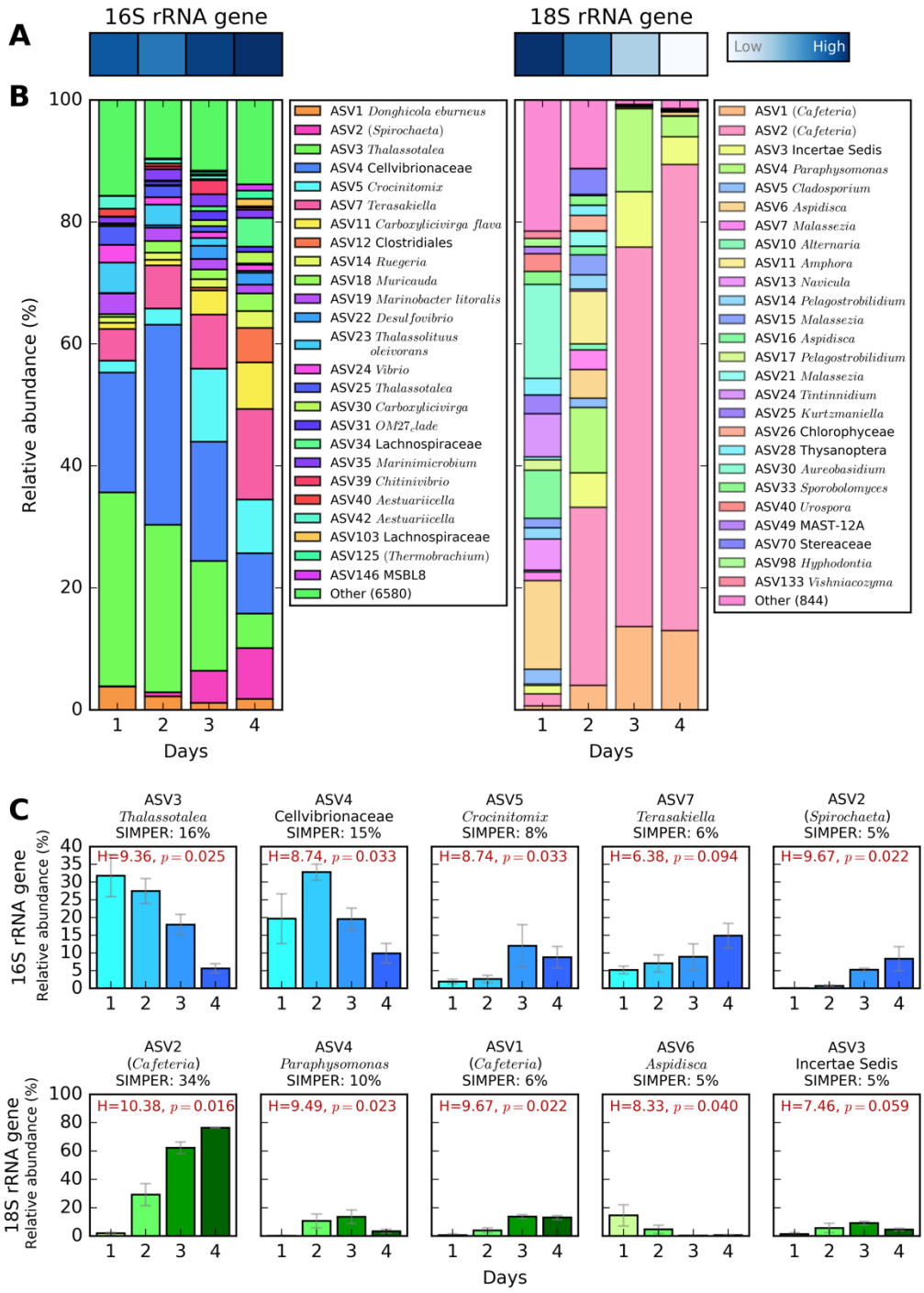

Figure 2.7. Daily microbial community analysis over the four-day incubation period within generation 20. The analysis was performed on the three communities that showed highest chitinase activity by the end of the four days and which would have been used to inoculate the next generation. **(A)** Simpsons index of diversity of the 16S (left) and 18S rRNA gene (right) amplicon analysis. Scale ranges between 0.38 (low) and 0.93 (high). **(B)** Community relative abundance over the four-day incubation period. Only ASVs with abundance above 1% in at least one time point are shown. The abundance for each ASV is a mean value from the three communities. ASVs were classified to genus level using the SILVA database (v132). Names in brackets were not identifiable with the standard analysis pipeline and were identified through a BLAST search of the NCBI database. **(C)** Five 16S and 18S rRNA gene ASVs that contributed the most to the community variations over time according to a SIMPER analysis. The percentage of variation to which each ASV contributes is indicated. Error bars represent the standard deviations of the three communities used to inoculate the next generation.

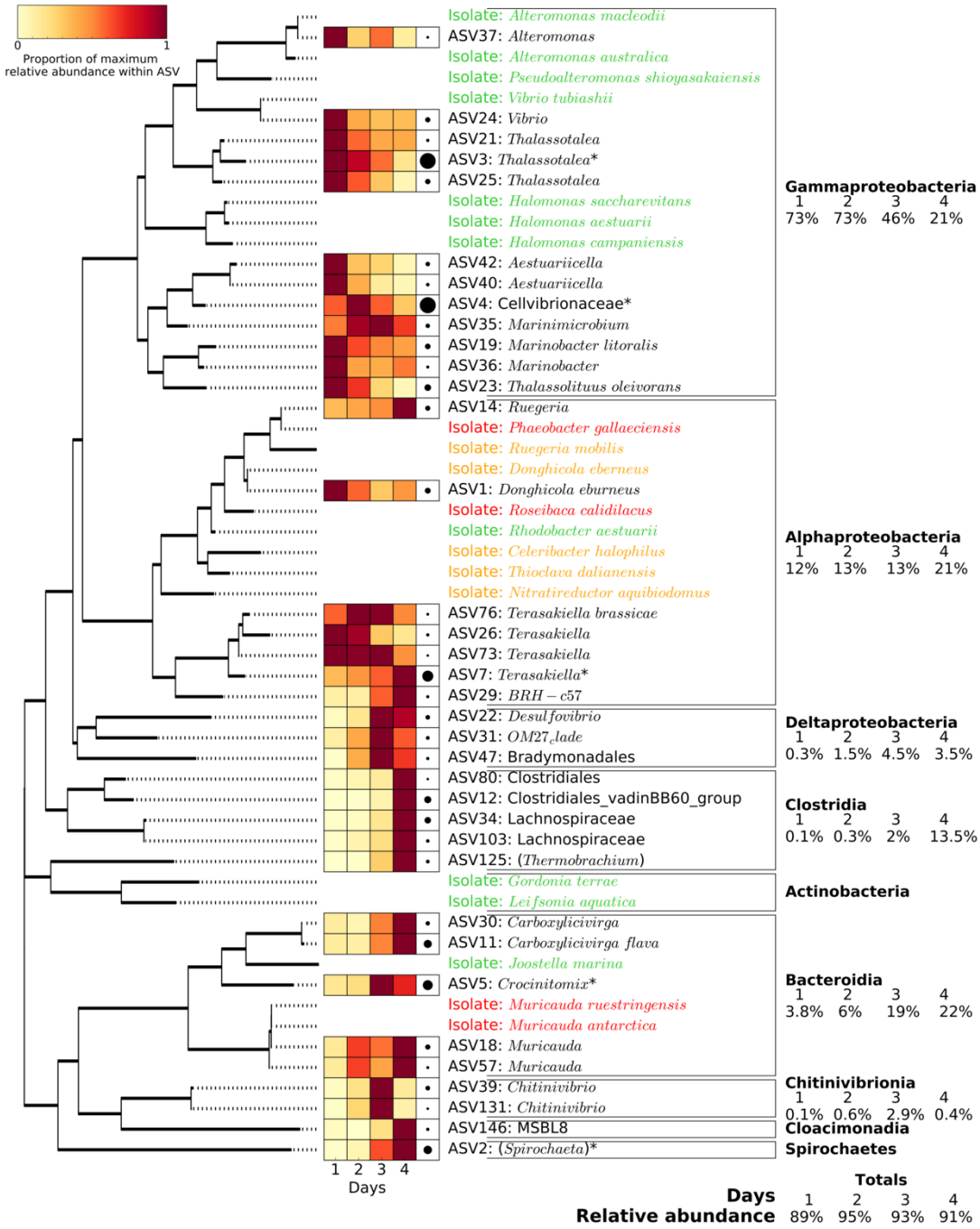

Figure 2.8. Phylogenetic analysis and relative abundance of the major 16S rRNA gene ASVs and bacterial isolates obtained at the end of the artificial selection experiment. The major 16S rRNA gene ASVs are defined as those with relative abundance above 0.5% in at least one of the four days (Figure 2.7 shows only those ASVs that were above 1% relative abundance). Phylogenetic grouping is represented by a mid-point rooted maximum likelihood phylogenetic tree. The 36 ASVs represented in the figure (out of the 6605 total ASVs detected) accounted for 92% of all 16S rRNA gene relative abundance. The heatmap represents the relative abundance of each ASV over the four days, with darker red showing the day at which the ASV showed maximum abundance. Black circles on the right of the heatmap represent the maximum relative abundance for that ASV amongst the entire community. The 20 isolates are coloured depending on their ability to grow on chitin and the monomer, GlcNAc (green), the GlcNAc only (orange), or neither (red).

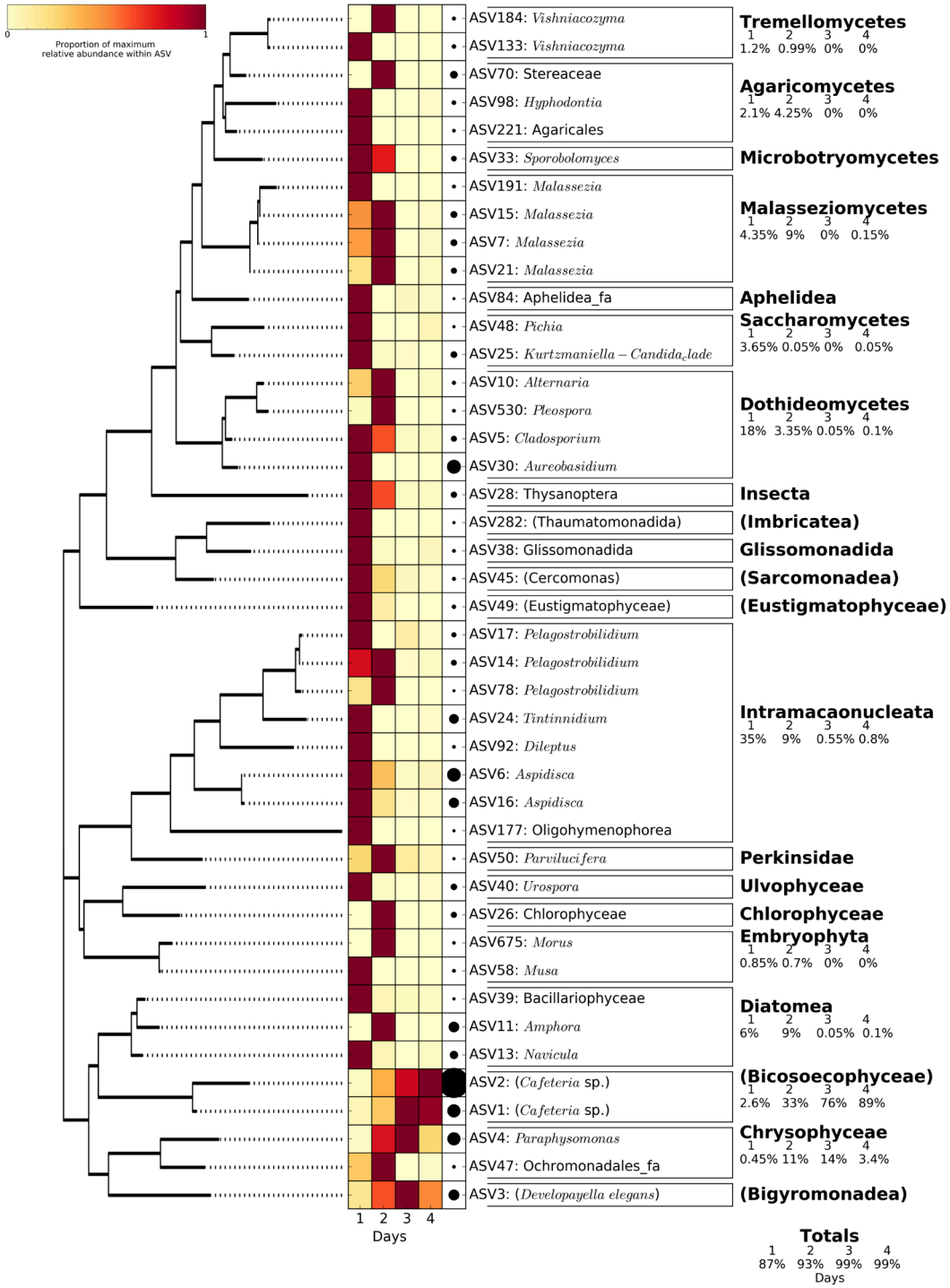

Figure 2.9. Phylogenetic analysis and relative abundance of the major 18S rRNA gene ASVs. The major 18S rRNA gene ASVs are defined as those with relative abundance above 0.5% in at least one of the four days (Figure 2.7 shows only those ASVs that were above 1% relative abundance). Phylogenetic grouping is represented by a mid-point rooted maximum likelihood phylogenetic tree. The 43 ASVs represented in the figure (out of the 870 total ASVs detected) accounted for 95% of all 18S rRNA gene relative abundance. The heatmap represents the relative abundance of each ASV over the four days, being the darker red the day at which the ASV showed maximum abundance. Black circles on the right of the heatmap represents the maximum relative abundance for that ASV amongst the entire community.

The SIMPER analysis of the 18S rRNA gene highlighted ASV2 (*Cafeteria* sp., contributing to 34% of the community variation between the four days, *p*=0.016), ASV4 (*Paraphysomonas*, 10% variation, p=0.023), ASV1 (*Cafeteria* sp., 6% variation, *p*=0.392), ASV6 (*Apsidica*, 5% variation, *p*=0.040) and ASV3 (Incertae Sedis, 5% variation, *p*=0.059) as the five main ASVs contributing to 60% of the community variation over the four days (Figure 2.7C). ASV2, which was 96% similar to the bactivorous marine flagellate *Cafeteria* sp., was by far the most striking Eukaryotic organism, showing an increase in relative abundance from 2% on day 1 up to over 76% on day 4 (Figure 2.7B and C). As observed in prokaryotes, Eukaryotic phylogenetic groups also showed a large variation between the beginning and the end of the incubation period, mainly due to the increase of *Bicosoecophyceae* over time (*i.e.* from 2.6 to 89% relative abundance, driven by both ASV1 and ASV2; Figure 2.9).

2.3.4 Community succession over the entire artificial selection experiment

The 16S and 18S rRNA gene community composition (Figure 2.10 and Figure 2.11) at each transfer was analysed in order to determine the effect that positive or random selection of communities had across the 20 transfers, both for the nine-day incubation experiment (*i.e.* transfers 0 to 20) and shortened four-day incubation experiment (*i.e.* transfers 16 to 20). Most interestingly, the overall community variability across all transfers (16S and 18S rRNA gene nMDS analysis; Figure 2.10A) showed that only the positive selection of the shortened four-day incubations differentiated the community from the random selection, which was confirmed by a PerMANOVA test using Bray-Curtis distance (16S rRNA gene *p*=0.001; 18S rRNA gene *p*=0.002; Table 2.4), while the nine-day selection mostly clustered with the random control communities. This is a clear explanation as to why the nine-day incubation time was not allowing a progressive selection of a community with better chitinase activities than those obtained randomly and, only when the time was shortened, was an effect of the positive selection over the random selection observed.

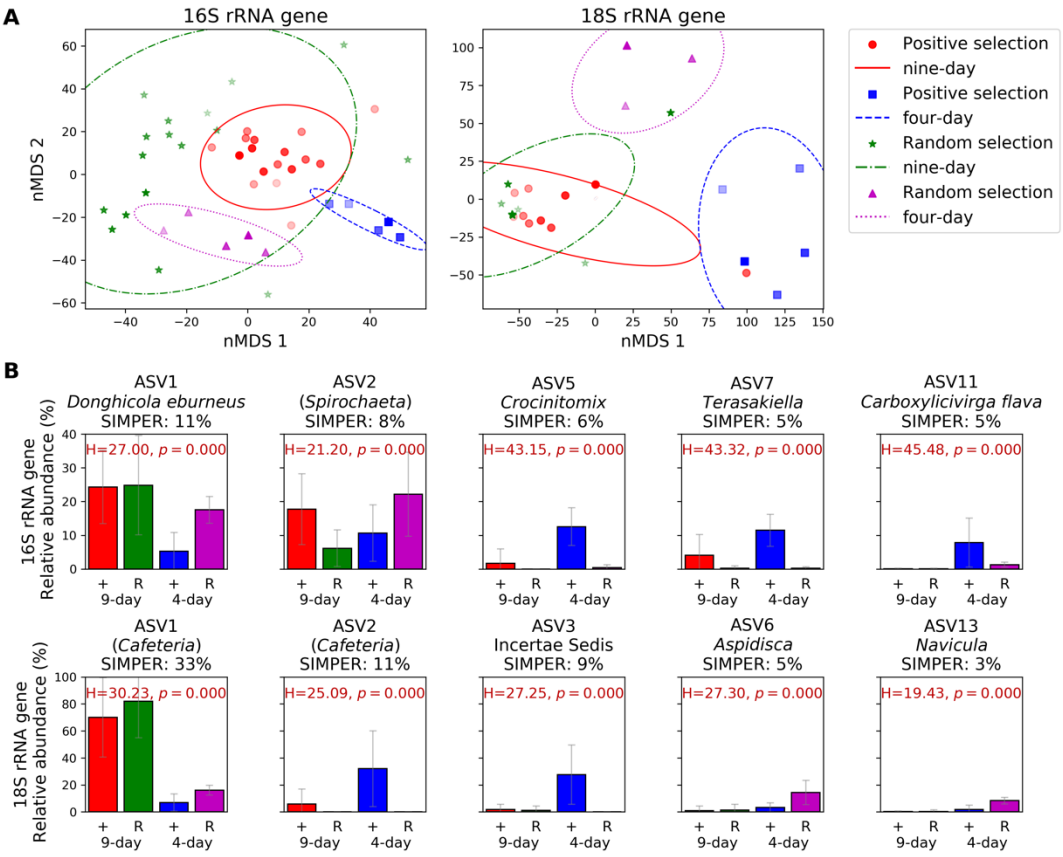

Figure 2.10. Microbial community variation over the entre artificial selection experiment. **(A)** nMDS plot showing Bray-Curtis distance of 16S (left) and 18S rRNA gene communities (right). Distance between the community composition obtained from nine-day (red circles) and four-day incubations (blue squares) of the positive selection and nine-day (green stars) and four-day incubations (purple triangles) of the random controls are shown. Marker colour intensity correlates to generation number, where progressive darker colours represent later generations. Each point represents the mean of the three communities selected from one generation used to inoculate the following one, for the positive selection. Random communities were pooled before sequencing. Ellipses show the mean plus the standard deviation of each group of samples. Stress values are 0.175 for the 16S rRNA gene and 0.063 for the 18S rRNA gene. **(B)** Five 16S (top panel) and 18S rRNA gene ASVs (bottom panel) that contributed the most towards community variations between the nine-day (generations 0-20) and four-day (generations 16-20) positive (+) and random I selections according to SIMPER analyses. The percentage of variation to which each ASV contributes is indicated. ASVs were classified to the species level with the standard analysis pipeline using the SILVA database (v132) where possible. Names in brackets were not identifiable and were identified through a BLAST search of the NCBI database. Relative abundances and error bars shown are the mean and standard deviations of all generations within that treatment.

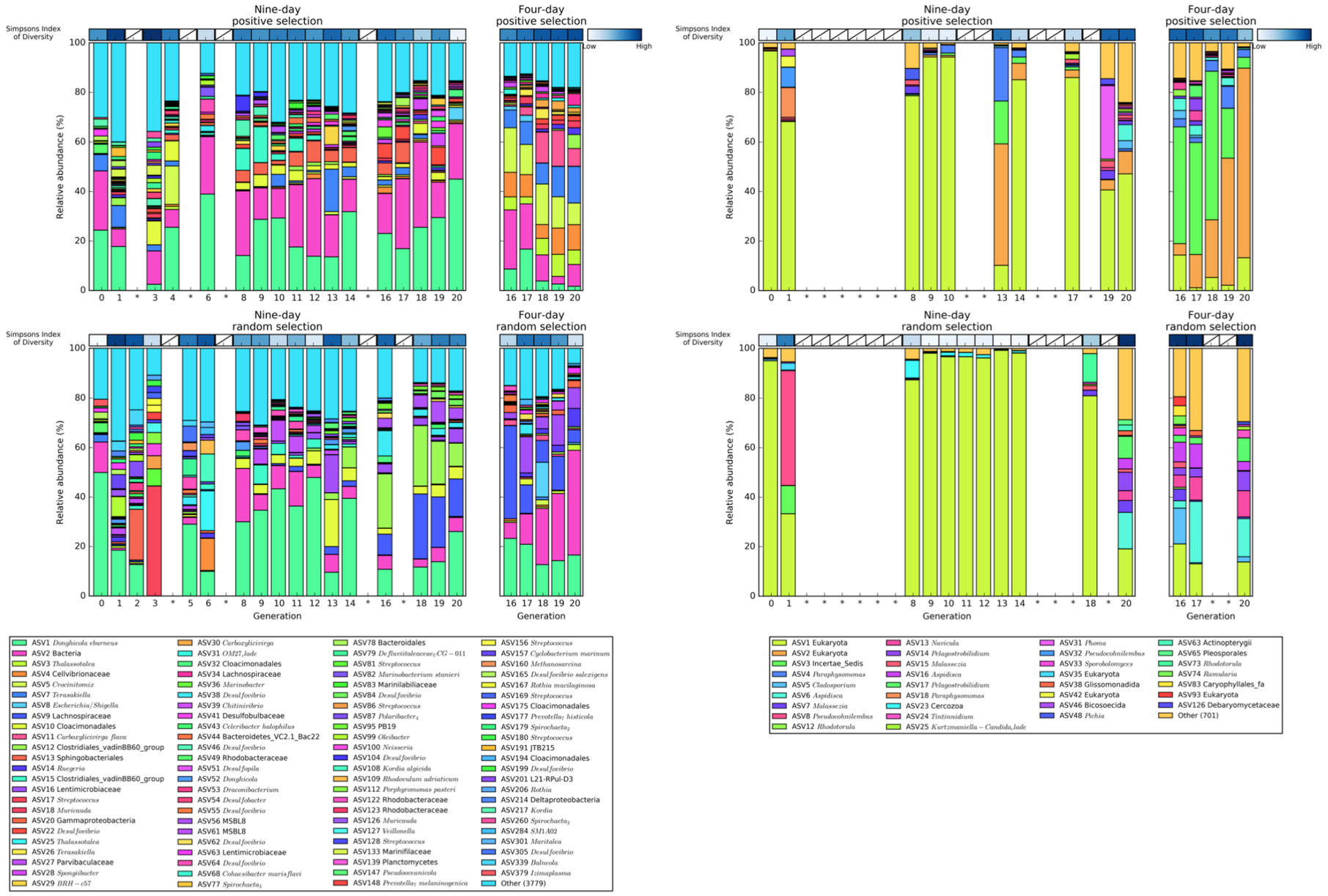

Figure 2.11. 16S and 18S rRNA gene community analysis of each generation within the first selection experiment. 16S (left) and 18S (right) rRNA gene community analysis of each generation within the artificial evolution experiment, both positive (top panel) and random selection (bottom panel). Simpsons index of diversity is represented above each panel, ranging between 0.73 (low diversity, white) to 0.96 (high diversity, dark blue) for the 16S rRNA gene and 0.015 (low diversity, white) to 0.92 (high diversity, dark blue) for the 18S rRNA gene. The stacked bar charts represent the relative abundance of those ASVs with abundances above 2% in at least one sample. All low abundance ASVs (3,779 and 701 ASVs for the 16S and 18S rRNA genes, respectively) are grouped into the category 'Other'. Each bar chart is the mean value of the three communities that were pooled together for inoculating the following generation. Asterisks indicate those generations where the number of reads were too low (*i.e.* below 1,000) and these samples were removed.

Table 2.4. Values for PerMDISP, PerMANOVA and ANOSIM statistical tests between the positive and random selections for both nine- and four-day incubation times of the chitin artificial selection experiment.

Comparison		PerMDISP		PerMANOVA		ANOSIM	
		F	*p*	Pseudo-F	*p*	R	*p*
Positive vs random (four-day)	16S	0.0105	**0.909**	16.7	**0.001**	0.960	**0.001**
	18S	1.006	**0.321**	4.91	**0.002**	0.638	**0.006**
Positive vs random (nine-day)	16S	4.004	0.043	(6.69)*	(0.001)*	(0.430)*	(0.001)*
	18S	1.000	**0.355**	1.204	0.232	-0.023	0.532
Samples vs controls (all)[1]	16S	0.161	**0.797**	0.905	**0.002**	4.883	**0.001**
	18S	0.0001	**0.991**	0.732	**0.001**	5.338	**0.002**

*Tests were not statistically valid due to significant PerMDISP result.
[1] Controls include chitin only and negative DNA extraction controls as well as negative PCR controls.
Bold and shaded values indicate significant test results.

SIMPER analyses were carried out to determine the ASVs that most strongly contributed to the differences between groups (*i.e.* positive *versus* random selections and nine-day *versus* four-day incubation times; Figure 2.10B). For the 16S rRNA gene, the top five ASVs identified by the SIMPER analysis contributed to 35% of the community variation, while for the 18S rRNA gene, they accounted for 61% (Figure 2.10B). The 16S rRNA gene ASVs 5, 7 and 11 (*Crocinitomix*, *Terasakiella* and *Carboxylicivirga flava*, respectively) presented a much higher abundance in the four-day positive selection than in any other selection (13%, 11% and 8%, respectively), suggesting that these species were the major contributors to the differentiation of these communities, as seen in Figure 2.10A. As observed above for the four-day incubation analysis, *Cafeteria* sp. (18S rRNA gene ASV1 and ASV2, both 96% similar) were again the most conspicuous Eukaryotic organisms. ASV2 was more abundant in the positive four-day selection (32% of the relative abundance), while ASV1 was highest in the three other selections (70% and 82% in the positive and random nine-day selection, respectively and 16% in the random four-day selection; Figure 2.10B).

2.3.5 Chitinase gene copies in artificially assembled metagenome

Artificially-assembled metagenomes, generated by PICRUSt (Langille et al., 2013) from the 16S rRNA gene amplicon sequences, were used to search for enzymes involved in chitin degradation: KEGG orthologs K01183 for chitinase, K01207 and K12373 for chitobiosidase, K01452 for chitin deacetylase and K00884, K01443, K18676 and K02564 for the conversion of GlcNAc to fructose-6-phosphate (Figure 2.12 and Table 2.3) (Kanehisa et al., 2017, 2016a; Kanehisa and Goto, 2000). As expected from the measured chitinase activities, the shortened four-day incubation experiment showed over 30 times more chitinase (K01183) gene copies than the nine-day incubation experiment (*i.e.* an average of 0.66 copies per bacterium were

observed in the four-day incubation experiment while only 0.025 copies per bacterium were observed over the same transfers in the nine-day experiment). Also, from the daily analysis of transfer 20, the chitinase activity was positively correlated with the normalised chitinase gene copy number (r^2=0.57), with a peak in chitinase activity *and* chitinase gene copies on day 2 (*i.e.* over one chitinase gene copy per bacterium). The most striking result from this analysis was the strong bias of taxonomic groups that contributed to the chitinase and chitin deacetylase genes; chitinase genes were mainly detected in *Gammaproteobacteria* and some *Bacteroidia*, whereas the chitin deacetylase genes were almost exclusively present in *Alphaproteobacteria*. It is worth highlighting that the chitosanase gene (K01233), the enzyme required to hydrolyse the product from chitin deacetylation, chitosan, was not detected in any of the artificial metagenomes. Chitobiosidases (K01207 and K12373) and enzymes involved in the conversion of GlcNAc to Fructose-6-phosphate (K00884, K01443, K18676 and K02564) were more widespread. Nevertheless, this data needs to be taken with caution as these were not real metagenomes.

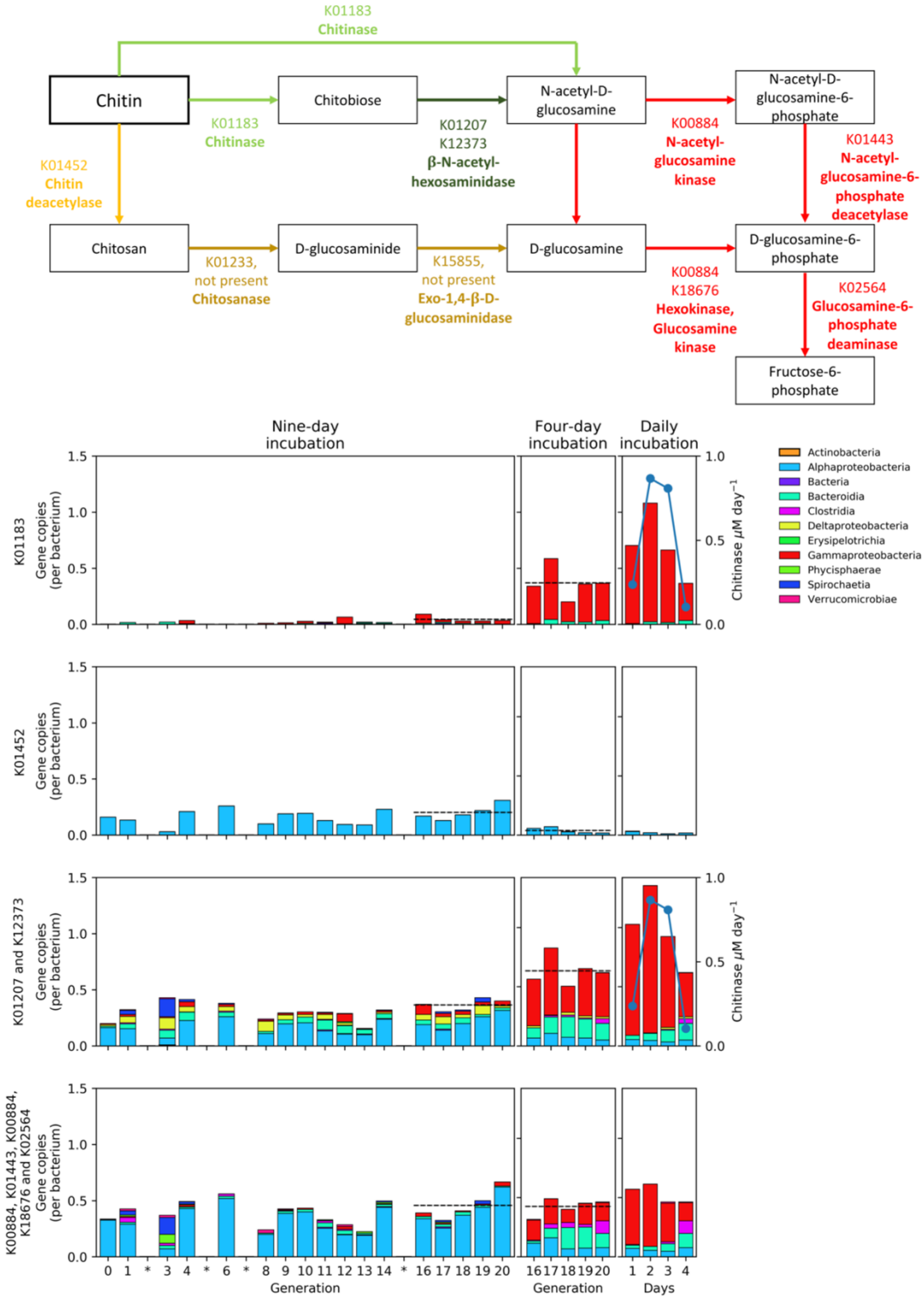

Figure 2.12. Chitin degradation pathway and the enzymes involved that were present in the PICRUSt artificial metagenome analysis. Adapted from KEGG pathway KO00520 for amino sugar and nucleotide sugar metabolism, showing KEGG orthologs that were searched for in the PICRUSt artificial metagenome (top). Transportation into the cell, or periplasm, likely occurs after the action of the action of chitinases or chitosanases (*i.e.* on the oligomers chitobiose and D-glucosaminide or monomers N-acetyl-D-glucosamine or D-glucosamine) (Bassler et al., 1991). The PICRUSt analysis includes almost 35% of all ASVs, accounting for a mean relative abundance of 53%, 68% and 81% for the nine-day, four-day and daily analyses, respectively. Only the positive selection of generations 0-20 of the nine-day incubation analysis and generations 16-20 from the shortened

four-day incubations are shown. The daily analysis within generation 20 of the four-day incubation is also shown. The blue points are for chitinase activity during the daily analysis of generation 20 and are shown in the panels where the KEGG orthologs would be able to produce a chitinase activity signal using the enzyme assay. Dashed black lines show means of gene copy numbers in generations 16-20. Copies of KEGG orthologs were predicted separately for each taxonomic class. Generations with asterisks indicated sample that were removed due to the low number of reads.

2.3.6 Isolation and identification of chitin degraders

Bacterial isolates were obtained from the end of the artificial selection experiments to confirm the ability of the identified groups to degrade chitin. From the 50 isolates obtained, 20 were unique according to their 16S rRNA gene sequences. From these, 18 showed at least 98% similarity with one or more of the MiSeq ASVs (Table 2.5) although, unfortunately, none belonged to the most abundant ASVs detected during the community analysis. The ability for chitin and GlcNAc degradation by each one of the isolates was assessed. It was found that 16 of these isolates could grow using GlcNAc as the sole carbon source, but only 11 of these strains could grow on chitin (Figure 2.8). The four remaining bacteria from the 20 isolated could not grow using chitin or GlcNAc. Most interestingly, all isolates from the class *Gammaproteobacteria* (*n*=7) were capable of chitin degradation whereas only a smaller subset of isolates had this phenotype in other abundant taxonomic groups, such as *Bacteroidia* (1 out of 3) or *Alphaproteobacteria* (1 out of 8; Figure 2.8).

Table 2.5. Information on isolates obtained from generation 20 of the positive selections.

Species match (%)[1]	ASV most similar to[2]	Chitin/GlcNAc growth[3]	Other information
Joostella marina (100%)	ASV1137 (90%)	C+ G+	N-acetylglucosamine not utilised as sole carbon source, chitin not tested (Quan et al., 2008)
Muricauda antarctica (97%)	ASV57 (99%)		Positive for N-acetyl-β-glucosaminidase, chitin not tested (Wu et al., 2013)
Muricauda ruestringensis (96%)	ASV18 (100%)		No report of GlcNAc or chitin testing (Bruns et al., 2001)
Gordonia terrae (99%)	ASV3386 (99%)	C+ G+	No report of GlcNAc or chitin testing. Genus is metabolically diverse (Arenskötter et al., 2004)
Leifsonia aquatica (99%)	ASV3205 (99%)	C+ G+	No report of GlcNAc or chitin testing (Evtushenko et al., 2000)
Phaeobacter gallaeciensis (100%)	ASV14 (100%)		No report of GlcNAc or chitin testing (Martens et al., 2006)
Ruegeria mobilis (99%)	ASV88 (100%)	G+	Not able to degrade chitin, GlcNAc not tested (Muramatsu et al., 2007)

Species match (%)[1]	ASV most similar to[2]	Chitin/GlcNAc growth[3]	Other information
Donghicola eberneus (99%)	ASV1 (99%)	G+	Negative for N-acetyl-β-glucosaminidase, chitin not tested (Sung et al., 2015)
Roseibaca calidilacus (98%)	-		No available information
Rhodobacter aestuarii (98%)	ASV3991 (99%) ASV1 (98%)	C+ G+	No report of GlcNAc or chitin testing (Ramana et al., 2009)
Celeribacter halophilus (99%)	ASV43 (99%)	G+	Previously Huaishuia halophila (Wang et al., 2012). Negative for N-acetyl-β-glucosaminidase, chitin not tested (Lai et al., 2014)
Thioclava dalianensis (100%)	ASV1566 (100%) ASV0043 (95%)	G+	Positive for N-acetylglucosamine utilisation, chitin not tested (Rongqiu Zhang et al., 2013)
Nitratireductor aquibiodomus (98%)	ASV1008 (97%) ASV14 (90%)	G+	Positive for N-acetyl-β-glucosaminidase (Labbé et al., 2004)
Alteromonas macleodii (99%)	ASV37 (99%)	C+ G+	No report of GlcNAc or chitin testing (López-Pérez et al., 2012)
Alteromonas australica (97%)	ASV321 (99%) ASV37 (98%)	C+ G+	Weakly utilises N-acetylglucosamine, chitin not tested (Ivanova et al., 2013)
Pseudoalteromonas shioyasakaiensis (99%)	ASV72 (99%)	C+ G+	Produces N-acetyl-β-glucosaminidase, chitin not tested (Matsuyama et al., 2014)
Vibrio tubiashii (100%)	ASV6516 (100%) ASV24 (100%)	C+ G+	Chitin hydrolysed extracellularly, GlcNAc not tested (Hada et al., 1984)
Halomonas saccharevitans (98%)	ASV59 (100%)	C+ G+	No report of GlcNAc or chitin testing (Xu et al., 2007)
Halomonas aestuarii (97%)	-	C+ G+	Negative for N-acetyl-β-glucosaminidase, chitin not tested (Koh et al., 2018)
Halomonas campaniensis (99%)	ASV3659 (99%)	C+ G+	No report of GlcNAc or chitin testing (Romano et al., 2005)

[1] Species matches were determined using BLAST searches of the NCBI database.
[2] ASV matches were determined using a local BLAST search with a database made with all 16S sequences from the first artificial selection experiment.
[3] Purple indicates that the isolate was able to grow using both chitin (C+) and GlcNAc (G+), red that it could grow using GlcNAc only and black that it could not grow using either (-).

2.3.7 Co-cultures using isolates

It was confirmed that both a cheater (*i.e.* isolate able to grow on GlcNAc but not chitin; *Donghicola eburneus*, *Alphaproteobacteria*) and a cross-feeder (*i.e.* isolate not capable of growth with GlcNAc or chitin; *Phaeobacter gallaeciensis*, *Alphaproteobacteria*) were only able to grow with chitin in the presence of a chitin degrading isolate (*Pseudoalteromonas shioyasakaiensis*, *Gammaproteobacteria*; Figure 2.13). As expected, while no growth was

observed in the absence of the chitin degrader, both the cheater and the cross-feeder grew over two orders of magnitude more when co-cultured with the degrader (Figure 2.13).

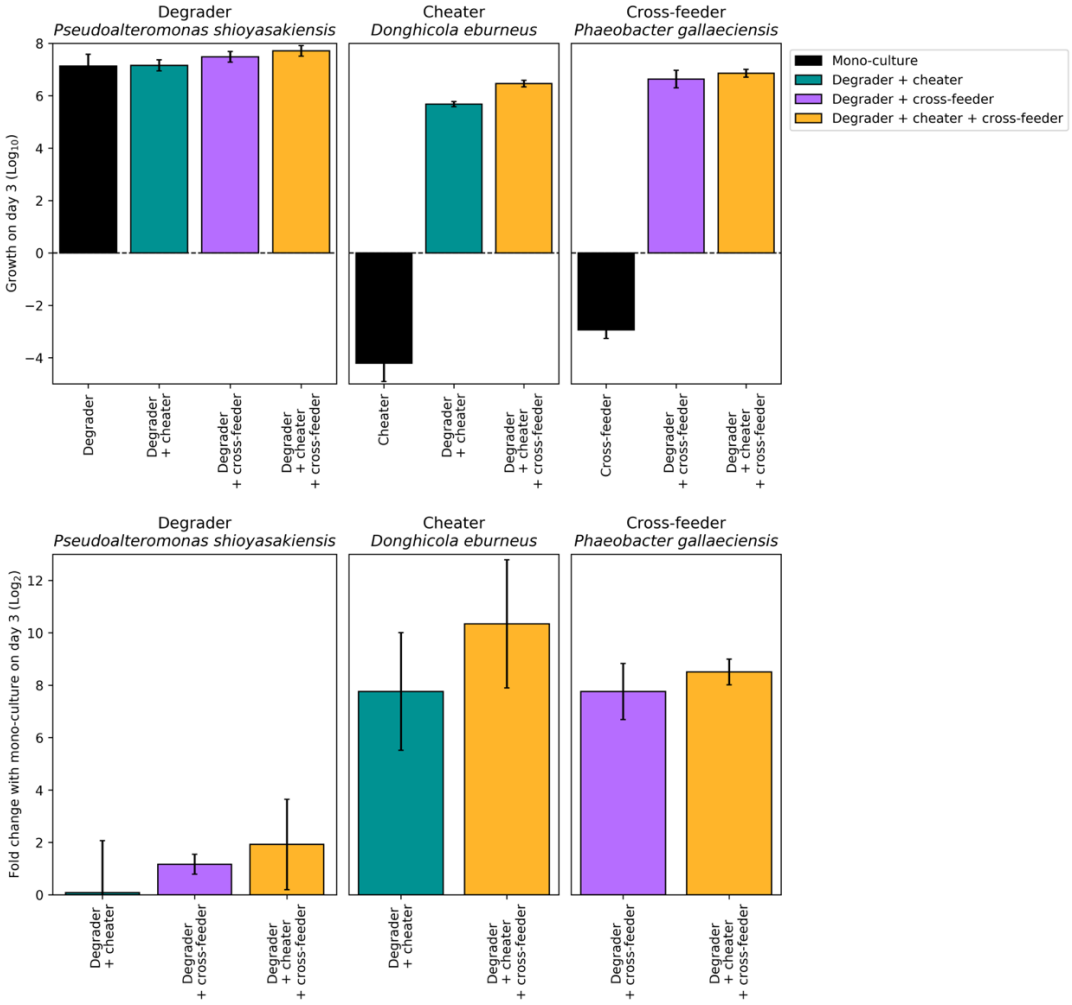

Figure 2.13. Growth of a chitin degrader, cheater and cross-feeder when grown in mono- and co-cultures with chitin as a sole carbon source. The chitin degrader (*Pseudoalteromonas shioyasakaiensis*) is capable of growth on chitin, the cheater (*Donghicola eburneus*) is capable of growth with GlcNAc but not chitin and the cross-feeder (*Phaeobacter gallaeciensis*) is not capable of growth on either chitin or GlcNAc. Growth was quantified through qPCR measurements with primers specific to each isolate. Top panels show growth on the third day of incubation (*i.e.* the difference between the measurements on day 0 and day 3) while bottom panels show $\log_2$ fold change between the mono-cultures and the different co-culture conditions for each isolate (on day 3). Points shown are means of three biological replicates and error bars show standard deviations.

2.3.8 Second artificial selection experiment; implementing an improved selection process

A second selection experiment showed an extremely rapid boost in chitinase activity, demonstrating that implementing an optimised incubation time between transfers largely enhances the selection of a desired trait. For this experiment, chitinase activity was measured daily until a peak in chitinase activity was observed. The communities with the

highest chitinase activity on this day were used to transfer to the next set of microcosms. By implementing this improved technique, chitinase activity of almost 90 µM day^{-1} was measured in only 7 transfers (Figure 2.14 and Figure 2.15), when the maximum activity achieved in the first experiment was just 0.9 µM day^{-1} (Figure 2.3C). While the different culture conditions between both experiments may have exacerbated the differences (*i.e.* the first artificial selection was carried out in 22 mL vials, with intermittent shaking and incubated at 23˚C and the second artificial selection was carried out in 2 mL 96-well plates, with constant shaking and incubated at 30˚C), the fact that the randomly selected control from the second artificial selection experiment reached similar chitinase activity levels to those observed in the first experiment (*i.e.* ~0.08 µM day^{-1}; Figure 2.15) suggests the culture conditions were not the underlying reason behind the strong increase in chitinase activity observed during the second experiment where the conditions were optimised.

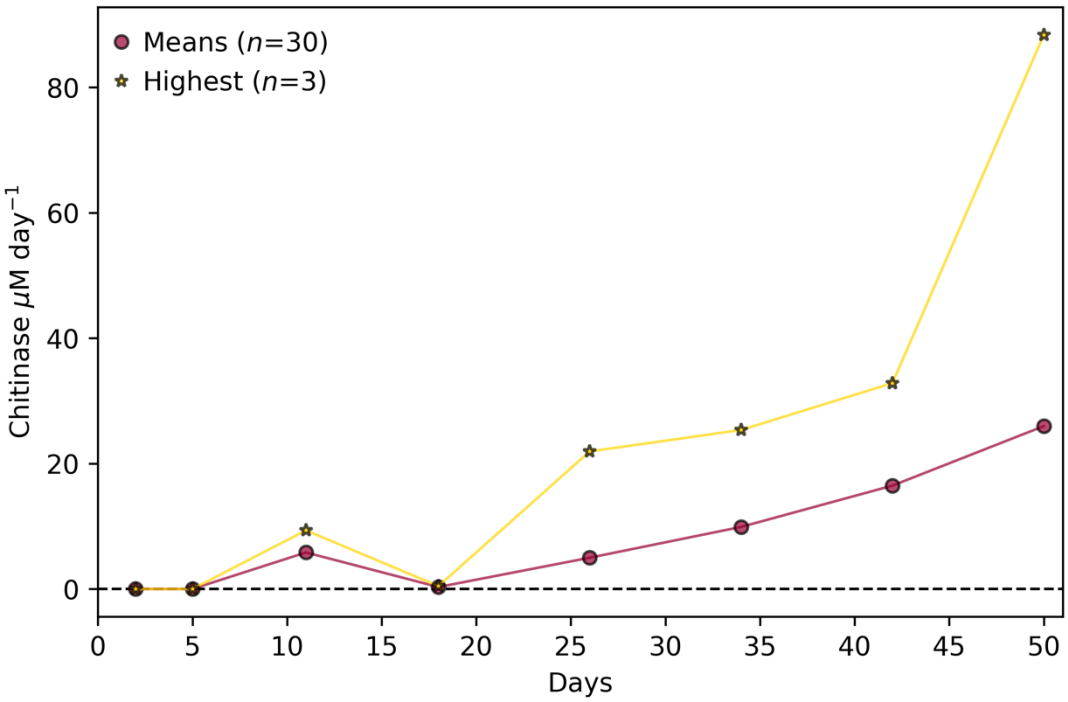

Figure 2.14. Chitinase activity of artificial selection experiment 2. Graph shows the mean chitinase activity of the positive selection, from which the mean of the random selection was subtracted. The means of all communities within the generation (*n*=30; red) and those of only the three communities that were pooled for the inoculum of the next generation (yellow) are shown.

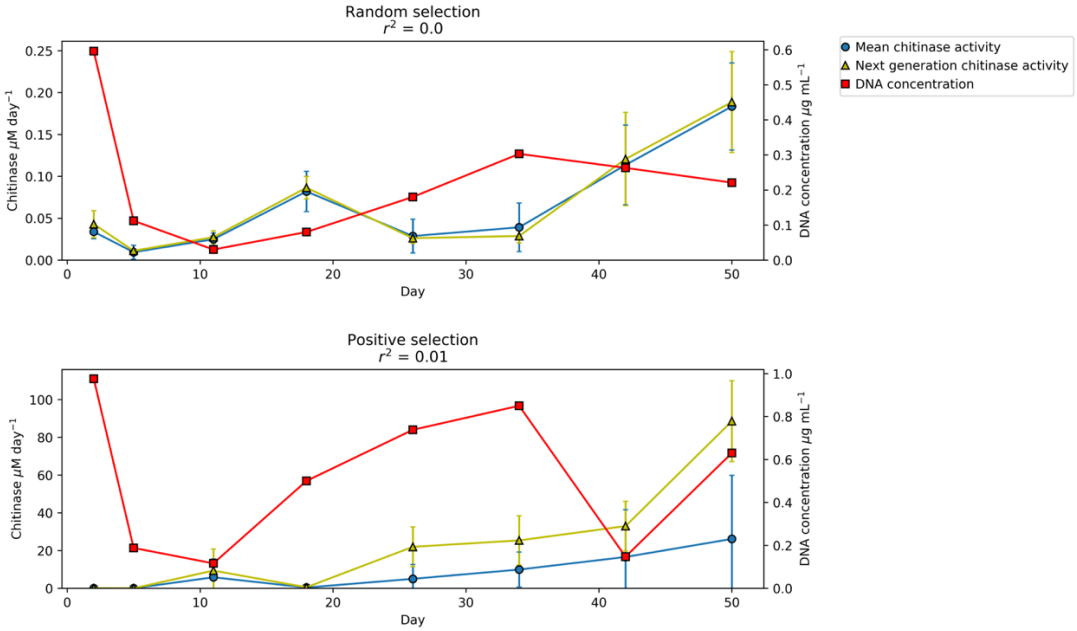

Figure 2.15. Averaged absolute chitinase activity and DNA concentration in the second artificial selection experiment. Averaged absolute chitinase activity measured from all communities (*n*=30; blue lines with circular markers) within each generation and from the three selected communities used to inoculate the following generation (yellow lines with triangular markers) during artificial selection experiment 2. Red lines with square markers show DNA concentrations for the three communities used to inoculate the next generation and used for 16S rRNA gene amplicon sequencing. Error bars show standard deviations. Note that scales differ between all axis. r^2 values indicate Pearson's correlation coefficients between chitinase activity (next generation) and DNA concentration.

2.4 Discussion

Artificial selection of microbial communities is, in principle, a powerful and attractive technique which has surprisingly been used in only a limited number of studies to date (Blouin et al., 2015; Swenson et al., 2000b, 2000a), possibly due to the lack of success as a consequence of poor process optimisation. Here, using chitin degradation as a case study and a detailed analysis of the community succession, it has been shown that artificial selection of microbial communities can be greatly improved by controlling the incubation times between transfers. We believe that the rapid succession of microbial community structure means transfers need to be done at the peak of the selected phenotypic activity (*e.g.* chitinase activity) or these get swiftly replaced by less efficient communities of cross-feeding microorganisms (*i.e.* "cheaters" and grazers). Previous studies that have artificially selected microbial communities for a particular phenotype did not report optimisation of the incubation time between transfers (Blouin et al., 2015; Swenson et al., 2000b, 2000a) which, in our hands, would have resulted in a negative selection (Figure 2.3). In agreement with our results, Penn and Harvey (2004) suggested that the observed phenotype in artificial ecosystem selection experiments could be significantly affected by interactions between different species and therefore microbial community structure.

A comprehensive understanding of microbial ecology helps to explain the importance of the timing during transfers. Datta et al. (2016) observed three distinct stages of community structure during the colonisation of chitin particles: (a) attachment, (b) selection and (c) succession. Each phase was characterised by having relatively higher abundances of organisms that were: (a) good at attaching to chitin particles; (b) good at degrading chitin particles and; (c) not able to degrade chitin, but able to benefit from others that could, *i.e.* "cheaters" and cross-feeders (Beier and Bertilsson, 2011; Enke et al., 2019, 2018; Keyhani and Roseman, 1999). During our first experiment, as communities became better and faster at degrading chitin, the chitinase activity was being measured when the communities were in the succession rather than in the selection stage and, by that point, the active chitinolytic community had decayed and was dominated by a cross-feeding community (Figure 2.7 and Figure 2.8). Hence, it was only when selecting at phenotypic time optima when chitinase activity improved and the overall community differentiated from the random control communities (Figure 2.10 and Figure 2.14). Due to the stochasticity of complex microbial communities, this time optimum is difficult to predict and continuous phenotypic monitoring is required. It is also interesting to note the selection of the grazer *Cafeteria* sp. (90% of the

Eukaryotic community), a genus of bactivorous marine flagellates that are commonly associated with marine detritus (Patterson et al., 1993). The predator-prey dynamics postulated by Lotka–Volterra's equations would also support the need to shorten transfer times to favour the prey's growth *i.e.* chitinolytic bacteria (Lotka, 1926; Volterra, 1926). It is noted however, that there may be a lower limit to optimal transfer times (possibly around two to three days; Figure 2.3C) as sufficient time has to be given for slower growing marine taxa (Joint et al., 2010) to i) develop a biofilm (Sutherland, 2001), ii) initiate the hydrolysis of the polymer to access the sugars and iii) allow the generation of sufficient biomass to overcome the dilution between transfers.

Interestingly, a strong successional pattern was observed at a higher taxonomic level. While *Gammaproteobacteria* dominated during the initial stages when chitinase activity was at its peak (accounting for over 70% of the prokaryotic community), other groups increased in abundance during the later stages (*i.e. Alphaproteobacteria*, *Bacteroidia* and *Clostridia*), similarly to the pattern previously observed by Datta et al. (2016) and Enke et al., (2018, 2019). The fact that *Gammaproteobacteria* are major contributors to chitin degradation is not new (Aunkham et al., 2018; Das et al., 2010; Fontanez et al., 2015; Giubergia et al., 2017; Kielak et al., 2013; Lecleir et al., 2007). All *Gammaproteobacteria* isolates obtained from the end of the experiments were able to grow using chitin as the only source of carbon and energy (Figure 2.8) confirming that this class is likely responsible for most of the chitinase activity observed. On the other hand, *Alphaproteobacteria*, the numerically dominant class of heterotrophic bacteria in surface oceans (Billerbeck et al., 2016; Morris et al., 2002), follow a cross-feeding and/or cheating life-strategy as five out of eight *Alphaproteobacterial* isolates could only use N-acetyl-D-glucosamine (GlcNAc) and only one could use chitin (Table 2.5). The dependence of cheaters and cross-feeders on the presence of a chitin-degrader was confirmed with co-cultures (Figure 2.13) and agreed with the results generated by others (Enke et al., 2019).

The PICRUSt metagenome analysis (Figure 2.12) further confirmed that almost all chitinase gene copies were encoded by *Gammaproteobacteria* (*i.e.* 90%; almost one gene copy encoded per bacterium) and, to a lesser extent, by some *Bacteroidia*. Chitin is made up of molecules of GlcNAc linked by (1,4)-β-glycosidic bonds and it has previously been found that initial degradation of chitin takes place predominantly by: i) chitinases which depolymerise the (1,4)-β-glycosidic bonds either at the ends or in the middle of chains, or ii) chitobiosidase enzymes which also hydrolyse (1,4)-β-glycosidic bonds but only at the ends of chitin chains.

Genes for the intracellular enzymes involved in GlcNAc utilisation (*i.e.* transformation of GlcNAc to Fructose-6-phosphate) were much more widespread amongst different taxonomic groups, highlighting the broader distribution of cross-feeding or cheating organisms, which can benefit from the extracellular depolymerisation of chitin which generates freely available GlcNAc to the community. Alternative degradation of chitin may also occur by deacetylation and deamination of the GlcNAc amino sugar, transforming chitin into chitosan and cellulose, respectively, after which they can be depolymerised by a range of other enzymes (*e.g.* chitosanases or cellulases) (Beier and Bertilsson, 2013; Beygmoradi and Homaei, 2018; Patil et al., 2000). While *Alphaproteobacteria* did not contribute to chitinase enzymes, they *did* potentially encode for most of the chitin deacetylases in the system, although no chitosanases were detected in the PICRUSt analysis (these also would not have been measured by the chitinase enzymatic activity assay).

Chitinolytic organisms have previously been found to make up between 0.1 and almost 6% of prokaryotic organisms in aquatic ecosystems (Beier and Bertilsson, 2011; Cottrell et al., 1999), while over a third of the organisms in these habitats can utilise only the products of chitin hydrolysis (*i.e.* GlcNAc) (Beier and Bertilsson, 2011; Eckert et al., 2013; Nedoma et al., 1994; Riemann and Azam, 2002). With *Gammaproteobacteria* being primarily responsible for the degradation of chitin here, the success of the artificial selection for an enhanced chitinolytic community was possibly achieved by the selective enrichment of this group between the beginning (5% of the prokaryotic community, within the expected range of *Gammaproteobacteria* found within natural environments) (Beier and Bertilsson, 2011; Cottrell et al., 1999) and end of the experiment (75% of the community).

Finally, chitin degradation is a task that single microorganisms can perform efficiently, but other more laborious phenotypic traits are rarely carried out entirely by a single microorganism in nature. It is now well documented that a distribution of labour is favoured in natural microbial communities (Cavaliere et al., 2017; Delgado-Baquerizo et al., 2017; Hug and Co, 2018; Ponomarova and Patil, 2015; Zhang et al., 2016). The detrimental effects of community dynamics and drift described here could be overcome by synthetically-assembled microbial communities, preventing the system from moving away from the high-performing desired community to a community in the succession phase (c) that is full of cheaters, cross-feeders and grazers. Nevertheless, this still requires a comprehensive understanding of the community structure and the necessity to select and isolate the microbes of interest (de Lorenzo et al., 2016; Ponomarova and Patil, 2015).

This chapter has proven the validity of artificially selecting a natural microbial community to better degrade chitin, but has highlighted the caveats for achieving this goal, which require a better understanding of the ecology of the system. It was found that continuous optimisation of incubation times was essential in order to successfully implement this process, as optimal communities rapidly decay due to their replacement by cheaters and cross-feeders, as well as the increase of potential predators such as grazers and, although not tested here, viruses. Hence, future artificial selection experiments should adjust transfer incubation times to activity maxima to successfully evolve enhanced community phenotypes and, eventually, allow the enrichment and isolation of microbes of interest.

Chapter 3

The PET Plastisphere: a proteogenomic characterisation of marine PET-degrading isolates and analysis of microbial community succession

3.1 Introduction

Plastics are now both ubiquitous and problematic in the marine environment (Law, 2017). Since the mass-production of plastic began almost 70 years ago, annual production has reached hundreds of millions of tonnes (PlasticsEurope, 2018). Current estimates put plastic input into the oceans at 4.8 to 12.7 million tonnes every year (Jambeck et al., 2015) and, although their ultimate fate and durability is currently unknown, some suggest a persistence of hundreds of years (Avio et al., 2016). Unfortunately, the properties that make plastics so widely used also underlie the reasons that they are so difficult to break down. For example, plastics are often manufactured with a high crystallinity, but the crystallinity also makes the polymer chains less accessible for microbial attack (Andrady, 2017). Estimates state that over 8 billion tonnes of plastics have been produced since the 1950s and approximately 80% of this ends up in landfills or in the environment. There is a plethora of routes for plastic to end up in the ocean, for example through the mismanagement of waste (Geyer et al., 2017), lost or discarded fishing gear (Gilman, 2015), fibres released during the washing of clothes (Napper and Thompson, 2016) or microplastics in cosmetic products (Napper et al., 2015).

Wherever people have looked in the oceans, plastics have been found; from coastal areas (Frias et al., 2016) to the deep sea (Courtene-Jones et al., 2017) and from the Arctic (Bergmann et al., 2017) and Antarctic (Reed et al., 2018) oceans to other remote and uninhabited areas, such as mid-oceanic Archipelagos (Readman et al., 2013), with concentrations of ~10^3 – 10^4 particles m^{-3} in intertidal sediments, ~0.1 – 1 particle m^{-3} in surface waters and >10^4 particles m^{-3} on deep sea sediments (Erni-cassola et al., 2019). Some plastics, such as polyethylene (PE), polypropylene (PP) and expanded polystyrene (PS), are less dense than seawater (Andrady, 2017), so they float and are carried by ocean currents. These have a tendency to accumulate in gyres in the middle of oceans, often termed “garbage patches” (Sebille et al., 2012; Van Sebille et al., 2016). Other plastics, including polyethylene terephthalate (PET) and polyvinyl chloride (PVC), are denser than seawater and therefore sink (Andrady, 2017). Floating plastics might also sink out of the surface seawater following colonisation by microorganisms and larvae of larger organisms, termed the “Plastisphere” (Zettler et al., 2013), which can be distinct from microbial assemblages found in the surrounding water (Bryant et al., 2016a) and colonising natural surfaces (Oberbeckmann et al., 2018). Plastics that consist of a carbon-carbon backbone without the addition of heteroatoms (*e.g.* PE, PP, PS, PVC) are expected to be less easily degradable than those with heteroatoms (*e.g.* PET and polyurethane), due to the presence of hydrolysable

functional groups (Wei and Zimmermann, 2017). Nevertheless, while there has been a larger focus on the marine degradation of PE and PP (Devi et al., 2019), there is little known on the degradation of plastics such as PET in marine environments (Webb et al., 2013).

A terrestrial bacterium capable of PET degradation, *Ideonella sakaiensis*, has been isolated and the enzymes involved have been characterised (Tanasupawat et al., 2016; Yoshida et al., 2016a). This bacterium was found to use an extracellular hydrolase, termed PETase, to break the PET down to the oligomer mono(2-hydroxyethyl) terephthalate (MHET) which was further broken down to terephthalic acid (TPA) and ethylene glycol (EG) by a second hydrolase, MHETase. Small amounts of bis(2-hydroxy ethyl) terephthalate (BHET) were also produced. The PETase was different from previously identified enzymes capable of PET degradation in that it has higher hydrolytic activity on PET than on other substrates and is active at lower temperatures. It has therefore since received considerable scientific attention: its crystal structure has been resolved and characterised (Han et al., 2017); it has been engineered to become more efficient at PET degradation (Austin et al., 2018); and it has been used – along with other enzymes known to be capable of PET degradation – for the construction of a Hidden Markov Model (HMM) to search available environmental metagenomes for homologs (Danso et al., 2018). The metagenome mining revealed 392 (present in 31 of 108 metagenomes) and 182 (present in 11 of 25 metagenomes) PETases in marine and terrestrial environments, respectively, and, interestingly, whilst in the terrestrial environment these belonged predominantly to the phylum *Actinobacteri*a, in the marine environment they were predominantly *Bacteroidetes*. One of these marine PETases was expressed in *Escherichia coli* and found to be capable of PET degradation, however, to our knowledge, no PETases have been identified *de novo* in the marine environment, nor have the bacteria possessing them been isolated. The larger number of PETases found in the marine metagenomes in comparison with the terrestrial metagenomes suggests that the marine potential for PET degradation is underexploited.

Previous studies on the biofilms found colonising particles in the marine environment have identified three distinct stages in the microbial community succession on these particles: i) colonisation, characterised by an abundance of organisms that are good at adhering to particles; ii) selection, characterised by an abundance of organisms that are good at degrading that particle; and iii) succession, where the efficient, degrading community is overtaken by cheaters, grazers and viruses (Datta et al., 2016; Enke et al., 2019, 2018). This means that if the time at which a microbial biofilm community is being studied is not right,

then a community efficient at degrading that compound will not be identified (Chapter 2), which could impact the differences found between those microbial communities attached to plastics and those attached to glass (Kirstein et al., 2018; Oberbeckmann et al., 2016; Woodall et al., 2018) or natural particles (De Tender et al., 2015; Oberbeckmann et al., 2018). Previous studies characterising succession on marine plastics have also found that plastic-specific communities are only found at earlier time points and these communities tend to converge at later time points (Dang et al., 2008; Pollet et al., 2018).

In this chapter, the microbial community succession and dynamics across six weeks of incubation with PET as a sole carbon source were characterised in a closed marine system. It was found that, where evidence of a community that was significantly different from the no carbon control existed, the taxa that were driving these differences were generally more abundant in the early rather than late colonisation phases. Two marine bacteria were also isolated, *Thioclava* sp. BHET1 and *Bacillus* sp. BHET2, that were capable of growing on amorphous PET as well as the PET oligomer, BHET and monomer, TPA. The proteogenomic characterisation of these two strains allowed the identification of potential PETases as well as the catabolic pathway involved in the degradation of TPA.

3.2 Method

3.2.1 Enrichment, isolation and characterisation of bacteria capable of PET degradation

Enrichment

Tissue culture flasks (25 cm^2) containing 25 mL Bushnell-Haas mineral media (Table 2.1, Section 2.2.3) supplemented with 0.005% (w/v) yeast extract (Merck KGaA, Germany), 0.1% w/v bis(2-hydroxy ethyl) terephthalate (3.9 mM; BHET; Sigma Aldrich, UK) and polyethylene terephthalate (PET; powder, below 300 µm; Goodfellow, UK) were inoculated with 1 mL of a microbial community obtained from bulk marine plastic debris during boat tows from both Plymouth Sound (Devon, UK; June 2016) and Portaferry (Northern Ireland, UK; August 2016). Cultures were incubated for four weeks at 30˚C in the dark with shaking at 150 rpm. When growth could be seen (assessed visually as a change in turbidity), 1 mL of these cultures was used for a second enrichment step.

Isolation and genome sequencing

Agar plates were made with Bushnell-Haas mineral medium, as above, containing 0.1% BHET and 1.5% agar. 100 µL of the microbial community from each enrichment step was spread on to replicate plates and these were incubated for three weeks at 30˚C. Morphologically distinct colonies were picked and streaked onto fresh plates until isolates were obtained. The identification of isolates was carried out by partial sequencing of the 16S rRNA gene (GATC BioTech, Germany) using primers 27F and 1492R (Table 2.2, Section 2.2.4) (Lane, 1991) after DNA extraction using the DNeasy Plant Mini Kit (Qiagen) with modifications as in Section 2.2.4 and purification using the QIAquick PCR purification kit (Qiagen). Two fast growing isolates were sent to MicrobesNG (Birmingham, UK) for whole genome sequencing and were used for further characterisation of their ability to degrade PET. The complete genome sequences of the two selected strains, *i.e. Thioclava* sp. BHET1 and *Bacillus* sp. BHET2, were deposited in the GenBank database under the accession numbers PRJNA544734 and PRJNA525098, respectively. Assembled genomes were annotated using Prokka (Seemann, 2014) and Blast KEGG Orthology and Links Annotation (BlastKOALA) (Kanehisa et al., 2016b). Following the methods of Danso et al. (2018) an amino acid sequence alignment of known PET hydrolases (Table 3.1) was constructed using the T-Coffee multiple sequence alignment server. This alignment was used for the construction of a Hidden Markov Model (HMM; Eddy, 2011) which was used to search the genomes of the isolates for PETase homologs.

Table 3.1. Known PET hydrolase sequences that were used to construct the Hidden Markov Model (HMM).

PDB entry	Gene name	Organism	Reference
W0TJ64	Cut190	*Saccharomonospora viridis*	Kawai et al. (2014)
E9LVI0	cut1	*Thermobifida fusca*	Dresler et al. (2006)
E5BBQ3	cut-2	*Thermobifida fusca*	Chen et al. (2008)
D1A9G5	Tcur-1278	*Thermanospora curvata*	Wang et al. (2014)
E9LVH7	cut1	*Thermobifida alba*	Hu et al. (2010)
H6WX58	NA	*Thermobifida halotolerans*	Ribitsch et al. (2012)
E9LVH9	cut2	*Thermobifida celluloysilityca*	Herrero Acero et al. (2011)
A0A0K8P6T7	ISF6-4831	*Ideonella sakaiensis*	Yoshida et al. (2016a)
G9BY57	NA	Uncultured bacterium	Sulaiman et al. (2012)
E8U721	Deima_1209	*Deinococcus maricopensis*	Danso et al. (2018)
C3RYL0	lipIAF5-2	Uncultured bacterium	Danso et al. (2018)
A0A0F9X315	LCGC14_0200860	Marine sediment metagenome	Danso et al. (2018)
N6VY44	J057_15340	*Marinobacter nanhaiticus*	Danso et al. (2018)
R4YKL9	lipA OLEAN_C07960	*Oleispira antarctica* RB-8	Danso et al. (2018)
UPI0003945E1F	n.d	*Vibrio gazogenes*	Danso et al. (2018)
Q8RR62	pbsA	*Acidovorax delafieldii*	Danso et al. (2018)
P19833	lip1 L1	*Moraxella* sp.	Danso et al. (2018)
A0A0D4L7E6	est	*Psychrobacter* sp.	Danso et al. (2018)
UPI00064655D2	n.d	*Methylibium* sp.	Danso et al. (2018)
UPI0003660256	n.d	*Caldimonas manganoxidans*	Danso et al. (2018)
A0A0G3BI90	AAW51_2473	*[Polyangium] brachysporum*	Danso et al. (2018)
A0A1F4G492	A2711_12500	*Burkholderiales bacterium*	Danso et al. (2018)

Characterisation

Both isolates were grown with marine broth 2216 (BD Difco™) or Bushnell-Haas mineral medium (as above), supplemented with 0.1% (w/v) glucose, fructose, succinate, glycerol, pyruvate, N-acetyl-D-glucosamine or BHET. Their growth on each substrate was measured over three days by absorbance (600 nm) measurements every 30 mins on a Synergy HTX microplate reader. Material for cellular and exo-proteomics was generated by growing each isolate in 50 mL glass Erlenmeyer flasks with 40 mL Bushnell-Haas mineral medium, as above, supplemented with either 0.1% (w/v) of fructose or BHET, 0.02% terephthalic acid (TPA) or three 0.5 x 0.75 cm amorphous PET pieces (Goodfellow, UK). These were incubated at 30˚C in the dark with shaking at 150 rpm. Samples (1 mL) were taken on days 0, 1, 3, 7 and 14 to monitor growth through absorbance (600 nm) measurements. When there was visible growth, or the incubation time was 2 weeks (whichever was sooner), cultures were centrifuged (4,000 rpm for 15 mins). Cellular pellets were immediately stored at -20˚C for later proteomic analysis. The supernatant was further filtered through a 0.2 µm filter prior

to freezing. Cultures with *Ideonella sakaiensis* and no inoculum controls were also incubated at the same time but were used only for absorbance measurements and not proteomics.

3.2.2 Proteomic analysis of isolates

Preparation of proteome samples

The collected exoproteomes were processed in accordance with Christie-Oleza et al. (2015) and Kaur et al. (2018) by using a trichloroacetic acid precipitation of the proteins contained in 40 mL of culture supernatants. The resulting protein pellets as well as the whole cellular pellets, were dissolved in LDS loading buffer (Invitrogen, USA) and the equivalent of 20 mL of culture was loaded on a precast Tris-Bis NuPAGE gel (Invitrogen, USA) using 1 x MOPS solution (Invitrogen, USA) as the running buffer. SDS-PAGE was performed for a short gel migration (5 min). This allows removal of contaminants and purification of the polypeptides in the polyacrylamide gel.

Trypsin in-gel proteolysis and nanoLC-MS/MS analysis

Polyacrylamide gel bands containing the cellular or exo-proteomes were excised and standard in-gel reduction with dithiothreitol and alkylation with iodoacetamide was performed prior to trypsin (Roche, Switzerland) proteolysis. The resulting tryptic peptide mixture was extracted using 5% formic acid in 25% acetonitrile and concentrated at 40˚C in a speed-vac. For mass spectrometry, the samples were resuspended in 2.5% acetonitrile containing 0.05% trifluoroacetic acid and filtered using a 0.22 µm cellulose acetate spin column at 16,000 x g for 5 mins, in order to eliminate undissolved aggregates. Samples were analysed by means of nanoLC-ESI-MS/MS using an Ultimate 2000 LC system (Dionex-LC Packings) coupled to an Orbitrap Fusion mass spectrometer (Thermo-Scientific, USA) using a 60 minute LC separation (exo-proteomes) or a 120 minute LC separation (cellular-proteomes) on a 25 cm column and settings as described previously (Christie-Oleza et al., 2015).

Bioinformatic and statistical analysis of proteomic data

Raw proteomics files were processed using MaxQuant version 1.5.5.1 (Cox and Mann, 2008) for protein identification and quantification, using default parameters, match between runs and in-house protein databases obtained from the whole genome sequences for each bacterium. The comparative proteomic analysis between samples was carried out using Perseus version 1.5.5.3 (Tyanova et al., 2016) following the pipeline described previously (Kaur et al., 2018), but including a stringent rule where only proteins confidently detected in

all three biological replicates of any one condition were considered. Proteins that were only identified by site, decoy and potential contaminants were removed. Data was then imported into Python where custom scripts (Python version 3.6.8 with modules numpy, os, csv and math) were used to carry out two-sample Student's T-tests for significance and calculate fold changes. Conserved domain searches were carried out for manual curation of the functions assigned to all key proteins identified and further mapped onto KEGG degradation pathways (Kanehisa et al., 2017; Marchler-Bauer et al., 2017).

3.2.3 Marine microbial community succession when grown with PET as a sole carbon source

The microbial community used as an inoculum was obtained from bulk marine plastic debris collected from Porthcawl beach (Wales, UK) in July 2018. Immediately after transport to the laboratory, the debris were washed with sterile seawater and sonicated to detach the biofilm from the plastic. For sonication, the plastics were placed into 50 mL falcon tubes containing 50 mL Bushnell-Haas mineral medium (as above) and were placed into a Branson 2510 Ultrasonic water bath for 10 mins followed by 30 s vortexing. The removed biofilm was collected by centrifugation (4,000 rpm for 5 mins) and used as the inoculum for five treatments: (a) No additional carbon (control); (b) 10 pieces 1.5 x 0.5 cm amorphous PET (as above); (c) PET powder (as above); (d) weathered PET powder (artificially weathered through incubation at 80˚C for 9 months); and (e) BHET (as above). Three independent biological replicates were performed for each treatment (total number of cultures *n*=30). Cultures were grown in 75 cm^2 tissue culture flasks containing 50 mL Bushnell-Haas mineral medium (as above) supplemented with one of the four substrates or no additional carbon (control) and incubated at 30˚C in the dark with constant shaking at 150 rpm. Aliquots of 1.5 mL were collected from each flask on days 1, 3, 7, 14, 21, 30 and 42 of incubation and centrifuged at 14,000 rpm for 5 mins after which the pellet (for community analysis) was stored at -20˚C. For treatment (b), one piece of 1.5 x 0.5 cm amorphous PET was also taken at each sampling point. Pellets and amorphous PET pieces were stored in Buffer AL (Qiagen, UK) for later DNA extraction and community analysis.

3.2.4 DNA extraction and amplicon sequencing

DNA extraction method determination

In order to determine the optimal method for DNA extraction from biofilms, four DNA extraction methods were tested: (a) DNeasy Plant Mini Kit (Qiagen) with modifications (as

detailed in Chapter 2, Section 2.2.4); (b) DNeasy Blood and Tissue Kit (Qiagen) with modifications as in (a); (c) DNeasy Power Biofilm Kit (Qiagen), following the manufacturer's instructions; and (d) GeneJET Genomic DNA Purification Kit (Thermofisher Scientific) following the manufacturer's instructions for gram-positive bacteria with an additional bead beating step, as in (a). These methods were tested on additional plastic pieces that were incubated with the microbial community, as in Section 3.2.3, as well as procedural blanks. Additional DNA extractions were carried out with pure *Synechococcus* sp. cultures (supplied by Audam Chhun), amorphous PET pieces from a preliminary experiment and the liquid medium that these were in. A Qubit® HS DNA kit (Life Technologies Corporation) was used for DNA quantification. The GeneJet Genomic DNA Purification Kit was found to yield the highest concentrations of DNA (Table 3.2) and was therefore used for all DNA extractions on samples collected for community characterisation from Section 3.2.3. A Qubit® HS DNA kit was again used for DNA quantification after which all samples were diluted to equalise the concentrations across samples.

Table 3.2. Comparison of different kits for DNA extraction from plastic pieces incubated with microbial communities.

Extraction kit	Manufacturer	Time taken[1]	Mean yield (*n*=3)	Mean control yield (*n*=3)	Price per sample (£)
(a) DNeasy Plant Mini Kit	Qiagen	~1 h	4.12 ng mL^{-1}	Not detected	2.39
(b) DNeasy Blood and Tissue Kit	Qiagen	~4 h	3.03 ng mL^{-1}	Not detected	2.63
(c) DNeasy Power Biofilm Kit	Qiagen (previously MoBIO)	<1 h	7.28 ng mL^{-1}	Not detected	6.20
(d) GeneJET Genomic DNA Purification Kit	ThermoFisher	~2 h	13.57 ng mL^{-1}	Not detected	1.86

[1] Times shown are for processing six samples (*i.e.* three samples and three controls per kit).

Amplicon sequencing

16S rRNA gene and index PCR as well as purification and normalisation steps were carried out as in Section 2.2.4 of Chapter 2. Pooled libraries were additionally quantified using the NEBNext Library Quant Kit for Illumina (New England Biolabs, UK) and diluted to 4 nM. Libraries were denatured using 0.2N NaOH and MiSeq amplicon sequencing was carried out using the MiSeq Reagent Kit v3 (600 cycles; Illumina, UK), following the manufacturer's instructions for a 14 pM library with 2% phiX as an internal reference. Reads were demultiplexed using Illumina BaseSpace and all sequences have been deposited in the NCBI Short Read Archive (SRA) under Bioproject accession number PRJNA544783.

Microbial community structure determination and statistical analysis

Sequencing data were processed following the DADA2 (version 1.8.0) pipeline (Callahan et al., 2016b), as in Section 2.2.5 of Chapter 2. Statistical analyses were also carried out as in Section 2.2.8 of Chapter 2, with some additional analyses: principal response curves (Brink and Besten, 2009) were calculated using the vegan package (Dixon, 2003); and PICRUSt2 – rather than PICRUSt1 – artificial metagenome analyses (Langille, 2018; Langille et al., 2013) were carried out in QIIME2 (Bolyen et al., 2018) on a Cloud Infrastructure for Microbial Bioinformatics (CLIMB; MRC, UK) server using the additional packages HMMER (Eddy, 2011), EPA-NG (Barbera et al., 2019) and gappa (Czech and Stamatakis, 2018). Nearest sequenced taxon indices (NSTI) are shown in Table 3.3.

Table 3.3. Nearest Sequenced Taxon Indices (NSTI) for all amorphous PET biofilm and BHET samples included in the PICRUSt analysis.

Day	Replicate	NSTI	
		Amorphous PET biofilm	BHET
Inoculum	1	0.05699618	
	2	0.06484307	
	3	0.06733378	
Day 1	1	0.02868844	0.05786394
	2	0.02657238	0.05531136
	3	0.02230206	0.05805919
Day 3	1	0.02427176	0.04830625
	2	0.02275862	0.04295512
	3	0.02161615	0.04409823
Day 7	1	0.02131736	0.04544387
	2	0.02149432	0.047748
	3	0.02261355	0.04465364
Day 14	1	0.01837236	0.05126617
	2	0.02514824	0.04908569
	3	0.02201042	0.04572072
Day 21	1	0.01886922	0.05163998
	2	0.02175451	0.05072131
	3	0.02167706	0.04990867
Day 30	1	0.01658053	0.0557198
	2	0.01618666	0.05662277
	3	0.0188591	0.04482693
Day 42	1	0.01738465	0.05996997
	2	NA	0.05436207
	3	0.02281332	0.05235447

3.2.5 Growth of isolates and microbial communities on PET

Microbial communities (as for the community succession experiment in Section 3.2.3), isolates (*Thioclava* sp. BHET1 and *Bacillus* sp. BHET2) or controls with no inoculum were

incubated in 25 cm^2 tissue culture flasks with 25 mL Bushnell-Haas mineral medium (as above) with carbon sources as follows (*n*=48 total); (a) no additional carbon (control); (b) five pieces of 1 x 3 cm amorphous PET (Goodfellow, UK); (c) approximately 100 mg PET powder (Goodfellow, UK); (d) approximately 100 mg weathered PET powder (as above). Flasks were incubated at 30˚C in the dark for five months with constant shaking at 150 rpm and were topped up with sterile water as necessary to keep the volume at 25 mL. At three months of incubation, the growth in each of these flasks was measured using the QuantiPro™ BCA Assay Kit (Sigma-Aldrich, UK) to quantify protein content as a proxy for growth. At the end of the incubation period the plastics were removed from the cultures and were fixed immediately in 4% (v/v) paraformaldehyde.

Biofilm removal from plastic samples

Digestion of biofilms was performed as described by Erni-Cassola et al. (2017). Briefly, enough 15% H_2O_2 was added to plastic samples in order to fully immerse them (approximately 5 mL for 1 x 3 cm amorphous PET pieces and 1 mL for weathered or non-weathered PET powders). These were then kept at 60˚C for 90 mins with shaking at 100 rpm after which plastics were placed into fresh H_2O_2 and incubated overnight at 60˚C. These were then washed thoroughly with MilliQ water at least three times and were dried overnight at 60˚C.

Fourier Transform Infrared Spectroscopy (FTIR)

In order to search for the presence of additional carboxyl and hydroxyl functional groups, indicative of the degradation of PET (Yoshida et al., 2016b), FTIR was performed on the plastics used in the five month incubations as well as on procedural controls that were not incubated with the microbial inoculums or digested with H_2O_2. Following the removal of the biofilm and drying, three measurements were taken on each PET piece and three measurements were taken on random PET powder pieces using an Agilent Technologies Cary 630 FTIR spectrometer. FTIR spectra were normalised to their respective baselines and differences were calculated between the absorbance at 2500 cm^{-1} and the absorbances at 1710, 2920, 1235, 1090 and 3300 cm^{-1} for the carboxylic acid C=O, O-H and C-O and alcohol C-O and O-H functional groups, respectively, using a custom python script.

The genomic analyses of *Thioclava* sp. BHET1 and *Bacillus* sp. BHET2, complete lists of detected peptides and polypeptides, files showing fold changes between treatments and

analysis scripts for this chapter can be found at https://github.com/R-Wright-1/PET-Plastisphere.

3.3 Results

3.3.1 Enrichment, isolation and characterisation of marine bacteria capable of PET degradation

Microbial enrichments with PET and BHET led to the isolation of two bacteria that grew on agar plates with BHET as the sole carbon source. These were identified through partial sequencing of their 16S rRNA genes as *Thioclava dalianensis* (99%; *Rhodobacteraceae, Alphaproteobacteria*) and *Bacillus aquimaris* (99%; *Bacillales, Firmicutes*) and were selected for further proteogenomic characterisation; they are named hereafter as *Thioclava* sp. BHET1 and *Bacillus* sp. BHET2. Their genomes were sequenced, revealing that *Thioclava* sp. BHET1 has a genome size of 7.66 Mb, with 7,568 coding sequences, including 3,265 hypothetical proteins, and a GC content of 63.26%. *Bacillus* sp. BHET2 has a genome size of 4.23 Mb with 4,368 coding sequences, including 1,719 hypothetical proteins, and a GC content of 40.97%. A search of their genomes was carried out for potential PETases using a HMM constructed from the known PETase sequences in Table 3.1. This revealed that *Thioclava* sp. BHET1 has seven enzymes that were above the inclusion threshold while *Bacillus* sp. BHET2 has four (Table 3.4; Appendix 2 and Appendix 3, respectively). The growth dynamics of the two isolates were determined on a range of typical microbial growth substrates (Figure 3.1) and were incubated with amorphous PET pieces, BHET, TPA and fructose (Figure 3.2). BHET is turbid in solution and an initial decrease in absorbance is therefore observed in the BHET incubations, while there was a minimal increase in absorbance in the PET treatments (for both isolates as well as the confirmed PET-degrader, *Ideonella sakaiensis*), likely because most growth in the PET treatments is as a biofilm on the surface of the pieces. Growth on TPA was low for both isolates, likely due to its toxicity in high concentrations (Vamsee-Krishna and Phale, 2008). Cellular and exo-proteomic analyses were performed in order to identify the enzymes and pathways used for PET degradation.

Table 3.4. Potential PETases found in the genomes of *Thioclava* sp. BHET1 and *Bacillus* sp. BHET2 using a Hidden Markov Model (HMM) constructed with known PETases (in Table 3.1).

Bacterium	Prokka annotation	Genome position	E-value	Score	SecretomeP[1]	SignalP[2]
Thioclava sp. BHET1	Lipase 1	3428	$4.9e^{-10}$	37.7	0.287	0.005
	Thermostable monoacylglycerol lipase	1741	$9.9e^{-9}$	33.5	0.062	0.988
	S-formylglutathione hydrolase	0051	$4.5e^{-6}$	24.8	0.538	0.047
	Hypothetical protein	3993	$2.1e^{-5}$	22.5	0.074	0.019
	Arylesterase	2746	$3.2e^{-5}$	22.0	0.081	0.041

Bacterium	Prokka annotation	Genome position	E-value	Score	SecretomeP[1]	SignalP[2]
Bacillus sp. BHET2	Non-heme chloroperoxidase	4046	0.0052	14.7	0.488	0.011
	Non-heme chloroperoxidase	6354	0.0073	14.2	0.093	0.006
	Di-peptidyl peptidase 5	2434	0.00013	19.1	0.847	0.014
	2-succinyl-6-hydroxy-2,4-cyclohexadiene-1-carboxylate synthase	2574	0.00081	16.5	0.064	0.034
	Thermostable monoacylglycerol lipase	3830	0.0013	15.8	0.056	0.032
	2-hydroxy-6-oxo-6-phenylhexa-2,4-dienoate hydrolase	3456	0.0068	13.5	0.085	0.003

[1] Values above 0.5 indicate that the protein is predicted to be secreted.
[2] Values are probabilities that the protein has a signal peptide.

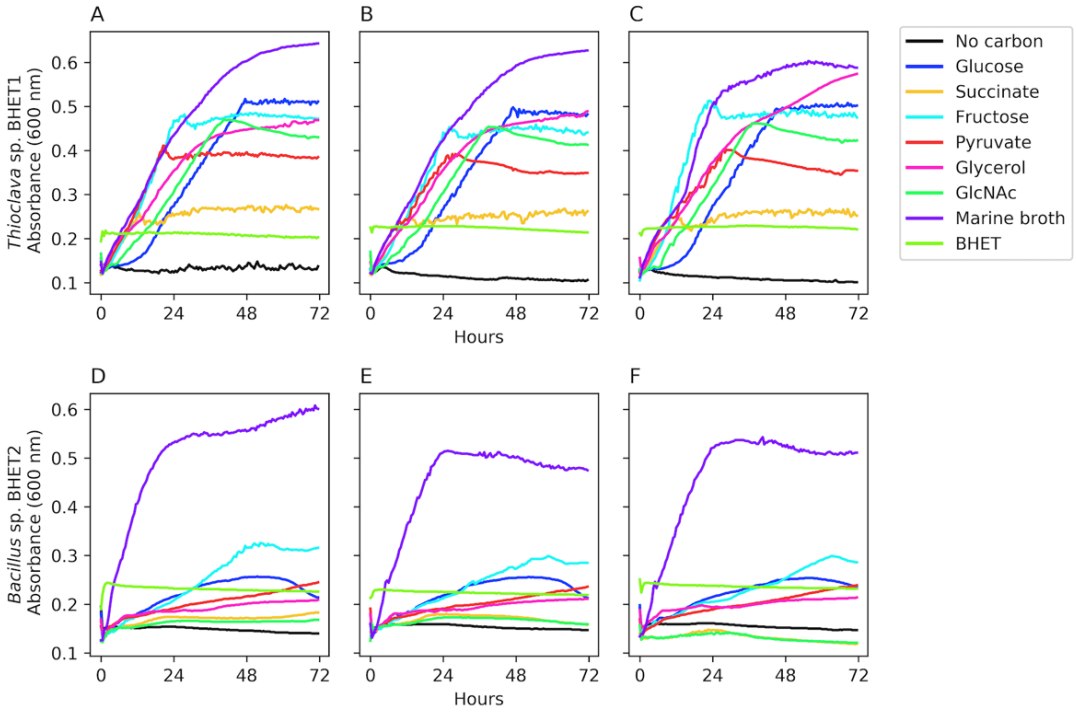

Figure 3.1. Growth of the isolates *Thioclava* sp. BHET1 (**A**-**C**) and *Bacillus* sp. BHET2 (**D**-**F**) on a range of common growth substrates across three days of incubation. Panels show biological replicates.

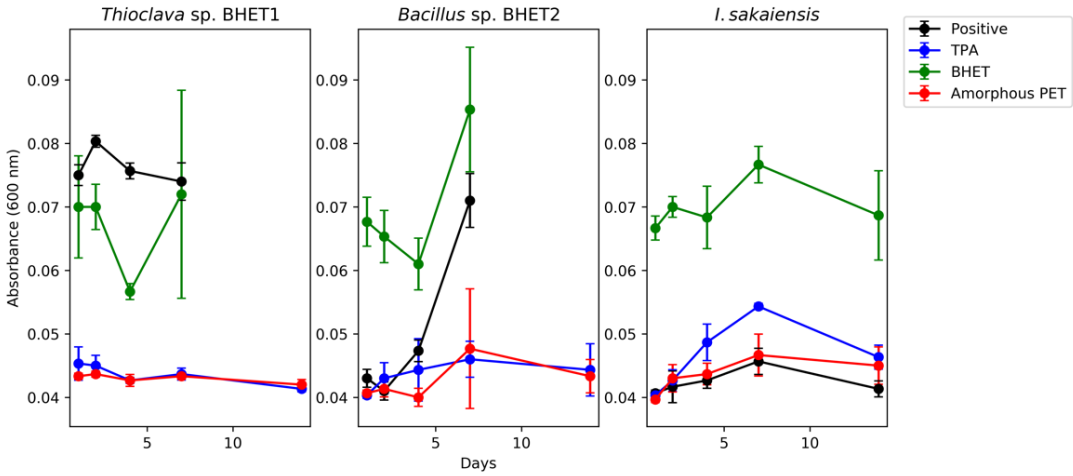

Figure 3.2. Incubation of isolates *Thioclava* sp. BHET1, *Bacillus* sp. BHET2 and *Ideonella sakaiensis* with fructose (positive control), terephthalic acid (TPA), BHET and amorphous PET. Points show the mean of absorbance measurements (600 nm) for three biological replicates and error bars show standard deviations. Samples were taken for proteomics on the last day shown for each treatment for the two isolates. Note that growth was generally more apparent by visual assessment due to the formation of cell aggregates. BHET is semi-soluble and produces a turbid mixture in the media and a reduction in optical density therefore indicates removal of the BHET.

3.3.2 Identification of the pathway used by *Thioclava* sp. BHET1 for PET degradation

In order for PET to be degraded, it must first be hydrolysed to its monomeric subunits, ethylene glycol (EG) and TPA (Figure 3.3). There was no enzyme that was clearly solely responsible for this step, however, there were two proteins present that were putatively involved, both of which were among the seven enzymes detected by the HMM search as potential PETases (Table 3.4). One was a carboxylesterase (1741) and was at least 2-fold upregulated in the cellular proteome in all treatments (Figure 3.4). Although it was predicted to be a secreted protein by SecretomeP, it was not detected in the exoproteome (Table 3.5). The other was a hydrolase (0051) that was not predicted to be secreted and was approximately 1.4-, 1.3- and 1.3-fold upregulated in the cellular proteomes of the PET, BHET and TPA treatments (relative to the fructose positive control), respectively. An enzyme similar to polyhydroxyalkanoate depolymerase (1504) was found – also not predicted to be secreted – that was over 7-fold upregulated in the BHET treatment cellular proteome that was likely capable of the hydrolysis of BHET, removing the EG molecules and leaving TPA (Figure 3.4). No enzymes that were similar to the *Ideonella sakaiensis* MHETase, responsible for the hydrolysis of MHET to TPA and EG, were found, however, it has previously been found that PETases also exhibit activity against BHET and MHET (Joo et al., 2018; Yoshida et al., 2016a). There were also several Tripartite ATP-independent periplasmic (TRAP) transporters that were upregulated in all treatments when compared with the positive control. These would be used for the transport of TPA into the cell, after which it should be metabolised to

protocatechuate by a series of dioxygenases (Salvador et al., 2019). Although *Thioclava* sp. BHET1 has a terephthalic acid degradation operon in its genome (Figure 3.4), these proteins were not detected in the proteome. Dioxygenases are involved in both the metabolisation of TPA and protocatechuate and it is known that some dioxygenases have very wide substrate specificity, acting on at least 100 compounds (Aukema et al., 2014; Wackett, 2015), hence, it is difficult to determine which enzymes carry out each one of the steps in TPA and protocatechuate degradation. These dioxygenases are listed in Table 3.5, several of which are very highly upregulated in some of the treatments when compared with the fructose positive control. One protein, annotated as a catechol 1,2-dioxygenase (1817) – that shared 35% protein identity with the *I. sakaiensis* protocatechuate 3,4-dioxygenase – was almost 9,000-fold upregulated in the TPA treatment and 16- and 14-fold upregulated in the BHET and PET treatments, respectively. Genes encoding the benzoate degradation pathway, necessary for the degradation of protocatechuate, usually appear together in the genome and are controlled by a single transcriptional regulator (Vamsee-Krishna and Phale, 2008). *Thioclava* sp. BHET1 possesses most of these genes, but the cluster is split by ectoine utilisation genes (Figure 3.4). Although most proteins of the TPA degradation pathway were not detected in the proteome (Figure 3.4), other detected proteins could potentially carry out some of these steps (Table 3.5). EG metabolism usually takes place either *via* conversion to acetaldehyde and acetate (Trifunovic et al., 2016; Wiegant and de Bont, 1980), or *via* the formation of glyoxylate (Salvador et al., 2019). Enzymes were found here that would be used for the conversion of EG to acetaldehyde, acetate and acetyl-CoA that are particularly upregulated in the BHET treatment and the acetaldehyde dehydrogenase, necessary for the conversion of acetaldehyde to acetate, is very abundant in the cellular proteomes (3.33 and 1.42% relative abundance in the BHET and PET treatments, respectively; Figure 3.4).

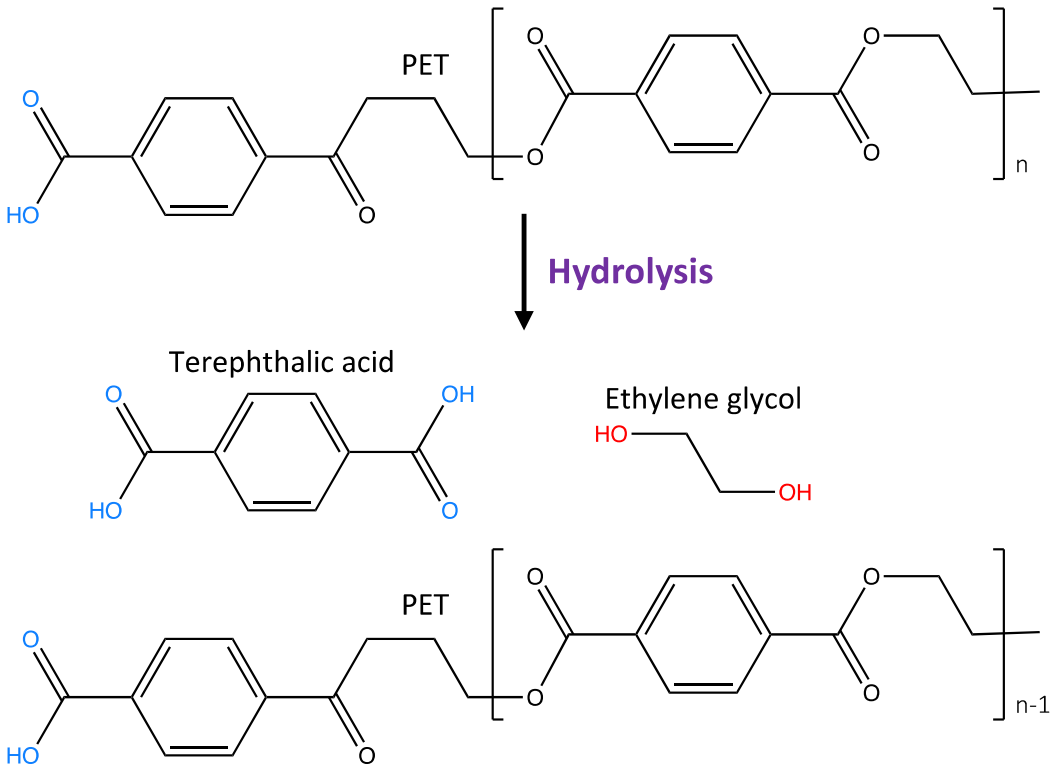

Figure 3.3. Diagram depicting the mechanism by which PET degradation leads to the generation of additional C-O and O-H alcohol bonds (blue) and C=O, O-H and C-O carboxylic acid bonds (red) that will be detected by FTIR analyses.

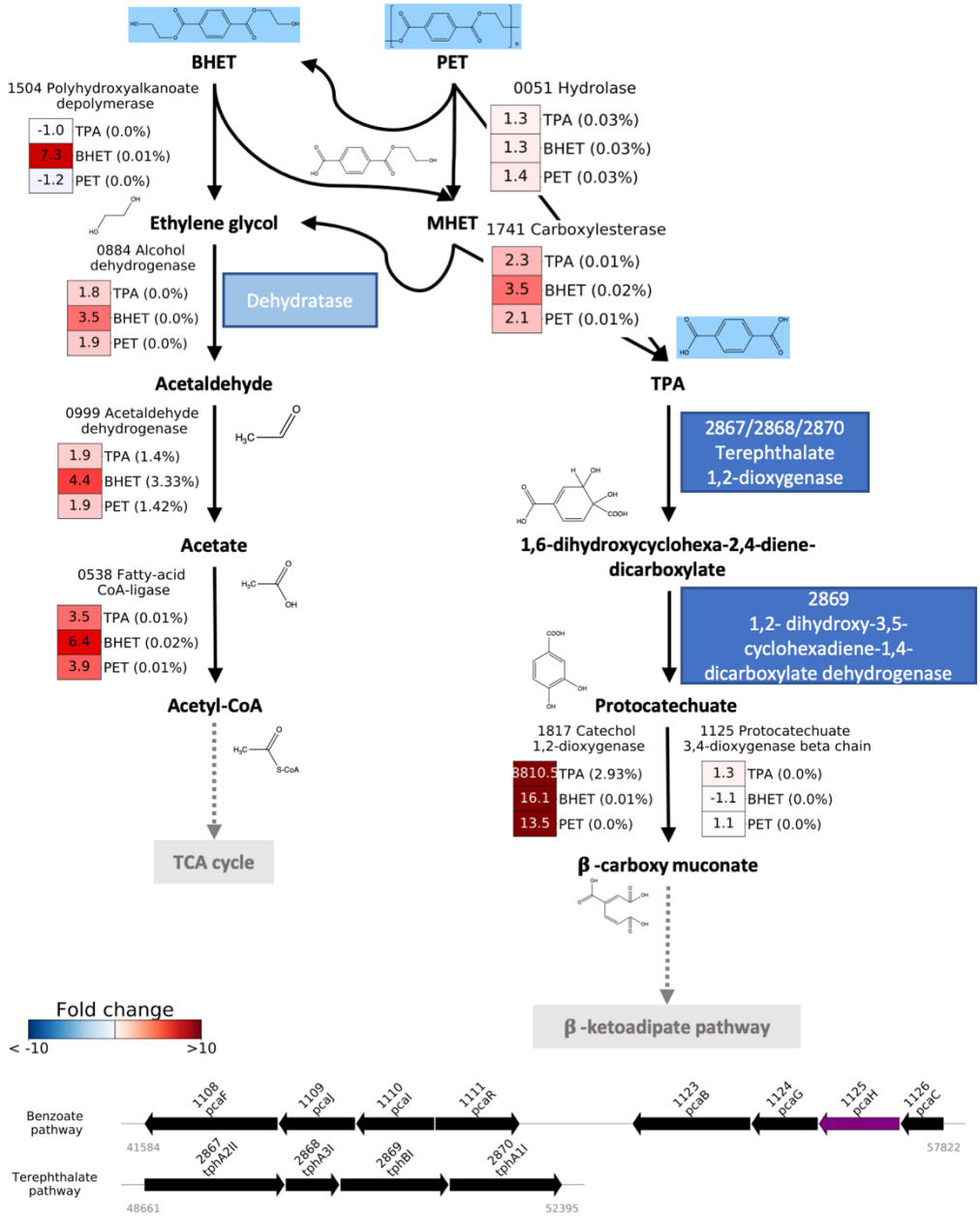

Figure 3.4. Putative pathway for PET, BHET and TPA degradation by *Thioclava* sp. BHET1 and genomic location of related genes. Initial substrates are shown with blue boxes around them. Boxes show the genome position of the enzyme used for that step alongside the fold-change (when compared with the positive control, *Thioclava* sp. BHET1 grown with fructose) and the percentage relative abundance within the proteomes. Although several of these processes are predicted to occur outside the cell, these proteins were found in the cellular proteome. For the benzoate and terephthalate pathway operons, arrows show the direction of transcription and are proportional to gene size, while purple indicates that the protein was detected in the proteome and black that it wasn't. 1108 *pcaF* β-ketoadipyl CoA-thiolase, 1109 *pcaJ* 3-oxoadipate CoA-transferase subunit beta, 1110 *pcaI* 3-oxoadipate CoA-transferase subunit alpha, 1111 *pcaR* β-ketoadipate pathway transcriptional regulator PCA regulon, 1123 *pcaB* 3-carboxy-*cis, cis*-muconate cycloisomerase, 1124 *pcaG* Protocatechuate 3,4-dioxygenase subunit alpha, 1125 *pcaH* Protocatechuate 3,4-dioxygenase subunit beta, 1126 *pcaC* 4-carboxymuconolactone decarboxylase, 2867 *tphA2II* Terephthalate 1,2-dioxygenase subunit alpha 2, 2868 *tphA3II* Terephthalate 1,2-dioxygenase subunit beta 1, 2869 *tphBI* 1,2-dihydroxy-3,5-cyclohexadiene-1,4-dicarboxylate dehydrogenase and 2870 *tphA1I* Terephthalate 1,2-dioxygenase reductase component.

Table 3.5. Proteins in the *Thioclava* sp. BHET1 cellular proteome that are potentially related to PET, BHET and TPA degradation, including relative abundance within the proteome and fold change when compared with the positive control.

Genome	Annotation	Relative abundance (%)				Fold change (with fructose) [1]		
		Fructose	TPA	BHET	PET	TPA	BHET	PET
0051	Hydrolase	0.018	0.025	0.027	0.027	**1.27**	**1.34**	**1.38**
1741	Carboxylesterase	0.004	0.011	0.017	0.010	**2.25**	**3.52**	**2.09**
1504	PHA depolymerase	0.001	0.001	0.010	0.001	1.00	**7.28**	0.81
2242	TRAP-type transporter	0.001	0.013	0.014	0.013	**10.42**	**11.07**	**10.75**
1143	Anthranilate 1,2-dioxygenase	0.002	0.022	0.002	0.003	**12.51**	0.94	**1.83**
2475	Anthranilate 1,2-dioxygenase	0.002	0.008	0.011	0.008	**3.58**	**4.56**	**3.33**
2780	Homogentisate 1,2-dioxygenase	0.002	0.016	0.030	0.017	**7.02**	**12.51**	**7.44**
3571	Tryptophan 2,3-dioxygenase	0.001	0.004	0.002	0.004	**2.81**	1.31	**3.00**
1817	Catechol 1,2-dioxygenase	0.000	2.925	0.005	0.004	**8810.47**	**16.13**	**13.54**
1125	Protocatechuate 3,4-dioxygenase beta chain	0.002	0.002	0.002	0.002	1.25	0.90	1.07
1816	Muconate cycloisomerase	0.001	0.090	0.002	0.001	**57.27**	1.29	0.75
2472	3-oxoadipate enol-lactonase	0.022	0.033	0.030	0.030	**1.39**	1.25	**1.28**
1581	3-oxoadipyl-CoA thiolase	0.011	0.084	0.053	0.087	**7.01**	**4.37**	**7.32**
2958	Succinate-semialdehyde dehydrogenase	0.010	0.065	0.059	0.068	**5.73**	**5.15**	**6.04**
2576	Acetyl-coenzyme A synthetase	0.030	0.090	0.081	0.092	**2.70**	**2.39**	**2.79**
1195	Alcohol dehydrogenase	0.053	0.099	0.147	0.143	**1.72**	**2.49**	**2.50**
0999	Acetaldehyde dehydrogenase	0.677	1.401	3.335	1.423	**1.89**	**4.41**	**1.94**
0538	Fatty-acid CoA-ligase	0.002	0.010	0.017	0.010	**3.53**	**6.36**	**3.88**
0884	Alcohol dehydrogenase	0.001	0.002	0.005	0.003	1.79	**3.49**	1.93

[1] The darker the red colour, the higher the upregulation relative to the positive control in that treatment. Values in bold indicate that this fold change was significant (Two-sample T-test < 0.05).

3.3.3 Identification of the pathway used by *Bacillus* sp. BHET2 for PET degradation

The pathway used for PET, BHET and TPA degradation by *Bacillus* sp. BHET2 was not determined. Almost half of the proteins in the genome were not annotated by Prokka (1,719 hypothetical proteins of 4,368 total) and a further 311 were assigned only a putative function. The genome annotations by both Prokka and KOALA did not reveal any of the genes necessary for TPA or protocatechuate degradation and subsequent local BLAST searches with

proteins known to be capable of these functions and searches of the conserved domain database did not identify any proteins with significant homology. There were, though, a large number of proteins that are usually involved in the degradation of xenobiotics, such as Cytochrome C oxidases and monooxygenases (Table 3.6), that were upregulated in the PET, BHET and TPA treatments compared with the positive control (*i.e.* with fructose), which suggests that these compounds are being degraded, possibly using a mechanism that is currently unknown. In order to confirm this hypothesis, however, metabolomic analyses searching for any degradation sub-products should be carried out to inform on the pathway used by this strain for catabolising these compounds.

Table 3.6. Proteins that are potentially involved in xenobiotics degradation that were upregulated in one or more treatments in the *Bacillus* sp. BHET2 cellular proteome, including relative abundance within the proteome and fold change when compared with the positive control.

Protein	Annotation	Relative abundance (%)				Fold change (with fructose) [1]		
		Fructose	TPA	BHET	PET	TPA	BHET	PET
0149	Cytochrome c biogenesis protein CcsB	0.002	0.017	0.014	0.018	5.77	**8.88**	**6.90**
0150	Cytochrome c biogenesis protein CcsA	0.002	0.010	0.003	0.009	3.09	2.00	3.06
0213	Cytochrome b6-f complex iron-sulphur subunit	0.049	0.298	0.088	0.315	**3.23**	1.73	**3.75**
0214	Menaquinol-cytochrome c reductase cytochrome b subunit	0.132	0.446	0.161	0.508	**1.78**	1.17	**2.22**
0215	Cytochrome c-551	0.075	0.370	0.254	0.382	**2.61**	**3.25**	**2.95**
0258	Cytochrome c oxidase subunit 2	0.001	0.010	0.008	0.021	3.66	**5.32**	**8.52**
1044	Putative monooxygenase	0.001	0.006	0.002	0.004	2.30	1.73	1.62
1495	Cytochrome c oxidase subunit 4B	0.008	0.050	0.035	0.018	**3.35**	**4.23**	1.29
1496	Cytochrome c oxidase subunit 3	0.035	0.290	0.041	0.326	**4.37**	1.12	**5.38**
1497	Cytochrome c oxidase subunit 1	0.160	0.669	0.091	0.657	**2.22**	0.55	**2.38**
1498	Cytochrome c oxidase subunit 2	0.119	0.991	0.548	1.111	**4.40**	**4.41**	**5.40**
1535	Putative cytochrome bd menaquinol oxidase subunit I	0.002	0.010	0.002	0.010	**2.54**	0.92	**2.77**
2081	Cytochrome c-550	0.170	0.449	1.036	0.544	1.39	**5.82**	1.85
2649	Heme-degrading monooxygenase HmoA	0.001	0.005	0.002	0.004	**2.57**	1.38	**2.21**

[1] The darker the red colour, the higher the upregulation relative to the positive control in that treatment. Values in bold indicate that this fold change was significant (Two-sample T-test < 0.05).

3.3.4 Microbial community succession on PET

For the microbial community succession experiments, the biofilm removed from beached plastics was used to inoculate microcosms with mineral media and (a) no additional carbon (control), (b) amorphous PET pieces, (c) PET powder, (d) weathered PET powder (weathering was confirmed by FTIR analyses; Figure 3.5) or (e) BHET. Samples were taken across six weeks of incubation and were taken separately for the planktonic and biofilm communities growing with the amorphous PET. It was determined that the GeneJET Genomic DNA Purification Kit was the cheapest and most efficient of those tested for extracting DNA from colonised plastics (Table 3.2). MiSeq amplicon sequencing of the 16S rRNA gene in these communities, as well as in the inoculum, was carried out in order to gain insight into the microbial community dynamics and succession that occurred during the incubation (DNA yields from these samples are shown in Figure 3.6). These data were processed using the DADA2 workflow and unique taxa are therefore called amplicon sequence variants (ASVs), which were classified down to species level where possible. DNA extraction and PCR negative controls as well as two samples (Day 42 amorphous PET biofilm replicate 2 and Day 42 PET powder replicate 1) were removed from further analyses due to low numbers of reads (<1000); all other samples had a minimum of 4,000 and a mean of 19,000 reads. Figure 3.7, Figure 3.8 and Figure 3.9 summarise the community composition of all samples: Figure 3.7 and Figure 3.8 show relative abundance of all ASVs and Simpsons index of diversity as well as species richness for all samples, respectively and Figure 3.9 shows a phylogenetic analysis and relative abundance of the major 16S rRNA gene ASVs (*i.e.* with a relative abundance of above 0.5% in at least one sample) alongside hierarchical clustering of all samples.

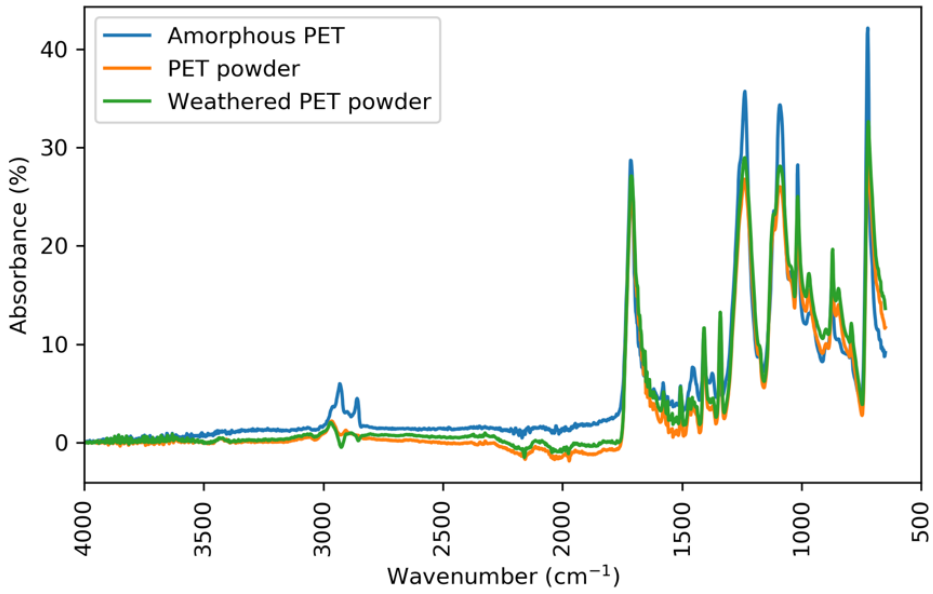

Figure 3.5. Fourier transform infrared spectra of amorphous PET, PET powder and weathered PET powder before incubation with communities or isolates. Differences between the spectra of the PET powder and the weathered PET powder are confirmation of small chemical changes to the weathered PET powder due to weathering.

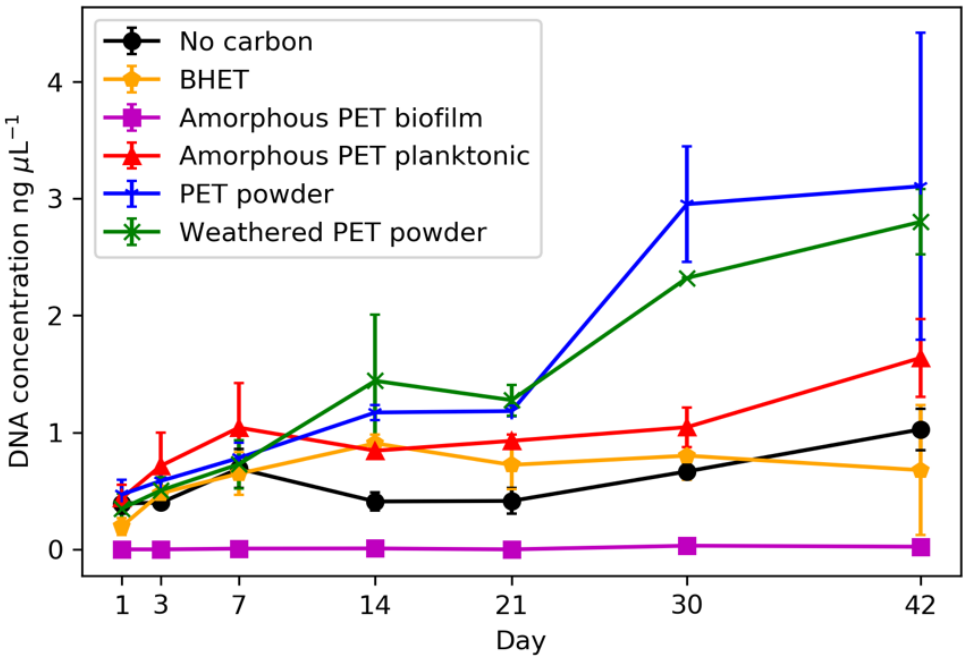

Figure 3.6. DNA yields from all PET succession experiment mesocosms. Points and error bars show means and standard deviations, respectively, of three biological replicates. The DNA concentration in all negative extraction controls was too low to measure aside from day 30 (0.04 ng µL^{-1}). The inoculum for all samples had a mean DNA concentration of 4.36 ng µL^{-1} (n=4). The DNA yields of the majority of Amorphous PET biofilm samples before day 30 of the incubation were below the detection limit but were measurable on days 30 and 42.

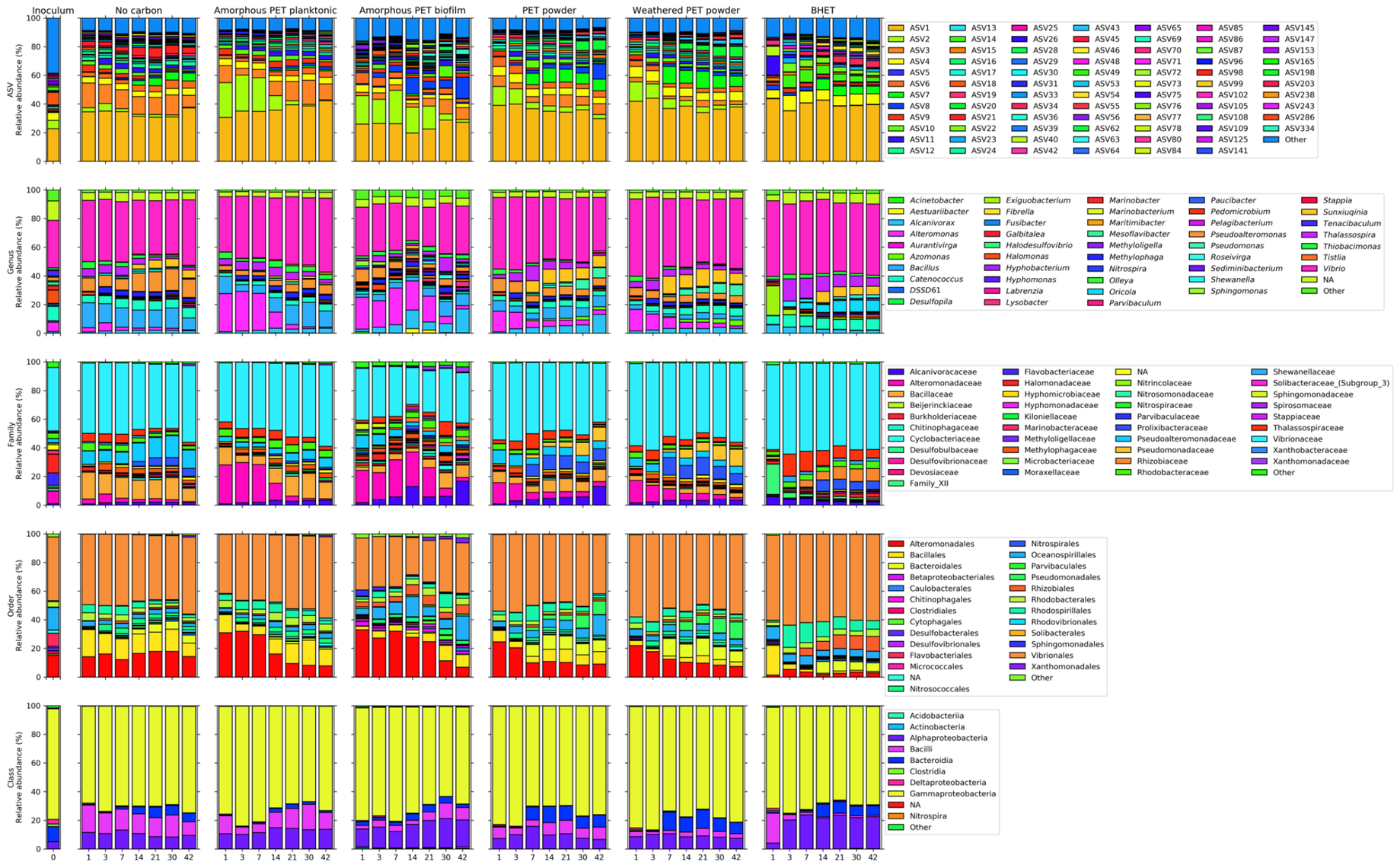

Figure 3.7. Relative abundances of taxa within all samples, with each bar representing the mean of three biological replicates. Each row shows taxa grouped to a different taxonomic level (shown on y label) and other represents all that were present at below 0.5% relative abundance at that level. ASVs are classified to species level where possible: ASV1 *Vibrio*, ASV2 *Alteromonas*, ASV3 *Bacillus*, ASV4 *Vibrio*, ASV5 *Sediminibacterium salmoneum*, ASV6 *Pseudoalteromonas*, ASV7 *Sunxiuqinia*, ASV8 *Alcanivorax*, ASV9 *Thiobacimonas profunda*, ASV10 *Thalassospira lucentensis*, ASV11 *Methylophaga*, ASV12 *Pseudoalteromonas*, ASV13 *Vibrio*, ASV14 *Thalassospira*, ASV15 *Alcanivorax*, ASV16 *Thalassospira*, ASV17 *Vibrio alginolyticus*, ASV18 *Halomonas*, ASV19 *Catenococcus*, ASV20 *Pseudomonas*, ASV21 *Pseudoalteromonas*, ASV22 *Thalassospira*, ASV23 *Shewanella*, ASV24 Beijerinckiaceae, ASV25 DSSD61, ASV26 *Exiguobacterium*, ASV28 *Roseivirga*, ASV29 *Vibrio alginolyticus*, ASV30 *Pedomicrobium*, ASV31 *Alteromonas*, ASV33 *Paucibacter*, ASV34 *Oricola cellulosilytica*, ASV36 *Lysobacter maris*, ASV39 *Catenococcus*, ASV40 *Exiguobacterium*, ASV42 *Tistlia*, ASV43 *Azomonas*, ASV45 Rhizobiaceae, ASV46 *Maritimibacter*, ASV48 *Catenococcus*, ASV49 Halomonadaceae, ASV53 Vibrionaceae, ASV54 *Oricola*, ASV55 *Catenococcus*, ASV56 *Sphingomonas*, ASV62 *Halomonas*, ASV63 Vibrionaceae, ASV64 *Parvibaculum*, ASV65 *Catenococcus*, ASV69 Alphaproteobacteria, ASV70 *Catenococcus*, ASV71 *Hyphomonas*, ASV72 *Marinobacter*, ASV73 *Catenococcus*, ASV75 Vibrionaceae, ASV76 *Aestuariibacter aggregatus*, ASV77 *Vibrio pacinii*, ASV78 *Catenococcus*, ASV80 *Labrenzia aggregata*, ASV84 *Catenococcus*, ASV85 *Hyphobacterium*, ASV86 Vibrionaceae, ASV87 *Stappia*, ASV96 Bacillaceae, ASV98 Gammaproteobacteria, ASV99 *Pseudoalteromonas*, ASV102 *Vibrio*, ASV105 *Marinobacter*, ASV108 *Acinetobacter*, ASV109 Bacillaceae, ASV125 *Pelagibacterium halotolerans*, ASV141 *Sunxiuqinia*, ASV145 *Tenacibaculum litoreum*, ASV147 Halomonadaceae, ASV153 *Mesoflavibacter zeaxanthinifaciens*, ASV165 Rhodobacteraceae, ASV198 *Pseudoalteromonas*, ASV203 *Tenacibaculum*, ASV238 *Catenococcus*, ASV243 *Aurantivirga*, ASV286 *Catenococcus*, ASV334 *Fibrella*.

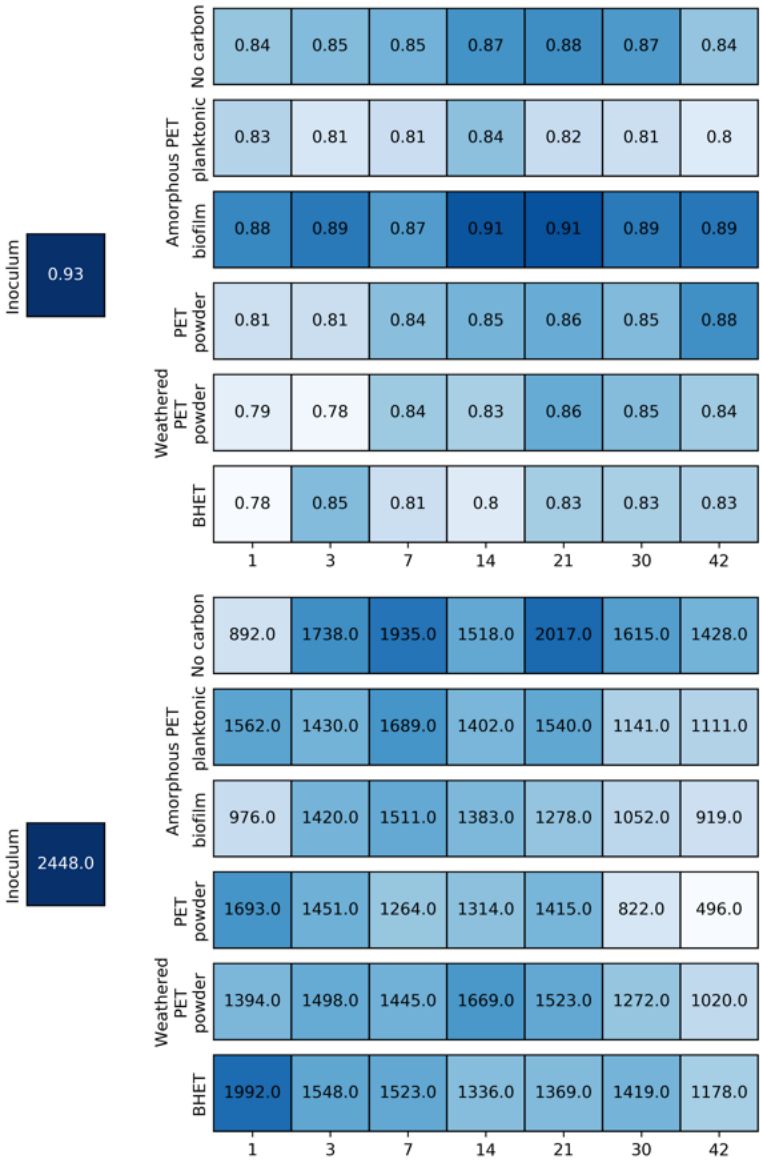

Figure 3.8. Diversity for all samples across 42 days of incubation. Showing Simpsons index of diversity (top) and species richness (bottom). Dark blue colours indicate higher diversity/richness while white indicates low diversity/richness.

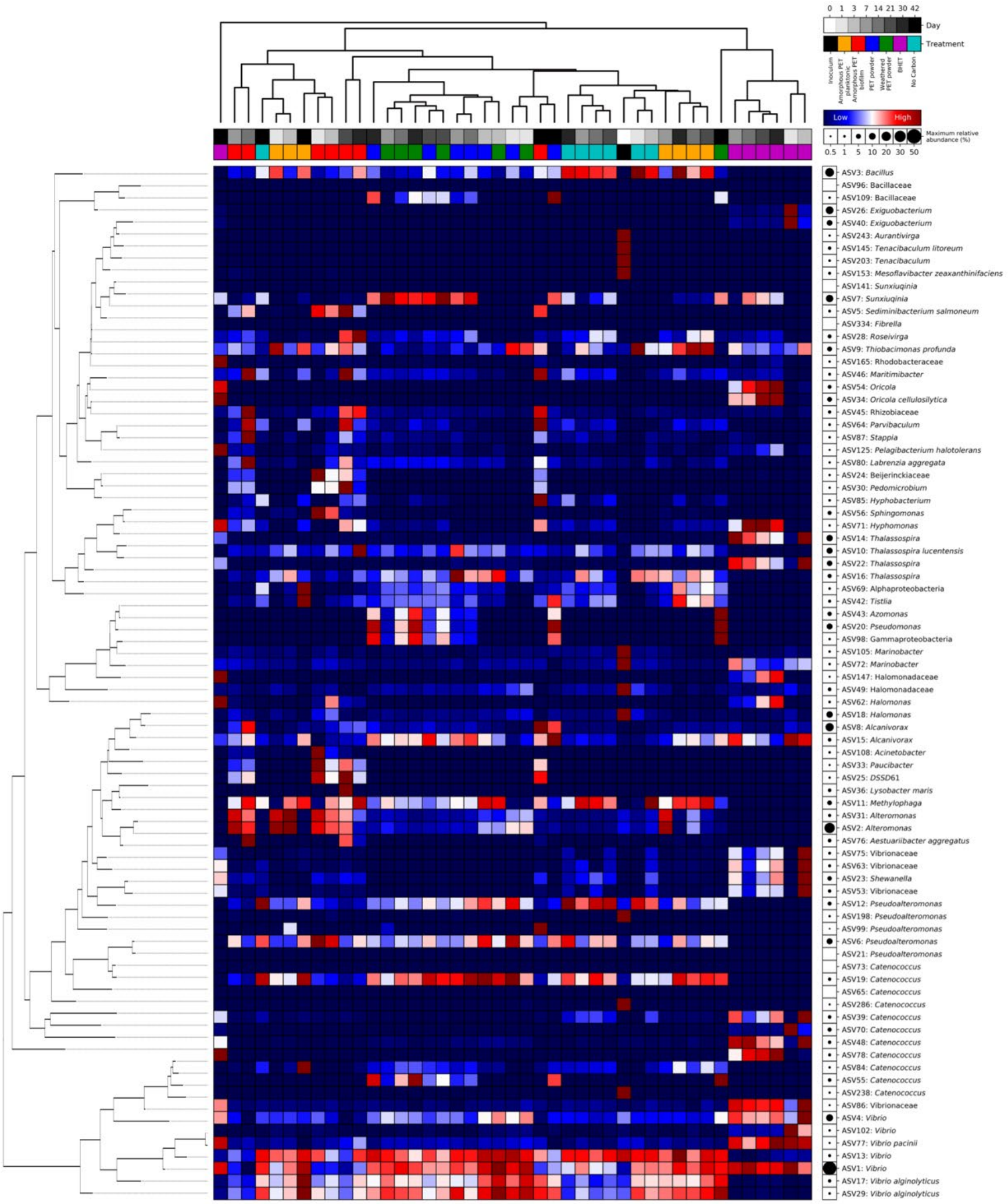

Figure 3.9. Phylogenetic analysis and relative abundance of the major 16S rRNA gene ASVs. Left dendrogram shows phylogenetic grouping of all ASVs with relative abundance above 0.5% in at least one sample (represented by a mid-point rooted maximum likelihood phylogenetic tree). The relative abundance of each ASV (shown by the heatmap) is normalised within each ASV, while black circles on the right of the heatmap represent the maximum relative abundance for that ASV across all samples. Samples are clustered (top) based on Bray-Curtis distance and are coloured by day and treatment. Each row of the heatmap represents the normalised relative abundance for an ASV, while each column represents the abundance for all ASVs (above 0.5% relative abundance) within a treatment at one time point.

Analysis of all communities

Analysis of all 16S rRNA gene communities revealed that only the inoculum, BHET and amorphous PET biofilm samples were statistically significantly different from all other communities (ANOSIM based on Bray-Curtis distance R=0.885, *p*=0.001; R=0.709, *p*=0.001; and R=0.446; *p*=0.001, respectively; Table 3.7). These communities also grouped separately from all others in the nMDS plot and the distances between communities became greater over time (Figure 3.10A). Interestingly, no distinct community succession at the class level was observed, with *Gammaproteobacteria* dominating all samples across all time points and only decreasing slightly in abundance towards the end in the amorphous PET biofilm and planktonic samples. There were, however, differences at levels lower than class, for example, the order *Alteromonodales* (*Gammaproteobacteria*) decreased in abundance in most treatments over time. This appears to be due to the dominance of *Vibrio* spp. in all treatments, possibly masking the effect of other community members (Figure 3.7). The principal response curve redundancy analysis (PRC) revealed the treatment effects that were being concealed by the effect of time (Brink and Besten, 2009), thereby identifying the ASVs that are driving the differences (*i.e.* had the highest or lowest weights) or contributing to similarities (*i.e.* had weights close to one) between treatments (Figure 3.10B). This showed that many of the ASVs that were contributing towards the differences between the amorphous PET biofilm and no carbon control treatments were not present in the BHET treatment, or were present only in very low relative abundances and *vice versa* (Figure 3.10C; Table 3.8). The PET and weathered PET powder communities remained similar to the no carbon control communities throughout and whilst the amorphous PET planktonic communities initially showed small differences with the no carbon control communities, these had almost disappeared by the last time point on day 42. The top ASVs identified by SIMPER analyses as contributing to differences between treatments (Figure 3.11) were also included in the PRC analysis and the ASVs identified by the PRC analysis were therefore focused on.

Table 3.7. Results of PERMANOVA and ANOSIM tests for statistical significance (using Bray-Curtis distance) on all succession experiment samples. ANOSIM results are mentioned in the text as these values are more conservative.

Test		PERMANOVA		ANOSIM	
		Statistic	***p***	**Statistic**	***p***
Inoculum *vs*	All others	8.534	**0.001**	0.885	**0.001**
	No carbon control	16.882	**0.003**	1	**0.002**
	Amorphous PET planktonic	21.152	**0.002**	1	**0.002**
	Amorphous PET biofilm	13.033	**0.003**	1	**0.001**
	PET powder	20.209	**0.001**	1	**0.001**
	Weathered PET powder	20.259	**0.001**	1	**0.001**
	BHET	23.069	**0.003**	1	**0.001**
NCC *vs*	All others	9.463	**0.001**	0.0392	0.249
	Amorphous PET planktonic	8.390	**0.001**	0.315	**0.001**
	Amorphous PET biofilm	24.965	**0.001**	0.792	**0.001**
	PET powder	10.854	**0.001**	0.448	**0.001**
	Weathered PET powder	16.805	**0.001**	0.624	**0.001**
	BHET	42.031	**0.001**	0.964	**0.001**
Amorphous PET planktonic *vs*	All others	5.582	**0.001**	-0.154	0.995
	Amorphous PET biofilm	16.489	**0.001**	0.540	**0.001**
	PET powder	9.640	**0.001**	0.409	**0.001**
	Weathered PET powder	13.990	**0.001**	0.550	**0.001**
	BHET	49.144	**0.001**	0.997	**0.001**
Amorphous PET biofilm *vs*	All others	22.943	**0.001**	0.446	**0.001**
	PET powder	21.319	**0.001**	0.726	**0.001**
	Weathered PET powder	27.019	**0.001**	0.828	**0.001**
	BHET	57.622	**0.001**	1	**0.001**
PET powder *vs*	All others	3.758	**0.002**	-0.212	1
	Weathered PET powder	2.968	**0.025**	0.089	**0.031**
	BHET	41.771	**0.001**	0.982	**0.001**
Weathered PET powder *vs*	All others	5.909	**0.001**	-0.134	0.987
	BHET	37.656	**0.001**	0.961	**0.001**
BHET *vs*	All others	39.508	**0.001**	0.709	**0.001**

Shading indicates the statistical test between that treatment and all other treatments, while non-shaded cells show tests against individual treatments. Bold values indicate statistically significant results.

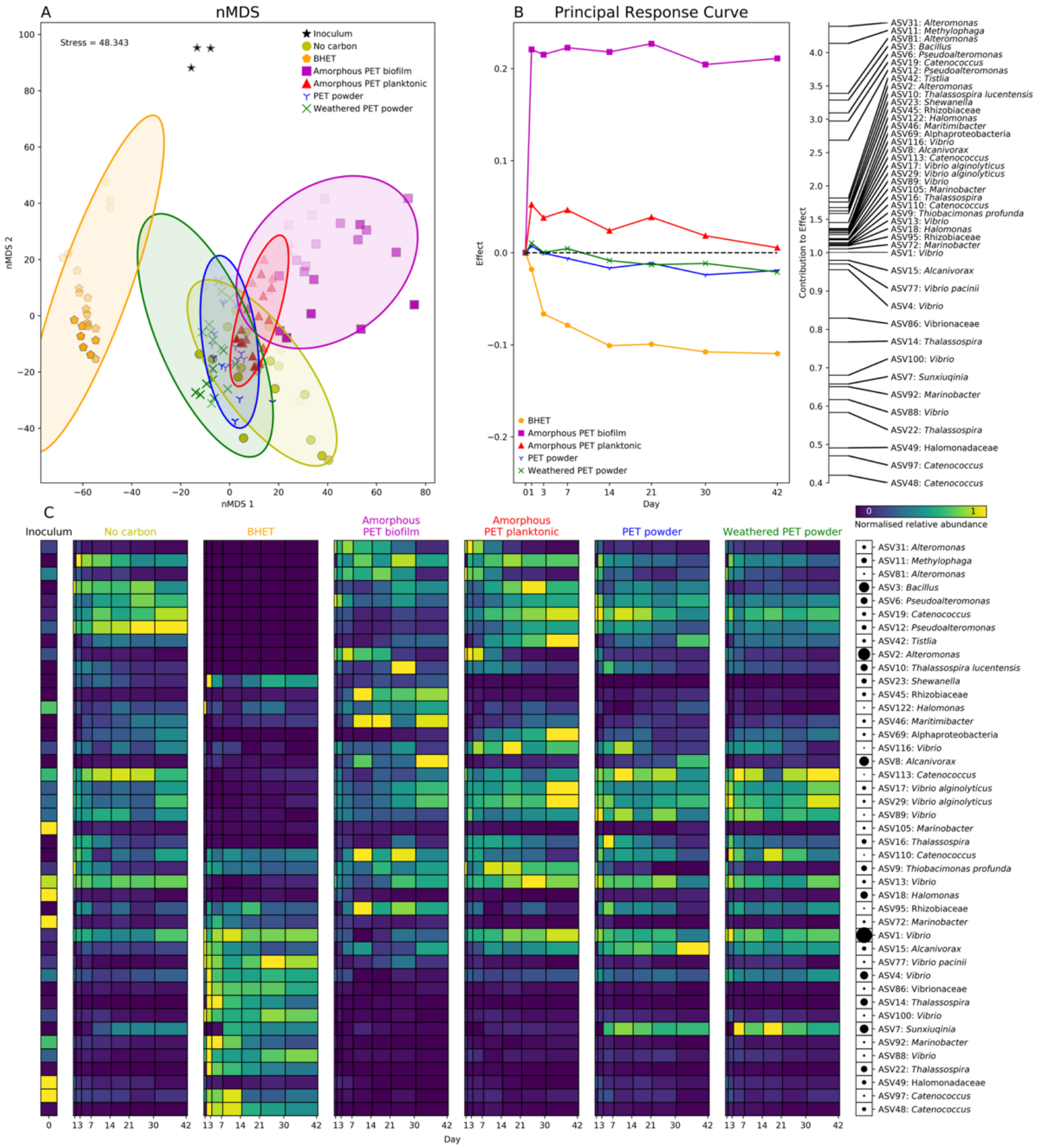

Figure 3.10. Microbial community variation of all succession experiment samples. (**A**) nMDS plot showing Bray-Curtis distance between 16S rRNA gene communities. Each treatment is shown by a different marker and colour and marker colour intensity correlates to day of incubation, where darker colours represent later days. Biological replicates are shown separately, and ellipses show the mean plus the standard deviation for each treatment. (**B**) Principal Response Curve (PRC) using log-transformed absolute abundance, showing the effect of treatment against the no carbon control (*y*=0; left) for all time points with the ASVs that are contributing most to this effect (*i.e.* with a sum of log abundance above 100; right). Values shown are species weights (no unit). (**C**) Heatmap showing normalised relative abundance for all ASVs identified in the PRC analysis, plotted over time. Black circles on the right of the heatmap show the maximum relative abundance for that ASV.

Table 3.8. ASVs identified by the PRC analysis. This includes ASV classifications using DADA2 and BLAST, PRC species weights, the closest representative whole genomes (from the NCBI database, where this was >97% similarity), whether these genomes potentially contain PETases and MHETases, PICRUSt2 nearest sequenced taxon indices (NSTI), the KEGG orthologs present in the genomes according to PICRUSt2 and other relevant information.

ASV	Classification		PRC [1]	NCBI genome reference	PETase HMM	BLAST with MHETase [2]	PICRUSt NSTI [3]	PICRUSt KEGG [4]	Information
	DADA2	BLAST							
ASV31	*Alteromonas*	*Alteromonas macleodii* (100%)	1.48	NC_018632.1 *Alteromonas macleodii* ATCC 27126, complete genome	Score 65.5, E value $8.9e^{-19}$	35% identity, E value 2.3	0.001698	K00632 (2)	*Gammaproteobacteria.* High in abundance in 8-month PET enrichment cultures (Webb, 2012)
ASV11	*Methylophaga*	*Methylophaga thiooxydans (99.19%)*	1.42	NC_017857.3 *Methylophaga nitratireducenticrescens* strain JAM1, complete genome	Score 14.3, E value 0.0026	36% identity, E value 0.70	0.017998	-	*Gammaproteobacteria. Methylophaga* spp. were hydrocarbon degraders involved in the deepwater horizon oil spill (Gutierrez and Aitken, 2014)
ASV81	*Alteromonas*	*Alteromonas macleodii (99.73%)*	1.22	NC_018632.1 *Alteromonas macleodii* ATCC 27126, complete genome	Score 65.5, E value $8.9e^{-19}$	35% identity, E value 2.3	0.003353	K00632 (2)	*Gammaproteobacteria.* High in abundance in 8-month PET enrichment cultures (Webb, 2012)
ASV3	*Bacillus*	*Bacillus pumilus/subtilus (100%)*	1.19	NZ_CP011007.1 *Bacillus pumilus* strain SH-B9, complete genome	Score 19.1, E value 0.00012	31% identity, E value 0.43	0.001639	K00632, K01607, K01821	*Firmicutes.* Possesses a *p*-nitrobenzylesterase that hydrolyses PET (Ribitsch et al., 2012)
ASV6	*Pseudoalteromonas*	*Pseudoalteromonas shioyasakiensis (100%)*	1.13	NZ_CP011028.1 *Pseudoalteromonas espejiana* strain ATCC 29659 chromosome I, complete sequence	Score 66.6, E value $3.6e^{-19}$	43% identity, E value 0.03	0.006766	K00632 (2)	*Gammaproteobacteria.* Previously isolated aerobically on crude oil (Catania et al., 2018) and marine plastic debris (Zadjelovic, *personal communication*)

ASV	Classification		PRC [1]	NCBI genome reference	PETase HMM	BLAST with MHETase [2]	PICRUSt NSTI [3]	PICRUSt KEGG [4]	Information
	DADA2	BLAST							
ASV19	*Pseudomonas*	*Vibrio coralliilyticus/alginolyticus* (95.42%)	1.09	-	-	-	0.031144	K00632 (2), K01607, K01821	*Gammaproteobacteria. Pseudomonas* spp. have previously been found to be capable of degrading PET and a range of other synthetic polymers (PE, PP, PS, PES, PEG, PVC, PUR, PVA) (Wilkes and Aristilde, 2017)
ASV12	*Pseudoalteromonas*	Pseudoalteromonas prydzensis/ shioyasakiensis/ espejiana (95.42%)	0.99	-	-	-	0.033146	K00632 (2)	*Gammaproteobacteria.* Previously isolated aerobically on crude oil (Catania et al., 2018) and marine plastic debris (Zadjelovic, *personal communication*)
ASV42	*Tistlia*	*Tistlia consotensis* (98.65%)	0.60	NZ_FWZX01000015.1 *Tistlia consotensis* USBA 355, whole genome shotgun sequence	NA	27% identity, E value 0.48	0.015072	K00449, K01607 (2)	*Alphaproteobacteria.* Isolated from a saline spring (Dıaz-Cardenas et al., 2010). Ability to degrade plastics or associated compounds not tested
ASV2	*Alteromonas*	*Alteromonas macleodii (99.73%)*	0.57	NC_018632.1 *Alteromonas macleodii* ATCC 27126, complete genome	Score 65.5, E value $8.9e^{-19}$	35% identity, E value 2.3	0.001698	K00632 (2)	*Gammaproteobacteria.* High in abundance in 8-month PET enrichment cultures (Webb, 2012)
ASV10	*Thalassospira lucentensis*	*Thalassospira alkalitolerans (100%)*	0.52	NZ_CP004388.1 *Thalassospira xiamenensis* M-5 = DSM	Score 36.1, E value $8.5e^{-10}$	32% identity, E value 2.6	0.008663	K00448, K00449, K00632 (2),	*Alphaproteobacteria.* High in abundance in 8-month PET enrichment cultures (Webb, 2012)

ASV	Classification		PRC [1]	NCBI genome reference	PETase HMM	BLAST with MHETase [2]	PICRUSt NSTI [3]	PICRUSt KEGG [4]	Information
	DADA2	BLAST							
				17429, complete genome				K01055, K01607 (2), K01857, K14727	and capable of degrading polycyclic aromatic hydrocarbons such as *p*-hydroxybenzoic acid, protocatechuate and catechol (Tsubouchi et al., 2014)
ASV23	*Shewanella*	*Shewanella algae (100%)*	0.49	NZ_LN810019.1 *Shewanella algae* strain MARS 14, whole genome shotgun sequence	Score 32.6, E value $9.8e^{-9}$	38% identity, E value 0.4	0.001695	K00632 (2)	*Gammaproteobacteria.* Human pathogens found in warm marine habitats and infecting ears, skin and soft tissue (Holt and Bruun, 2005)
ASV45	Rhizobiaceae	*Nitratireductor basaltis (98.11%)*	0.46	NZ_KK073880.1 *Aquamicrobium defluvii* strain W13Z1 V9__scaffold_04, whole genome shotgun sequence	NA	44% identity, E value 2.9	0.011687	K00448, K00449, K00632, K01055, K01607 (2), K01857, K04101, K10217, K10218, K16514, K16515	*Alphaproteobacteria.* Other closely-related *Nitratireductor* spp. are capable of degrading the PAH pyrene (Lai et al., 2011)
ASV122	*Halomonas*	*Halomonas desiderata (99.46%)*	0.37	NZ_CP014226.1 *Halomonas chromatireducens* strain AGD 8-3, complete genome	Score 18.1, E value 0.00024	26% identity, E value 0.47	0.016664	K00632, K01607, K01821, K14727	*Gammaproteobacteria.* Isolated from municipal sewage works for nitrocellulose degradation (Berendes et al., 1996)

ASV	Classification		PRC [1]	NCBI genome reference	PETase HMM	BLAST with MHETase [2]	PICRUSt NSTI [3]	PICRUSt KEGG [4]	Information
	DADA2	BLAST							
ASV46	*Maritimibacter*	*Pseudoruegeria lutimaris (99.46%)*	0.31	NZ_CYSF01000012.1 *Thalassobius mediterraneus* strain CECT 5383, whole genome shotgun sequence	Score 20.9, E value $3.1e^{-6}$	25% identity, E value 0.01	0.003386	K01055, K01607 (2)	*Gammaproteobacteria.*
ASV69	Alphaproteobacteria	*Tistlia consotensis (98.61%)*	0.30	NZ_FWZX01000015.1 *Tistlia consotensis* USBA 355, whole genome shotgun sequence	NA	27% identity, E value 0.48	0.05688	K00449, K01607 (2)	Isolated from a saline spring (Dıaz-Cardenas et al., 2010). Ability to degrade plastics or associated compounds not tested
ASV116	*Vibrio*	*Vibrio coralliilyticus/alginolyticus (99.73%)*	0.30	NZ_CP009264.1 *Vibrio coralliilyticus* strain OCN014 chromosome 1, complete sequence	Score 15.2, E value 0.0015	27% identity, E value 0.41	0.006594	K00632 (2)	*Gammaproteobacteria.* Consortia of *V. alginolyticus* and *V. parahaemolyticus* previously shown to degrade PVA-LLDPE (Raghul et al., 2014)
ASV8	*Alcanivorax*	*Alcanivorax dieselolei (98.39%)*	0.28	NC_018691.1 *Alcanivorax dieselolei* B5, complete genome	Score 33.7, E value $5.1e^{-9}$	33% identity, E value $2e^{-68}$ (annotated as MHETase)	0.015576	K00632 (2)	*Gammaproteobacteria.* Similar species previously isolated from marine plastic debris and shown to degrade hydrocarbons and polyesters (Zadjelovic et al., 2019)
ASV113	*Catenococcus*	*Vibrio coralliilyticus/alginolyticus (99.73%)*	0.27	NZ_CP009264.1 *Vibrio coralliilyticus* strain OCN014 chromosome 1, complete sequence	Score 15.2, E value 0.0015	27% identity, E value 0.41	0.003357	K00632 (2), K01607, K01821	*Gammaproteobacteria.* Consortia of *V. alginolyticus* and *V. parahaemolyticus* previously shown to

ASV	Classification		PRC [1]	NCBI genome reference	PETase HMM	BLAST with MHETase [2]	PICRUSt NSTI [3]	PICRUSt KEGG [4]	Information
	DADA2	BLAST							
									degrade PVA-LLDPE (Raghul et al., 2014)
ASV17	*Vibrio alginolyticus*	*Vibrio coralliilyticus/alginolyticus (99.73%)*	0.26	NZ_CP009264.1 *Vibrio coralliilyticus* strain OCN014 chromosome 1, complete sequence	Score 15.2, E value 0.0015	27% identity, E value 0.41	0.003354	K00632 (2), K01607, K01821	*Gammaproteobacteria.* Consortia of *V. alginolyticus* and *V. parahaemolyticus* previously shown to degrade PVA-LLDPE (Raghul et al., 2014)
ASV29	*Vibrio alginolyticus*	*Vibrio coralliilyticus/alginolyticus (99.73%)*	0.24	NZ_CP009264.1 *Vibrio coralliilyticus* strain OCN014 chromosome 1, complete sequence	Score 15.2, E value 0.0015	27% identity, E value 0.41	0.004935	K00632 (2), K01607	*Gammaproteobacteria.* Consortia of *V. alginolyticus* and *V. parahaemolyticus* previously shown to degrade PVA-LLDPE (Raghul et al., 2014)
ASV89	*Vibrio*	*Vibrio diazotrophicus/ coralliilyticus/ alginolyticus/ tubiashii/ fluvialis/ parahaemolyticus (99.73%)*	0.19	NZ_CP009264.1 *Vibrio coralliilyticus* strain OCN014 chromosome 1, complete sequence	Score 15.2, E value 0.0015	27% identity, E value 0.41	0.004829	K00632 (2), K01607	*Gammaproteobacteria.* Consortia of *V. alginolyticus* and *V. parahaemolyticus* previously shown to degrade PVA-LLDPE (Raghul et al., 2014)
ASV105	*Marinobacter*	*Marinobacter salarius (100%)*	0.18	NZ_CP007152.1 *Marinobacter salarius* strain R9SW1, complete genome	Score 19.9, E value $9.6e^{-5}$	27% identity, E value 0.25	0.004956	K00449, K00632, K01055, K01617, K01821 (2), K10217	*Gammaproteobacteria.* Similar *Marinobacter* spp. were high in abundance in 8-month PET enrichment cultures (Webb, 2012)

ASV	Classification		PRC [1]	NCBI genome reference	PETase HMM	BLAST with MHETase [2]	PICRUSt NSTI [3]	PICRUSt KEGG [4]	Information
	DADA2	BLAST							
ASV16	*Thalassospira*	*Thalassospira alkalitolerans (93.57%)*	0.18	-	-	-	0.077993	K00448, K00449, K00632 (2), K01055, K01607 (2), K01857, K14727, K16514	*Alphaproteobacteria.* High in abundance in 8-month PET enrichment cultures (Webb, 2012) and capable of degrading polycyclic aromatic hydrocarbons such as *p*-hydroxybenzoic acid, protocatechuate and catechol (Tsubouchi et al., 2014)
ASV110	*Catenococcus*	*Vibrio coralliilyticus/alginolyticus (93.12%)*	0.14	-	-	-	0.04831	K00632 (2), K01607, K01821	*Gammaproteobacteria.* Consortia of *V. alginolyticus* and *V. parahaemolyticus* previously shown to degrade PVA-LLDPE (Raghul et al., 2014)
ASV9	*Thiobacimonas profunda*	*Salipiger nanhaiensis /Thiobacimonas profunda (100%)*	0.13	NZ_CP014796.1 *Salipiger profundus* strain JLT2016 chromosome, complete genome	Score 23.1, E value $8.5e^{-6}$	38% identity, E value $2e^{-97}$ (annotated as MHETase)	0.000101	K00632, K01055, K01607 (2), K01857	*Alphaproteobacteria. Salipiger nanhaiensis* is a later heterotypic synonym of *Thiobacimonas profunda* (Huang et al., 2017).
ASV13	*Vibrio*	*Vibrio coralliilyticus/alginolyticus (99.73%)*	0.11	NZ_CP009264.1 *Vibrio coralliilyticus* strain OCN014 chromosome 1, complete sequence	Score 15.2, E value 0.0015	27% identity, E value 0.41	0.001694	K00632 (2)	*Gammaproteobacteria.* Consortia of *V. alginolyticus* and *V. parahaemolyticus* previously shown to degrade PVA-LLDPE (Raghul et al., 2014)

ASV	Classification		PRC [1]	NCBI genome reference	PETase HMM	BLAST with MHETase [2]	PICRUSt NSTI [3]	PICRUSt KEGG [4]	Information
	DADA2	BLAST							
ASV18	*Halomonas*	*Halomonas pantelleriense (98.92%)*	0.11	NZ_CP013106.1 *Halomonas huangheensis* strain BJGMM-B45, complete genome	Score 25.5, E value $1.5e^{-6}$	33% identity, E value 0.3	0.021214	K00448, K00449, K00632, K01607, K01821, K01857, K14727	*Gammaproteobacteria.* Similar bacterium, *H. xianhensis* was isolated from crude oil (Zhao et al., 2012)
ASV95	Rhizobiaceae	*Nitratireductor basaltis (91.80%)*	0.10	-	-	-	0.055618	K00448, K00449, K00632, K01055, K01607 (2), K01857, K04101, K10217, K10218, K16514, K16515	*Alphaproteobacteria.* Other closely-related *Nitratireductor* spp. are capable of degrading the PAH pyrene (Lai et al., 2011)
ASV72	*Marinobacter*	*Marinobacter nanhaiticus (99.19%)*	0.06	NZ_KB822693.1 *Marinobacter nanhaiticus* D15-8W super1, whole genome shotgun sequence	Score 423.9, E value $6.4e^{-128}$	30% identity, E value 0.42	0.032605	K00632, K01821	*Gammaproteobacteria.* Hydrocarbon-degrading bacterium able to degrade naphthalene, phenanthrene and anthracene (Gao et al., 2013)
ASV1	*Vibrio*	*Vibrio coralliilyticus/alginolyticus (100%)*	0.01	NZ_CP009264.1 *Vibrio coralliilyticus* strain OCN014 chromosome 1, complete sequence	Score 15.2, E value 0.0015	27% identity, E value 0.41	0.0017	K00632 (2), K01607, K01821	*Gammaproteobacteria.* Consortia of *V. alginolyticus* and *V. parahaemolyticus* previously shown to

ASV	Classification		PRC [1]	NCBI genome reference	PETase HMM	BLAST with MHETase [2]	PICRUSt NSTI [3]	PICRUSt KEGG [4]	Information
	DADA2	BLAST							
									degrade PVA-LLDPE (Raghul et al., 2014)
ASV15	*Alcanivorax*	*Alcanivorax dieselolei (94.64%)*	-0.02	-	-	-	0.060091	K00632 (2)	*Gammaproteobacteria.* Similar species previously isolated from marine plastic debris and shown to degrade hydrocarbons and polyesters (Zadjelovic et al., 2019)
ASV77	*Vibrio pacinii*	*Vibrio ostreicida (99.73%)*	-0.03	NZ_CP009264.1 *Vibrio coralliilyticus* strain OCN014 chromosome 1, complete sequence	Score 15.2, E value 0.0015	27% identity, E value 0.41	0.020211	K00632 (2)	*Gammaproteobacteria.* Bivalve larvae pathogen (Prado et al., 2014)
ASV4	*Vibrio*	*Vibrio tubiashii (100%)*	-0.05	NZ_CP009354.1 *Vibrio tubiashii* ATCC 19109 chromosome 1, complete sequence	Score 14.1, E value 0.003	32% identity, E value 0.62	0.017995	K00632 (2)	*Gammaproteobacteria.* Oyster larvae pathogen (Hasegawa et al., 2008)
ASV86	Vibrionaceae	*Vibrio coralliilyticus/alginolyticus (99.73%)*	-0.11	NZ_CP009264.1 *Vibrio coralliilyticus* strain OCN014 chromosome 1, complete sequence	Score 15.2, E value 0.0015	27% identity, E value 0.41	0.003357	K00632 (2), K01607, K01821	*Gammaproteobacteria.* Consortia of *V. alginolyticus* and *V. parahaemolyticus* previously shown to degrade PVA-LLDPE (Raghul et al., 2014)
ASV14	*Thalassospira*	*Thalassospira australica (98.37%)*	-0.27	-	-	-	0.005428	K00448 (2), K00449 (2), K00632 (2), K01055,	*Alphaproteobacteria.* High in abundance in 8-month PET enrichment cultures (Webb, 2012) and other *Thalassospira* spp. are capable of degrading polycyclic

ASV	Classification		PRC [1]	NCBI genome reference	PETase HMM	BLAST with MHETase [2]	PICRUSt NSTI [3]	PICRUSt KEGG [4]	Information
	DADA2	BLAST							
								K01607 (2), K01821, K01857	aromatic hydrocarbons such as *p*-hydroxybenzoic acid, protocatechuate and catechol (Tsubouchi et al., 2014)
ASV100	*Vibrio*	*Vibrio coralliilyticus/alginolyticus (100%)*	-0.39	NZ_CP009264.1 *Vibrio coralliilyticus* strain OCN014 chromosome 1, complete sequence	Score 15.2, E value 0.0015	27% identity, E value 0.41	0.021972	K00632 (2)	*Gammaproteobacteria.* Consortia of *V. alginolyticus* and *V. parahaemolyticus* previously shown to degrade PVA-LLDPE (Raghul et al., 2014)
ASV7	*Sunxiuqinia*	*Sunxiuqinia elliptica (99.18%)*	-0.42	-	-	-	0.005011	-	*Bacteroidia.* Isolated from sediment in a sea cucumber farm (Qu et al., 2011)
ASV92	*Marinobacter*	*Marinobacter daqiaonensis (94.10%)*	-0.43	-	-	-	0.181633	K00632, K01607, K01821	*Gammaproteobacteria.* Other similar species are hydrocarbon-degrading and able to degrade naphthalene, phenanthrene and anthracene (Gao et al., 2013)
ASV88	*Vibrio*	*Vibrio ostreicida (99.46%)*	-0.48	NZ_CP009264.1 *Vibrio coralliilyticus* strain OCN014 chromosome 1, complete sequence	Score 15.2, E value 0.0015	27% identity, E value 0.41	0.018522	K00632 (2)	*Gammaproteobacteria.* Bivalve larvae pathogen (Prado et al., 2014)
ASV22	*Thalassospira*	*Thalassospira australica (92.49%)*	-0.54	-	-	-	0.079532	K00448 (2), K00449	*Alphaproteobacteria.* High in abundance in 8-month PET enrichment

ASV	Classification		PRC [1]	NCBI genome reference	PETase HMM	BLAST with MHETase [2]	PICRUSt NSTI [3]	PICRUSt KEGG [4]	Information
	DADA2	BLAST							
								(2), K00632 (2), K01055, K01607 (2), K01821, K01857	cultures (Webb, 2012) and other *Thalassospira* spp. are capable of degrading polycyclic aromatic hydrocarbons such as *p*-hydroxybenzoic acid, protocatechuate and catechol (Tsubouchi et al., 2014)
ASV49	Halomonadaceae	*Halomonas cupida (94.12%)*	-0.71	-	-	-	0.083501	K00632, K01607, K14727	*Gammaproteobacteria.* Similar bacterium, *H. xianhensis* was isolated from crude oil (Zhao et al., 2012)
ASV97	*Catenococcus*	*Vibrio coralliilyticus/alginolyticus (94.91%)*	-0.75	-	-	-	0.175895	K00632, K01607, K01857	*Gammaproteobacteria.* Consortia of *V. alginolyticus* and *V. parahaemolyticus* previously shown to degrade PVA-LLDPE (Raghul et al., 2014)
ASV48	*Catenococcus*	*Vibrio coralliilyticus/alginolyticus (93.55%)*	-0.87	-	-	-	0.048576	K00632 (2), K01607, K01821	*Gammaproteobacteria.* Consortia of *V. alginolyticus* and *V. parahaemolyticus* previously shown to degrade PVA-LLDPE (Raghul et al., 2014)

[1] Principal response curve species weights.

[2] Values for the closest match within the genome for local BLAST searches against the *Ideonella sakaiensis* MHETase protein sequence.

[3] PICRUSt nearest sequences taxon index (NSTI).

[4] KEGG orthologs related to phthalate, terephthalate and benzoate degradation present in the PICRUSt artificial metagenomes. Numbers in brackets indicate how many copies of this gene were present, if more than one. Including: K00448 Protocatechuate 3,4-dioxygenase beta subunit, K00449 Protocatechuate 3,4-dioxygenase alpha subunit, K00455 Protocatechuate 2,3-dioxygenase, K00624 Phthalate 3,4-dihydrodiol dehydrogenase, K00632 Acetyl-CoA acetyltransferase, K01031 3-oxoadipate CoA-transferase alpha subunit, K01032 3-oxoadipate CoA-transferase beta subunit, K01055 3-oxoadipate enol-lactonase, K01607 4-carboxymuconolactone decarboxylase, K01617 2-oxo-3-hexenedioate decarboxylase, K01821, K01857, K04100, K04101, K04102, K07823, K10217, K10218, K10219, K10220, K10221, K14727 4-carboxymuconolactone decarboxylase, K15556 Phthalate transporter *ophF*, K15557 Phthalate transporter *ophG*, K15558 Phthalate transporter *ophH*, K16514 4-oxalomesaconate tautomerase, K16515 4-oxalomesaconate hydratase, K18067 Phthalate 4,5-dihydrodiol dehydrogenase, K18068 Phthalate 4,5-dioxygenase, K18074 Terephthalate 1,2-dioxygenase, K18075 Terephthalate 1,2-dioxygenase, K18076 1,2-dihydroxy-3,5-cyclohexadiene-1,4-dicarboxylate dehydrogenase, K18077 Terephthalate 1,2-dioxygenase, K18252 Phthalate 3,4-dioxygenase and K18256 3,4-dihydroxyphthalate decarboxylase.

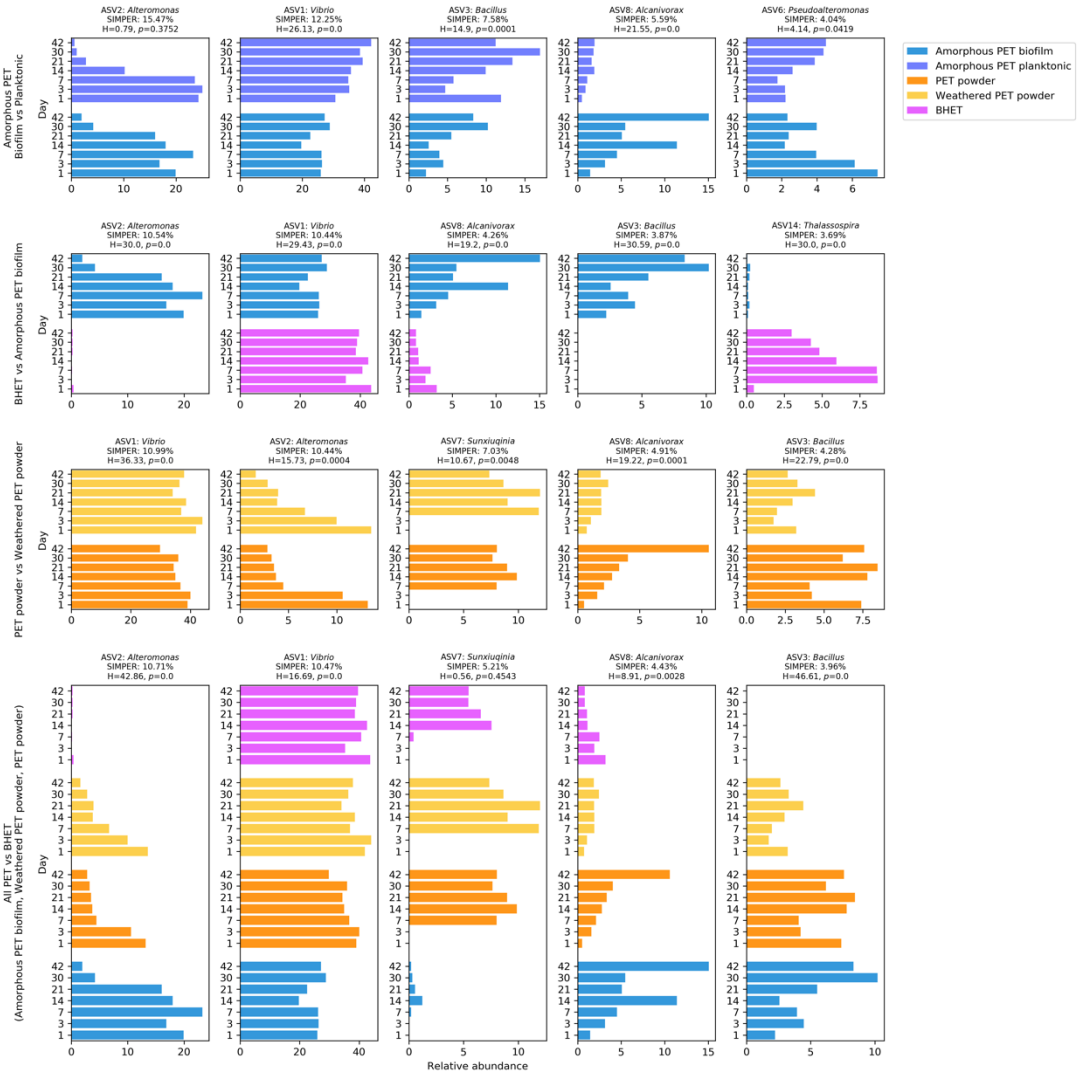

Figure 3.11. Graphs showing the relative abundances of the top five ASVs identified by SIMPER analyses. Tests were carried out between the amorphous PET biofilm and planktonic treatments, BHET and amorphous PET biofilm treatments, PET powder and weathered PET powder treatments and all PET (amorphous PET biofilm, PET powder and weathered PET powder grouped) and BHET treatments. Relative abundances are shown across all sampling time points and titles show ASV, classification, SIMPER contribution to differences between treatments and results of Kruskal-Wallis tests for significance.

Determination of early, middle or late colonisers

ASVs were defined as early, middle or late colonisers depending on whether they peaked in abundance on days 1-7, 14-30 or 42, respectively. This was carried out separately for each treatment and ASVs were only included if they were above 0.5% abundance in at least one time point for that treatment (Figure 3.12 and Table 3.9). Overall, this analysis identified 77 ASVs; 24 that were early, 15 that were middle and 2 that were late colonisers. The others did not clearly differentiate between different time points. This revealed that there were 19 ASVs unique (above 0.5% abundance only in this treatment) to each of the BHET (11 early colonisers, 3 middle and 5 late) and amorphous PET biofilm treatments (9 early, 8 middle and

2 late), 4 ASVs unique to the no carbon control treatment (1 early and 3 middle) and 1 ASV unique to each of the PET powder and weathered PET powder treatments (both late). There were also 4 ASVs that were only in the PET powder and weathered PET powder treatments (1 late, 3 that were middle in PET powder and late in weathered PET powder).

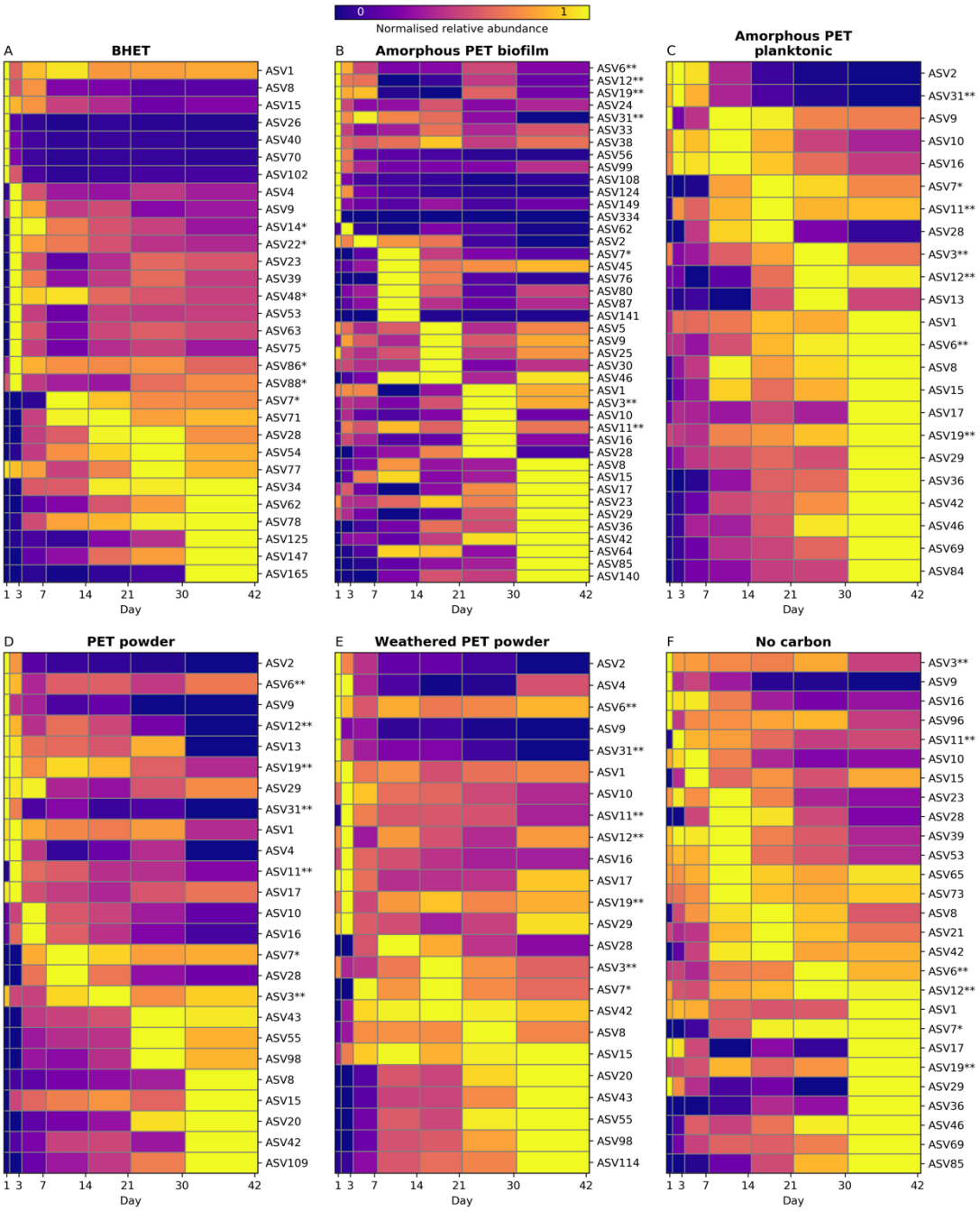

Figure 3.12. Heatmap showing colonisation dynamics for early, middle and late colonisers. **(A)** BHET, **(B)** amorphous PET biofilm, **(C)** amorphous PET planktonic, **(D)** PET powder, **(E)** Weathered PET powder and **(F)** No carbon control communities for all ASVs with abundance above 0.5% in at least one time point. ASV abundance is normalised within each ASV for each treatment and ASVs were plotted in order of the day on which they had the highest relative abundance, with those that were most abundant on days 1-7, 14-30 and 42 classified as early, middle and late colonisers, respectively. ASVs with a PRC weight (effect value) of below 0.9 (Figure 3.10B), *i.e.* those most associated with the BHET treatment, are denoted with *, while those with a PRC weight of above two, *i.e.* those most associated with the amorphous PET biofilm treatment, are denoted with **. Details on these ASVs, including taxonomic classification, are shown in Table 3.9.

Table 3.9. Analysis of early, middle or late colonisers, showing the day on which that ASV was most abundant in that treatment. Only ASVs that were above 0.5% in abundance in at least one time point in that treatment were included.

ASV	Class	No carbon control	Amorphous PET biofilm	Amorphous PET planktonic	PET powder	Weathered PET powder	BHET	Early, middle or late coloniser
ASV001: *Vibrio*	*Gammaproteobacteria*	42	30	42	3	3	1	
ASV002: *Alteromonas*	*Gammaproteobacteria*		7	3	1	1		Early
ASV003: *Bacillus*	*Bacilli*	1	30	30	21	21		
ASV004: *Vibrio*	*Gammaproteobacteria*				3	1	3	Early
ASV005: *Sediminibacterium salmoneum*	*Bacteroidia*		21					Middle
ASV006: *Pseudoalteromonas*	*Gammaproteobacteria*	30	1	42	1	1		
ASV007: *Sunxiuqinia*	*Bacteroidia*	42	14	21	14	21	14	
ASV008: *Alcanivorax*	*Gammaproteobacteria*	21	42	42	42	30	1	
ASV009: *Thiobacimonas profunda*	*Alphaproteobacteria*	1	21	14	1	1	3	
ASV010: *Thalassospira lucentensis*	*Alphaproteobacteria*	7	30	14	7	3		
ASV011: *Methylophaga*	*Gammaproteobacteria*	3	30	21	3	3		
ASV012: *Pseudoalteromonas*	*Gammaproteobacteria*	30	1	30	1	3		
ASV013: *Vibrio*	*Gammaproteobacteria*			30	1			
ASV014: *Thalassospira*	*Alphaproteobacteria*						3	Early
ASV015: *Alcanivorax*	*Gammaproteobacteria*	7	42	42	42	42	1	
ASV016: *Thalassospira*	*Alphaproteobacteria*	1	30	14	7	3		
ASV017: *Vibrio alginolyticus*	*Gammaproteobacteria*	42	42	42	3	3		
ASV019: *Catenococcus*	*Gammaproteobacteria*	42	1	42	1	3		
ASV020: *Pseudomonas*	*Gammaproteobacteria*				42	42		Late
ASV021: *Pseudoalteromonas*	*Gammaproteobacteria*	21						Middle
ASV022: *Thalassospira*	*Alphaproteobacteria*						3	Early
ASV023: *Shewanella*	*Gammaproteobacteria*	14	42				3	
ASV024: Beijerinckiaceae	*Alphaproteobacteria*		1					Early
ASV025: *DSSD61*	*Gammaproteobacteria*		21					Middle
ASV026: *Exiguobacterium*	*Bacilli*						1	Early
ASV028: *Roseivirga*	*Bacteroidia*	14	30	21	14	14	30	Middle
ASV029: *Vibrio alginolyticus*	*Gammaproteobacteria*	42	42	42	1	3		

ASV	Class	No carbon control	Amorphous PET biofilm	Amorphous PET planktonic	PET powder	Weathered PET powder	BHET	Early, middle or late coloniser
ASV030: *Pedomicrobium*	*Alphaproteobacteria*		21					Middle
ASV031: *Alteromonas*	*Gammaproteobacteria*		1	3	1	1		Early
ASV033: *Paucibacter*	*Gammaproteobacteria*		1					Early
ASV034: *Oricola cellulosilytica*	*Alphaproteobacteria*						42	Late
ASV036: *Lysobacter maris*	*Gammaproteobacteria*	42	42	42				Late
ASV038: *Nitrospira*	*Nitrospira*		1					Early
ASV039: *Catenococcus*	*Gammaproteobacteria*	14					3	
ASV040: *Exiguobacterium*	*Bacilli*						1	Early
ASV042: *Tistlia*	*Alphaproteobacteria*	21	42	42	42	21		
ASV043: *Azomonas*	*Gammaproteobacteria*				30	42		Middle/late
ASV045: Rhizobiaceae	*Alphaproteobacteria*		14					Middle
ASV046: *Maritimibacter*	*Alphaproteobacteria*	42	21	42				
ASV048: *Catenococcus*	*Gammaproteobacteria*						3	Early
ASV053: Vibrionaceae	*Gammaproteobacteria*	14					3	
ASV054: *Oricola*	*Alphaproteobacteria*						30	Middle
ASV055: *Catenococcus*	*Gammaproteobacteria*				30	42		Middle/late
ASV056: *Sphingomonas*	*Alphaproteobacteria*		1					Early
ASV062: *Halomonas*	*Gammaproteobacteria*		3				42	
ASV063: Vibrionaceae	*Gammaproteobacteria*						3	Early
ASV064: *Parvibaculum*	*Alphaproteobacteria*		42					Late
ASV065: *Catenococcus*	*Gammaproteobacteria*	14						Middle
ASV069: Alphaproteobacteria	*Alphaproteobacteria*	42		42				Late
ASV070: *Catenococcus*	*Gammaproteobacteria*						1	Early
ASV071: *Hyphomonas*	*Alphaproteobacteria*						21	Middle
ASV073: *Catenococcus*	*Gammaproteobacteria*	14						Middle
ASV075: Vibrionaceae	*Gammaproteobacteria*						3	Early
ASV076: *Aestuariibacter aggregatus*	*Gammaproteobacteria*		14					Middle
ASV077: *Vibrio pacinii*	*Gammaproteobacteria*						30	Middle
ASV078: *Catenococcus*	*Gammaproteobacteria*						42	Late

ASV	Class	No carbon control	Amorphous PET biofilm	Amorphous PET planktonic	PET powder	Weathered PET powder	BHET	Early, middle or late coloniser
ASV080: *Labrenzia aggregate*	*Alphaproteobacteria*		14					Middle
ASV084: *Catenococcus*	*Gammaproteobacteria*			42				Late
ASV085: *Hyphobacterium*	*Alphaproteobacteria*	42	42					Late
ASV086: Vibrionaceae	*Gammaproteobacteria*						3	Early
ASV087: *Stappia*	*Alphaproteobacteria*		14					Middle
ASV088: *Vibrio*	*Gammaproteobacteria*						3	Early
ASV096: Bacillaceae	*Bacilli*	1			30			Early
ASV098: Gammaproteobacteria	*Gammaproteobacteria*					42		Middle/late
ASV099: *Pseudoalteromonas*	*Gammaproteobacteria*		1					Early
ASV102: *Vibrio*	*Gammaproteobacteria*						1	Early
ASV108: *Acinetobacter*	*Gammaproteobacteria*		1					Early
ASV109: Bacillaceae	*Bacilli*				42			Late
ASV114: *Vibrio*	*Gammaproteobacteria*					42		Late
ASV124: *Stakelama*	*Alphaproteobacteria*		1					Early
ASV125: *Pelagibacterium halotolerans*	*Alphaproteobacteria*						42	Late
ASV140: *Methyloligella*	*Alphaproteobacteria*		42					Late
ASV141: *Sunxiuqinia*	*Bacteroidia*		14					Middle
ASV147: Halomonadaceae	*Gammaproteobacteria*						42	Late
ASV149: *Galbitalea*	*Actinobacteria*		1					Early
ASV165: Rhodobacteraceae	*Alphaproteobacteria*						42	Late
ASV334: *Fibrella*	*Bacteroidia*		1					Early

Interestingly, both the ASVs with a weight (contribution to effect) in the PRC analysis of above two (ASV31 *Alteromonas*, ASV11 *Methylophaga*, ASV81 *Alteromonas*, ASV3 *Bacillus*, ASV6 *Pseudoalteromonas*, ASV19 *Catenococcus* and ASV12 *Pseudoalteromonas*) and below 0.9 (ASV48 *Catenococcus*, ASV97 *Catenococcus*, ASV49 Halomonadaceae, ASV22 *Thalassospira*, ASV88 *Vibrio*, ASV92 *Marinobacter*, ASV7 *Sunxiuqinia*, ASV100 *Vibrio*, ASV14 *Thalassospira* and ASV86 Vibrionaceae), *i.e.* those that were most associated with the amorphous PET biofilm or BHET treatments, respectively (Figure 3.10B), were predominantly early colonisers that were only present above 0.5% relative abundance in those treatments (Figure 3.12). Other ASVs, with weights closer to one, were generally middle or late colonisers, or varied between treatments and were more widespread across the treatments. This suggests that in both the amorphous PET biofilm and BHET treatments, an initial selection for organisms that are capable of the degradation of PET or BHET, respectively, is observed and then a succession at later time points, with an abundance of organisms that are likely not capable of degradation themselves but may benefit from the production of sub-products or other metabolic products from others that do degrade (Christie-Oleza et al., 2017; Noriega-Ortega et al., 2019). This was confirmed by the hierarchical clustering, showing that the amorphous PET biofilm samples from days 7-30 group closely to the BHET samples from days 1 and 3 (Figure 3.9).

3.3.5 Artificially assembled metagenome

An artificial metagenome analysis was carried out using PICRUSt2 (Langille, 2018) to determine the predicted abundance of genes related to protocatechuate degradation in the inoculum, BHET and amorphous PET biofilm samples (Figure 3.13). The genes that are necessary for the conversion of PET or BHET to TPA and then protocatechuate are not currently available in PICRUSt. This showed that protocatechuate degradation genes peaked in abundance on days 3 and 7 in the BHET treatment and on days 21 and 30 in the amorphous PET biofilm treatment. For example, protocatechuate 3,4-dioxygenase alpha (K00448) and beta (K00449) subunits, responsible for the initial conversion of protocatechuate to β-carboxymuconate, are present in approximately 30% of the BHET communities on days 3 and 7 and in 10-15% of the amorphous PET biofilm communities on days 21 and 30. This supports the idea that organisms specialised in degradation may be present at the earlier time points because for BHET there are fewer challenging steps involved in metabolising it to protocatechuate than there are for PET, and the genes are therefore abundant earlier on – as also evidenced by the faster growth on BHET compared with amorphous PET by both

isolates (Figure 3.2) and that there were more ASVs unique to the BHET treatment that were early colonisers as opposed to middle colonisers (11 *vs* three), while the split was more equal for the amorphous PET biofilm treatment (nine *vs* eight; Figure 3.12). The closest available complete genomes for all of those ASVs that were identified by the PRC analysis were also obtained (where these were above 97% similar to the ASV, determined by BLAST searches using the 16S rRNA gene sequence; Table 3.8). These genomes were annotated using Prokka (as above; Seemann, 2014) and the HMM, constructed above, was used to search them for PETases. This determined that 27 out of these 32 genomes possessed enzymes that were above the inclusion threshold. In general, the genomes with the highest scores were those matched to the ASVs that were more abundant in the amorphous PET biofilm treatment (Table 3.8), however, there were no close genome matches to half of the top ten ASVs contributing to the differences in the BHET treatment.

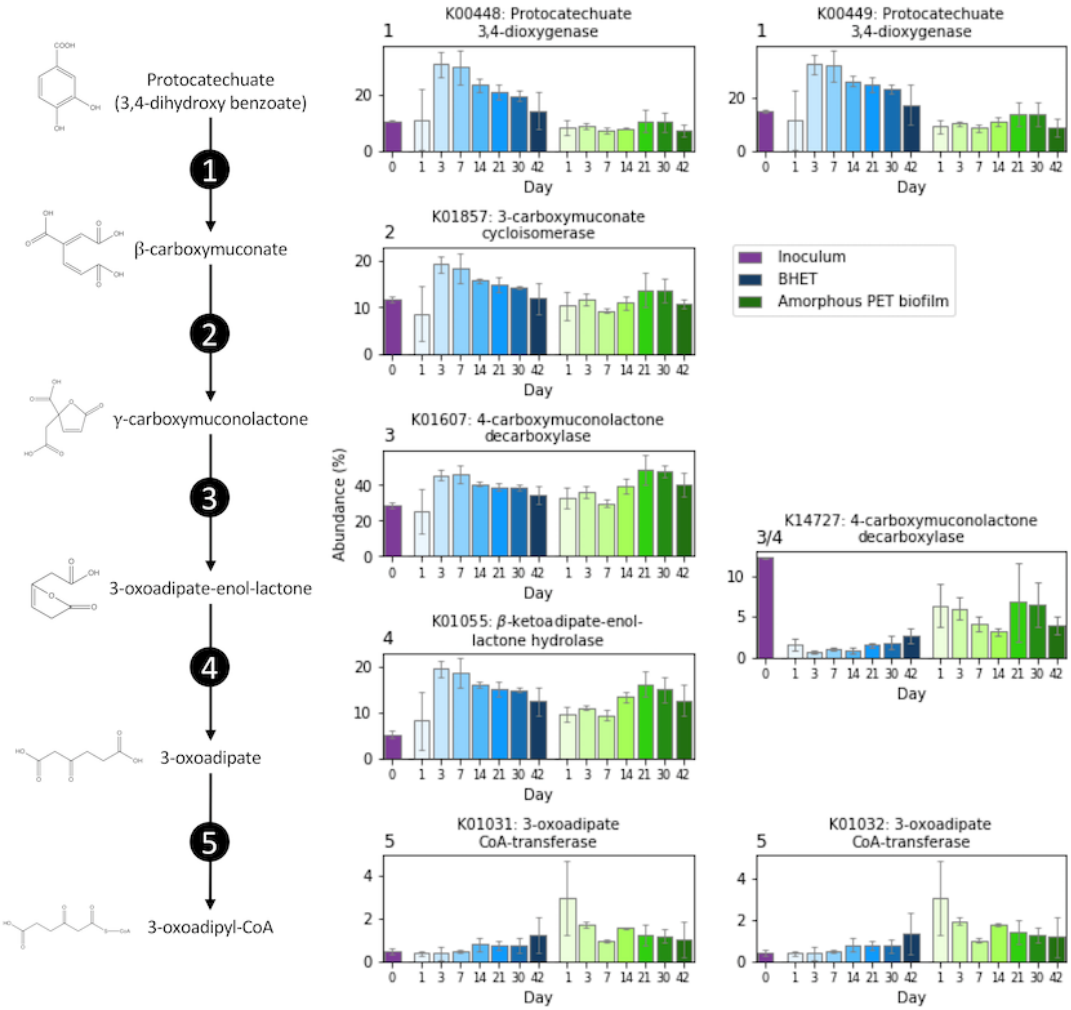

Figure 3.13. Predicted abundance of protocatechuate degradation pathway genes in PICRUSt2-assembled artificial metagenomes for BHET and amorphous PET biofilm communities over time. Bars shown are means of biological replicates (*n*=3) and error bars show standard deviation. Numbers in black circles correspond to numbers at the top left of axes. Average weighted nearest sequenced taxon indices (NSTI) were 0.06, 0.02 and 0.05 for the inoculum, amorphous PET biofilm and BHET samples, respectively (see Table 3.9 for values for individual ASVs).

3.3.6 Long-term degradative ability of isolates and communities

In parallel to the community succession experiment, the inoculum (*i.e.* the same microbial community as used previously) as well as both of the isolates, *Thioclava* sp. BHET1 and *Bacillus* sp. BHET2, were incubated with amorphous PET pieces, PET powder, weathered PET powder (as above) and no additional carbon (control), in order to determine whether a microbial community is better at degrading plastics than an individual bacterium. Controls were also incubated with no inoculum. After three months of incubation, samples were taken to measure growth and after five months of incubation, samples were taken to assess the degradation of the plastics. At three months of incubation, the community showed significantly higher growth with the amorphous PET than either of the isolates (Figure 3.14). FTIR was performed on the plastics that were incubated in this experiment and this indicated that there were changes in the relative populations at certain wavelengths between the treated and control plastics (Figure 3.15, Figure 3.16, Figure 3.17 and Figure 3.18). For the amorphous PET pieces (Figure 3.15A), there were significant (two independent samples T-test, $p < 0.05$) increases in the absorbance at wavelengths associated with carboxylic acid C=O (1710 cm^{-1}), O-H (2920 cm^{-1}) and C-O (1235 cm^{-1}) and alcohol O-H (3300 cm^{-1}) and C-O (1090 cm^{-1}) bonds, when compared with the absorbance at 2500 cm^{-1} for both *Thioclava* sp. BHET1 and *Bacillus* sp. BHET2. Figure 3.3 **Error! Reference source not found.**shows the degradation mechanism that leads to the generation of additional carboxylic acid and alcohol end groups; for each terephthalic acid and ethylene glycol group removed from the end of the polymer, there are two additional alcohol C-O and O-H bonds and two additional carboxylic acid C-O, C=O and O-H bonds. For the community, there were significant increases in the absorbance at carboxylic acid and alcohol O-H bond wavelengths and non-significant increases (with high variability) at carboxylic acid C=O and C-O and alcohol C-O bond wavelengths (Figure 3.15A). For the weathered PET powder, the only significant increase was shown for carboxylic acid O-H bonds in the community incubation (Figure 3.15B) and for PET powder the only significant increase was with *Bacillus* sp. BHET2 for the carboxylic acid C=O and C-O and alcohol C-O bonds (Figure 3.15C). These results together indicate that there was hydrolysis of PET polymer chains to produce MHET, TPA and EG, as evidenced by the increase in carboxylic acid and alcohol end groups, as would be on the end of MHET and TPA or MHET and EG chains, respectively, but these results depended upon the microorganisms incubated with them as well as the polymer type.

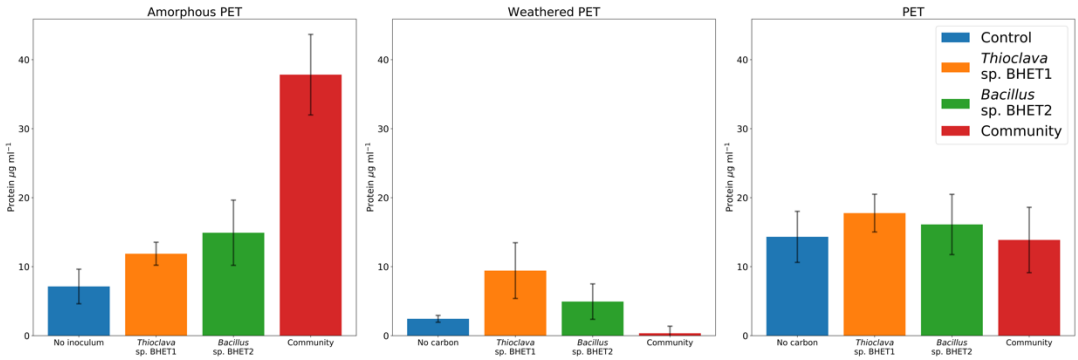

Figure 3.14. Protein content when the isolates *Thioclava* sp. BHET1 and *Bacillus* sp. BHET2 and the microbial community are grown with amorphous PET, weathered PET and PET. Bars show means for three biological replicates and error bars show standard deviations. The means for negative controls with no inoculum were subtracted from all values. Results are from three months of growth. Note that measurements with weathered PET and PET may not be reliable due to the possible presence of small particulates, interfering with the absorbance-based method, although samples were centrifuged, and the supernatant removed prior to measurements.

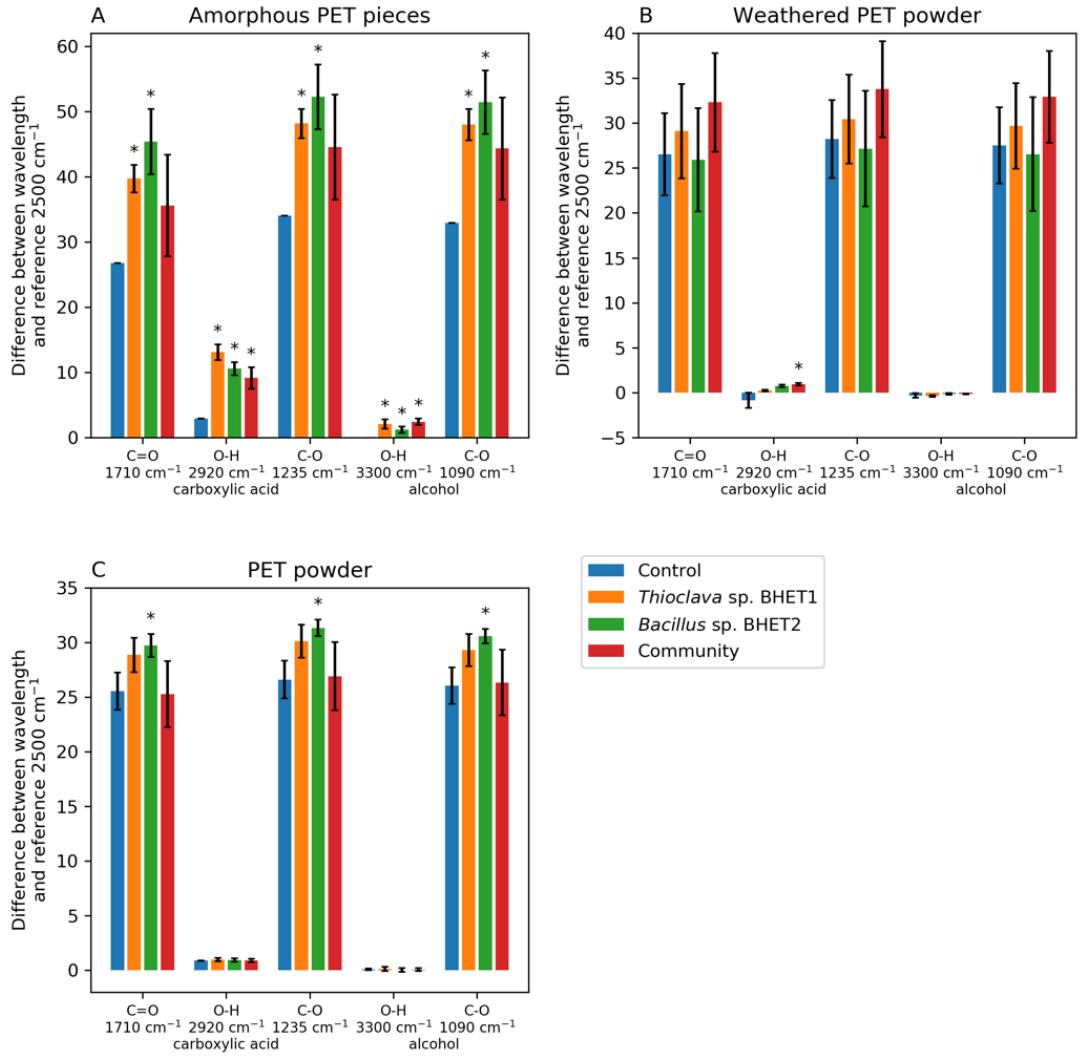

Figure 3.15. Results of FT-IR analyses on amorphous PET pieces **(A)**, weathered PET powder **(B)** and PET powder **(C)** after five months of incubation with either of the two isolates, *Thioclava* sp. BHET1 or *Bacillus* sp. BHET2, the microbial community or no inoculum controls. Bars show the difference between the absorbance at 2500 cm^{-1} and each of the C=O, O-H and C-O carboxylic acid bonds, at

wavelengths of 1710, 2920 and 1235 cm^{-1}, respectively and the O-H and C-O alcohol bonds at 3300 cm^{-1} and 1090 cm^{-1}. Figure 3.3 shows how PET degradation leads to the generation of additional carboxylic acid and alcohol bonds Bars and error bars show means and standard deviations, respectively, of three biological replicates. Asterisks denote significant results for T-tests between the treatment and the control, *i.e.* indicative that degradation has occurred in these treatments. Full FT-IR spectra are shown in Figure 3.16, Figure 3.17 and Figure 3.18 for amorphous PET pieces, weathered PET powder and PET powder, respectively.

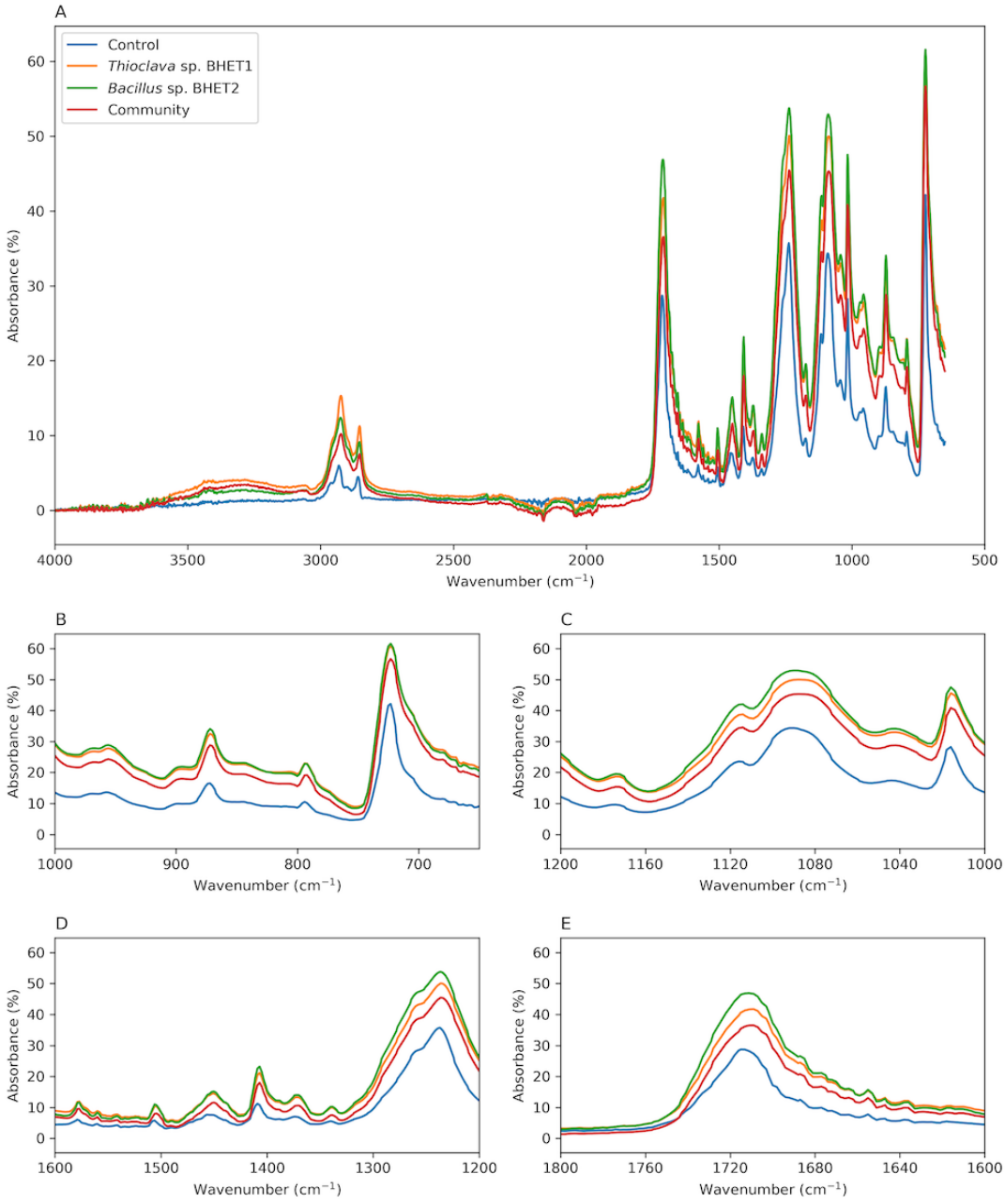

Figure 3.16. FT-IR spectra for control, *Thioclava* sp. BHET1, *Bacillus* sp. BHET2 and community-incubated amorphous PET pieces. All wavelengths are shown in **(A)**, while **(B)**, **(C)**, **(D)** and **(E)** show 1000-600, 1200-1000, 1600-1200 and 1800-1600 cm^{-1}, respectively. Each line shows the mean absorbance for three technical replicates for each of three biological replicates (*i.e.* nine total measurements) per treatment.

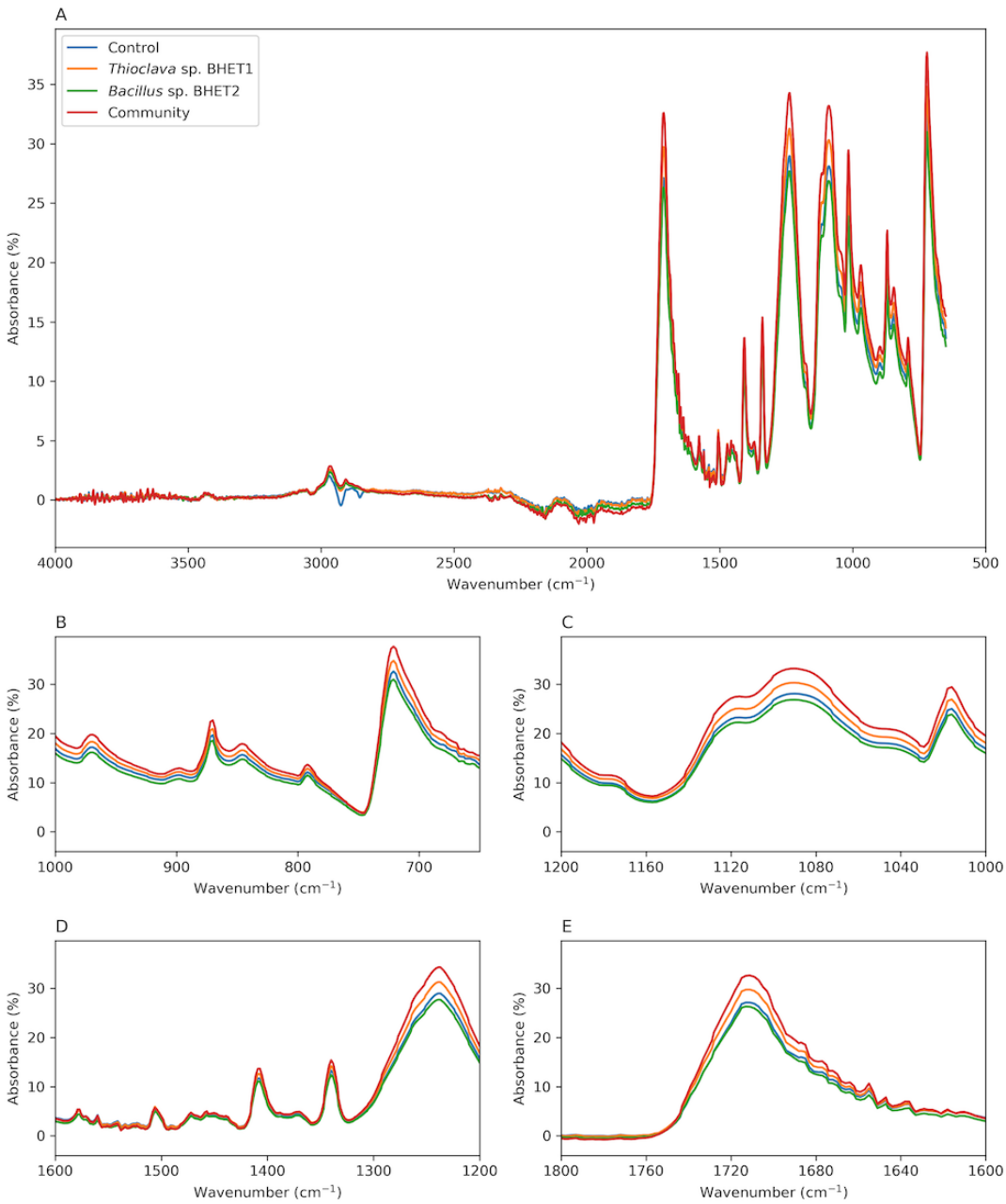

Figure 3.17. FT-IR spectra for control, *Thioclava* sp. BHET1, *Bacillus* sp. BHET2 and community-incubated weathered PET powder. All wavelengths are shown in **(A)**, while **(B)**, **(C)**, **(D)** and **(E)** show 1000-600, 1200-1000, 1600-1200 and 1800-1600 cm^{-1}, respectively. Each line shows the mean absorbance for three technical replicates for each of three biological replicates (*i.e.* nine total measurements) per treatment.

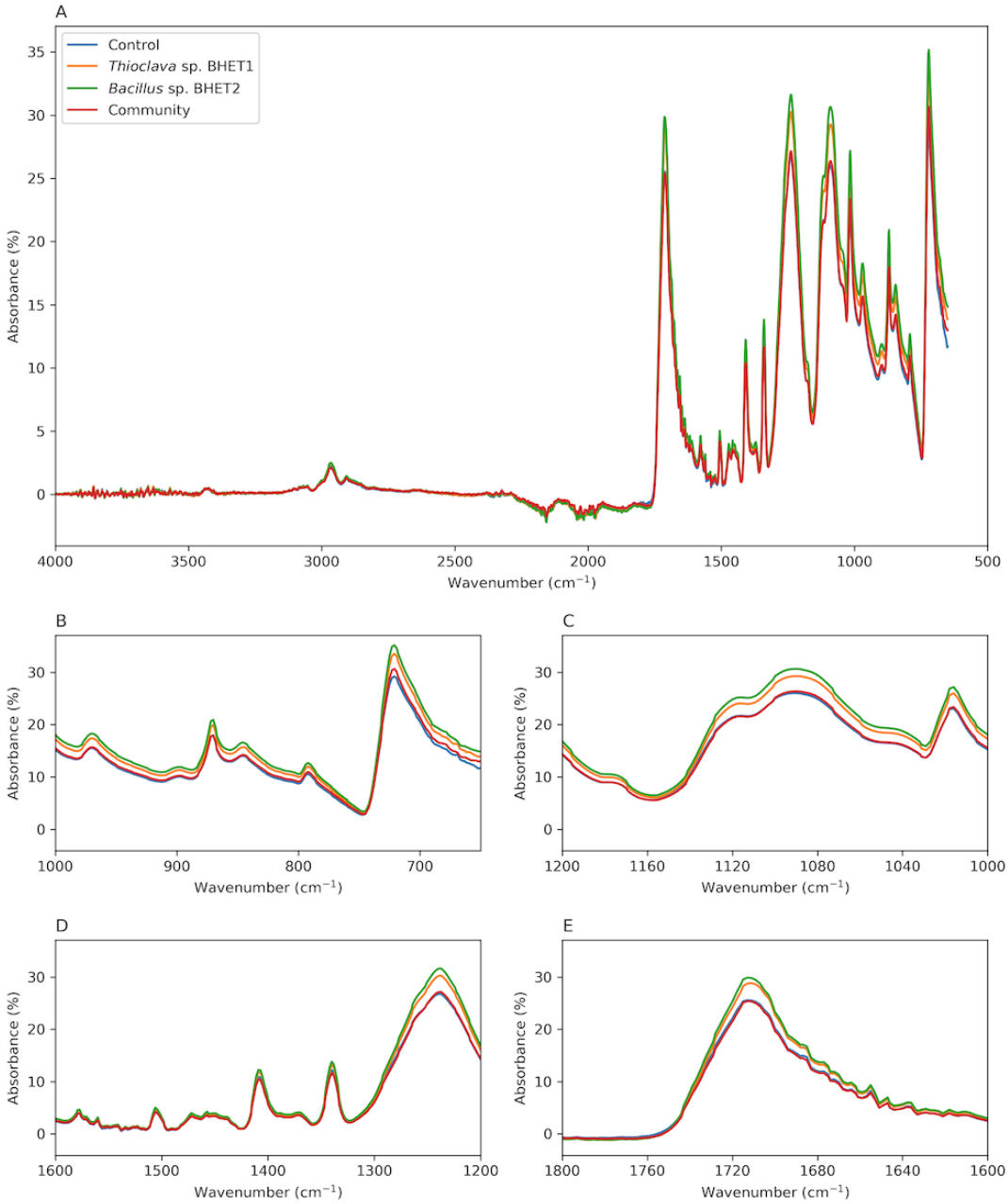

Figure 3.18. FT-IR spectra for control, *Thioclava* sp. BHET1, *Bacillus* sp. BHET2 and community-incubated PET powder. All wavelengths are shown in **(A)**, while **(B)**, **(C)**, **(D)** and **(E)** show 1000-600, 1200-1000, 1600-1200 and 1800-1600 cm^{-1}, respectively. Each line shows the mean absorbance for three technical replicates for each of three biological replicates (*i.e.* nine total measurements) per treatment.

3.4 Discussion

The results in this chapter give a more comprehensive overview of the steps involved in the marine degradation of PET. Initially, the PET oligomer bis(2-hydroxy ethyl) terephthalate (BHET) was used to isolate marine bacteria that were potentially capable of PET degradation, *Thioclava* sp. BHET1 and *Bacillus* sp. BHET2. A full proteogenomic characterisation of the growth of these isolates on amorphous PET pieces, BHET and terephthalic acid (TPA) was then performed. The microbial community succession was also characterised across six weeks of laboratory incubation – in order to prevent confounding variables (Ogonowski et al., 2018) – with amorphous PET pieces, PET powder, weathered PET powder and BHET and both the isolates and the community were incubated with amorphous PET pieces, PET powder and weathered PET powder for five months in order to quantify their potential to degrade PET. The pathway used for PET degradation by *Bacillus* sp. BHET2 was not determined, although the FTIR results suggest that the amorphous PET was being degraded by *Bacillus* sp. BHET2 (Figure 3.15), so it is possible that this bacterium uses a currently uncharacterised pathway for PET degradation. However, it has been confirmed that for *Thioclava* sp. BHET1, PET degradation takes place through an initial hydrolysis of PET to MHET and TPA, after which the TPA is converted to protocatechuate *via* a range of dioxygenases (Figure 3.4), which tend to be abundant in the marine environment (Quero and Luna, 2017) and on marine plastics (Bryant et al., 2016a; Didier et al., 2017; Dussud et al., 2018b). This suggests that while enzymes capable of the hydrolysis of PET itself, PETases, are generally present in low abundances (Danso et al., 2018), the enzymes involved in the metabolism of the products of PET degradation may be more widely abundant in the marine environment. It is worth noting, however, that the enzymes that have been identified here as PETases share much lower homology with previous PETases than those identified by Danso et al. (2018) and should therefore be tested more comprehensively to confirm PETase activity. The dioxygenases, as well as other enzymes from the benzoate degradation pathway, are also involved in the degradation of phthalic acid ester (PAE) plasticizers (Vamsee-Krishna and Phale, 2008), which are frequently used as plastic additives (Groh et al., 2019; Hahladakis et al., 2018).

Both *Bacillus* and *Thioclava* spp. have previously been found to be colonisers of plastics in the marine environment (Carson et al., 2013; Curren and Leong, 2019; Syranidou et al., 2019, 2017b, 2017a). *Thioclava* spp. have also been found to be potent degraders of crude oil (Wanpeng Wang et al., 2014), while the degradative ability of *Bacillus* spp. has previously

been reported in the terrestrial environment for PET (Nakkabi et al., 2015) and also for PE in the marine environment. In Sudhakar et al. (2008), growth was substantially higher on PE that was thermally pre-treated and it was also suggested that an initial abiotic oxidation step was necessary for *Bacillus* spp. to be capable of PE degradation. Abiotic degradation, for example by UV radiation (Andrady, 2017), is likely a necessary prerequisite for the biodegradation of many plastics, particularly for plastics that do not contain heteroatoms in their backbone, such as PE and PP (Gewert et al., 2015) and the products of this abiotic degradation for PE, PP, PS and PET are low-molecular weight compounds with oxidised end groups (Gewert et al., 2018) that share structural similarity with BHET, MHET and TPA. Intriguingly, although an increase was observed in the absorbance at wavelengths relating to carboxyl and hydroxyl end groups in FTIR spectra after thermal pre-treatment of PET powder (weathered PET powder; Figure 3.5), this did not lead to large differences between the microbial communities growing on the weathered and non-weathered PET powder (Figure 3.10 and Figure 3.12). Furthermore, indications of microbial degradation having occurred in all conditions were only observed for the amorphous PET (Figure 3.15).

Typically, on particle surfaces in the marine environment, microbial community succession leads to an initial dominance of *Gammaproteobacteria* before these are overtaken by *Alphaproteobacteria*, which stands true for both natural particles such as chitin (Datta et al., 2016; Chapter 2) as well as marine plastics (Pollet et al., 2018). Interestingly, in our six-week succession experiment, we do not see this and *Gammaproteobacteria* remain dominant throughout, making up 60-80% relative abundance of the microbial community, while *Alphaproteobacteria* make up 10-30% of the communities (Figure 3.7), similarly to Oberbeckmann et al. (2014), who incubated PET in coastal marine environments. Of these *Gammaproteobacteria*, *Vibrio* spp. are highly abundant and one ASV, ASV1 (identified as either *V. parahaemolyticus* or *V. alginolyticus*), makes up approximately 20-40% of all communities. The inoculum used for all samples was removed from plastics collected from a beach in Porthcawl, Wales, which is close to a wastewater treatment plant and this is one possible explanation for the dominance of *Vibrio* spp., both in the inoculum and in all samples at all time points (Figure 3.10). Several previous studies have also found *Vibrio* spp. in high abundances on some marine plastics (De Tender et al., 2015; Zettler et al., 2013) and others have investigated the presence of *Vibrio* spp. on marine plastics as potentially pathogenic microbial hitchhikers (Frere et al., 2018; Keswani et al., 2016; Kirstein et al., 2016; Quilliam et al., 2014). On the other hand, a consortia of *Vibrio* spp. has also been reported to degrade a polyvinyl alcohol-LLDPE plastic blend (Raghul et al., 2014). While we did not aim to

determine whether *Vibrio* spp. are capable of PET degradation, the PICRUSt artificial metagenome analysis showed that ASV1 did not possess any of the genes involved in protocatechuate degradation that are shown in Figure 3.13 (Table 3.8), suggesting that it is a cross-feeder, utilising the organic matter generated by other members of the microbial community (Christie-Oleza et al., 2017; Noriega-Ortega et al., 2019) rather than PET or any of its immediate breakdown products.

Several previous studies have noted that the effects of substrate type are only likely to be seen at early stages of biofilm formation (Datta et al., 2016; Ogonowski et al., 2018; Zhang et al., 2014). The same was seen to be true here, where those species with large contributions to differences between treatments were predominantly early colonisers (defined as those that peaked in abundance between days 1 and 7) in those treatments (Figure 3.10 and Figure 3.12). We also found that genes involved in protocatechuate degradation peaked in abundance on days 3 and 7 for the BHET and days 21 and 30 for the amorphous PET biofilm treatments, fitting with the hypothesis that organisms capable of degrading that substrate were abundant at earlier time points and that this would occur earlier in BHET than in amorphous PET, as it is less challenging to degrade. This also agrees with the pattern shown in Figure 3.9, where the amorphous PET biofilm samples from days 7-30 group with the BHET samples from days 1 and 3, and away from the amorphous PET biofilm samples from days 1, 3 and 42. This suggests that all of these samples see an enrichment in protocatechuate degradation that can only occur either after the removal of the BHET side chains producing TPA, or after the hydrolysis of the PET to TPA. This also correlates with the growth dynamics of pure cultures of the PET degrader *Ideonella sakaiensis*, where the highest growth is reached after approximately two days for BHET and six days for amorphous PET (Yoshida et al., 2016a). Those ASVs that were middle (highest in abundance on days 14-30) or late (highest in abundance on day 42) colonisers generally contributed to similarities between treatments (Figure 3.10) and this suggests that we are then seeing the succession phase at these time points in all treatments. This finding agrees with previous studies that have looked at early biofilm formation on plastics and have observed a distinct plastisphere only at early incubation stages (Pollet et al., 2018) and suggests that in order to identify other plastic-degrading bacteria in the oceans we should look at the early colonisation phases.

In this chapter, evidence has been provided for marine PET degradation by both microbial communities and isolates and the enzymes used for this degradation by the marine bacterial isolate, *Thioclava* sp. BHET1, have been identified. The results from the isolates suggest that

the enzymatic structure of a PETase may not need to be as heavily conserved as previously suggested, but the degradation that is seen here is relatively low, so it is possible that this would lead to little degradative activity for these isolates within a community. It has also been confirmed that the time must be right in order to see PET degradation as opposed to degradation of metabolic intermediates. The results presented in this chapter suggest that where studies collect plastics from the environment – and do not know the full chemical composition of these plastics, including additive concentrations – it is impossible to know whether any colonising microbes are degrading the plastic or the plasticizer, or are cheaters benefitting from the production of degradation intermediates by early colonisers.

Chapter 4

Plasticizer degradation by marine bacterial isolates: a proteogenomic and metabolomic characterisation

4.1 Introduction

Marine plastic pollution is both ubiquitous and well-acknowledged (Barnes et al., 2009; Derraik, 2002; Thompson et al., 2009) with estimates that 4.8 to 12.7 million tons of plastic waste enters the oceans every year (Jambeck et al., 2015). The ecotoxicological problems derived from environmental plastic pollution are direct, *e.g.* through ingestion or entanglement (Avio et al., 2016), or indirect, *e.g.* through the transfer of toxic chemicals to marine life (Rochman et al., 2013; Teuten et al., 2009). Plastics are known to harbour toxic chemicals in concentrations up to 10^6 times higher than in their surrounding environment (Mato et al., 2001), with up to 906 different chemicals associated with plastics (Groh et al., 2019). These chemical pollutants come from hydrophobic sorption to plastics, such as polychlorinated biphenyls (PCBs) and polyaromatic hydrocarbons (PAHs) (Bakir et al., 2012), or are directly added during manufacturing processes, such as stabilisers, flame retardants and plasticizers (Groh et al., 2019).

Plasticizers are added to plastics in order to change the physical and chemical properties of the material and can represent up to 10-70% of the material's weight, mainly in plasticized or flexible polyvinyl chloride (PVC), a material which comprises 80% of the global use of these chemicals (Hahladakis et al., 2018). There are several classes of plasticizers: phthalates, terephthalates, epoxies, aliphatics, trimellitates and citrates. Phthalic acid ester plasticizers (PAEs) represent ~65% of the global market share, with bis(2-ethyl hexyl) phthalate (DEHP) and dibutyl phthalate (DBP) being the two most widely used ("Plasticizers," 2019). Plasticizers are not chemically bound to the plastic and are therefore able to leach out of these materials, either during consumer use or on their subsequent release into the environment (Hahladakis et al., 2018; Paluselli et al., 2019; Rani et al., 2015; Staples et al., 1997). Both DEHP and DBP, in addition to other plasticizers, have been found on both new plastics and plastic marine debris (in the environment for an unknown period of time; Rani et al., 2015), as well as in a range of plastics ingested by marine wildlife (Savoca et al., 2018; Vered et al., 2019). Concerns have been raised over the continued use of plasticizers as they may not only be highly toxic – DBP and DEHP have recently been identified as some of the most hazardous chemicals associated with plastics (Groh et al., 2019) – but many are also known endocrine disruptors and carcinogens, even at low concentrations (Mathieu-Denoncourt et al., 2015). Due to their toxicity, there is now a push to replace the traditional PAEs with other less toxic alternatives, such as acetyl tributyl citrate (ATBC) (Erceg et al., 2005; Van Vliet et al., 2011).

ATBC is widely stated to be a non-toxic and biodegradable alternative to DEHP and other PAEs (Baiardo et al., 2002; Erceg et al., 2005), however, to our knowledge, the catabolic pathway for ATBC biodegradation has not been experimentally shown. In fact, one study found that using ATBC as a plasticizer actually decreased enzymatic degradation rates of the biodegradable plastic poly(lactic acid) (Labrecque et al., 1997). On the other hand, the pathways used for PAE biodegradation *have* been characterised to some extent in a number of terrestrial microorganisms (Ahuactzin-Pérez et al., 2016; Liang Feng et al., 2018; Hesselsoe et al., 2005; Kumar et al., 2017; Kumar and Maitra, 2016; Liang et al., 2008; Park et al., 2009, 2008; Xie et al., 2010; Yuan et al., 2002). Esterases have been suggested to carry out the first step of PAE biodegradation by hydrolysing the side chains and generating phthalate and short-chain alcohols and fatty acids (Ahuactzin-Pérez et al., 2018, 2016; Chen et al., 2007; Nai-xian Feng et al., 2018; Kumar et al., 2017; Li et al., 2018; Park et al., 2009, 2008; Stanislauskienė et al., 2011; Yang et al., 2018; Yue et al., 2017). However, only two of these studies (Stanislauskienė et al., 2011; Yue et al., 2017) actually identified the specific esterases involved and, furthermore, β-oxidation of the side chain fatty acids has even been suggested to occur directly on the PAE molecule (Amir et al., 2005; Li et al., 2018). Hence, it is not known whether the mechanism for biodegradation is the same for different PAE plasticizers. The metabolic pathway for phthalate degradation is well established, with a first conversion to protocatechuate (3,4-dihydroxybenzoate) prior to following one of the pathways for benzoate degradation (Liang et al., 2008; Vamsee-Krishna and Phale, 2008). Despite the widespread distribution of plastics and, consequently, plasticizers, in the oceans, the degradation of these additives by marine bacteria has been less extensively studied (Liang et al., 2008; Paluselli et al., 2019; Yang et al., 2018) and the catabolic pathways are unknown.

In this chapter, a natural microbial community obtained from marine plastic debris was enriched with each of six different plasticizers; DBP, DEHP, ATBC, diisononyl phthalate (DINP), diisodecyl phthalate (DIDP) and trioctyl trimellitate (TOTM). Forty-two strains were isolated and tested for their ability to grow on each of the six plasticizers. A detailed proteogenomic and metabolomic analysis was then performed on the two strains with the highest growth on a range of plasticizers, *i.e. Halomonas* sp. ATBC28 and *Mycobacterium* sp. DBP42, allowing the identification of the enzymes and pathways involved in phthalate, DBP, DEHP and ATBC biodegradation.

4.2 Method

4.2.1 Enrichments from marine plastic debris

Tissue culture flasks (25 cm^2) containing 25 mL of Bushnell-Haas mineral media (Table 2.1, Section 2.2.3) supplemented with 0.52 M of NaCl, 0.005% (w/v) of yeast extract (as a supplement of growth factors; Merck KGaA, Germany) and each one of six plasticizers (0.1% v/v of DBP, DEHP, DINP, DIDP, ATBC or TOTM; Sigma-Aldrich, UK; concentrations were 3.6, 2.6, 2.4, 2.2, 2.5 and 1.8 mM, respectively) were inoculated with 1 mL of a natural microbial community obtained from bulk marine plastic debris collected during boat tows from both Plymouth Sound (Devon, UK; June 2016) and Portaferry (Northern Ireland, UK; August 2016) and detached by thorough vortexing. Cultures were incubated at 30˚C in the dark with shaking at 150 rpm. 30˚C, rather than ambient environmental temperatures, was chosen in order to speed up growth rates rather than directly emulating the environment. When growth was apparent (after approximately four weeks and assessed by visual turbidity), 1 mL of these cultures was used to inoculate fresh tissue culture flasks (25 cm^2) with 25 mL custom media, as above, in a second enrichment step.

4.2.2 Microbial isolation

Agar plates were made with the supplemented Bushnell-Haas mineral medium, containing 0.1% (v/v) of one of the six plasticizers listed above and 1.5% agar. Media was blended immediately before pouring the plates to ensure homogeneous dispersal of the hydrophobic plasticizers. Marine agar (BD Difco™) plates were also used for isolation. 100 µL of the enrichment cultures was spread on to replicate plates and incubated for three weeks at 30˚C. Morphologically distinct colonies (*n*=42) were picked and streaked onto fresh plates until isolates were obtained.

4.2.3 Screening and selection of isolates

Each one of the 42 isolates was grown in a six-well plate, each well containing 2.5 mL of supplemented Bushnell Haas mineral media with 0.1% (v/v) of one of the six plasticizers and incubated for two weeks at 30˚C in the dark. Growth was monitored weekly through visual assessment. The ten isolates that showed highest potential for growth with several of the plasticizers were identified by partial amplification (using primers 27F and 1492R; Table 2.2) and sequencing (GATC BioTech, Germany) of the 16S rRNA gene.

4.2.4 Further characterisation and genome sequencing of two isolates

Two selected isolates were further tested on different growth substrates *i.e.* glucose, sodium succinate, pyruvate, glycerol, N-acetyl-D-glucosamine, fructose, phthalate and marine broth (BD Difco™). Each condition was tested in duplicate in 96-well plates, with each well containing 200 µL supplemented Bushnell Haas mineral media with 0.1% (w/v or v/v; concentrations were 5.5, 6.2, 11.4, 10.9, 4.5, 5.6 and 4.9 mM for glucose, sodium succinate, pyruvate, glycerol, N-acetyl-D-glucosamine, fructose and phthalate, respectively) substrate and incubated at 30˚C with shaking at 150 rpm for 72 hours. Growth was monitored by optical density measurements (600 nm; 30-minute intervals using a Synergy HTX microplate reader). The two selected isolates were also grown in triplicate in 22 mL glass vials containing 10 mL of supplemented Bushnell-Haas mineral medium with 0.1% (v/v) of each of the six plasticizers or 0.02% (w/v) phthalate and incubated at 30˚C in the dark with shaking at 150 rpm in order to confirm growth on these substrates. Growth was monitored by optical density measurements (600 nm) on days 1, 2, 4 and 7.

Whole genome sequencing, assembly and annotation of the two selected isolates was performed as in Section 3.2.1 of Chapter 3. The complete genome sequences of the two selected strains, *i.e. Halomonas* sp. ATBC28 and *Mycobacterium* sp. DBP42, were deposited in the GenBank database under the BioProject numbers PRJNA525098 and PRJNA525197, respectively. For *Halomonas* sp. ATBC28, genomic islands were predicted using IslandViewer 4 (Bertelli et al., 2017) and plasmid-encoded proteins were determined using SPAdes (Bankevich et al., 2012).

4.2.5 Preparation of cellular and extracellular proteome samples

The two selected isolates were grown in 100 mL Erlenmeyer flasks containing 40 mL of supplemented Bushnell-Haas mineral medium and 0.1% (v/v) of DBP, DEHP and ATBC and 0.02% (w/v) of phthalate as sole carbon sources. Pyruvate and glycerol (0.1% w/v) were used as the control growth conditions for *Halomonas* sp. ATBC28 and *Mycobacterium* sp. DBP42, respectively. Three independent cultures for each condition were incubated at 30˚C in the dark with shaking at 150 rpm until absorbance (600 nm) reached 0.3, or large clumps of cells were visible, at which point, cells and supernatants were harvested and processed for proteomics as in Section 3.2.2 of Chapter 3. Additional 1.5 mL samples of the supernatants were removed for metabolomic analyses (see below, Section 4.2.6). Cellular and extracellular proteomics as well as analysis of data was carried out as in Section 3.2.2 of Chapter 3.

4.2.6 Metabolomics for the identification of degradation intermediates in culture supernatants (LCMS)

Filtered supernatants (1.5 mL) were adjusted to pH 2.5 using 2M HCl after which 3 mL of ethyl acetate was added for hydrophobic compound extraction and purification. Briefly, samples were vortexed for 10 s and left for 10 mins for phase separation, after which the organic fraction was collected into a new tube and evaporated using a GeneVac EZ-2 Evaporator. Pellets were resuspended in 250 µL of phosphate buffer 16 mM (pH 2.5) containing 20% (v/v) of DMSO and filtered through a micro-centrifugal tube with a 0.2 µm nylon membrane (Thermo Fisher Scientific, UK) before analysis. An UHPLC system (Ultimate 3000; ThermoFisher Scientific, Waltham, MA, USA) coupled to a Q-Exactive Hybrid Quadrupole-Orbitrap mass spectrometer (ThermoFisher Scientific) operating with a heated electrospray interface (HESI) was employed and the spectra were recorded in both positive and negative modes.

Chromatographic separation was accomplished using two strategies: i) untargeted metabolomics were performed on a reversed-phase C18-core shell (100 x 2.1 mm ID, 1.6 µm; Luna Omega) chromatographic column preceded by a C18-security guard ultra-cartridge (2.1 mm ID), both from Phenomenex (Torrence, CA); ii) targeted metabolomics were performed on a reversed-phase C18-core shell (250 x 4.6 mm ID, 5.0 µm; Ultrasphere) chromatographic column preceded by a C18-security guard cartridge (45 x 4.6 mm ID, 5.0 µm; Ultrasphere), both from Hichrom (Leicester, UK). Both strategies used a mobile phase of (A) 0.1% (v/v) formic acid in water and (B) 0.1 %(v/v) formic acid in acetonitrile (ACN) at 0.2 mL min^{-1} (untargeted metabolomics) or 0.5 mL min^{-1} (targeted metabolomics). For untargeted metabolomics, the elution gradient started with 5% of solution B for 5 min, then increased to 55% over 5 min and was maintained at 55% for 3 min. Over 1 min, the proportion of solution B was reduced from 55 to 5% and it was maintained at 5% for 6 min. For targeted metabolomics, the elution gradient started with 5% of solution B for 6 min, then increased to 55% B over 8 minutes and was maintained at 55% for 4.25 minutes. Over 15 s the proportion of solution B was reduced from 55 to 5% and it was maintained at 5% for 7 min. For both strategies, the injection volume was 5 µL.

For MS and MS/MS acquisition the temperature of ion transfer capillary, spray voltage, sheath gas flow rate, auxiliary gas flow rate and S-lens RF level were set to 350 °C, 3.9 KV in

positive mode and 3.1 kV in negative mode, 35 arbitrary units (AU), 10 AU and 55 AU, respectively. Full scan acquisition over a range of 80–600 m/z was performed with a resolution of 70,000. During the MS/MS scans, precursors were fragmented with a normalised collisional energy of 50 AU. The top 5 ions were selected for MS/MS analysis with a dynamic exclusion of 1 s.

Xcalibur™ 4.1, Trace Finder 4.1 SP2 and Compound Discoverer 2.0 software (Thermo Fisher Scientific) were used for LC-MS and LC-MS/MS acquisition, targeted metabolomics and untargeted metabolomics data processing, respectively. Mass tolerance (Δ) was set for the analysis with Trace Finder 4.1 SP2 and Compound Discoverer 2.0 to 14 ppm and to 10 ppm, respectively, according to data obtained with external standards analysed in negative mode using FreeStyle 1.3 software (Thermo Fisher Scientific): salicylic acid (targeted, RT 21.02 min, Δ 10.22 ppm; untargeted, RT 15.11 min, Δ 6.46 ppm), phthalic acid (targeted, RT 18.12 min, Δ 8.67 ppm; untargeted, RT 12.08 min, Δ 4.99 ppm), catechol (targeted, RT 18.14 min, Δ 13.75 ppm; untargeted, RT 7.7 min, Δ 2.1 ppm), protocatechuate (3,4-dihydroxy benzoate; targeted, RT 16.7 min, Δ 8.49 ppm; untargeted, RT 12.23 min, Δ 6.18 ppm) and citric acid (targeted, RT 6.97 min, Δ 5.76 ppm; untargeted, RT 1.87 min, Δ 2.86 ppm). Additional basic parameters used for analysis were as follows: Trace Finder 4.1 SP2, negative mode, Genesis as detection algorithm and Highest peak as peak detection strategy; Compound Discoverer 2.0, minimum peak intensity of 5E6, signal-noise ratio of 5 and retention time tolerance 0.075 min.

The genomic analyses of *Halomonas* sp. ATBC28 and *Mycobacterium* sp. DBP42, complete lists of detected peptides and polypeptides, files showing fold changes between plasticizer treatments and control conditions, details of all compounds detected by metabolomics and analysis scripts can be found at https://github.com/R-Wright-1/Plasticizer-Degradation.

4.3 Results

4.3.1 Enrichment, isolation and selection of plasticizer-degrading bacteria

Microbial enrichments on each of the six plasticizers (DBP, DEHP, DINP, DIDP, ATBC and TOTM; Table 4.1) inoculated with a microbial community obtained from bulk marine plastic debris produced apparent turbidity on all substrates after three weeks of incubation. A second enrichment step produced growth after just one week. From the second enrichment, a total of 42 morphologically distinct bacterial isolates were obtained on either agar plates made with one of the plasticizers or marine broth, after which all isolates were screened for their ability to grow with each one of the six plasticizers in liquid cultures (Appendix 4. Screening of bacterial isolates ability to grow using plasticizers as a sole carbon source.). Curiously, only 17 out of the 42 isolates achieved considerable growth with at least one of the plasticizers in liquid cultures whereas others only produced weak growth (*n*=15) or emulsified the plasticizers (*n*=10). Interestingly, while each one of the PAEs and TOTM could be used by 11 to 14 of the isolates, clear growth on ATBC was only observed with one of the strains (*i.e.* isolate 40; Appendix 4. Screening of bacterial isolates ability to grow using plasticizers as a sole carbon source.). Those ten isolates that showed best growth on a wide range of plasticizers were further identified by partial sequencing of their 16S rRNA gene (Table 4.2). Isolates 28 and 42, identified as *Halomonas campaniensis* (99% 16S rRNA sequence identity) and *Mycobacterium houstonense* (99% 16S rRNA sequence identity), respectively, were selected for further growth (Figure 4.1) and genomic characterisation based on their robust growth on a variety of plasticizers (Table 4.2 and Figure 4.2) and diverse phylogenetic origin (*i.e. Gammaproteobacteria* and *Actinomycetales*, respectively). Strains were named hereafter as *Halomonas* sp. ATBC28 and *Mycobacterium* sp. DBP42.

Table 4.1. Characteristics of plasticizers used in this chapter.

Plasticizer (Abbreviation; CAS number)	**Plasticizer class**	**Chemical formula, molecular weight**	**Toxicity (Regulation (EC) 1272/2008)**	**Structure**	**Solubility (water, mg L^{-1})**	**Log K_{OW}**
Phthalate (88-99-3)	NA/ Precursor	$C_8H_6O_4$, 166.14	Skin irritation Eye irritation Specific organ toxicity – single exposure	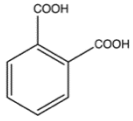	600	Not found

Plasticizer (Abbreviation; CAS number)	Plasticizer class	Chemical formula, molecular weight	Toxicity (Regulation (EC) 1272/2008)	Structure	Solubility (water, mg L^{-1})	Log K_{ow}
Dibutyl phthalate (DBP; 87-74-2)	Phthalate (classified)	$C_{16}H_{22}O_4$, 278.348	Reproductive toxicity Acute aquatic toxicity	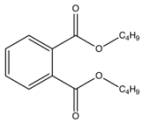	13	4.5 (Ellington, 1999)
Bis(2-ethyl hexyl) phthalate (DEHP; 117-81-7)	Phthalate (classified)	$C_{24}H_{38}O_4$, 390.564	Reproductive toxicity	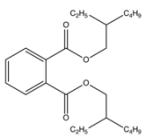	0.27	7.45 (Bui et al., 2016)
Diisononyl phthalate (DINP; 28553-12-0)	Phthalate	$C_{26}H_{42}O_4$, 418.618	Not hazardous (according to regulation)	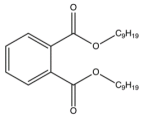	0.2	8.6 (Cousins and Mackay, 2000)
Diisodecyl phthalate (DIDP; 26741-40-0)	Phthalate	$C_{28}H_{46}O_4$, 446.672	Chronic aquatic toxicity	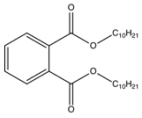	0.28	9.46 (Cousins and Mackay, 2000)
Acetyl tributyl citrate (ATBC; 77-90-7)	Citrate	$C_{20}H_{34}O_8$, 404.484	Not hazardous (according to regulation)	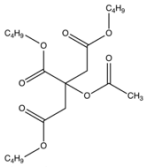	5	4.29 (Bui et al., 2016)
Trioctyl trimellitate (TOTM; 3319-31-1)	Trimellitate	$C_{33}H_{54}O_6$, 546.78	Not hazardous (according to regulation)	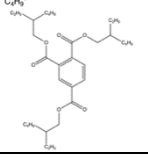	<0.1	Not found

Table 4.2. Ten isolates that showed the best growth on a range of plasticizers.

Isolate	Identification (16S rRNA gene)[1]	DBP[2]	DEHP[2]	DINP[2]	DIDP[2]	ATBC[2]	TOTM[2]
DINP8	*Idiomarina loihiensis* (99%)	+	w	+	+	-	+
DIDP14	*Pseudonocardia autotrophica* (96%)	+	+	+	+	-	+
DIDP15	*Cyclobacterium marinum* (98%)	w	+	+	+	s	+
DEHP23	*Idiomarina loihiensis* (99%)	+	+	+	+	s	+
ATBC28	***Halomonas campaniensis* (99%)**	+	+	+	+	s	+
ATBC29	*Halomonas boliviensis* (99%)	+	+	+	+	s	+

Isolate	Identification (16S rRNA gene)[1]	DBP[2]	DEHP[2]	DINP[2]	DIDP[2]	ATBC[2]	TOTM[2]
TOTM32	*Novosphingobium tardaugens* (100%)	w	w	w	w	w	w
BHET34	*Bacillus aquimaris* (99%)	w	+	w	+	-	+
ATBC40	*Microbacterium aurum* (99%)	w	-	-	-	+	s
DBP42	***Mycobacterium houstonense* (99%)**	+++	+++	+++	+++	w	+++

[1] Isolates were identified through partial sequencing of their 16S rRNA gene and subsequence BLAST searches of the NCBI database.
[2] + (green) indicates growth on a substrate, +++ (green) indicates strong growth, - (red) indicates no growth, w (orange) indicates weak growth and s (red) indicates that there was evidence that a surfactant was produced, but no growth was obvious.

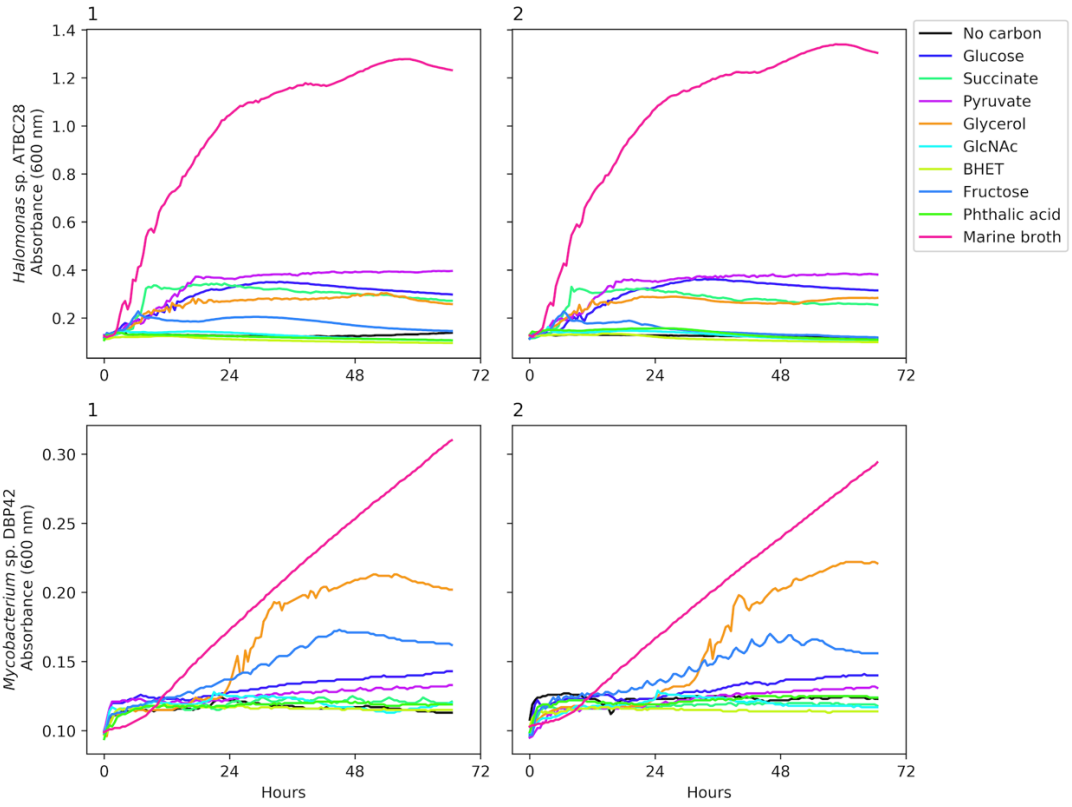

Figure 4.1. Growth of *Halomonas* sp. ATBC28 and *Mycobacterium* sp. DBP42 on a range of different substrates (0.1% w/v in supplemented Bushnell-Haas mineral media), as well as marine broth, over 72 hours. Measurements were taken every half an hour. Panels 1 and 2 show biological replicates.

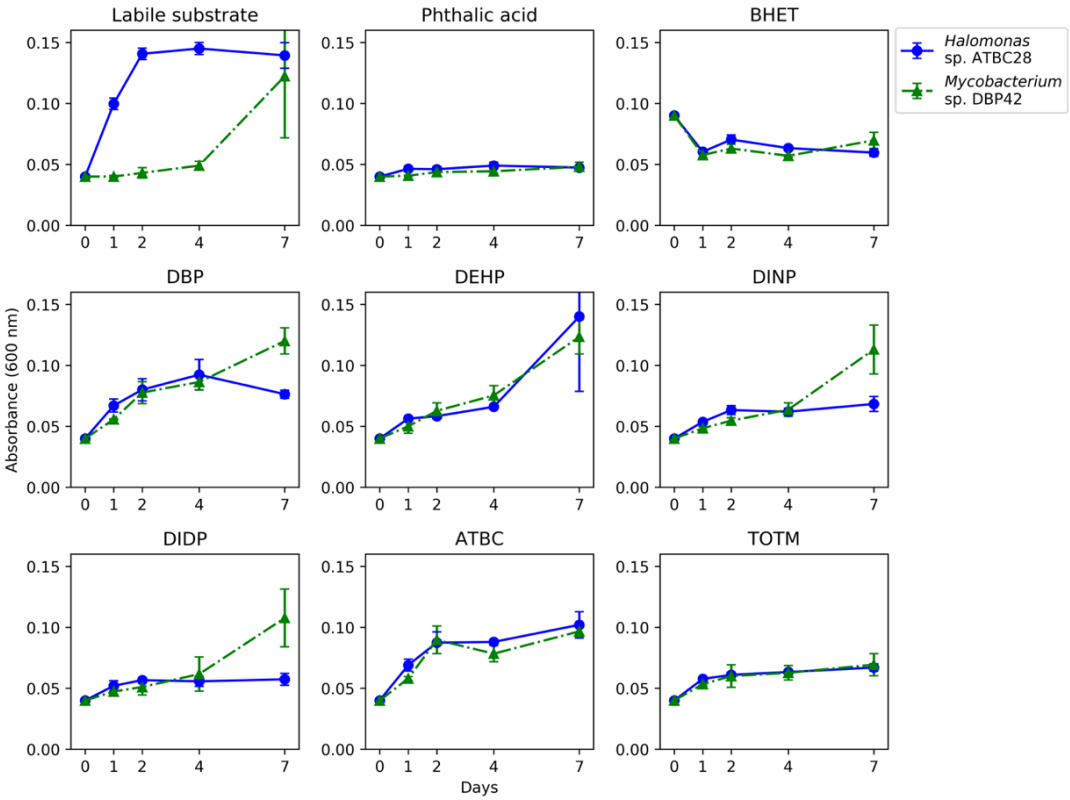

Figure 4.2. Growth of *Halomonas* sp. ATBC28 and *Mycobacterium* sp. DBP42 on a labile substrate (0.1% w/v of pyruvate and 0.1% v/v of glycerol, respectively, as tested in Figure 4.1 and six different plasticizers (0.1% v/v), as well as phthalate. Hereafter, growth with phthalate was carried out using 0.02% (w/v) as no growth was observed at 0.1%, potentially due to its toxicity. Error bars represent the standard deviation of three biological replicates.

4.3.2 Genome analysis of *Halomonas* sp. ATBC28 and *Mycobacterium* sp. DBP42

Genome sequencing revealed that *Halomonas* sp. ATBC28 had a genome size of 5.47 Mb, with 5,111 coding sequences, 2,367 of which were annotated as hypothetical proteins, and a GC content of 54.6%. *Mycobacterium* sp. DBP42 had a genome size of 6.52 Mb with 6,316 coding sequences, 1,581 of which were annotated as hypothetical proteins, and a GC content of 66.15%. As expected, the genomes of both organisms revealed a large potential for PAE biodegradation: i) both strains encoded genes involved in phthalate degradation and ii) a number of esterases, cutinases and lipases or enzymes from the β-oxidation of fatty acids, necessary for the removal of the ester side chains from the phthalate molecule, were also encoded. A comprehensive exo- and cellular-proteomic and metabolomic analysis was performed with *Halomonas* sp. ATBC28 (Appendix 5. Proteins identified through genomic analysis of *Halomonas* sp. ATBC28 as potentially involved with plasticizer degradation.) and *Mycobacterium* sp. DBP42 (Appendix 6. Proteins identified through genomic analysis of *Mycobacterium* sp. DBP42 as potentially involved with plasticizer degradation.) to ascertain

the pathways and enzymes used for degrading the plasticizers DBP, DEHP and ATBC, as summarised in Figure 4.3 and detailed below.

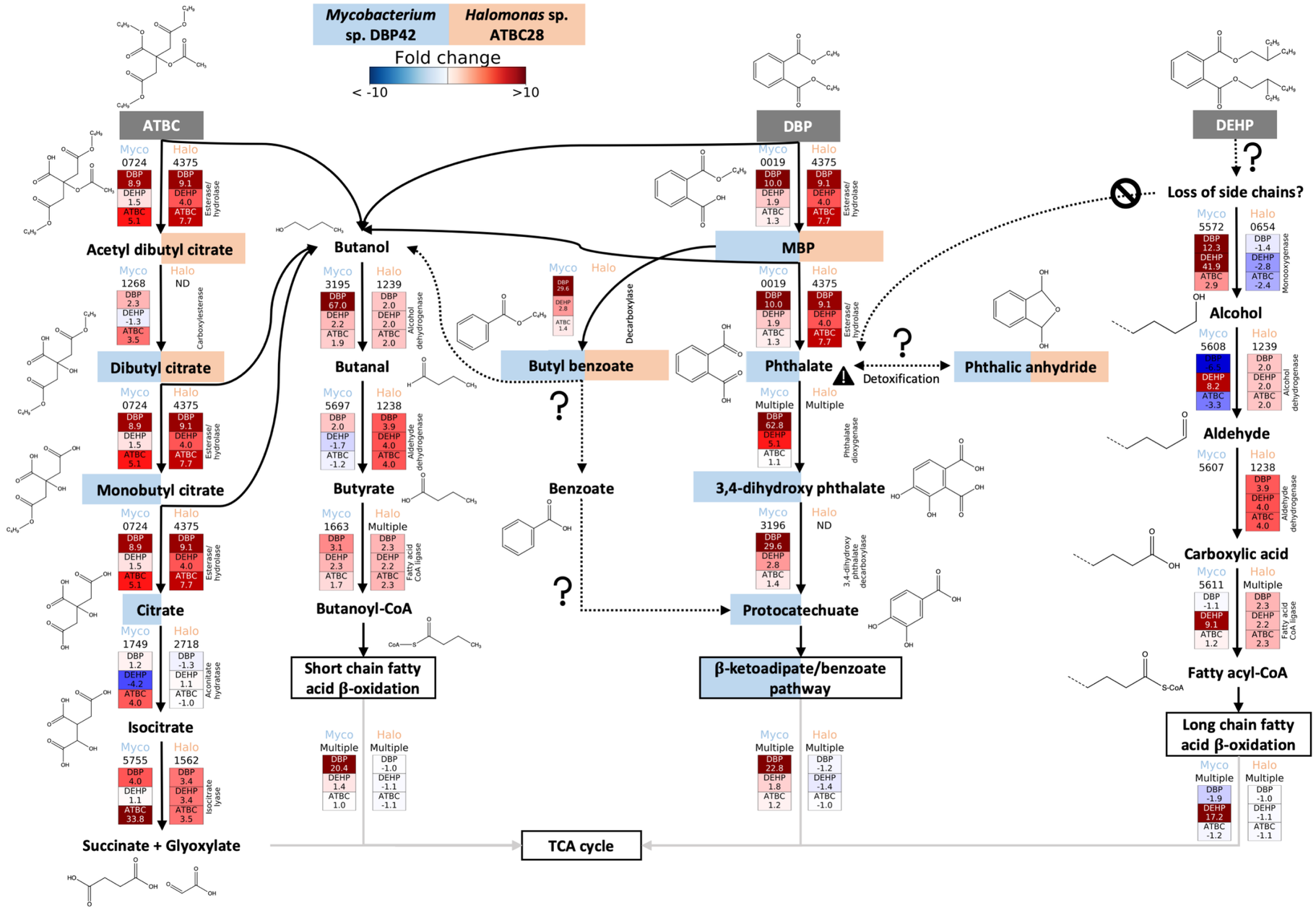

Figure 4.3. Catabolic pathways informed by genomic, proteomic and metabolomic analyses for DBP, DEHP and ATBC degradation by *Mycobacterium* sp. DBP42 and *Halomonas* sp. ATBC28. Initial plasticizer substrates are shown in dark grey boxes, while degradation intermediates that were detected by metabolomics are shown with blue and orange boxes if they were present in the *Mycobacterium* sp. DBP42 (Myco) or *Halomonas* sp. ATBC28 (Halo) treatments, respectively. General multi-step pathways are outlined in boxes. Dashed arrows show reactions inferred by metabolomics, although no enzyme catalysing the reaction could be confidently assigned by proteogenomics. Solid arrows indicate reactions catalysed by detected enzymes. Enzyme ID number and fold change in each treatment (DBP, DEHP and ATBC *vs* control) for both *Mycobacterium* sp. DBP42 and *Halomonas* sp. ATBC28 is shown for each reaction. All enzymes shown here were detected in the cellular proteome, aside from the isocitrate lyase 5755 in *Mycobacterium* sp. DBP42 and the esterase/hydrolase 4375 in *Halomonas* sp. ATBC28, which were detected in the exo-proteome. Dashed lines in chemical structures indicate uncertainty on composition.

4.3.3 Identification of the pathway used by *Mycobacterium* sp. DBP42 for plasticizer degradation

For *Mycobacterium* sp. DBP42, it was confirmed by metabolomics that DBP is degraded through a sequential removal of the ester side chains, first producing monobutyl phthalate and then phthalate, as well as two butanol molecules (Figure 4.3 and Figure 4.4). The strong proteomic upregulation of the cutinase 0019 in the presence of DBP (*i.e.* 10.0-fold) suggests that this enzyme may be involved in the cleavage of these side chains. Phthalate is then converted to protocatechuate and further processed via the β-ketoadipate/benzoate pathway, as indicated by the detection of the expected intermediates by metabolomics (Figure 4.3, Figure 4.4 and Appendix 7. Summary of compounds detected through targeted (T) and untargeted (UT) metabolomic analyses of *Mycobacterium* sp. DBP42 and *Halomonas* sp. ATBC28 culture supernatants when grown with phthalate, DBP, DEHP or ATBC as sole carbon sources.) and the up-regulation of all proteins encoded within the gene cluster 3196-3210 in the presence of DBP (*i.e.* Figure 4.3, Figure 4.4 and Figure 4.5). Interestingly, the metabolomic analysis flagged the possible accumulation of compounds derived from side reactions, *i.e.* butyl benzoate and phthalic anhydride (Figure 4.3 and Appendix 7. Summary of compounds detected through targeted (T) and untargeted (UT) metabolomic analyses of *Mycobacterium* sp. DBP42 and *Halomonas* sp. ATBC28 culture supernatants when grown with phthalate, DBP, DEHP or ATBC as sole carbon sources.). While butyl benzoate may come as a consequence of monobutyl phthalate decarboxylation (and it is unknown whether it is then further processed into benzoate as this intermediate was not detected), phthalic anhydride may function as a detoxification strategy during the build-up of phthalate. Phthalic anhydride was previously detected during the degradation of the long-chain PAEs DINP and DIDP (Park et al., 2009, 2008), as well as dipentyl phthalate (Ahn et al., 2006). A dihydroxy acid dehydratase (3668) that could be responsible for catalysing this reaction was slightly upregulated in both the presence of phthalate and DBP (*i.e.* 1.9-fold; Appendix 6. Proteins identified through genomic analysis of *Mycobacterium* sp. DBP42 as potentially involved with plasticizer degradation.), however, it is also possible that this could occur through a hydrolysis reaction, for which a number of enzymes could be responsible. The hydrolysed DBP side chains, *i.e.* two butanol molecules, are further metabolised through the action of alcohol and aldehyde dehydrogenases (3195 and 5697, respectively) and a fatty acid-CoA ligase (1663) before entering the short chain fatty acid β-oxidation pathway (4429-4434), a pathway previously suggested (Ahuactzin-Pérez et al., 2018) and for which all enzymes were strongly upregulated in this treatment (Figure 4.3, Figure 4.4 and Figure 4.5).

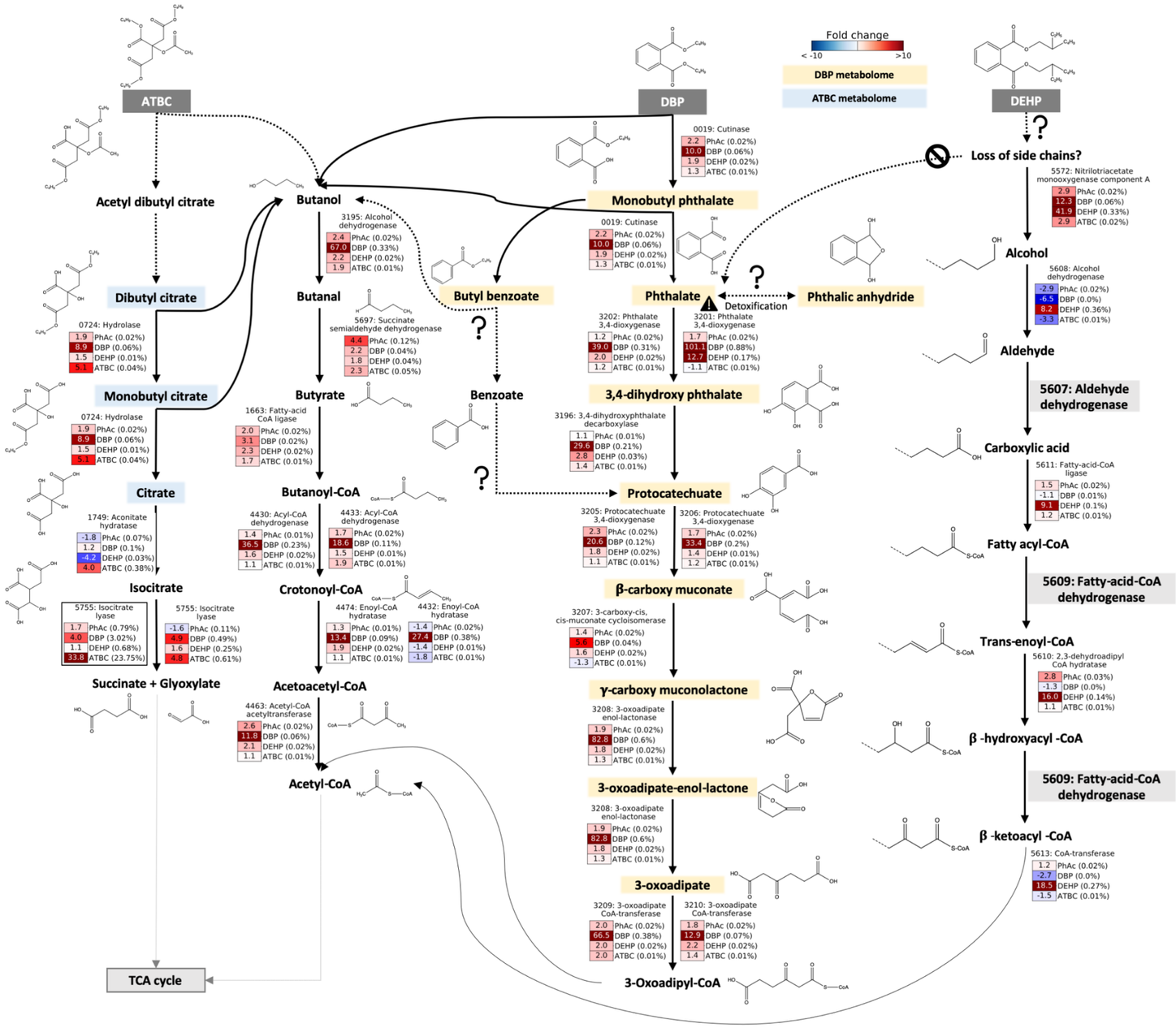

Figure 4.4. Catabolic pathways informed by genomic, proteomic and metabolomic analyses for DBP, DEHP and ATBC degradation by *Mycobacterium* sp. DBP42. Initial plasticizer substrates are shown in dark grey boxes, while degradation intermediates that were detected by metabolomics are shown with yellow or blue boxes if they were identified in the DBP or ATBC metabolomes, respectively. Dashed arrows show reactions inferred by metabolomics, although no enzyme catalysing the reaction could be confidently assigned by proteogenomics. Solid arrows indicate reactions catalysed by detected enzymes. Enzyme ID number and fold change in each treatment (DBP, DEHP and ATBC *vs* control) is shown for each reaction. All enzymes shown here were detected in the cellular proteome, aside from the isocitrate lyase 5755, which was detected in the exo-proteome. Light grey boxes with enzyme ID numbers show enzymes that were in the genome but were not detected in either the cellular or exo-proteomes. Dashed lines in chemical structures indicate uncertainty on composition.

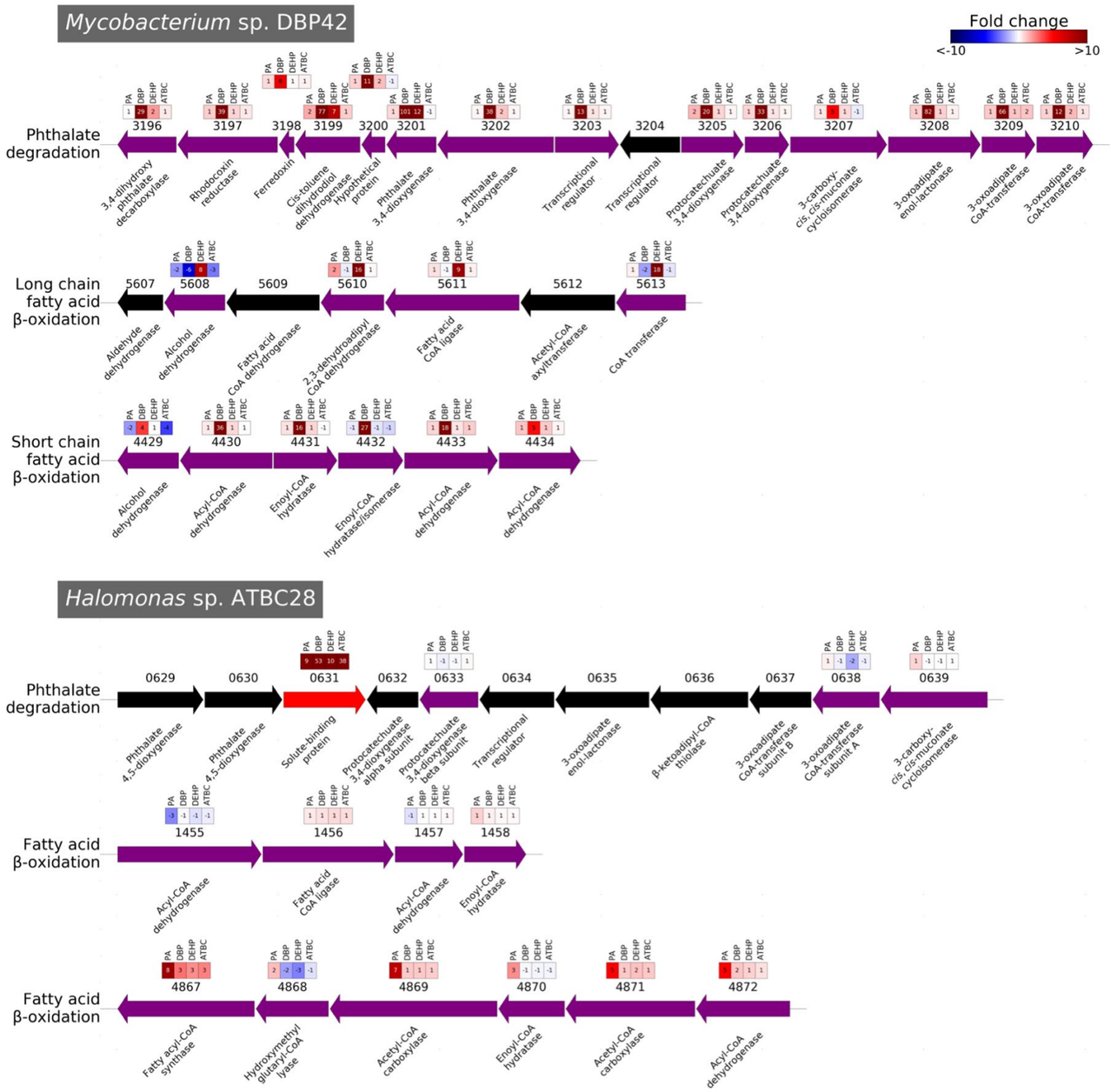

Figure 4.5. Operons within the genomes of *Mycobacterium* sp. DBP42 and *Halomonas* sp. ATBC28 that are used for either phthalate or fatty acid degradation. Arrows represent coding domain sequences that were detected in the cellular proteomes (purple), exo-proteomes (red) or neither (black). Numbers above the arrows indicate the gene ID within each genome. Boxes indicate the protein fold change in phthalate (PA), DBP, DEHP and ATBC treatments relative to the control growth (labile substrate).

Curiously, while the presence of DBP strongly induced the catabolic pathway for phthalate, this was not the case when *Mycobacterium* sp. DBP42 was grown in the presence of phthalate or DEHP (Figure 4.3). The transcriptional regulator encoded within the gene cluster (3203) increased 13.5-fold in the presence of DBP as opposed to just 1.2- to 1.4-fold in the phthalate, DEHP and ATBC treatments (Figure 4.4). Furthermore, metabolic intermediates of phthalate and protocatechuate degradation were only detected in the DBP treatment and not in the presence of phthalate or DEHP. All of this evidence in conjunction with i) the slow growth of this strain in the presence of phthalate (Figure 4.2), ii) the build-up of phthalic anhydride in the phthalate treatment (Appendix 7. Summary of compounds detected through targeted (T) and untargeted (UT) metabolomic analyses of *Mycobacterium* sp. DBP42 and *Halomonas* sp. ATBC28 culture supernatants when grown with phthalate, DBP, DEHP or ATBC as sole carbon sources.) and iii) the higher relative abundance of proteins involved in DNA protection (5706; 18.0-fold increase), potential antigens (2974; 14.6-fold increase) and stress proteins (3075; 8.8-fold increase; Appendix 6. Proteins identified through genomic analysis of *Mycobacterium* sp. DBP42 as potentially involved with plasticizer degradation.), suggests that growth using phthalate as the sole source of carbon and energy is challenging, if not toxic, for this strain.

The degradation of DEHP by *Mycobacterium* sp. DBP42 did not seem to follow the same pathway as observed for DBP. The lack of detection of the expected degradation intermediates (*e.g.* mono(2-ethyl hexyl) phthalate, phthalate or phthalic anhydride) and lower abundance of the cutinase 0019 involved in hydrolysing the ester side-chains, suggests that DEHP degradation does not occur via sequential cleavage of ester side-chains. The data indicates that degradation may occur as suggested previously (Amir et al., 2005), *i.e.* via the β-oxidation of the fatty acid side-chains directly on the DEHP molecule. In fact, enzymes from the long-chain fatty acid β-oxidation pathway were strongly induced by the presence of DEHP (an average of 17.2-fold; Figure 4.4 and Figure 4.5). It is therefore hypothesised here that DEHP degradation is initiated through hydroxylation of the ester side chains by a monooxygenase (5572; 42-fold protein increase in the DEHP treatment) and enters the β-oxidation pathway as suggested in Figure 4.3.

ATBC degradation in *Mycobacterium* sp. DBP42 occurs through a sequential removal of the ester side chains, generating citrate that is then funnelled into the central metabolism (Figure 4.3). The metabolomic analysis confirmed the presence of the ATBC degradation intermediates dibutyl citrate, monobutyl citrate and citrate (Appendix 7. Summary of

compounds detected through targeted (T) and untargeted (UT) metabolomic analyses of *Mycobacterium* sp. DBP42 and *Halomonas* sp. ATBC28 culture supernatants when grown with phthalate, DBP, DEHP or ATBC as sole carbon sources. and Figure 4.3). This suggests that ATBC degradation initiates by the removal of acetic acid and butanol, possibly by the carboxylesterase 1268 (3.5-fold increase) or hydrolase 0724 (5.1-fold increase), respectively. As indicated in Figure 4.3, it is tentatively suggested here that acetyl dibutyl citrate is generated first because this intermediate was detected in the *Halomonas* sp. ATBC28 metabolome (see below). The other two butanol molecules are then successively removed, presumably by the hydrolase 0724, to produce citrate. While the degradation pathway for butanol was not highly upregulated in the presence of ATBC, the two-step conversion of citrate to succinate and glyoxylate was (Figure 4.3). Curiously, the isocitrate lyase (5755), presumably responsible for the conversion of isocitrate to succinate and glyoxylate, with no prediction for secretion (Almagro Armenteros et al., 2019), was detected in high abundance in the exoproteome of *Mycobacterium* sp. DBP42 only in this treatment (24.7% of the exoproteome and 33.8-fold upregulated; Appendix 7. Summary of compounds detected through targeted (T) and untargeted (UT) metabolomic analyses of *Mycobacterium* sp. DBP42 and *Halomonas* sp. ATBC28 culture supernatants when grown with phthalate, DBP, DEHP or ATBC as sole carbon sources.).

4.3.4 Proteomic and metabolomic identification of the pathway used by *Halomonas* sp. ATBC28 for plasticizer degradation

The metabolic pathways used for the degradation of plasticizers and phthalate were less clear in *Halomonas* sp. ATBC28 (Figure 4.3 and Figure 4.6). Surprisingly, whilst this bacterium encoded the necessary pathway for phthalate and protocatechuate degradation (Figure 4.5), most of the enzymes and degradation intermediates were not detected in the proteomes or metabolomes of any of the treatments (Figure 4.6, Appendix 5. Proteins identified through genomic analysis of *Halomonas* sp. ATBC28 as potentially involved with plasticizer degradation. and Appendix 7. Summary of compounds detected through targeted (T) and untargeted (UT) metabolomic analyses of *Mycobacterium* sp. DBP42 and *Halomonas* sp. ATBC28 culture supernatants when grown with phthalate, DBP, DEHP or ATBC as sole carbon sources.), suggesting a lack of induction of this pathway under the conditions tested. Based on their predicted fragmentation pattern with trypsin digestion, these should have been detected if they were present and they were also not in a genomic island (Figure 4.7) or plasmid encoded. Interestingly, though, *Halomonas* sp. ATBC28 *was* able to carry out the first

steps of DBP degradation as the metabolic intermediates monobutyl phthalate, phthalic anhydride and butyl benzoate were detected in this treatment (Figure 4.3 and Appendix 7. Summary of compounds detected through targeted (T) and untargeted (UT) metabolomic analyses of *Mycobacterium* sp. DBP42 and *Halomonas* sp. ATBC28 culture supernatants when grown with phthalate, DBP, DEHP or ATBC as sole carbon sources.). We propose the hydrolysis of the butyl side chains of DBP is catalysed by the esterase 4375, a serine hydrolase with a signal peptide for secretion (Almagro Armenteros et al., 2019) which showed a 9.1-fold increase in the exoproteome under this treatment (Figure 4.3). Esterase 4375 also showed an increased abundance in the presence of other plasticizers (4- and 7.7-fold in the DEHP and ATBC treatments, respectively) suggesting it may also be induced by other metabolites. As observed for *Mycobacterium* sp. DBP42, the side chains of the plasticizers are likely to enter the β-oxidation pathway for fatty acid degradation, however, in *Halomonas* sp. ATBC28 there was no clear differentiation between the short- and long-chain pathways when growing with either DBP or DEHP (Figure 4.5). Intriguingly, some of these enzymes were not largely upregulated in the cellular proteome but were in the exo-proteome (Appendix 5. Proteins identified through genomic analysis of *Halomonas* sp. ATBC28 as potentially involved with plasticizer degradation.).

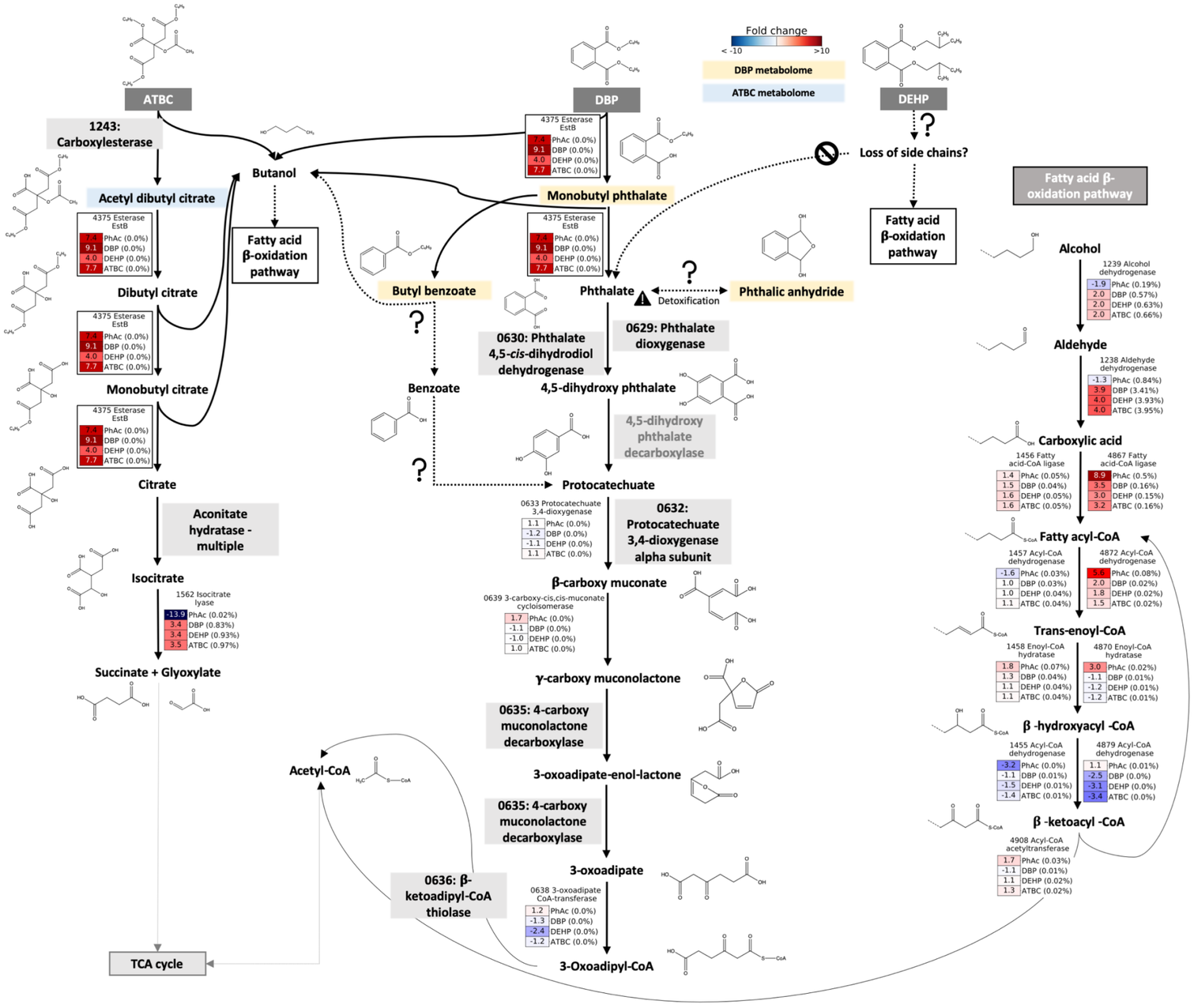

Figure 4.6. Catabolic pathways informed by genomic, proteomic and metabolomic analyses for DBP, DEHP and ATBC degradation by *Halomonas* sp. ATBC28. Initial plasticizer substrates are shown in dark grey boxes, while degradation intermediates that were detected by metabolomics are shown with yellow or blue boxes if they were identified in the DBP or ATBC metabolomes, respectively. Dashed arrows show reactions inferred by metabolomics, although no enzyme catalysing the reaction could be confidently assigned by proteogenomics. Solid arrows indicate reactions catalysed by detected enzymes. Enzyme ID number and fold change in each treatment (DBP, DEHP and ATBC *vs* control) is shown for each reaction. All enzymes shown here were detected in the cellular proteome, aside from the esterase/hydrolase 4375, which was detected in the exo-proteome. Light grey boxes with enzyme ID numbers show enzymes that were in the genome but were not detected in either the cellular or exo-proteomes. Dashed lines in chemical structures indicate uncertainty on composition.

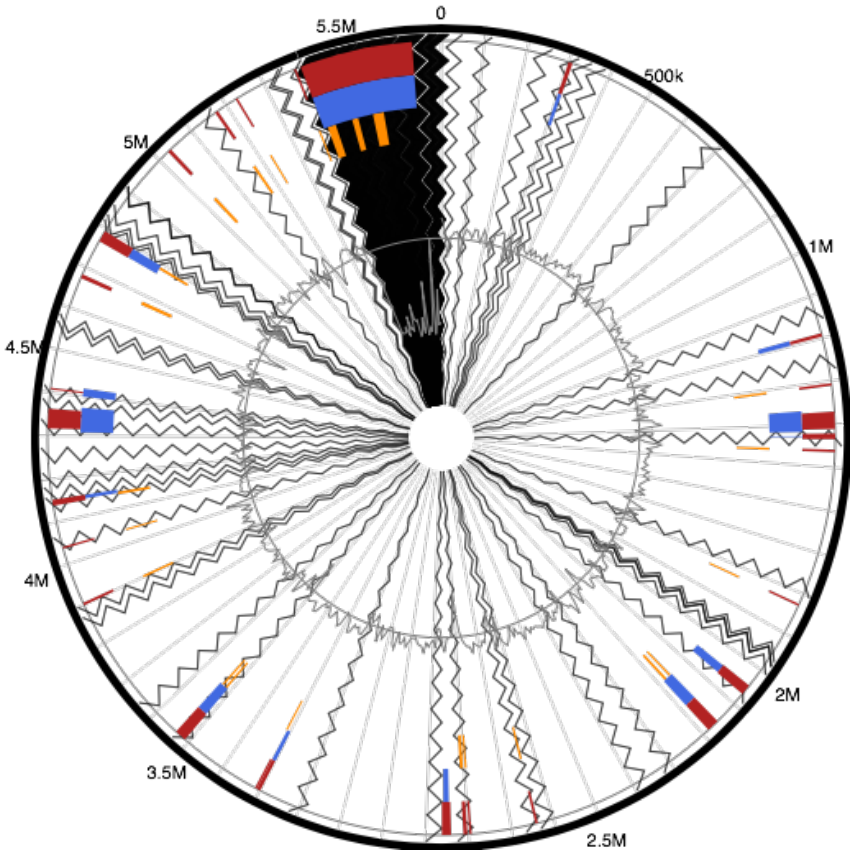

Figure 4.7. Circular visualisation of *Halomonas* sp. ATBC28 genome with genomic islands, as predicted by Island Viewer 4. Blocks are coloured according to the prediction method; Integrated results (*i.e.* multiple methods; dark red), IslandPath-DIMOB (blue) or SIGI-HMM (orange). Radial lines indicate contig gap regions and the inner circle shows GC content.

For ATBC, the intermediates acetyl dibutyl citrate and dibutyl citrate were detected in the metabolome of *Halomonas* sp. ATBC28 in this treatment (Figure 4.3) confirming the ability of this strain to metabolise ATBC. It is therefore again suggested that esterase 4375 is involved in hydrolysing the side-chains of ATBC, although the promiscuity of substrates for this enzyme requires further characterisation.

The strong increase of 20 transporters and efflux pumps in *Halomonas* sp. ATBC28 in one or more of the treatments, when compared with growth on pyruvate (Figure 4.8 and Appendix 5. Proteins identified through genomic analysis of *Halomonas* sp. ATBC28 as potentially involved with plasticizer degradation.), is also remarkable. The tripartite ATP-independent periplasmic (TRAP) transporter 0631, that is encoded in close proximity to the phthalate degradation gene cluster (Figure 4.5), was strongly upregulated in the exo-proteomes of all treatments and a second TRAP transporter (0264) was strongly upregulated in the cellular proteomes of the plasticizer treatments (Figure 4.6). Transporters are likely detected in the

exo-proteome because the exo-proteome often includes proteins that are attached to the surface of the cell (Armengaud et al., 2012). Also upregulated more strongly in the plasticizer treatments was a cation/acetate symporter previously suggested to be involved in phthalate degradation (Kumar and Maitra, 2016) and a sodium/hydrogen ion antiporter (2103). The fact that the phthalate degradation pathway was not induced in *Halomonas* sp. ATBC28 opens the question as to whether these transporters are maybe exporting phthalate to reduce its cellular toxicity or importing the cleaved side chains into the cell. Other interesting cellular responses of *Halomonas* sp. ATBC28 to the presence of the different plasticizers were the strong increase in iron acquisition (*e.g.* bacterioferritin 2469 and three different iron binding transport systems) and extracellular superoxide dismutase 4604 to deal with oxidative stress (Appendix 5. Proteins identified through genomic analysis of *Halomonas* sp. ATBC28 as potentially involved with plasticizer degradation.). There was also an ompA-like protein (3348) that was abundant in the exo-proteomes of phthalate, DBP, DEHP and ATBC (49, 204, 90 and 264-fold increases, respectively; Figure 4.8 and Appendix 5. Proteins identified through genomic analysis of *Halomonas* sp. ATBC28 as potentially involved with plasticizer degradation.) that could be used as a surfactant to solubilise the plasticizers and aid in their detoxification.

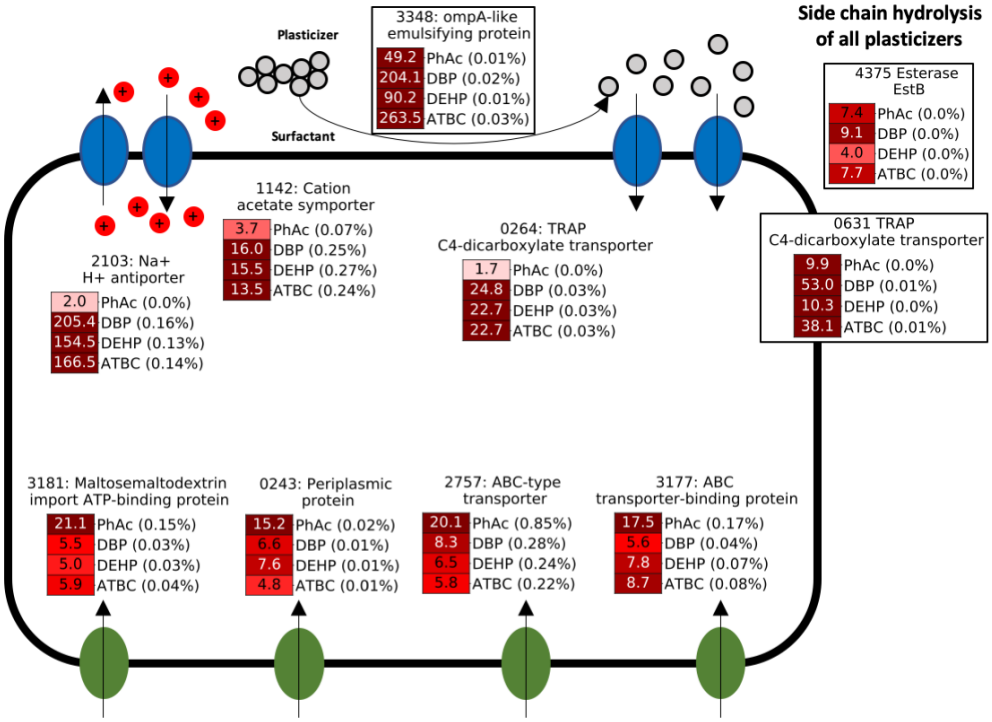

Figure 4.8. Proteins in Halomonas sp. ATBC28 that may be involved in the solubilisation, hydrolysis or transport into the cell of plasticizers and phthalate. Black outlines around the boxes indicate that this protein was detected in the exo-proteome. Boxes show the genome position of the enzyme used for that step alongside the fold-change (when compared with the positive control, *Halomonas* sp. ATBC28 grown with pyruvate) and the percentage relative abundance within the proteomes.

4.4 Discussion

The microbial isolation and integrated multi-OMIC characterisation presented here has allowed a comprehensive understanding of plasticizer biodegradation in bacteria obtained from marine plastic debris. Through the enrichment and isolation of 42 bacterial isolates capable of plasticizer degradation it was found that, while the ability to grow using PAE plasticizers (*e.g.* DBP and DEHP) was fairly widespread, surprisingly, ATBC was the plasticizer that the lowest number of isolates were able to use for growth (Table 4.2 and Appendix 4. Screening of bacterial isolates ability to grow using plasticizers as a sole carbon source.). ATBC is sold as a biodegradable and less toxic alternative to DEHP and other PAE plasticizers (Baiardo et al., 2002; Erceg et al., 2005), however, to our knowledge, there are no studies that have reported microbial ATBC degradation or identified the enzymes involved. It is possible though that the side chains of the ATBC molecules can hydrolyse spontaneously, however, this only occurs at high temperatures and ATBC has a predicted half-life of two years under the conditions applied here, *i.e.* pH 7 (FR-MSCA, 2013). Hence, it is suggested that ATBC side-chain hydrolysis is facilitated by encoded hydrolases in a reduced number of bacteria as only a small number of isolates could grow in the presence of this plasticizer.

The biodegradation of most plasticizers requires an initial hydrolysis of the ester side-chains, generating intermediates that are then funnelled through known catabolic pathways into the central metabolism (Ahuactzin-Pérez et al., 2018, 2016; Nai-xian Feng et al., 2018; Vamsee-Krishna and Phale, 2008; Yang et al., 2018). The proteogenomic approach used here helped to identify these esterases (*i.e.* cutinase 0019 and hydrolase 0724 for DBP and ATBC hydrolysis, respectively, in *Mycobacterium* sp. DBP42; and the possibly more promiscuous esterase 4375 in *Halomonas* sp. ATBC28; Figure 4.3) and flags these enzymes as candidates for future biochemical characterisation. Although cutinases are enzymes that were initially described for the hydrolysis of the plant polyester cutin (Carvalho et al., 1998), a previously identified cutinase-like enzyme was also shown to hydrolyse the PAE dipentyl phthalate to phthalate (Ahn et al., 2006). Esterases acting on PAEs can catalyse a wide range of compounds, *e.g. p*-nitrophenols (Ahn et al., 2006) and triacylglycerols (Martínez-Martínez et al., 2014) and hence the promiscuity of the enzymes identified in this chapter is not surprising but needs to be tested. Nevertheless, while for DBP and ATBC a sequential removal of the ester-bound side-chains was observed by metabolomics (*i.e.* producing phthalate and citrate, respectively, as well as butanol), DEHP presumably follows a sequential shortening of the

side-chains directly on the molecule by enzymes involved in the β-oxidation pathway for fatty acid degradation, as previously suggested (Li et al., 2018).

The use of two phylogenetically distinct bacteria to characterise the biodegradation of different plasticizers has highlighted the biological complexity behind the metabolic regulation of the different pathways. In this sense, while both isolates investigated potentially encoded the catabolic pathway for phthalate biodegradation, these enzymes were only detected in *Mycobacterium* sp. DBP42 and were mainly upregulated under the DBP treatment, suggesting that either DBP or monobutyl phthalate may act as inducers of this pathway. This stresses the fact that more microbes may be capable of biodegrading recalcitrant compounds, although their pathways might be silenced or only induced by very specific chemicals. The conversion of phthalate into protocatechuate is the most common pathway for phthalate degradation (Vamsee-Krishna and Phale, 2008). Interestingly, in *Mycobacterium* sp. DBP42 it was found that these genes (*i.e.* phthalate dioxygenase and dihydroxy phthalate decarboxylase) clustered with the protocatechuate and benzoate degradation pathway (Figure 4.5) as reported previously in *Mycobacterium vanbaalenii* PYR-1 (Stingley et al., 2004), although in *M. vanbaalenii* the decarboxylase (responsible for the conversion of 3,4-dihydroxy phthalate to protocatechuate) was located elsewhere in the genome. The fact that here all genes were found to be clustered in *Mycobacterium* sp. DBP42 suggests a higher level of specialisation in degrading these aromatic compounds. In *Halomonas* sp. ATBC28, though, despite encoding for a potential phthalate dioxygenase within the protocatechuate degradation gene cluster, we failed to identify the dihydroxy phthalate decarboxylase. Hence, it is uncertain if this isolate can process phthalate as the metabolomic analysis showed no degradation intermediates beyond phthalate and none of the enzymes were detected by proteomics (Figure 4.6).

Phthalate and its isomers are known toxic compounds (Fajardo et al., 1997; Vamsee-Krishna and Phale, 2008; Yi-Mei Zhang et al., 2013). There are few studies on the mechanisms of this toxicity to bacteria, but phthalate is likely to be more toxic than PAEs due to its higher solubility and it is found to be toxic to other organisms due to a number of mechanisms, for example, by acting as a competitive inhibitor to key enzymes or by suppressing calcium signalling and inducing oestrogenic responses (Vamsee-Krishna and Phale, 2008). Here a number of adaptations adopted by the two isolates to deal with phthalate toxicity are shown *e.g.* via conversion into phthalic anhydride, as observed by metabolomics, or the production of stress response mechanisms and efflux pumps, as shown by proteomics. While phthalic

anhydride was previously reported in other PAE biodegradation studies (Ahn et al., 2006; Park et al., 2009, 2008) and is known to be less toxic than phthalic acid (Bang et al., 2011), the mechanisms or reasons for its production were not identified in these studies. Whilst it is possible that the dehydration of phthalate could occur spontaneously, many previous PAE degradation studies have not reported phthalic anhydride production (*e.g.* Ahuactzin-Pérez et al., 2018, 2016; N. Feng et al., 2018; Yang et al., 2018) and carboxylic acid anhydride production usually requires the presence of a catalyst or an enzyme. It is therefore suggested here that this conversion is catalysed biologically by the dihydroxy acid dehydratase 3668 in *Mycobacterium* sp. DBP42, which is theoretically capable of this conversion and was slightly upregulated in both the presence of phthalate and DBP. This reaction deserves further biochemical characterisation to confirm its involvement in phthalate detoxification.

Twenty active membrane transporters were upregulated in *Halomonas* sp. ATBC28 in the presence of one or more of the plasticizers, including two TRAP transporters (0264 and 0631), the latter of which is located within the phthalate degradation gene cluster (Figure 4.5). These TRAP transporters were more abundantly detected in the PAE and ATBC treatments than with phthalate, which suggests that they may be aiding in side-chain utilisation by transporting these ester side-chains after removal from the phthalate and citrate molecules, respectively, rather than the plasticizers themselves as suggested previously (Kumar et al., 2017). The transporters used for PAEs are identified in very few studies to date (Kumar et al., 2017; Kumar and Maitra, 2016; Stingley et al., 2004) and thus remain under-studied. It is even possible that either the aforementioned TRAP or other transporters and efflux pumps (Du et al., 2018; Figure 4.8, Appendix 5. Proteins identified through genomic analysis of *Halomonas* sp. ATBC28 as potentially involved with plasticizer degradation. and Appendix 7. Summary of compounds detected through targeted (T) and untargeted (UT) metabolomic analyses of *Mycobacterium* sp. DBP42 and *Halomonas* sp. ATBC28 culture supernatants when grown with phthalate, DBP, DEHP or ATBC as sole carbon sources.) are being used as a detoxification mechanism, secreting the toxic phthalate out of the cell. We also identified an ompA-like protein in the exo-proteome of *Halomonas* sp. ATBC28 (3348; Figure 4.8), which could be involved in both detoxification and facilitating biodegradation; ompA proteins are the active components in the biosurfactant alasan and have been previously implicated in the degradation of xenobiotic compounds such as alkanes in other *Gammaproteobacteria* (Schneiker et al., 2006). Further work should be carried out in the future to determine the exact role of these transporters and mechanisms for cellular detoxification.

This chapter presents, for the first time, a comprehensive characterisation of the plasticizer biodegrading potential extant in biofilms on marine plastic debris; from the enrichment and isolation of microbes to the proteogenomic and metabolomic analysis of degradation. The molecular analysis of the degradation of phthalate and three of the most widely-used plasticizers, *i.e.* DBP, DEHP and ATBC, in two newly isolated bacteria, *i.e. Mycobacterium* sp. DBP42 and *Halomonas* sp. ATBC28, has revealed: i) an array of esterases involved in the first steps of DBP and ATBC degradation, ii) the use of different mechanisms for the removal of the ester side-chains from different PAEs (DBP and DEHP), iii) the complexity of induction of the catabolic pathways involved in in the degradation of such compounds and iv) a number of strategies used by the microbes to deal with these toxic compounds. Non-covalently bound compounds linked to plastics are likely to be leached into the surrounding environment. Microbial biofilms that grow on these materials are the first to encounter such chemicals and, as proven here, are able to catabolise them for growth.

Chapter 5

Conclusions and future directions

In this thesis, the aims (Section 1.7) were to: (i) evaluate current knowledge on the colonisation and degradation of plastics by marine microbial communities; (ii) gain a fundamental understanding of microbial community succession and how this impacts the degradation of polymers such as plastics by marine microbial communities, using the natural polymer chitin as a case study; (iii) determine whether the general principles of microbial community succession also apply to the colonisation of and growth on the common packaging plastic polyethylene terephthalate (PET); (iv) isolate marine bacteria that are capable of degrading PET and characterise the enzymes and pathways used for degradation; and (v) determine whether marine microbes have the potential to degrade plastic additives, *i.e.* plasticizers, and characterise the enzymes and pathways involved. Figure 5.1 provides a summary of the motivation, major questions and key results for each results chapter.

Chapter 2 aimed to determine whether a microbial community could be artificially selected to become better at the degradation of a polymer (using the natural polymer chitin as a case study) and how the microbial community responds to this selection. The ability to select a community for the degradation of a recalcitrant polymer requires a test for enzymatic activity that may be performed in a high-throughput manner and is indicative of the ability to degrade that polymer specifically. Because chitin degradation is already well-characterised and the metabolic pathways involved are known (Beier and Bertilsson, 2013), an enzymatic activity test that is both rapid and accurate – that relied on the liberation and measurement of the fluorescent molecule methylumbelliferyl – was used as a proxy for chitin degradation. The validity of artificially selecting a natural microbial community to better degrade a recalcitrant polymer, chitin, was proven for the first time, but the requirements for achieving this goal became apparent, *i.e.* it requires a better understanding of the ecology of the system. It was found that continuous optimisation of incubation times is essential in order to successfully implement this process, as optimal degrading communities rapidly decay due to their replacement by cheaters and cross-feeders, as well as the increase in potential predators such as grazers and, although not tested here, viruses. These optimal communities, in the case of chitin degradation, were composed of a large proportion of *Gammaproteobacteria* and it was this group that predominantly possessed the ability to degrade chitin. Other groups that increased in abundance at later time points, such as the *Alphaproteobacteria*, were, in general, merely capable of utilising the sub-products of chitin degradation such as the

sugar molecules of the chitin monomer, N-acetyl-D-glucosamine, GlcNAc, and organic matter produced by the community.

Chapter 2	Chapter 3	Chapter 4
Motivation: Before studying the degradation of synthetic polymers, *i.e.* plastics, in the marine environment, it is important to understand the factors influencing the degradation of natural polymers, *i.e.* chitin. Artificial selection has been previously used on whole microbial communities to improve the degradation of toxic environmental contaminants – with limited success – but the mechanisms behind its success have not been determined and it has not been used on polymers.	**Motivation:** It is suggested that PET is easier to degrade than other plastics due to an ester linkage between monomeric units, and PETases (a sub-group of esterases) have been characterised. Artificial selection cannot be applied currently because esterases are produced for a variety of processes in microbial communities and degradation times for PET in the marine environment are currently unknown, although communities are expected to perform better than isolates at PET biodegradation.	**Motivation:** Plasticizers (a highly toxic group of plastic additives) are not covalently bound to plastics and therefore leach out when the plastics reach the environment. Phthalic acid ester plasticizer (PAEs) degradation has been characterised in some terrestrial microorganisms but studies in the marine environment are limited and few studies have identified the enzymes involved in initiating biodegradation. These are now increasingly being replaced by less toxic alternatives for which the biodegradation pathways are unknown.
Major questions • Can a microbial community be artificially selected to become better at the degradation of a polymer (for which the degradation pathways and colonisation dynamics are known) – chitin? • Are there any caveats to the success of this selection? • What effect does artificial selection have on the 16S and 18S rRNA gene community structure and composition? • Is actively selecting for a community with high chitinase activity better than randomly selecting a community (when both are grown with chitin as a sole carbon and nitrogen source)?	**Major questions** • Do the general principles of microbial community succession also apply to the colonisation (and degradation) of PET? • How does the 16S rRNA gene community change across six weeks of incubation with PET? • Are these changes the same on different types of PET and the PET precursor, BHET? • Can marine bacteria be isolated that are capable of degrading PET? • What are the enzymes and pathways used for this degradation? Are they the same as for terrestrial PET degraders? • Are microbial communities or isolates better at PET degradation?	**Major questions** • Does the potential for plasticizer degradation exist within the microbial community that colonises plastics? • Are the mechanisms for the degradation of PAEs the same in the marine environment as in the terrestrial environment? • Are the same pathways/enzymes used for the degradation of different PAEs (*i.e.* DBP and DEHP)? • Is a less toxic plasticizer (*i.e.* ATBC) degraded? What is the pathway used for ATBC degradation? • Are the pathways used for this degradation the same in two phylogenetically distinct bacteria?
Key results • Artificial selection of microbial communities only increases chitinase activity when incubation times between transfers are constantly optimised. • If incubation times between transfers are too long then the community enters the succession (*i.e.* high relative abundance of cheaters, cross-feeders and grazers) rather than the selection (*i.e.* high relative abundance of chitin degraders) phase. • The high-performing chitinolytic community is composed predominantly of *Gammaproteobacteria*. • Most chitinase gene copies are possessed by the *Gammaproteobacteria* (and their abundance correlates with measured chitinase activity) while other taxonomic groups (*e.g. Alphaproteobacteria*) possess mainly chitin deacetylases. • The succession phase is composed predominantly of *Alphaproteobacteria* and *Cafeteria* sp. • The largest effects on community composition are within an incubation and only after incubation times have been reduced to four days is the positively selected community significantly different from the randomly selected control community.	**Key results** • The community colonising PET does go through the common phases of community succession, but these are less distinct than for chitin and incubation times required are much longer. • Most ASVs that differentiate the communities colonising different types of PET and BHET are abundant at earlier (days 1-7) stages of incubation. • Two marine bacteria (*Thioclava* sp. BHET1 and *Bacillus* sp. BHET2) were isolated using BHET that were potentially capable of degrading PET. • Putative enzymes similar to those used for PET degradation in the terrestrial environment were identified through a proteogenomic approach for *Thioclava* sp. BHET1 but those that were potentially involved in PET degradation for *Bacillus* sp. BHET2 were not similar to known PET degradation enzymes. • The community showed higher growth with PET than either isolate and the FTIR results suggest that the community and both isolates were able to degrade PET.	**Key results** • Two marine bacteria (*Halomonas* sp. ATBC28 and *Mycobacterium* sp. DBP42) were isolated that were able to degrade two PAEs (DBP and DEHP) and one citrate plasticizer (ATBC), which was confirmed by a multi-OMIC approach. • Different mechanisms are used for the utilisation of the ester side-chains from different PAEs (*i.e.* esterases are used on DBP and enzymes from the β-oxidation pathway of fatty acids for DEHP). • An array of esterases are involved in the first steps of DBP and ATBC degradation • The induction of the catabolic pathways for these compounds is complex: *Mycobacterium* sp. DBP42 only utilises the phthalate produced from DBP degradation while *Halomonas* sp. ATBC42 possesses the genomic potential for phthalate degradation but this pathway was not induced under any of the conditions tested. • A number of strategies are used by these bacteria to cope with phthalate, a toxic intermediate of PAE degradation.

Figure 5.1. Summary of the motivation, major questions and key results for each results chapter of this thesis.

Chapter 3 of this thesis aimed to: i) determine whether the general principles of microbial community succession also apply to the colonisation of and growth on the common packaging plastic polyethylene terephthalate (PET); ii) isolate marine bacteria that are capable of degrading PET; and iii) characterise their degradation pathways using a proteogenomic approach. It was shown that microbial communities growing with PET as a sole carbon source go through distinct stages of succession, but that the extent to which this occurs and the time at which members of these specific communities are highest in abundance is dependent upon the properties of the polymer. Curiously, although community succession is seen on different types of PET, there is no typical shift in the dominant microbial community from *Gammaproteobacteria* at early stages of incubation to *Alphaproteobacteria* at later time points, which has also been shown in *in situ* incubations with PET (Oberbeckmann et al., 2014). Here, this is possibly due to the dominance of *Vibrio* spp. in the seeding community, as a consequence of collection of the inoculum from a coastal site close to a wastewater treatment plant. Also in Chapter 3, two marine bacteria were isolated that were potentially capable of degrading PET, *Thioclava* sp. BHET1 and *Bacillus* sp. BHET2, using the PET monomer, bis(2-hydroxy ethyl) terephthalate (BHET). Putative pathways were identified for PET degradation by *Thioclava* sp. BHET1, but the pathway used by *Bacillus* sp. BHET2 for PET degradation was not determined, although degradation was shown through FTIR analyses and a large number of proteins that are potentially involved in the metabolism of xenobiotic compounds were present in its cellular and exo-proteomes. It is possible that *Bacillus* sp. BHET2 encodes a novel pathway for PET degradation and work to confirm this using metabolomics is ongoing. This is the first time that microbial community succession has been characterised using different types of PET, *i.e.* high and low crystallinity as well as weathered PET and PET oligomers, *i.e.* BHET, and the first time that the pathway used for PET degradation by marine microbial isolates has been described.

Chapter 4 aimed to determine whether the potential exists in the marine environment for the degradation of common plastic additives, plasticizers, and to identify the degradation pathways involved using a proteogenomic approach. Initially, 42 bacteria were isolated that were capable of growing on one or more of six plasticizers (dibutyl phthalate, DBP; bis(2-ethyl hexyl) phthalate, DEHP; diisononyl phthalate, DINP; diisodecyl phthalate, DIDP; acetyl tributyl citrate, ATBC; and trioctyl trimellitate, TOTM) as a sole carbon source and then this was narrowed down to two bacteria that could grow on most of these plasticizers, *Halomonas* sp. ATBC28 and *Mycobacterium* sp. DBP42. The growth of these

two isolates was characterised on two phthalic acid ester (PAE) plasticizers, DBP and DEHP, and one biodegradable plasticizer, ATBC, using proteomics and a thorough genomic analysis. The pathway used by *Mycobacterium* sp. DBP42 to degrade the plasticizers was confirmed, although the pathway used by *Halomonas* sp. ATBC28 was less clear. Interestingly, *Mycobacterium* sp. DBP42 uses different mechanisms for the removal of the side chains from each of the phthalic acid ester (PAE) plasticizers, DBP and DEHP, and apparently only the phthalic acid generated from DBP degradation goes on to enter the benzoate (β-ketoadipate) degradation pathway. This is the first time that the enzymes used for PAE plasticizer degradation in the marine environment have been identified and is one of only a few studies to identify the enzymes used for side-chain removal from these compounds. The pathway used for ATBC degradation was also identified for the first time and showed that the side chains are progressively removed by esterases and cutinases before the citrate enters the glyoxylate pathway.

Overall, this thesis has confirmed that general principles in marine microbial ecology govern the colonisation and degradation dynamics on both natural, *i.e.* chitin, and synthetic, *i.e.* PET, polymers. Both communities go through typical stages of community succession: (i) an initial colonisation phase; (ii) a selection phase, characterised by an enrichment of organisms that are capable of polymer degradation; and (iii) a succession phase, where efficient degraders are overtaken by cheaters, cross-feeders and grazers (Datta et al., 2016) (Figure 5.2). The interactions between microbial community members often arise from metabolites produced by one species being used by another species (Cavaliere et al., 2017). These interactions can be antagonistic, for example in the case of the marine degradation of some polysaccharides, where one species broadcasts degrading enzymes and a secondary consumer uses the products of this degradation and actually eventually inhibits the particle degradation and therefore growth of both species (Enke et al., 2018). However, in other cases the degradation of a compound by one species may lead to a build-up of a potentially toxic intermediate, for which they do not possess the metabolic machinery to degrade, although another organism may be readily able to degrade this intermediate, thereby decreasing the toxicity to the first species (Figure 5.3). This is shown in the degradation of lignin, where toxic phenolic intermediates build up in the media (Wei Wang et al., 2014) and terephthalic and phthalic acid produced by PET and PAE degradation, respectively, can also become toxic at high concentrations (Fajardo et al., 1997; Yi-Mei Zhang et al., 2013). The interactions between community members may also be beneficial to only one of these species, although not antagonistic to the other

(commensalism), for example when microbial communities “leak” a large diversity of organic matter which in turn may be used by the rest of the community (Christie-Oleza et al., 2017; Cordero et al., 2012), or when they simply do not have the metabolic machinery to use a degradation intermediate, although it is not toxic to them. A distribution of labour is often favoured in natural microbial communities (Cavaliere et al., 2017; Delgado-Baquerizo et al., 2017; Ponomarova and Patil, 2015; Zhang et al., 2016), although we have seen in Chapter 2 how community succession in natural microbial communities can lead to a loss of degradative ability in this community. If we wish to exploit microbial communities for the degradation of recalcitrant polymers, then it is therefore important to reduce antagonistic interactions between these organisms and avoid the inevitable microbial community decay and shift towards an abundance of cheaters and grazers; using synthetic microbial communities would remove the natural element of microbial community succession, while also avoiding the build-up of toxic intermediates, allowing for complete and efficient degradation (Figure 5.2 and Figure 5.3).

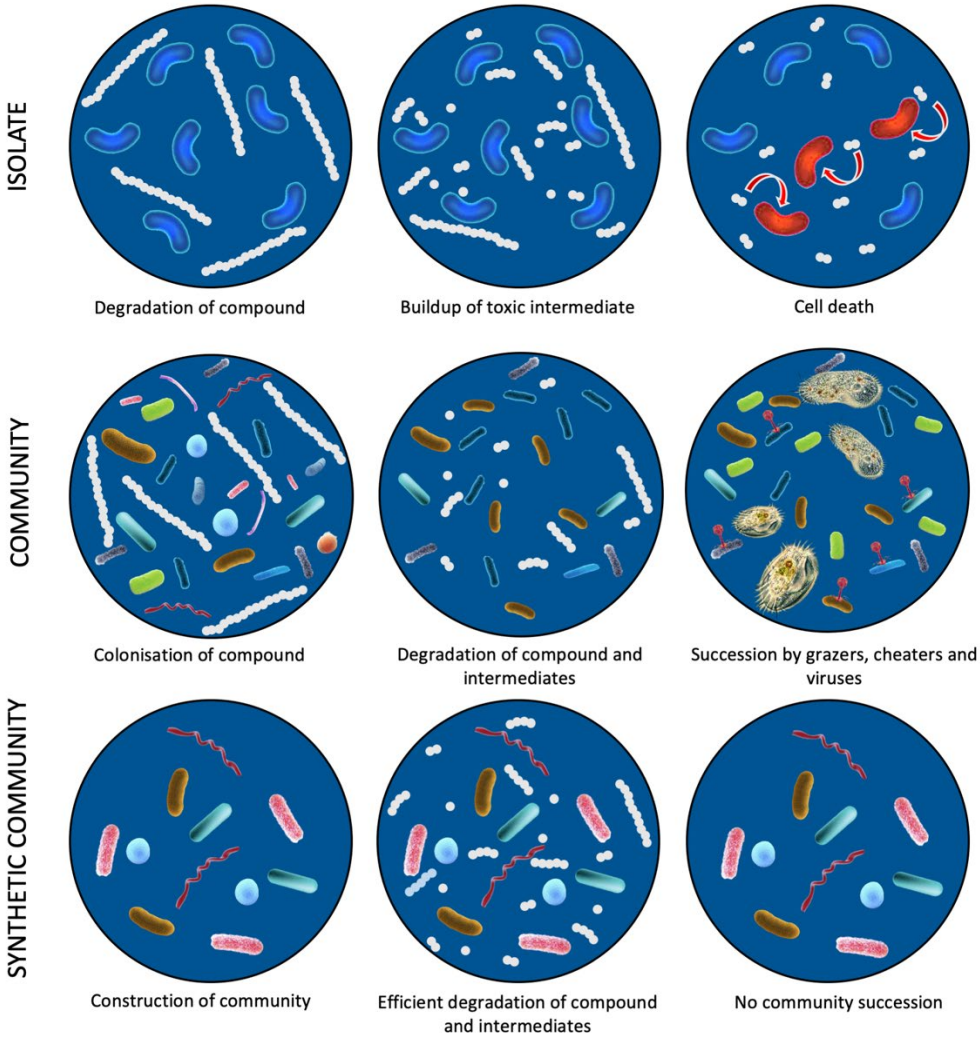

Figure 5.2. Degradation of polymers by isolates, communities and synthetic communities.

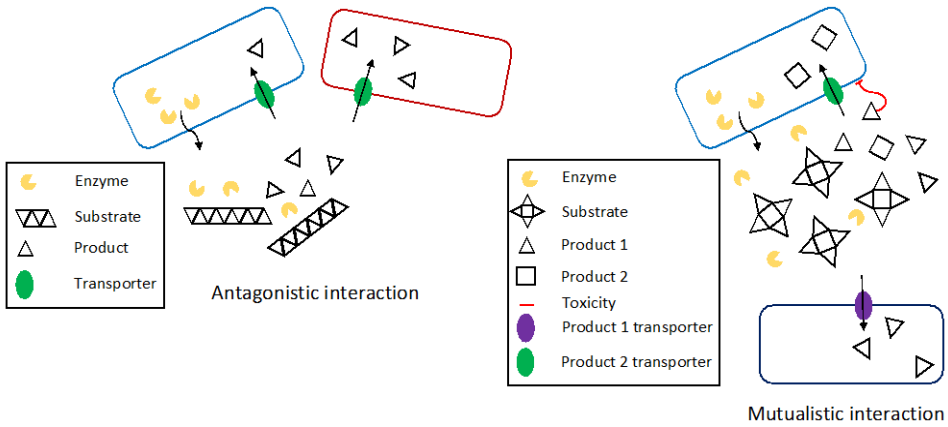

Figure 5.3. Antagonistic and mutualistic interactions. Antagonistic interactions show the case where one species is producing enzymes to produce a product from a substrate and a second species is unable to produce the enzyme but is able to take up the product. The Mutualistic interaction shows the case where one of the products produced by the enzymes of the first species is toxic (Product 1) to this first species while the second species is able to utilise this toxic product, thus reducing toxicity to the first species.

Synthetic communities are useful as model systems due to their reduced complexity, allowing for a greater degree of characterisation of microbial community members and the interactions between them (Großkopf and Soyer, 2014; Ponomarova and Patil, 2015; Tecon et al., 2019). Besides being easier to study than natural microbial communities, synthetic communities and consortia are often able to achieve higher rates of biodegradation than natural microbial communities (Syranidou et al., 2017b) or isolated organisms (Krishnan and Saramma, 2005). Constructing these synthetic communities, however, requires a prior, comprehensive understanding of the system or process for which they are being designed, as well as the possession of microbial isolates that are capable of each of the steps in this process (de Lorenzo et al., 2016; Ponomarova and Patil, 2015). In order to construct and maintain these communities, or consortia, the optimisation of a number of different factors is required, for example, size of inoculum, nutritional dependencies and requirements and compatible growth conditions (Roell et al., 2019). Synthetic communities have been validated for some processes that are known to occur naturally in the environment, for example, the production of methane often depends upon interactions between sulphate-reducing bacteria and methanogens (Stolyar et al., 2007). In order to construct synthetic communities, or consortia, however, microbial isolates that are capable of carrying out a process must first be obtained. Although these isolates of interest may be identified using methods such as amplicon sequencing or metagenomics, it may still be time-consuming to obtain pure cultures of these, as their nutritional requirements are unknown and there are still a large number of microorganisms for which culture conditions have not yet been determined (Stewart, 2012). Nevertheless, future work could look to grow the isolates that have been obtained here, for chitin, PET and plasticizer degradation, to determine whether degradation is more efficient when carried out by more than one isolate, as touched on in the chitin isolate co-culture experiment (Figure 2.13) and to optimise the system, for example, by determining the optimal number of species for the degradation of each compound and whether there is an upper limit to the number of species for efficient degradation.

To expand on the work characterising microbial community succession on PET, future work should look to apply the improved community artificial selection method, developed in Chapter 2, to synthetic polymers such as plastics. Coupling this with a thorough analysis of microbial community structure would aid in identifying the key players in marine PET degradation, although applying the community artificial selection method requires the development of a high-throughput method for determining the PET-degradative ability of

the community. Enzymes that are active against PET have previously been identified through the use of a Hidden Markov Model to search environmental metagenomes (Danso et al., 2018), however, whilst these enzymes shared a considerable degree of homology at the amino acid level, this is not necessarily the case at the nucleotide level. The development of universal primers for PETases, that would allow the use of methods such as quantitative PCR to determine levels of PET-degrading enzymes in the environment, would therefore be very challenging and more high-throughput methods would still be necessary for the community artificial selection method to be applied to PET degradation. The PETases that have been found so far have been capable of the hydrolysis of esterase substrates that can be used in colorimetric or fluorometric enzymatic activity assays (Danso et al., 2018; Hajighasemi et al., 2018; Yoshida et al., 2016a), for example *p*-nitrophenyl or 4-methylumbelliferyl acetate, butyrate or octanoate, however, these tests are not specific to PETases and esterases are produced in an abundance in microbial communities for a range of other processes (Sayali et al., 2013). If we wish to screen more specifically for PETase activity, then enzymatic activity tests with specificity to PET must be developed, for example 4-methylumbelliferyl substrates with terephthalate or BHET, rather than acetate or butyrate, attached to them.

It would also be interesting to determine how an ability to degrade a particular compound is conferred, *i.e.* is it conserved within phylogenetically similar groups, or could it be transferred through horizontal gene transfer? Studying the phylogenetic origin and distribution of chitinases, along with genes for the degradation of the chitin monomer, GlcNAc, may help to elucidate how genes for the degradation of recalcitrant compounds are spread, particularly as the abundance of plastics in the oceans increases (Geyer et al., 2017; Jambeck et al., 2015). For example, chitinases are shown to be more, or less, conserved within different groups of microorganisms, likely depending on how advantageous they are in the ecological niches generally inhabited by those organisms (Karlsson and Stenlid, 2009). The case is slightly different for the β-ketoadipate pathway, one branch of which converts protocatechuate to β-ketoadipate (3-oxoadipate), which is highly conserved amongst prokaryotes (where not lost), but evidence suggests an independent and convergent evolutionary origin in eukaryotes (Harwood and Parales, 1996). For PETases, the majority in the terrestrial environment were found within the *Actinobacteria*, while in the marine environment the majority originated from the *Bacteroidetes* (Danso et al., 2018). However, it is worth noting that *Proteobacteria* were the second most abundant carriers of PETases in both environments (Danso et al., 2018)

and the PET-degrading bacterium *Ideonella sakaiensis* is from the *Betaproteobacteria* (Yoshida et al., 2016a) and *Thioclava* sp. BHET1 is from the *Alphaproteobacteria*. It is then even more interesting that we appear to see an as-yet unknown pathway for PET and presumably terephthalate and protocatechuate, degradation, in *Bacillus* sp. BHET2, as these processes appear to typically be conserved even amongst diverse phylogenetic origins. Metabolomic analyses to identify biodegradation intermediates would help to confirm this, however, they may also show that the pathway for PET degradation is similar, or the same, as with other bacteria, but the enzymes share little homology with others and were therefore not detected by the software used for genome annotation and subsequent searches of the conserved domain database. If it is indeed a new pathway, then it would be of utmost importance to determine its abundance in environmental metagenomes and within other microbial isolates that may possess it but have not been previously known to be capable of PET or protocatechuate degradation.

It has also been seen here, in Chapter 3 and Chapter 4, how, for both PET and phthalic acid ester (PAE) plasticizers, the protocatechuate resulting from their initial degradation enters the same branch of the β-ketoadipate pathway. This is then acted upon by protocatechuate dioxygenases, for which a high relative abundance in marine metagenomes has previously been correlated with high local concentrations on plastic debris (Quero and Luna, 2017). As plastics are known to be contaminated with high levels of PAEs or related compounds, such as polyaromatic hydrocarbons (PAHs) (Groh et al., 2019; Hahladakis et al., 2018), it is not possible to determine whether these enzymes are being used for the degradation of either PET or PAEs, or neither, but this is something that should be addressed by future studies. It has also been uncovered here that in the degradation of PAEs, the β-ketoadipate pathway may not be induced by all PAEs or even by phthalate, as it was only upregulated in the DBP treatment with *Mycobacterium* sp. DBP42 and not the treatments with DEHP or phthalate, or indeed with any of the substrates with *Halomonas* sp. ATBC28. It would be interesting to determine which of these substrates is inducing the pathway in *Mycobacterium* sp. DBP42 and if there are other substrates that would induce this in *Halomonas* sp. ATBC28. Determining the mechanisms by which phthalate degradation is 'switched on' and whether this is the same in other species, may help to elucidate which substrates these enzymes are being used for in environmental metagenomes and therefore help to increase our understanding of the function of the marine Plastisphere community. An isocitrate lyase enzyme was also identified in *Mycobacterium* sp. DBP42 that is highly upregulated and abundant in the

exoproteome when grown with ATBC, although it is not predicted to be secreted. Isocitrate lyases are usually responsible for the conversion of isocitrate to succinate and glyoxylate (Bentrup et al., 1999), but other Mycobacterial isocitrate lyases have previously been proven to be capable of the degradation of other compounds, such as fatty acids (Gould et al., 2006) and ethylene glycol (Wiegant and de Bont, 1980) and have been suggested to be important in determining the pathogenicity of Mycobacteria (Muñoz-Elías and McKinney, 2006). It would therefore be interesting to purify this enzyme and carry out work looking at its kinetics, specificity and activity, which would help to determine why it was so abundant in this proteome.

There are also a number of other enzymes that it would be interesting to overexpress, purify and characterise, such as the esterases used for PET and PAE degradation. It could be important to determine whether the esterases used for PET degradation by *Thioclava* sp. BHET1 may also be used for PAE degradation and *vice versa* for the esterases produced by *Mycobacterium* sp. DBP42 and *Halomonas* sp. ATBC28 for PAE degradation. Preliminary results suggested that *Mycobacterium* sp. DBP42 and *Halomonas* sp. ATBC28 could grow with BHET and *Thioclava* sp. BHET1 and *Bacillus* sp. BHET2 could grow with PAEs, but this should be confirmed with further, comprehensive testing. This will aid in not only determining how widespread the ability to degrade PET and PAEs is, but also in identifying enzymes that may be useful in biotechnological applications and the enzymatic recycling of recalcitrant compounds (Kawai et al., 2019; Salvador et al., 2019). Identifying key enzymes, and the degree of homology necessary for carrying out a particular process, will also be fundamental for determining their abundance in both existing and future metagenomic studies as well as in identifying core Plastisphere communities and determining whether they are indeed degrading the plastics that they are colonising.

Whilst the experiments shown in this thesis aimed to determine whether marine microbial communities were, or could be, capable of degrading recalcitrant compounds, the conditions used were not typical of those found in the environment. For example, most experiments were carried out in the dark and at 30˚C, although the inoculums used were collected from coastal surface waters of the UK where typical temperatures reach an annual maximum of approximately 20˚C (Morris et al., 2018) and light varies diurnally. The 30˚C temperature used could be a heat shock to many of the microorganisms found and the dark conditions used do not allow the growth of phototrophic organisms, which typically make up 5-24% of bacterial (Sato-Takabe et al., 2016) and up to 20% of

eukaryotic (de Vargas et al., 2015) microbial communities in the photic ocean. Because plastics are predicted to take hundreds of years to degrade in the environment (Avio et al., 2016), we used temperatures that were much higher than in the environment in order to speed up growth (Nedwell, 1999). Experiments were also carried out in the dark in order to ensure that the substrate given was the only carbon source in the microcosms, avoiding the generation of labile photosynthate which would most likely become the preferred substrate of the community. The presence of light, and particularly UV light, could also contribute to the abiotic degradation of plastics through oxidation of the polymer chains (Andrady, 2017), and reactive oxygen species produced as a by-product of carrying out photosynthesis (Pospíšil, 2016) may also contribute to plastic degradation in the environment, although it is likely that the biofilms formed on plastics protect from this effect (Rummel et al., 2017). Furthermore, the concentrations of substrates that were used here are generally much higher than those found in the environment, which is a common criticism given to laboratory studies that investigate the ecotoxicological effects of plastics (de Sá et al., 2018). In fact, it is thought that it is unlikely that synthetic polymers will reach levels in the ocean that are high enough to produce a positive selection for their degradation (Oberbeckmann and Labrenz, 2020). Nevertheless, the aim here was not to give a comprehensive overview of all factors governing the colonisation and biodegradation of recalcitrant polymers in the environment, but to expand the current knowledge on microbial communities and isolates that potentially degrade xenobiotics by exploring a few specific aspects of this under laboratory conditions.

In conclusion, this thesis represents a significant step forwards in our understanding of microbial processes that control the degradation of recalcitrant polymers in marine conditions, as well as the enzymes and pathways used for this degradation by several bacterial isolates. However, it has also led to the creation of new questions, that should be addressed by future studies in this area, which should also aim to determine the effect of using environmentally relevant parameters on polymer degradation.

References

Abraham, W.-R., Nogales, B., Golyshin, P., Pieper, D., Timmis, K., 2002. Polychlorinated biphenyl-degrading microbial communities in soils and sediments. Curr. Opin. Microbiol. 5, 246–253.

Ahn, J.Y., Kim, Y.H., Min, J., Lee, J., 2006. Accelerated degradation of dipentyl phthalate by Fusarium oxysporum f. sp. pisi cutinase and toxicity evaluation of its degradation products using bioluminescent bacteria. Curr. Microbiol. 52, 340–344.

Ahuactzin-Pérez, M., Tlecuitl-Beristain, S., García-Dávila, J., González-Pérez, M., Gutiérrez-Ruíz, M.C., Sánchez, C., 2016. Degradation of di(2-ethyl hexyl) phthalate by *Fusarium culmorum*: Kinetics, enzymatic activities and biodegradation pathway based on quantum chemical modelingpathway based on quantum chemical modeling. Sci. Total Environ. 566–567, 1186–1193.

Ahuactzin-Pérez, M., Tlécuitl-Beristain, S., García-Dávila, J., Santacruz-Juárez, E., González-Pérez, M., Gutiérrez-Ruíz, M.C., Sánchez, C., 2018. Kinetics and pathway of biodegradation of dibutyl phthalate by *Pleurotus ostreatus*. Fungal Biol. 122, 991–997.

Albertsson, A.-C., Barenstedt, C., Karlsson, S., Lindberg, T., 1995. Degradation product pattern and morphology changes as means to differentiate abiotically and biotically aged polyethylene. Polymer (Guildf). 36, 3075–3083.

Almagro Armenteros, J.J., Tsirigos, K.D., Sønderby, C.K., Petersen, T.N., Winther, O., Brunak, S., von Heijne, G., Nielsen, H., 2019. SignalP 5.0 improves signal peptide predictions using deep neural networks. Nat. Biotechnol. 37, 420–423.

Amaral-Zettler, L.A., Zettler, E.R., Slikas, B., Boyd, G.D., Melvin, D.W., Morrall, C.E., Proskurowski, G., Mincer, T.J., 2015. The biogeography of the Plastisphere: implications for policy. Front. Ecol. Environ. 13, 541–546.

Amir, S., Hafidi, M., Merlina, G., Hamdi, H., Jouraiphy, A., 2005. Fate of phthalic acid esters during composting of both lagooning and activated sludges. Process Biochem. 40, 2183–2190.

Andrady, A.L., 2017. The plastic in microplastics: A review. Mar. Pollut. Bull. 119, 12–22.

Andrady, A.L., 2011. Microplastics in the marine environment. Mar. Pollut. Bull. 62, 1596–1605.

Andrady, A.L., Neal, M.A., 2009. Applications and societal benefits of plastics. Philos. Trans. R. Soc. Lond. B. Biol. Sci. 364, 1977–84.

Arenskötter, M., Bröker, D., Steinbüchel, A., 2004. Biology of the metabolically diverse genus Gordonia. Appl. Environ. Microbiol. 70, 3195–3204.

Armengaud, J., Christie-Oleza, J.A., Clair, G., Malard, V., Duport, C., 2012. Exoproteomics: Exploring the world around biological systems. Expert Rev. Proteomics 9, 561–575.

Arutchelvi, J., Sudhakar, M., Arkatkar, A., Doble, M., Bhaduri, S., Uppara, P.V., 2008. Biodegradation of polyethylene and polypropylene 7, 9–22.

Aukema, K.G., Kasinkas, L., Aksan, A., Wackett, L.P., 2014. Use of silica-encapsulated *Pseudomonas* sp. Strain NCIB 9816-4 in biodegradation of novel hydrocarbon ring Structures found in hydraulic fracturing waters. Appl. Environ. Microbiol. 80, 4968–4976.

Aunkham, A., Zahn, M., Kesireddy, A., Pothula, K.R., Schulte, A., Baslé, A., Kleinekathöfer, U., Suginta, W., Van Den Berg, B., 2018. Structural basis for chitin acquisition by marine *Vibrio* species. Nat. Commun. 9, 1–13.

Austin, H.P., Allen, M.D., Donohoe, B.S., Rorrer, N.A., Kearns, F.L., Silveira, R.L., Pollard, B.C., Dominick, G., Duman, R., Omari, K. El, Mykhaylyk, V., Wagner, A., Michener, W.E., Amore, A., Skaf, M.S., Crowley, M.F., Thorne, A.W., Johnson, C.W., Woodcock, H.L., McGeehan, J.E., Beckham, G.T., 2018. Characterization and engineering of a plastic-degrading aromatic polyesterase. Proc. Natl. Acad. Sci. 115, E4350–E4357.

Avio, C.G., Gorbi, S., Regoli, F., 2016. Plastics and microplastics in the oceans: From emerging pollutants to emerged threat. Mar. Environ. Res. 128, 2–11.

Azeredo, J., Azevedo, N.F., Briandet, R., Cerca, N., Costa, A.R., Desvaux, M., Bonaventura, G. Di, Jaglic, Z., Kačániová, M., Knøchel, S., Mergulhão, F., Meyer, R.L., Nychas, G., Tresse, O., Sternberg, C., Azeredo, J., Azevedo, N.F., Briandet, R., Cerca, N., Costa, A.R., Desvaux, M., Bonaventura, G. Di, Hébraud, M., Kačániová, M., Knøchel, S., Lourenço, A., Mergulhão, F., Meyer, L., Nychas, G., Simões, M., Tresse, O., Sternberg, C., Rita, A., Di, G., Michel, H., Meyer, R.L., Nychas, G., Sim, M., Tresse, O., 2017. Critical review on biofilm methods. Crit. Rev. Microbiol. 43, 315–351.

Baiardo, M., Frisoni, G., Scandola, M., Rimelen, M., Lips, D., Ruffieux, K., Wintermantel, E., 2002. Thermal and mechanical properties of plasticized poly(L-lactic acid). J. Appl. Polym. Sci. 90, 1731–1738.

Bakir, A., Rowland, S.J., Thompson, R.C., 2012. Competitive sorption of persistent organic pollutants onto microplastics in the marine environment. Mar. Pollut. Bull. 64, 2782–2789.

Bang, D.Y., Lee, I.K., Lee, B., 2011. Toxicological Characterization of Phthalic Acid. Off. J. Korean Soc. Toxicol. 27, 191–203.

Bankevich, A., Nurk, S., Antipov, D., Gurevich, A.A., Dvorkin, M., Kulikov, A.S., Lesin, V.M., Nikolenko, S.I., Pham, S.O.N., Prjibelski, A.D., Pyshkin, A. V, Sirotkin, A. V, Vyahhi, N.,

Tesler, G., Alekseyev, M.A.X.A., Pevzner, P.A., 2012. SPAdes: A new genome assembly algorithm and Its applications to single-cell sequencing. J. Comput. Biol. 19, 455–477.

Barakat, A.O., Khairy, M., Aukaily, I., 2013. Persistent organochlorine pesticide and PCB residues in surface sediments of Lake Qarun, a protected area of Egypt. Chemosphere 90, 2467–76.

Barbera, P., Kozlov, A.M., Czech, L., Morel, B., Darriba, D., Flouri, T., Stamatakis, A., 2019. EPA-ng: Massively parallel evolutionary placement of genetic sequences. Syst. Biol. (Stevenage). 68, 365–369.

Barnes, D.K.A., Galgani, F., Thompson, R.C., Barlaz, M., 2009. Accumulation and fragmentation of plastic debris in global environments. Phil. Trans. R. Soc. B 364, 1985–1998.

Bassler, B.L., Yu, C., Roseman, S., 1991. Chitin Utilization by Marine Bacteria. J. Biol. Chem. 266, 24260–24267.

Beier, S., Bertilsson, S., 2013. Bacterial chitin degradation-mechanisms and ecophysiological strategies. Front. Microbiol. 4, 1–12.

Beier, S., Bertilsson, S., 2011. Uncoupling of chitinase activity and uptake of hydrolysis products in freshwater bacterioplankton. Limnol. Ocean. 56, 1179–1188.

Bentrup, K., Miczak, A., Swenson, D.L., Russell, D.G., 1999. Characterization of Activity and Expression of Isocitrate Lyase in *Mycobacterium avium* and *Mycobacterium tuberculosis*. J. Bacteriol. 181, 7161–7167.

Berendes, F., Goitschalk, G., Heine-Dobbernack, E., Moore, E.R.B., Tindall, B.J., 1996. *Halomonas desiderata* sp. nov., a new alkaliphilic, halotolerant and denitrifying bacterium isolated from a municipal sewage works. Syst. Appl. Microbiol. Appl. Microbiol. 19, 158–167.

Bergmann, M., Wirzberger, V., Krumpen, T., Lorenz, C., Primpke, S., Tekman, M.B., Gerdts, G., 2017. High quantities of microplastic in Arctic deep-sea sediments from the HAUSGARTEN observatory. Environ. Sci. Technol. 51, 11000–11010.

Berry, D., Gutierrez, T., Waite, D.W., 2017. Evaluating the detection of hydrocarbon-degrading bacteria in 16S rRNA gene sequencing surveys. Front. Microbiol. 8, 1–6.

Bertelli, C., Laird, M.R., Williams, K.P., Fraser, S., Group, C., Lau, B.Y., Hoad, G., Winsor, G.L., Brinkman, F.S.L., 2017. IslandViewer 4: expanded prediction of genomic islands for larger-scale datasets. Nucleic Acids Res. 45, 30–35.

Besseling, E., Wegner, A., Foekema, E.M., van den Heuvel-Greve, M.J., Koelmans, A.A., 2013. Effects of microplastic on fitness and PCB bioaccumulation by the lugworm *Arenicola marina* (L.). Environ. Sci. Technol. 47, 593–600.

Beygmoradi, A., Homaei, A., 2018. Marine chitinolytic enzymes, a biotechnological treasure hidden in the ocean? Appl. Microbiol. Biotechnol. 1–12.

Billerbeck, S., Wemheuer, B., Voget, S., Poehlein, A., Giebel, H.A., Brinkhoff, T., Gram, L., Jeffrey, W.H., Daniel, R., Simon, M., 2016. Biogeography and environmental genomics of the *Roseobacter*-affiliated pelagic CHAB-I-5 lineage. Nat. Microbiol. 1, 1–8.

Blouin, M., Karimi, B., Mathieu, J., Lerch, T.Z., 2015. Levels and limits in artificial selection of communities. Ecol. Lett. 1040–1048.

Boerger, C.M., Lattin, G.L., Moore, S.L., Moore, C.J., 2010. Plastic ingestion by planktivorous fishes in the North Pacific Central Gyre. Mar. Pollut. Bull. 60, 2275–2278.

Bolyen, E., Rideout, J.R., Dillon, M.R., Bokulich, N.A., Abnet, C.C., Gabriel, A., Ghalith, A., Alexander, H., Alm, E.J., Arumugam, M., Asnicar, F., Bai, Y., Bisanz, J.E., Bittinger, K., Brejnrod, A., Brislawn, C.J., Brown, C.T., Benjamin, J., Mauricio, A., Rodríguez, C., Chase, J., Cope, E.K., Silva, R. Da, Dorrestein, P.C., Douglas, G.M., Durall, D.M., Duvallet, C., Edwardson, C.F., Ernst, M., Estaki, M., Fouquier, J., Gauglitz, J.M., Gibson, D.L., Gorlick, K., Guo, J., Hillmann, B., Holmes, S., Holste, H., Huttley, G.A., Janssen, S., Jarmusch, A.K., Jiang, L., Benjamin, D., Kang, K. Bin, Keefe, C.R., Keim, P., Kelley, S.T., Knights, D., Loftfield, E., Lozupone, C., Maher, M., Marotz, C., Martin, B.D., Metcalf, J.L., Morgan, S.C., Jamie, T., Nothias, L.F., Orchanian, S.B., Segata, N., Willis, A.D., 2018. QIIME 2: Reproducible, interactive, scalable, and extensible microbiome data science. PeerJ Prepr.

Bradley, I.M., Pinto, A.J., Guest, J.S., 2016. Design and evaluation of Illumina MiSeq-compatible, 18S rRNA gene-specific primers for improved characterization of mixed phototrophic communities. Appl. Environ. Microbiol. 82, 5878–5891.

Brennecke, D., Duarte, B., Paiva, F., Caçador, I., 2016. Microplastics as vector for heavy metal contamination from the marine environment. Estuar. Coast. Shelf Sci. 178, 189–195.

Brink, P.J. Van Den, Besten, P.J. Den, 2009. Principal response curves technique for the analysis of multivariate biomonitoring time series 271–281.

Browne, M.A., Dissanayake, A., Galloway, T.S., Lowe, D.M., Thompson, R.C., 2008. Ingested microscopic plastic translocates to the circulatory system of the mussel, *Mytilus edulis* (L.). Environ. Sci. Technol. 42, 5026–5031.

Browne, M.A., Galloway, T.S., Thompson, R.C., 2010. Spatial patterns of plastic debris along estuarine shorelines. Environ. Sci. Technol. 44, 3404–3409.

Bruns, A., Rohde, M., Berthe-Corti, L., 2001. Muricauda ruestringensis gen. nov., sp. nov., a facultatively anaerobic, appendaged bacterium from German North Sea intertidal sediment. Int. J. Syst. Evol. Microbiol. 51, 1997–2006.

Bryant, J.A., Clemente, T.M., Viviani, D.A., Fong, A.A., Thomas, K.A., Kemp, P., Karl, D.M., White, A.E., DeLong, E.F., 2016a. Diversity and Activity of Communities Inhabiting Plastic Debris in the North Pacific Gyre. mSystems 1, e00024-16.

Bryant, J.A., Clemente, T.M., Viviani, D.A., Fong, A.A., Thomas, K.A., Kemp, P., Karl, D.M., White, A.E., DeLong, E.F., 2016b. Diversity and activity of communities inhabiting plastic debris in the North Pacific Gyre. mSystems 1, e00024-16.

Bui, T.T., Giovanoulis, G., Palm, A., Magnér, J., Cousins, I.T., Wit, C.A. De, 2016. Human exposure, hazard and risk of alternative plasticizers to phthalate esters. Sci. Total Environ. 541, 451–467.

Bushnell, L.D., Haas, H.F., 1941. The utilization of certain hydrocarbons by microorganisms. J. Bacteriol. 41, 653–673.

Callahan, B.J., McMurdie, P.J., Holmes, S.P., 2017. Exact sequence variants should replace operational taxonomic units in marker-gene data analysis. ISME J. 11, 2639–2643.

Callahan, B.J., McMurdie, P.J., Rosen, M.J., Han, A.W., Johnson, A.J.A., Holmes, S.P., 2016. DADA2: High-resolution sample inference from Illumina amplicon data. Nat. Methods 13, 581–583.

Callahan, B.J., Sankaran, K., Fukuyama, J.A., McMurdie, P.J., Holmes, S.P., 2016. Bioconductor workflow for microbiome data analysis: from raw reads to community analyses. F1000Research 5, 1492.

Caporaso, J.G., Kuczynski, J., Stombaugh, J., Bittinger, K., Bushman, F.D., Costello, E.K., Fierer, N., Peña, A.G., Goodrich, J.K., Gordon, J.I., Huttley, G. a, Kelley, S.T., Knights, D., Koenig, J.E., Ley, R.E., Lozupone, C. a, Mcdonald, D., Muegge, B.D., Pirrung, M., Reeder, J., Sevinsky, J.R., Turnbaugh, P.J., Walters, W. a, Widmann, J., Yatsunenko, T., Zaneveld, J., Knight, R., 2010. QIIME allows analysis of high- throughput community sequencing data. Nat. Methods 7, 335–336.

Carr, A., 1987. Impact of nondegradable marine debris on the ecology and survival outlook of sea turtles. Mar. Pollut. Bull. 18, 352–356.

Carson, H.S., Nerheim, M.S., Carroll, K.A., Eriksen, M., 2013. The plastic-associated microorganisms of the North Pacific Gyre. Mar. Pollut. Bull. 75, 126–132.

Carvalho, C.M.L., Aires-Barros, M.R., Cabral, J.M.S., 1998. Cutinase structure, function and biocatalytic applications. Electron. J. Biotechnol. 1, 160–173.

Catania, V., Cappello, S., Giorgi, V. Di, Santisi, S., Maria, R. Di, 2018. Microbial communities of polluted sub-surface marine sediments. Mar. Pollut. Bull. 131, 396–406.

Cavaliere, M., Feng, S., Soyer, O., Jiminez, J., 2017. Cooperation in microbial communities and their biotechnological applications. Environ. Microbiol. 19, 2949–2963.

Chen, J., Li, X., Li, J., Cao, J., Qiu, Z., Zhao, Q., Xu, C., Shu, W., 2007. Degradation of environmental endocrine disruptor di-2-ethylhexyl phthalate by a newly discovered bacterium, *Microbacterium* sp . strain CQ0110Y. Appl. Microbiol. Biotechnol. 74, 676–682.

Chen, S., Tong, X., Woodard, R.W., Du, G., Wu, J., Chen, J., 2008. Identification and characterization of bacterial cutinase. J. Biol. Chem. 283, 25854–25862.

Christie-Oleza, J.A., Scanlan, D.J., Armengaud, J., 2015. "You produce while I clean up", a strategy revealed by exoproteomics during *Synechococcus-Roseobacter* interactions. Proteomics 15, 3454–3462.

Christie-Oleza, J.A., Sousoni, D., Lloyd, M., Armengaud, J., Scanlan, D.J., 2017. Nutrient recycling facilitates long-term stability of marine microbial phototroph-heterotroph interactions. Nat. Microbiol. 2, 1–10.

Claessens, M., De Meester, S., Van Landuyt, L., De Clerck, K., Janssen, C.R., 2011. Occurrence and distribution of microplastics in marine sediments along the Belgian coast. Mar. Pollut. Bull. 62, 2199–204.

Colabuono, F.I., Taniguchi, S., Montone, R.C., 2010. Polychlorinated biphenyls and organochlorine pesticides in plastics ingested by seabirds. Mar. Pollut. Bull. 60, 630–634.

Cole, M., Lindeque, P., Halsband, C., Galloway, T.S., 2011. Microplastics as contaminants in the marine environment: A review. Mar. Pollut. Bull. 62, 2588–2597.

Cordero, O.X., Ventouras, L., Delong, E.F., Polz, M.F., 2012. Public good dynamics drive evolution of iron acquisition strategies in natural bacterioplankton populations. Proc. Natl. Acad. Sci. 109, 20059–20064.

Cottrell, M.T., Moore, J.A., David, L., Kirchman, D.L., 1999. Chitinases from Uncultured Marine Microorganisms. Appl. Environ. Microbiol. 65, 2553–2557.

Courtene-Jones, W., Quinn, B., Gary, S.F., Mogg, A.O.M., Narayanaswamy, B.E., 2017. Microplastic pollution identified in deep-sea water and ingested by benthic invertebrates in the Rockall Trough, North Atlantic Ocean. Environ. Pollut. 231, 271–280.

Cousins, I., Mackay, D., 2000. Correlating the physical-chemical properties of phthalate esters using the `three solubility' approach. Chemosphere 41, 1389–1399.

Cox, J., Mann, M., 2008. MaxQuant enables high peptide identification rates, individualized p.p.b.-range mass accuracies and proteome-wide protein quantification. Nat. Biotechnol. 26, 1367–1372.

Cózar, A., Echevarría, F., González-Gordillo, J.I., Irigoien, X., Ubeda, B., Hernández-Léon, S.,

Palma, Á.T., Navarro, S., García-de-Lomas, J., Ruiz, A., Fernández-de-Puelles, M.L., Duarte, C.M., 2014. Plastic debris in the open ocean. Proc. Natl. Acad. Sci. 111, 10239–10244.

Curren, E., Leong, S.C.Y., 2019. Profiles of bacterial assemblages from microplastics of tropical coastal environments. Sci. Total Environ. 655, 313–320.

Czech, L., Stamatakis, A., 2018. Scalable methods for analyzing and visualizing phylogenetic placement of metagenomic samples. BioRxiv 1–72.

Dang, H., Li, T., Chen, M., Huang, G., 2008. Cross-ocean distribution of *Rhodobacterales* bacteria as primary surface colonizers in temperate coastal marine waters. Appl. Environ. Microbiol. 74, 52–60.

Dang, H., Lovell, C.R., 2016. Microbial Surface Colonization and Biofilm Development in Marine Environments. Microbiol. Mol. Biol. Rev. 80, 91–138.

Dang, H., Lovell, C.R., 2000. Bacterial primary colonization and early succession on surfaces in marine waters as determined by amplified rRNA gene restriction analysis and sequence analysis of 16S rRNA genes. Appl. Environ. Microbiol. 66, 467–475.

Danso, D., Zimmermann, Schmeisser, C., Chow, J., Zimmermann, W., Wei, R., Leggewie, C., Li, X., Hazen, T., Streit, W.R., 2018. New insights into the function and global distribution of polyethylene terephthalate (PET) degrading bacteria and enzymes in marine and terrestrial metagenomes. Appl. Environ. Microbiol. 84, AEM.02773-17.

Das, S.N., Sarma, P.V.S.R.N., Neeraja, C., Malati, N., Podile, A.R., 2010. Members of Gammaproteobacteria and Bacilli represent the culturable diversity of chitinolytic bacteria in chitin-enriched soils. World J. Microbiol. Biotechnol. 26, 1875–1881.

Datta, M.S., Sliwerska, E., Gore, J., Polz, M.F., Cordero, O.X., 2016. Microbial interactions lead to rapid micro-scale successions on model marine particles. Nat. Commun. 7, 1–7.

Day, M.D., Beck, D., Foster, J.A., 2011. Microbial communities as experimental units. Bioscience 61, 398–406.

de Lorenzo, V., Marlière, P., Solé, R., 2016. Bioremediation at a global scale: from the test tube to planet Earth. Microb. Biotechnol.

de Sá, L.C., Oliveira, M., Ribeiro, F., Rocha, T.L., Futter, M.N., 2018. Studies of the effects of microplastics on aquatic organisms: What do we know and where should we focus our efforts in the future? Sci. Total Environ. 645, 1029–1039.

De Tender, C.A., Devriese, L.I., Haegeman, A., Maes, S., Ruttink, T., Dawyndt, P., 2015. Bacterial community profiling of plastic litter in the Belgian part of the North Sea. Environ. Sci. Technol. 49, 9629–9638.

De Tender, C.A., Devriese, L.I., Haegeman, A., Maes, S., Vangeyte, J., Cattrijsse, A., Dawyndt,

P., Ruttink, T., 2017. The temporal dynamics of bacterial and fungal colonization on plastic debris in the North Sea. Environ. Sci. Technol. 51, 7350–7360.

de Vargas, C., Audic, S., Henry, N., Decelle, J., Mahe, F., Logares, R., Lara, E., Berney, C., Le Bescot, N., Probert, I., Carmichael, M., Poulain, J., Romac, S., Colin, S., Aury, J.-M., Bittner, L., Chaffron, S., Dunthorn, M., Engelen, S., Flegontova, O., Guidi, L., Horak, A., Jaillon, O., Lima-Mendez, G., Lukes, J., Malviya, S., Morard, R., Mulot, M., Scalco, E., Siano, R., Vincent, F., Zingone, A., Dimier, C., Picheral, M., Searson, S., Kandels-Lewis, S., Coordinators, T.O., Acinas, S.G., Bork, P., Bowler, C., Gorsky, G., Grimsley, N., Hingamp, P., Iudicone, D., Not, F., Ogata, H., Pesant, S., Raes, J., Sieracki, M.E., Speich, S., Stemman, L., Sunagawa, S., Weissenbach, J., Wincker, P., Karsenti, E., 2015. Eukaryotic plankton diversity in the sunlit ocean. Science (80-.). 348, 1261605–1/11.

Delgado-Baquerizo, M., Eldridge, D.J., Ochoa, V., Gozalo, B., Singh, B.K., Maestre, F.T., 2017. Soil microbial communities drive the resistance of ecosystem multifunctionality to global change in drylands across the globe. Ecol. Lett. 20, 1295–1305.

Derraik, J.G.B., 2002. The pollution of the marine environment by plastic debris: A review. Mar. Pollut. Bull. 44, 842–852.

Desantis, T.Z., Hugenholtz, P., Larsen, N., Rojas, M., Brodie, E.L., Keller, K., Huber, T., Dalevi, D., Hu, P., Andersen, G.L., 2006. Greengenes, a chimera-checked 16S rRNA gene database and workbench compatible with ARB. Appl. Environ. Microbiol. 72, 5069–5072.

Devi, R.S., Ramya, R., Kannan, K., Antony, A.R., Kannan, V.R., 2019. Investigation of biodegradation potentials of high density polyethylene degrading marine bacteria isolated from the coastal regions of Tamil Nadu , India. Mar. Pollut. Bull. 138, 549–560.

Didier, D., Anne, M., Alexandra, T.H., 2017. Plastics in the North Atlantic garbage patch: A boat-microbe for hitchhikers and plastic degraders. Sci. Total Environ. 599–600, 1222–1232.

Dixon, P., 2003. VEGAN, a package of R functions for community ecology. J. Veg. Sci. 14, 927–930.

Dıaz-Cardenas, C., Patel, B.K.C., Baena, S., 2010. *Tistlia consotensis* gen. nov., sp. nov., an aerobic, chemoheterotrophic, free-living, nitrogen-fixing alphaproteobacterium, isolated from a Colombian saline spring. Int. J. Syst. Evol. Microbiol. 60, 1437–1443.

Dresler, K., Van Den Heuvel, J., Müller, R.J., Deckwer, W.D., 2006. Production of a recombinant polyester-cleaving hydrolase from *Thermobifida fusca* in *Escherichia coli*. Bioprocess Biosyst. Eng. 29, 169–183.

Du, D., Wang-Kan, X., Neuberger, A., van Veen, H.W., Pos, K.M., Piddock, L.J.V., Luisi, B.F.,

2018. Multidrug efflux pumps: structure, function and regulation. Nat. Rev. Microbiol. 16, 523–539.

Dussud, C., Hudec, C., George, M., Fabre, P., Higgs, P., Bruzaud, S., Delort, A., Eyheraguibel, B., Meistertzheim, A., Jacquin, J., Cheng, J., Callac, N., 2018a. Colonization of non-biodegradable and biodegradable plastics by marine microorganisms. Front. Microbiol. 9, 1–13.

Dussud, C., Meistertzheim, A.L., Conan, P., Pujo-pay, M., George, M., Fabre, P., Coudane, J., Higgs, P., Elineau, A., Pedrotti, M.L., Gorsky, G., Ghiglione, J.F., 2018b. Evidence of niche partitioning among bacteria living on plastics , organic particles and surrounding seawaters. Environ. Pollut. 236, 807–816.

Eckert, E.M., Baumgartner, M., Huber, I.M., Pernthaler, J., 2013. Grazing resistant freshwater bacteria profit from chitin and cell-wall-derived organic carbon. Environ. Microbiol. 15, 2019–2030.

Eddy, S.R., 2011. Accelerated profile HMM searches. PLoS Comput. Biol. 7.

Ellington, J.J., 1999. Octanol / Water partition coefficients and water solubilities of phthalate esters. J. Chem. Eng. Data 44, 1414–1418.

Endo, S., Takizawa, R., Okuda, K., Takada, H., Chiba, K., Kanehiro, H., Ogi, H., Yamashita, R., Date, T., 2005. Concentration of polychlorinated biphenyls (PCBs) in beached resin pellets: Variability among individual particles and regional differences. Mar. Pollut. Bull. 50, 1103–1114.

Enke, T.N., Datta, M.S., Schwartzman, J., Cermak, J., Schmitz, D., Barrere, J., Pascual-garcıa, A., Cordero, O.X., 2019. Modular assembly of polysaccharide- degrading marine microbial communities. Curr. Biol. 29, 1–8.

Enke, T.N., Leventhal, G.E., Metzger, M., Saavedra, J.T., Cordero, O.X., 2018. Microscale ecology regulates particulate organic matter turnover in model marine microbial communities. Nat. Commun. 9, 1–8.

Erceg, M., Kovačić, T., Klarić, I., 2005. Thermal degradation of poly(3-hydroxybutyrate) plasticized with acetyl tributyl citrate. Polym. Degrad. Stab. 90, 313–318.

Eren, A.M., Vineis, J.H., Morrison, H.G., Sogin, M.L., 2013. A filtering method to generate high quality short reads using Illumina paired-end technology. PLoS One 8, 6–11.

Erni-Cassola, G., Gibson, M.I., Thompson, R.C., Christie-Oleza, J.A., 2017. Lost, but found with Nile Red: A novel method for detecting and quantifying small microplastics (1 mm to 20 µm) in environmental samples. Environ. Sci. Technol. 51, 13641–13648.

Erni-Cassola, G., Wright, R.J., Gibson, M.I., Christie-Oleza, J.A., 2019. Early Colonization of Weathered Polyethylene by Distinct Bacteria in Marine Coastal Seawater. Microb. Ecol.

Erni-cassola, G., Zadjelovic, V., Gibson, M.I., Christie-oleza, J.A., 2019. Distribution of plastic polymer types in the marine environment ; A meta- analysis. J. Hazard. Mater. 369, 691–698.

Evtushenko, L.I., Dorofeeva, L. V., Subbotin, S.A., Cole, J.R., Tiedje, J.M., 2000. Leifsonia poae gen. nov., sp. nov., isolated from nematode galls on Poa annua, and reclassification of "*Corynebacterium aquaticum*" Leifson 1962 as *Leifsonia aquatica* (ex Leifson 1962) gen. nov., nom. rev., comb. nov. and *Clavibacter xyli* Davis et al. 1984. Int. J. Syst. Evol. Microbiol. 50, 371–380.

Fajardo, C., Guyot, P., Macarie, H., Monroy, O., 1997. Inhibition of anaerobic digestion by terephthalic acid and its aromatic by-products. Water Sci. Technol. 36, 83–90.

Feng, L., Liu, H., Cheng, D., Mao, X., Wang, Y., Wu, Z., Wu, Q., 2018. Characterization and genome analysis of a phthalate esters-degrading strain *Sphingobium yanoikuyae* SHJ. Biomed Res. Int. 2018, 1–8.

Feng, N., Yu, J., Mo, C., Zhao, H., Li, Y., Wu, B., Cai, Q., 2018. Biodegradation of di-n-butyl phthalate (DBP) by a novel endophytic *Bacillus megaterium* strain YJB3. Sci. Total Environ. 616–617, 117–127.

Fontanez, K.M., Eppley, J.M., Samo, T.J., Karl, D.M., DeLong, E.F., 2015. Microbial community structure and function on sinking particles in the North Pacific Subtropical Gyre. Front. Microbiol. 6, 1–14.

Fowler, C.W., 1987. Marine debris and Northern fur seals: a case study. Mar. Pollut. Bulleti 18, 326–335.

FR-MSCA, 2013. Analysis of the most appropriate risk management option for tributyl citrate.

Frere, L., Maignien, L., Chalopin, M., Huvet, A., Rinnert, E., Morrison, H., Kerninon, S., Cassone, A.-L., Lambert, C., Reveillaud, J., Paul-Pont, I., 2018. Microplastic bacterial communities in the Bay of Brest: Influence of polymer type and size. Environ. Pollut. 242, 614–625.

Frias, J.P.G.L., Gago, J., Otero, V., Sobral, P., 2016. Microplastics in coastal sediments from Southern Portuguese shelf waters. Mar. Environ. Res. 114, 24–30.

Gao, W., Cui, Z., Li, Q., Xu, G., 2013. *Marinobacter nanhaiticus* sp . nov ., polycyclic aromatic hydrocarbon-degrading bacterium isolated from the sediment of the South China Sea. Antonie van Leeuwenhoek, Int. J. Gen. Mol. Microbiol. 103, 485–491.

Gewert, B., Plassmann, M., Sandblom, O., Macleod, M., 2018. Identification of chain scission products released to water by plastic exposed to ultraviolet light. Environ. Sci. Technol. Lett. 5, 272–276.

Gewert, B., Plassmann, M.M., MacLeod, M., 2015. Pathways for degradation of plastic

polymers floating in the marine environment. Environ. Sci. Process. Impacts 17, 1513–21.

Geyer, R., Jambeck, J.R., Law, K.L., 2017. Production, use, and fate of all plastics ever made. Sci. Adv. 3, e1700782.

Gilman, E., 2015. Status of international monitoring and management of abandoned, lost and discarded fishing gear and ghost fishing. Mar. Policy 60, 225–239.

Giubergia, S., Phippen, C., Nielsen, K.F., Gram, L., 2017. Growth on chitin impacts the transcriptome and metabolite profiles of antibiotic-producing *Vibrio coralliilyticus* S2052 and Photobacterium galatheae S2753. mSystems 2, 1–12.

González-Soto, N., Hatfield, J., Katsumiti, A., Duroudier, N., Lacave, J.M., Bilbao, E., Orbea, A., Navarro, E., Cajaraville, M.P., 2019. Impacts of dietary exposure to different sized polystyrene microplastics alone and with sorbed benzo[a]pyrene on biomarkers and whole organism responses in mussels *Mytilus galloprovincialis*. Sci. Total Environ. 684, 548–566.

Goodnight, C.J., 2005. Multilevel selection: The evolution of cooperation in non-kin groups. Popul. Ecol. 47, 3–12.

Goodnight, C.J., 2000. Heritability at the ecosystem level. Proc. Natl. Acad. Sci. 97, 9365–9366.

Gould, T.A., Langemheen, H. Van De, Muñoz-elías, E.J., Mckinney, J.D., Sacchettini, J.C., 2006. Dual role of isocitrate lyase 1 in the glyoxylate and methylcitrate cycles in *Mycobacterium tuberculosis*. Mol. Microbiol. 61, 940–947.

Graham, E.R., Thompson, J.T., 2009. Deposit- and suspension-feeding sea cucumbers (Echinodermata) ingest plastic fragments. J. Exp. Mar. Bio. Ecol. 368, 22–29.

Gregory, M.R., 2009. Environmental implications of plastic debris in marine settings--entanglement, ingestion, smothering, hangers-on, hitch-hiking and alien invasions. Philos. Trans. R. Soc. Lond. B. Biol. Sci. 364, 2013–2025.

Gregory, M.R., 1978. Accumulation and distribution of virgin plastic granules on New Zealand beaches. New Zeal. J. Mar. Freshw. Res. 12, 399–414.

Groh, K.J., Backhaus, T., Carney-almroth, B., Geueke, B., Inostroza, P.A., Lennquist, A., Leslie, H.A., Maffini, M., Slunge, D., Trasande, L., Warhurst, A.M., Muncke, J., Maf, M., Slunge, D., Trasande, L., Warhurst, A.M., Muncke, J., 2019. Overview of known plastic packaging-associated chemicals and their hazards. Sci. Total Environ. 651, 3253–3268.

Großkopf, T., Soyer, O.S., 2014. Synthetic microbial communities. Curr. Opin. Microbiol. 18, 72–77.

Guillard, R.R.L., Ryther, J.H., 1962. Studies of marine planktonic diatoms: *I. cyclotella*, *Nana*

hustedt, and *Detonula confervacea* (cleve) gran. Can. J. Microbiol. 8, 229–239.

Gutierrez, T., Aitken, M.D., 2014. Role of methylotrophs in the degradation of hydrocarbons during the Deepwater Horizon oil spill. ISME J. 8, 2543–2545.

Hada, H.S., West, P.A., Lee, J. V., Stemmler, J., Colwell, R.R., 1984. *Vibrio tubiashii* sp. nov., a pathogen of bivalve mollusks. Int. J. Syst. Bacteriol. 34, 1–4.

Hahladakis, J.N., Velis, C.A., Weber, R., Iacovidou, E., Purnell, P., 2018. An overview of chemical additives present in plastics: Migration, release, fate and environmental impact during their use, disposal and recycling. J. Hazard. Mater. 344, 179–199.

Hajighasemi, M., Tchigvintsev, A., Nocek, B.P., Flick, R., Popovic, A., Hai, T., Khusnutdinova, A.N., Brown, G., Xu, X., Cui, H., Anstett, J., Chernikova, T.N., Bruls, T., Le Paslier, D., Yakimov, M.M., Joachimiak, A., Golyshina, O. V., Savchenko, A., Golyshin, P.N., Edwards, E.A., Yakunin, A.F., 2018. Screening and characterization of novel polyesterases from environmental metagenomes with high hydrolytic activity against synthetic polyesters. Environ. Sci. Technol. 52, 12388–12401.

Hall-Stoodley, L., Costerton, J.W., Stoodley, P., State, M., Engineering, B., 2004. Bacterial biofilms: from the natural environment to infectious diseases. Nat. Rev. Microbiol. 2, 95–108.

Han, X., Liu, W., Huang, J., Ma, J., Zheng, Y., Ko, T., Xu, L., Cheng, Y., Chen, C., Guo, R., 2017. Structural insight into catalytic mechanism of PET. Nat. Commun. 8, 1–6.

Harrison, J.P., Sapp, M., Schratzberger, M., Osborn, A.M., 2011. Interactions between microorganisms and marine microplastics: A call for research. Mar. Technol. Soc. J. 45, 12–20.

Harrison, J.P., Schratzberger, M., Sapp, M., Osborn, A.M., 2014. Rapid bacterial colonization of low-density polyethylene microplastics in coastal sediment microcosms. BMC Microbiol. 14, 1–15.

Harshvardhan, K., Jha, B., 2013. Biodegradation of low-density polyethylene by marine bacteria from pelagic waters, Arabian Sea, India. Mar. Pollut. Bull. 77, 100–106.

Hartmann, N., Hüffer, T., Thompson, R.C., Hassellöv, M., Verschoor, A., Daugaard, A.E., Rist, S., Karlsson, T.M., Brennholt, N., Cole, M., Herrling, M.P., Heß, M., Ivleva, N.P., Lusher, A.L., Wagner, M., 2019. Are we speaking the same language? Recommendations for a definition and categorization framework for plastic debris. Environ. Sci. Technol. 53, 1039–1047.

Harwood, C.S., Parales, R.E., 1996. the B-Ketoadipate pathway and the biology of self-identity. Annu. Rev. Microbiol. 50, 553–590.

Hasegawa, H., Lind, E.J., Boin, M.A., Ha, C.C., 2008. The extracellular metalloprotease of

Vibrio tubiashii Is a major virulence factor for Pacific oyster (*Crassostrea gigas*) larvae. Appl. Environ. Microbiol. 74, 4101–4110.

Herrero Acero, E., Ribitsch, D., Steinkellner, G., Gruber, K., Greimel, K., Eiteljoerg, I., Trotscha, E., Wei, R., Zimmermann, W., Zinn, M., Cavaco-Paulo, A., Freddi, G., Schwab, H., Guebitz, G., 2011. Enzymatic surface hydrolysis of PET: Effect of structural diversity on kinetic properties of cutinases from *Thermobifida*. Macromolecules 44, 4632–4640.

Heskett, M., Takada, H., Yamashita, R., Yuyama, M., Ito, M., Geok, Y.B., Ogata, Y., Kwan, C., Heckhausen, A., Taylor, H., Powell, T., Morishige, C., Young, D., Patterson, H., Robertson, B., Bailey, E., Mermoz, J., 2012. Measurement of persistent organic pollutants (POPs) in plastic resin pellets from remote islands: Toward establishment of background concentrations for International Pellet Watch. Mar. Pollut. Bull. 64, 445–448.

Hesselsoe, M., Boysen, S., Iversen, N., Jørgensen, L., Murrell, J.C., Mcdonald, I., Radajewski, S., Thestrup, H., Roslev, P., 2005. Degradation of organic pollutants by methane grown microbial consortia. Biodegradation 16, 435–448.

Hirai, H., Takada, H., Ogata, Y., Yamashita, R., Mizukawa, K., Saha, M., Kwan, C., Moore, C., Gray, H., Laursen, D., Zettler, E.R., Farrington, J.W., Reddy, C.M., Peacock, E.E., Ward, M.W., 2011. Organic micropollutants in marine plastics debris from the open ocean and remote and urban beaches. Mar. Pollut. Bull. 62, 1683–1692.

Holmes, L.A., Turner, A., Thompson, R.C., 2014. Interactions between trace metals and plastic production pellets under estuarine conditions. Mar. Chem. 167, 25–32.

Holt, H.M., Bruun, B., 2005. *Shewanella algae* and *Shewanella putrefaciens*: clinical and microbiological characteristics. Eur. Soc. Clin. Infect. Dis. 11, 347–352.

Hood, M.A., 1991. Comparison of four methods for measuring chitinase activity and the application of the 4-MUF assay in aquatic environments. J. Microbiol. Methods 13, 151–160.

Hu, X., Thumarat, U., Zhang, X., Tang, M., Kawai, F., 2010. Diversity of polyester-degrading bacteria in compost and molecular analysis of a thermoactive esterase from *Thermobifida alba* AHK119. Appl. Microbiol. Biotechnol. 87, 771–779.

Huang, Z., Lai, Q., Shao, Z., 2017. *Salipiger nanhaiensis* Dai et al . 2015 is a later heterotypic synonym of *Thiobacimonas profunda* Li et al . 2015. Int. J. Syst. Evol. Microbiol. 67, 2043–2045.

Hug, L.A., Co, R., 2018. It takes a village: Microbial communities thrive through interactions and metabolic handoffs. mSystems 3, e00152-17.

Hugerth, L.W., Andersson, A.F., 2017. Analysing microbial community composition through

amplicon sequencing: From sampling to hypothesis testing. Front. Microbiol. 8, 1–22.

Ivanova, E.P., Ng, H.J., Webb, H.K., Kurilenko, V. V., Zhukova, N. V., Mikhailov, V. V., Ponamoreva, O.N., Crawford, R.J., 2013. *Alteromonas australica* sp. nov., isolated from the Tasman Sea. Antonie van Leeuwenhoek, Int. J. Gen. Mol. Microbiol. 103, 877–884.

Jahnke, A., Arp, H.P., Escher, B.I., Gewert, B., Gorokhova, E., Kühnel, D., Ogonowski, M., Potthoff, A., Rummel, C.D., Schmitt-Jansen, M., Toorman, E., MacLeod, M., 2017. Reducing uncertainty and confronting ignorance about the possible impacts of weathering plastic in the marine environment. Environ. Sci. Technol. Lett. 4, 85–90.

Jambeck, J., Geyer, R., Wilcox, C., Siegler, T., Perryman, M., Andrady, A., Narayan, R., Law, K., 2015. Plastic waste inputs from land into the ocean. Science (80-.). 347, 768–771.

Jeon, H.J., Kim, M.N., 2016. Comparison of the functional characterization between alkane monooxygenases for low-molecular-weight polyethylene biodegradation. Int. Biodeterior. Biodegradation 114, 202–208.

Jiang, P., Zhao, S., Zhu, L., Li, D., 2018. Microplastic-associated bacterial assemblages in the intertidal zone of the Yangtze Estuary. Sci. Total Environ. 624, 48–54.

Johnson, C.R., Boerlijst, M.C., 2002. Selection at the level of the community: the importance of spatial structures. Trends Ecol. Evol. 17, 83–90.

Johnston, E.L., Mayer-pinto, M., Crowe, T.P., 2015. Chemical contaminant effects on marine ecosystem functioning. J. Appl. Ecol. 52, 140–149.

Joint, I., Mühling, M., Querellou, J., 2010. Culturing marine bacteria – an essential prerequisite for biodiscovery. Microb. Biotechnol. 3, 564–575.

Joo, S., Cho, I.J., Seo, H., Son, H.F., Sagong, H.-Y., Shin, T.J., Choi, S.Y., Lee, S.Y., Kim, K.-J., 2018. Structural insight into molecular mechanism of poly(ethylene terephthalate) degradation. Nat. Commun. 9, 1–12.

Kanehisa, M., Furumichi, M., Tanabe, M., Sato, Y., Morishima, K., 2017. KEGG: New perspectives on genomes, pathways, diseases and drugs. Nucleic Acids Res. 45, D353–D361.

Kanehisa, M., Goto, S., 2000. KEGG; Kyoto Encyclopedia of Genes and Genomes. Nucleic Acids Res. 28, 27–30.

Kanehisa, M., Sato, Y., Kawashima, M., Furumichi, M., Tanabe, M., 2016a. KEGG as a reference resource for gene and protein annotation. Nucleic Acids Res. 44, D457–D462.

Kanehisa, M., Sato, Y., Morishima, K., 2016b. BlastKOALA and GhostKOALA: KEGG tools for functional characterization of genome and metagenome sequences. J. Mol. Biol. 428, 726–731.

Karapanagioti, H.K., Endo, S., Ogata, Y., Takada, H., 2011. Diffuse pollution by persistent

organic pollutants as measured in plastic pellets sampled from various beaches in Greece. Mar. Pollut. Bull. 62, 312–7.

Karlsson, M., Stenlid, J., 2009. Evolution of family 18 glycoside hydrolases: Diversity, domain structures and phylogenetic relationships. J. Mol. Microbiol. Biotechnol. 16, 208–223.

Kathiresan, K., 2003. Polythene and plastics-degrading microbes from the mangrove soil. Rev. Biol. Trop. 51, 629–634.

Kaur, A., Hernandez-Fernaud, J.R., Aguilo-Ferretjans, M. del M., Wellington, E.M., Christie-Oleza, J.A., 2018. 100 Days of marine *Synechococcus–Ruegeria pomeroyi* interaction: A detailed analysis of the exoproteome. Environ. Microbiol. 20, 785–799.

Kawai, F., Kawabata, T., Oda, M., 2019. Current knowledge on enzymatic PET degradation and its possible application to waste stream management and other fields. Appl. Microbiol. Biotechnol. 103, 4253–4268.

Kawai, F., Oda, M., Tamashiro, T., Waku, T., Tanaka, N., Yamamoto, M., Mizushima, H., Miyakawa, T., Tanokura, M., 2014. A novel Ca2+-activated, thermostabilized polyesterase capable of hydrolyzing polyethylene terephthalate from *Saccharomonospora viridis* AHK190. Appl. Microbiol. Biotechnol. 98, 10053–10064.

Keswani, A., Oliver, D.M., Gutierrez, T., Quilliam, R.S., 2016. Microbial hitchhikers on marine plastic debris: Human exposure risks at bathing waters and beach environments. Mar. Environ. Res. 118, 10–19.

Kesy, K., Oberbeckmann, S., Müller, F., Labrenz, M., 2016. Polystyrene influences bacterial assemblages in *Arenicola marina*-populated aquatic environments in vitro. Environ. Pollut. 219, 219–227.

Kettner, M.T., Rojas-jimenez, K., Oberbeckmann, S., Labrenz, M., Latina, U., Rica, D.C., Pedro, C.S., Jose, S., Rica, C., 2017. Microplastics alter composition of fungal communities in aquatic ecosystems. Environ. Microbiol. 19, 4447–4459.

Keyhani, N.O., Roseman, S., 1999. Physiological aspects of chitin catabolism in marine bacteria. Biochim. Biophys. Acta 1473 1473, 108–122.

Kielak, A.M., Cretoiu, M.S., Semenov, A. V., Sørensen, S.J., Van Elsas, J.D., 2013. Bacterial chitinolytic communities respond to chitin and pH alteration in soil. Appl. Environ. Microbiol. 79, 263–272.

Kiørboe, T., Grossart, H.P., Ploug, H., Tang, K., 2002. Mechanisms and rates of colonisation of sinking aggregates. Appl. Environ. Microbiol. 68, 3996–4006.

Kiørboe, T., Tang, K., Grossart, H., Ploug, H., 2003. Dynamics of microbial communities on marine snow aggregates: Colonization, growth, detachment, and grazing mortality of attached bacteria. Appl. Environ. Microbiol. 69, 3036–3047.

Kirstein, I. V., Kirmizi, S., Wichels, A., Garin-Fernandez, A., Erler, R., Löder, M., Gerdts, G., 2016. Dangerous hitchhikers? Evidence for potentially pathogenic *Vibrio* spp. on microplastic particles. Mar. Environ. Res. 120, 1–8.

Kirstein, I. V., Wichels, A., Gullans, E., Krohne, G., Gerdts, G., 2019. The Plastisphere – Uncovering tightly attached plastic "specific" microorganisms. PLoS One 1–17.

Kirstein, I. V, Wichels, A., Krohne, G., Gerdts, G., 2018. Mature biofilm communities on synthetic polymers in seawater - Specific or general? Mar. Environ. Res. 142, 147–154.

Koelmans, A.A., Kooi, M., Law, K.L., Van Sebille, E., 2017. All is not lost: Deriving a top-down mass budget of plastic at sea. Environ. Res. Lett.

Koh, H., Rani, S., Kim, S., Moon, E., Nam, S.W., Rhee, S., Park, S., 2018. *Halomonas aestuarii* sp. nov ., a moderately halophilic bacterium isolated from a tidal flat. Int. J. Syst. Evol. Microbiol. 67, 4298–4303.

Köllner, K.E., Carstens, D., Keller, E., Vazquez, F., Schubert, C.J., Zeyer, J., Bürgmann, H., 2012. Bacterial chitin hydrolysis in two lakes with contrasting trophic statuses. Appl. Environ. Microbiol. 78, 695–704.

Kozich, J.J., Westcott, S.L., Baxter, N.T., Highlander, S.K., Schloss, P.D., 2013. Development of a dual-index sequencing strategy and curation pipeline for analyzing amplicon sequence data on the MiSeq Illumina sequencing platform. Appl. Environ. Microbiol. 79, 5112–5120.

Krishnan, K.P., Saramma, A. V, 2005. Mixed substrate degradation: Are consortia better than monocultures? Indian J. Mar. Sci. 34, 188–191.

Kühn, S., Rebolledo, E.L.B., Franeker, J.A. Van, 2015. Deleterious effects of litter on marine life, in: Bergmann, M., Gutow, L., Klages, M. (Eds.), Marine Anthropogenic Litter. Springer Open, pp. 75–116.

Kumar, M., Xie, A., Curley, J., 2016. Determining the potential secondary impacts associated with microorganismal biodegradation of microplastics in the marine environment. J. Exp. Second. Sci. 3, 1–11.

Kumar, S., Hatha, A.A.M., Christi, K.S., 2007. Diversity and effectiveness of tropical mangrove soil microflora on the degradation of polythene carry bags. Int. J. Trop. Biol. 55, 777–786.

Kumar, V., Maitra, S.S., 2016. Biodegradation of endocrine disruptor dibutyl phthalate (DBP) by a newly isolated *Methylobacillus* sp. V29b and the DBP degradation pathway. 3 Biotech 6, 1–12.

Kumar, V., Sharma, N., Maitra, S.S., 2017. Comparative study on the degradation of dibutyl phthalate by two newly isolated Pseudomonas sp. V21b and Comamonas sp. 51F.

Biotechnol. Reports 15, 1–10.

Labbé, N., Parent, S., Villemur, R., 2004. Nitratireductor aquibiodomus gen. nov., sp. nov., a novel α-proteobacterium from the marine denitrification system of the Montreal Biodome (Canada). Int. J. Syst. Evol. Microbiol. 54, 269–273.

Labrecque, L. V, Kumar, R.A., Davé, V., Gross, R.A., P, M.S., 1997. Citrate esters as plasticizers for poly(lactic acid). J. Appl. Polym. Sci. 66, 1507–1513.

Lacerda, A.L.F., Rodrigues, L.S., Sebille, E. Van, Rodrigues, F.L., Ribeiro, L., Secchi, E.R., Kessler, F., Proietti, M.C., 2019. Plastics in sea surface waters around the Antarctic Peninsula. Sci. Rep. 9, 1–12.

Laganà, P., Caruso, G., Corsi, I., Bergami, E., Venuti, V., Majolino, D., La, R., Azzaro, M., Cappello, S., 2019. Do plastics serve as a possible vector for the spread of antibiotic resistance? First insights from bacteria associated to a polystyrene piece from King George Island (Antarctica). Int. J. Hyg. Environ. Health 222, 89–100.

Lai, Q., Cao, J., Yuan, J., Li, F., Shao, Z., 2014. *Celeribacter indicus* sp. nov., a polycyclic aromatic hydrocarbon-degrading bacterium from deep-sea sediment and reclassification of *Huaishuia halophila* as *Celeribacter halophilus* comb. nov. Int. J. Syst. Evol. Microbiol. 64, 4160–4167.

Lai, Q., Yu, Z., Wang, J., Zhong, H., Sun, F., Wang, L., Wang, B., Shao, Z., 2011. *Nitratireductor pacificus* sp. nov., isolated from a pyrene-degrading consortium. Int. J. Syst. Evol. Microbiol. 61, 1386–1391.

Lane, D.J., 1991. 16S/23S rRNA Sequencing, in: Stackebrandt, E. and Goodfellow, M. (Ed.), Nucleic Acid Techniques in Bacterial Systematics. pp. 115–175.

Langille, M.G.I., 2018. Exploring linkages between taxonomic and functional profiles of the human microbiome. mSystems 3, 1–4.

Langille, M.G.I., Zaneveld, J., Caporaso, J.G., McDonald, D., Knights, D., Reyes, J.A., Clemente, J.C., Burkepile, D.F., Vega Thurber, R.L., Knight, R., Beiko, R.G., Huttenhower, C., 2013. Predictive functional profiling of microbial communities using 16S rRNA marker gene sequences. Nat. Biotechnol. 31, 1814–821.

Larimer, C., Winder, E., Jeters, R., Prowant, M., Nettleship, I., Addleman, R.S., Bonheyo, G.T., Addleman, R.S., 2016. A method for rapid quantitative assessment of biofilms with biomolecular staining and image analysis. Anal. Bioanal. Chem. 408, 999–1008.

Law, K.L., 2017. Plastics in the Marine Environment. Ann. Rev. Mar. Sci. 9, 205–29.

Lecleir, G.R., Buchan, A., Maurer, J., Moran, M.A., Hollibaugh, J.T., 2007. Comparison of chitinolytic enzymes from an alkaline, hypersaline lake and an estuary. Environ. Microbiol. 9, 197–205.

Li, F., Liu, Y., Wang, D., Zhang, C., Yang, Z., Lu, S., Id, Y.W., 2018. Biodegradation of di-(2-ethylhexyl) phthalate by a halotolerant consortium LF. PLoS One 13, 1–13.

Li, J., Duan, H., Shi, P., 2011. Heavy metal contamination of surface soil in electronic waste dismantling area : site investigation and source-apportionment analysis. Waste Manag. Res. 27, 727–738.

Liang, D.W., Zhang, T., Fang, H.H.P., He, J., 2008. Phthalates biodegradation in the environment. Appl. Microbiol. Biotechnol. 80, 183–198.

Lloyd, J.R., Lovley, D.R., 2001. Microbial detoxification of metals and radionuclides. Curr. Opin. Biotechnol. 12, 248–253.

Lobelle, D., Cunliffe, M., 2011. Early microbial biofilm formation on marine plastic debris. Mar. Pollut. Bull. 62, 197–200.

López-Pérez, M., Gonzaga, A., Martin-Cuadrado, A.B., Onyshchenko, O., Ghavidel, A., Ghai, R., Rodriguez-Valera, F., 2012. Genomes of surface isolates of *Alteromonas macleodii*: The life of a widespread marine opportunistic copiotroph. Sci. Rep. 2, 1–11.

Lotka, A.J., 1926. Elements of Physical Biology. Sci. Prog. Twent. Century 21, 341–343.

Lu, Q., Qiu, L., Yu, L., Zhang, S., Alves, R., Toledo, D., Shim, H., 2019. Microbial transformation of chiral organohalides: Distribution, microorganisms and mechanisms. J. Hazard. Mater. 368, 849–861.

Marchler-Bauer, A., Bo, Y., Han, L., He, J., Lanczycki, C.J., Lu, S., Chitsaz, F., Derbyshire, M.K., Geer, R.C., Gonzales, N.R., Gwadz, M., Hurwitz, D.I., Lu, F., Marchler, G.H., Song, J.S., Thanki, N., Wang, Z., Yamashita, R.A., Zhang, D., Zheng, C., Geer, L.Y., Bryant, S.H., 2017. CDD/SPARCLE: functional classification of proteins via subfamily domain architectures. Nucleic Acids Res. 45, 200–203.

Martens, T., Heidorn, T., Pukal, R., Simon, M., Tindall, B.J., Brinkhoff, T., 2006. Reclassification of Roseobacter gallaeciensis Ruiz-Ponte et al. 1998 as *Phaeobacter gallaeciensis* gen. nov., comb. nov., description of *Phaeobacter inhibens* sp. nov., reclassification of *Ruegeria algicola* (Lafay et al. 1995) Uchino et al. 1999 as *Marinovu*. Int. J. Syst. Evol. Microbiol. 56, 1293–1304.

Martínez-Martínez, M., Lores, I., Peña-García, C., Bargiela, R., Reyes-Duarte, D., Guazzaroni, M.E., Peláez, A.I., Sánchez, J., Ferrer, M., 2014. Biochemical studies on a versatile esterase that is most catalytically active with polyaromatic esters. Microb. Biotechnol. 7, 184–191.

Mathieu-Denoncourt, J., Wallace, S.J., de Solla, S.R., Langlois, V.S., 2015. Plasticizer endocrine disruption: Highlighting developmental and reproductive effects in mammals and non-mammalian aquatic species. Gen. Comp. Endocrinol. 219, 74–88.

Mato, Y., Isobe, T., Takada, H., Kanehiro, H., Ohtake, C., Kaminuma, T., 2001. Plastic resin pellets as a transport medium for toxic chemicals in the marine environment. Environ. Sci. Technol. 35, 318–324.

Matsuyama, H., Sawazaki, K., Minami, H., Kasahara, H., Horikawa, K., Yumoto, I., 2014. *Pseudoalteromonas shioyasakiensis* sp . nov., a marine polysaccharide-producing bacterium. Int. J. Syst. Evol. Microbiol. 64, 101–106.

McMurdie, P.J., Holmes, S., 2013. phyloseq: An R package for reproducible interactive analysis and graphics of microbiome census data. PLoS One 8, 1–11.

Michels, J., Stippkugel, A., Wirtz, K., Engel, A., 2018. Aggregation of microplastics with marine biogenic particles. Proc. R. Soc. B 285, 1–9.

Mohanrasu, K., Premnath, N., Prakash, G.S., Sudhakar, M., Boobalan, T., 2018. Exploring multi potential uses of marine bacteria; an intgrated approach for PHB production, PAHs and polyethylene biodegradation. J. Photochem. Photobiol. B Biol. 185, 55–65.

Moore, C.J., 2008. Synthetic polymers in the marine environment: A rapidly increasing, long-term threat. Environ. Res. 108, 131–139.

Moore, C.J., Lattin, G.L., Zellers, A.F., 2005. A brief analysis of organic pollutants sorbed to pre and post- production plastic particles from the Los Angeles and San Gabriel river watersheds, Algalita Marine Research Foundation.

Morris, D.J., Pinnegar, J.K., Maxwell, D.L., Dye, S.R., Fernand, L.J., Flatman, S., Williams, O.J., Rogers, S.I., 2018. Over 10 million seawater temperature records for the United Kingdom Continental Shelf between 1880 and 2014 from 17 Cefas (United Kingdom government) marine data systems. Earth Syst. Sci. Data 10, 27–51.

Morris, J.J., Lenski, R.E., Zinser, E.R., 2012. The Black Queen Hypothesis: Evolution of dependencies through adaptive gene loss. MBio 3, 1–9.

Morris, R.M., Rappé, M.S., Connon, S.A., Vergin, K.L., Siebold, W.A., Carlson, C.A., Giovannoni, S.J., 2002. SAR11 clade dominates ocean surface bacterioplankton communities. Nature 420, 806–810.

Muller-Karanassos, C., Turner, A., Arundel, W., Vance, T., Lindeque, P.K., Cole, M., 2019. Antifouling paint particles in intertidal estuarine sediments from southwest England and their ingestion by the harbour ragworm, *Hediste diversicolor*. Environ. Pollut. 249, 163–170.

Munier, B., Bendell, L.I., 2018. Macro and micro plastics sorb and desorb metals and act as a point source of trace metals to coastal ecosystems. PLoS One 13, 1–13.

Muñoz-Elías, E.J., McKinney, J.D., 2006. *M. tuberculosis* isocitrate lyases 1 and 2 are jointly required for in vivo growth and virulence. Nat. Med. 11, 638–644.

Muramatsu, Y., Uchino, Y., Kasai, H., Suzuki, K.I., Nakagawa, Y., 2007. *Ruegeria mobilis* sp. nov., a member of the *Alphaproteobacteria* isolated in Japan and Palau. Int. J. Syst. Evol. Microbiol. 57, 1304–1309.

Muthukrishnan, T., Khaburi, M. Al, Abed, R.M.M., 2018. Fouling microbial communities on plastics compared with wood and steel: Are they substrate- or location-specific? Microb. Ecol.

Nakkabi, A., Elmoualij, N., Sadiki, M., Ibnsouda Koraichi, S., Fahim, M., 2015. Biodegradation of poly (ethylene terephthalate) by *Bacillus Subtilis*. Int. J. Recent Adv. Multidiscip. Res. 2, 1060–1062.

Napper, I.E., Bakir, A., Rowland, S.J., Thompson, R.C., 2015. Characterisation, quantity and sorptive properties of microplastics extracted from cosmetics. Mar. Pollut. Bull. 99, 178–185.

Napper, I.E., Thompson, R.C., 2016. Release of synthetic microplastic plastic fibres from domestic washing machines: Effects of fabric type and washing conditions. Mar. Pollut. Bull. 112, 39–45.

Nauendorf, A., Krause, S., Bigalke, N.K., Gorb, E. V., Gorb, S.N., Haeckel, M., Wahl, M., Treude, T., 2016. Microbial colonization and degradation of polyethylene and biodegradable plastic bags in temperate fine-grained organic-rich marine sediments. Mar. Pollut. Bull. 103, 168–178.

Nedoma, J., Vrba, J., Hejzlar, J., Šimek, K., Straškrabová, V., 1994. N-acetylglucosamine dynamics in freshwater environments: Concentration of amino sugars, extracellular enzyme activities, and microbial uptake. Limnol. Oceanogr. 39, 1088–1100.

Nedwell, D.B., 1999. Effect of low temperature on microbial growth: Lowered affinity for substrates limits growth at low temperature. FEMS Microbiol. Ecol. 30, 101–111.

Neto, J.A.B., Gaylarde, C., Beech, I., Bastos, A.C., Quaresma, V. da S., de Carvalho, D.G., 2019. Microplastics and attached microorganisms in sediments of the Vitória bay estuarine system in SE Brazil. Ocean Coast. Manag. 169, 247–253.

Njiwa, J.R.K., Müller, P., Klein, R., 2004. Life cycle stages and length of Zebrafish (*Danio rerio*) exposed to DDT. J. Heal. Sci. 50, 220–225.

Noriega-Ortega, B.E., Wienhausen, G., Mentges, A., Dittmar, T., Simon, M., Niggemann, J., 2019. Does the chemodiversity of bacterial exometabolomes sustain the chemodiversity of marine dissolved organic matter? Front. Microbiol. 10, 1–13.

Oberbeckmann, S., Kreikemeyer, B., Labrenz, M., 2018. Environmental factors support the formation of specific bacterial assemblages on microplastics. Front. Microbiol. 8, 1–12.

Oberbeckmann, S., Labrenz, M., 2020. Marine Microbial Assemblages on Microplastics:

Diversity, Adaptation, and Role in Degradation. Ann. Rev. Mar. Sci. 12, 1–24.

Oberbeckmann, S., Loeder, M.G.J., Gerdts, G., Osborn, A.M., 2014. Spatial and seasonal variation in diversity and structure of microbial biofilms on marine plastics in Northern European waters. FEMS Microbiol. Ecol. 90, 478–492.

Oberbeckmann, S., Osborn, A.M., Duhaime, M.B., 2016. Microbes on a bottle: Substrate, season and geography influence community composition of microbes colonizing marine plastic debris. PLoS One 11, 1–24.

Ogata, Y., Takada, H., Mizukawa, K., Hirai, H., Iwasa, S., Endo, S., Mato, Y., Saha, M., Okuda, K., Nakashima, A., Murakami, M., Zurcher, N., Booyatumanondo, R., Zakaria, M.P., Dung, L.Q., Gordon, M., Miguez, C., Suzuki, S., Moore, C., Karapanagioti, H.K., Weerts, S., McClurg, T., Burres, E., Smith, W., Velkenburg, M. Van, Lang, J.S., Lang, R.C., Laursen, D., Danner, B., Stewardson, N., Thompson, R.C., 2009. International Pellet Watch: Global monitoring of persistent organic pollutants (POPs) in coastal waters. 1. Initial phase data on PCBs, DDTs, and HCHs. Mar. Pollut. Bull. 58, 1437–1446.

Ogonowski, M., Motiei, A., Ininbergs, K., Hell, E., Gerdes, Z., Udekwu, K.I., Bacsik, Z., 2018. Evidence for selective bacterial community structuring on microplastics. Environ. Microbiol. 20, 2796–2808.

Opsahl, S., Benner, R., 1997. Distribution and cycling of terrigenous dissolved organic matter in the ocean. Nature 386, 480–482.

Ortiz-Álvarez, R., Fierer, N., de los Ríos, A., Casamayor, E.O., Barberán, A., 2018. Consistent changes in the taxonomic structure and functional attributes of bacterial communities during primary succession. ISME J. 12, 1658–1667.

Paço, A., Duarte, K., da Costa, J.P., Santos, P.S.M., Pereira, R., Pereira, M.E., Freitas, A.C., Duarte, A.C., Rocha-Santos, T.A.P., 2017. Biodegradation of polyethylene microplastics by the marine fungus *Zalerion maritimum*. Sci. Total Environ. 586, 10–15.

Paluselli, A., Fauvelle, V., Galgani, F.F., Sempéré, R., 2019. Phthalate release from plastic fragments and degradation in seawater. Environ. Sci. Technol. 53, 166–175.

Parada, A.E., Needham, D.M., Fuhrman, J.A., 2016. Every base matters: assessing small subunit rRNA primers for marine microbiomes with mock communities, time series and global field samples. Environ. Microbiol. 18, 1403–1414.

Paradis, E., Claude, J., Strimmer, K., 2004. APE: Analyses of Phylogenetics and Evolution in R language. Bioinformatics 20, 289–290.

Park, J.M., Jeon, M., Lim, E.S., Um, H.J., Kim, Y.C., Min, J., Kim, Y.H., 2008. Biodegradation of a phthalate plasticizer, di-isononyl phthalate (DINP), by *Sphingobium chungbukense*. Curr. Microbiol. 57, 515–518.

Park, J.M., Kim, M., Yoon, J., Kobayashi, F., Iwasaka, Y., Hong, C.S., Min, J., Kim, Y.H., 2009. Biodegradation of diisodecyl phthalate (DIDP) by *Bacillus* sp. SB-007. J. Basic Microbiol. 49, 31–35.

Patil, R.S., Ghormade, V., Deshpande, M. V., 2000. Chitinolytic enzymes: An exploration. Enzyme Microb. Technol. 26, 473–483.

Patterson, D., Steinberg, G., Nygaard, K., Steinberg, G., 1993. Heterotrophic flagellates and other protists associated with oceanic detritus throughout the water column in the mid north atlantic. J. Mar. Biol. Assoc. U.K. 73, 67–95.

Pedregosa, F., Weiss, R., Brucher, M., 2011. Scikit-learn: Machine learning in Python. J. Mach. Learn. Res. 12, 2825–2830.

Penn, A., 2003. Modelling Artificial Ecosystem Selection: A Preliminary Investigation, in: ECAL.

Penn, A., Harvey, I., 2004. The role of non-genetic change in the heritability, variation, and response to selection of artificially selected ecosystems. Artif. Life IX 352–357.

Plasticizers, 2019. URL plasticizers.org (accessed 1.31.19).

PlasticsEurope, 2018. Plastics – the Facts 2018.

Pollet, T., Berdjeb, L., Garnier, C., Durrieu, G., Le Poupon, C., Misson, B., Briand, J.-F., 2018. Prokaryotic community successions and interactions in marine biofilms: the key role of *Flavobacteriia*. FEMS Microb. Ecol. 94, 1–13.

Ponomarova, O., Patil, K.R., 2015. Metabolic interactions in microbial communities: untangling the Gordian knot. Curr. Opin. Microbiol. 27, 37–44.

Pospíšil, P., 2016. Production of reactive oxygen species by photosystem II as a response to light and temperature stress. Front. Plant Sci. 7, 1–12.

Prado, S., Dubert, J., Romalde, L., Toranzo, A.E., Barja, J.L., 2014. *Vibrio ostreicida* sp. nov., a new pathogen of bivalve larvae. Int. J. Syst. Evol. Microbiol. 64, 1641–1646.

Pruesse, E., Peplies, J., Glöckner, F.O., 2012. SINA: Accurate high-throughput multiple sequence alignment of ribosomal RNA genes. Bioinformatics 28, 1823–1829.

Qu, L., Zhu, F., Hong, X., Gao, W., Chen, J., Sun, X., 2011. *Sunxiuqinia elliptica* gen. nov., sp. nov., a member of the phylum bacteroidetes isolated from sediment in a sea cucumber farm. Int. J. Syst. Evol. Microbiol. 61, 2885–2889.

Quan, Z.-X., Xiao, Y.-P., Roh, S.W., Nam, Y.-D., Chang, H.-W., Shin, K.-S., Rhee, S.-K., Park, Y.-H., Bae, J.-W., 2008. *Joostella marina* gen. nov., sp. nov., a novel member of the family *Flavobacteriaceae* isolated from the East Sea. Int. J. Syst. Evol. Microbiol. 58, 1388–1392.

Quast, C., Pruesse, E., Yilmaz, P., Gerken, J., Schweer, T., Glo, F.O., Yarza, P., 2013. The SILVA

ribosomal RNA gene database project: improved data processing and web-based tools. Nucleic Acids Res. 41, 590–596.

Quero, G.M., Luna, G.M., 2017. Surfing and dining on the “plastisphere”: Microbial life on plastic marine debris. Adv. Oceanogr. Limnol. 8, 199–207.

Quilliam, R.S., Jamieson, J., Oliver, D.M., 2014. Seaweeds and plastic debris can influence the survival of faecal indicator organisms in beach environments. Mar. Pollut. Bull. 84, 201–207.

R Core Team, 2017. R: A language and environment for statistical computing. R Found. Stat. Comput.

Raghul, S.S., Bhat, S.G., Chandrasekaran, M., Francis, V., Thachil, E.T., 2014. Biodegradation of polyvinyl alcohol-low linear density polyethylene-blended plastic film by consortium of marine benthic vibrios. Int. J. Environ. Sci. Technol. 11, 1827–1834.

Ramana, V.V., Kumar, P.A., Srinivas, T.N.R., Sasikala, C., Ramana, C. V, 2009. *Rhodobacter aestuarii* sp . nov ., a phototrophic alphaproteobacterium isolated from an estuarine environment. Int. J. Syst. Evol. Microbiol. 59, 1133–1136.

Rani, M., Shim, W.J., Han, G.M., Jang, M., Al-odaini, N.A., Song, Y.K., Hong, S.H., 2015. Qualitative Analysis of Additives in Plastic Marine Debris and Its New Products. Arch. Environ. Contam. Toxicol. 69, 352–66.

Readman, J.W., Deluna, F., Ebinghaus, R., Guzman, A., Price, A.R.G., Emily, E., Sheppard, A.L.S., Sleight, V.A., Thompson, R.C., Tonkin, A., Wright, R.J., Sheppard, C.R.C., 2013. Contaminants, Pollution and Potential Anthropogenic Impacts in Chagos/BIOT, in: Coral Reefs of the United Kingdom Overseas Territories. pp. 283–298.

Reed, S., Clark, M., Thompson, R., Hughes, K.A., 2018. Microplastics in marine sediments near Rothera Research Station, Antarctica. Mar. Pollut. Bull. 133, 460–463.

Reisser, J., Shaw, J., Hallegraeff, G., Proietti, M., Barnes, D.K.A., Thums, M., Wilcox, C., Hardesty, B.D., Pattiaratchi, C., 2014. Millimeter-sized marine plastics: A new pelagic habitat for microorganisms and invertebrates. PLoS One 9, 1–11.

Ribitsch, D., Acero, E.H., Greimel, K., Dellacher, A., Zitzenbacher, S., Marold, A., Rodriguez, R.D., Steinkellner, G., Gruber, K., Schwab, H., Guebitz, G.M., 2012. A new esterase from *Thermobifida halotolerans* hydrolyses polyethylene terephthalate (PET) and polylactic acid (PLA). Polymers (Basel). 4, 617–629.

Riemann, L., Azam, F., 2002. Widespread N -Acetyl-D-Glucosamine uptake among pelagic marine bacteria and its ecological implications. Appl. Environ. Microbiol. 68, 5554–5562.

Rochman, C.M., Hoh, E., Kurobe, T., Teh, S.J., 2013. Ingested plastic transfers chemicals to

fish and induces hepatic stress. Sci. Rep. 3, 1–7.

Rodrigues, A., Oliver, D.M., Mccarron, A., Quilliam, R.S., 2019. Colonisation of plastic pellets (nurdles) by E . coli at public bathing beaches. Mar. Pollut. Bull. 139, 376–380.

Roell, G.W., Zha, J., Carr, R.R., Koffas, M.A., Fong, S.S., Tang, Y.J., 2019. Engineering microbial consortia by division of labor. Microb. Cell Fact. 1–11.

Romano, I., Giordano, A., Lama, L., Nicolaus, B., Gambacorta, A., 2005. *Halomonas campaniensis* sp. nov., a haloalkaliphilic bacterium isolated from a mineral pool of Campania Region, Italy. Syst. Appl. Microbiol. 28, 610–618.

Romera-Castillo, C., Pinto, M., Langer, T.M., Álvarez-salgado, X.A., Herndl, G.J., 2018. Dissolved organic carbon leaching from plastics stimulates microbial activity in the ocean. Nat. Commun. 9, 1–7.

Roy, P.K., Titus, S., Surekha, P., Tulsi, E., Deshmukh, C., Rajagopal, C., 2008. Degradation of abiotically aged LDPE films containing pro-oxidant by bacterial consortium. Polym. Degrad. Stab. 93, 1917–1922.

Ruiz-Dueñas, F.J., Martínez, Á.T., 2009. Microbial degradation of lignin: how a bulky recalcitrant polymer is efficiently recycled in nature and how we can take advantage of this. Microb. Biotechnol. 2, 164–177.

Rummel, C.D., Jahnke, A., Gorokhova, E., Kühnel, D., Schmitt-Jansen, M., 2017. The impacts of biofilm formation on the fate and potential effects of microplastic in the aquatic environment. Environ. Sci. Technol. Lett. 4, 258–267.

Ryan, P.G., Connell, A.D., Gardner, B.D., 1988. Plastic ingestion and PCBs in seabirds: Is there a relationship? Mar. Pollut. Bull. 19, 174–176.

Salvador, M., Abdulmutalib, U., Gonzalez, J., Kim, J., Smith, A.A., Faulon, J.-L., Wei, R., Zimmerman, W., Jiminez, J.I., 2019. Microbial genes for a circular and sustainable Bio-PET economy. Genes (Basel). 10, 1–15.

Sato-Takabe, Y., Nakao, H., Kataoka, T., Yokokawa, T., Hamasaki, K., Ohta, K., Suzuki, S., 2016. Abundance of common aerobic anoxygenic phototrophic bacteria in a coastal aquaculture area. Front. Microbiol. 7, 1–10.

Savoca, D., Arculeo, M., Barreca, S., Buscemi, S., Caracappa, S., Gentile, A., Flaminia, M., Pace, A., 2018. Chasing phthalates in tissues of marine turtles from the Mediterranean sea. Mar. Pollut. Bull. 127, 165–169.

Sayali, K., Sadichha, P., Surekha, S., 2013. Microbial Esterases: An overview. Int. J. Curr. Microbiol. Appl. Sci. 2, 135–146.

Schliep, K.P., 2011. phangorn: phylogenetic analysis in R. Bioinformatics 27, 592–593.

Schloss, P.D., Westcott, S.L., Ryabin, T., Hall, J.R., Hartmann, M., Hollister, E.B., Lesniewski,

R.A., Oakley, B.B., Parks, D.H., Robinson, C.J., Sahl, J.W., Stres, B., Thallinger, G.G., Van Horn, D.J., Weber, C.F., 2009. Introducing mothur: Open-source, platform-independent, community-supported software for describing and comparing microbial communities. Appl. Environ. Microbiol. 75, 7537–7541.

Schneiker, S., dos Santos, V.A., Bartels, D., Bekel, T., Brecht, M., Buhrmester, J., Chernikova, T.N., Denaro, R., Ferrer, M., Gertler, C., Goesmass, A., Golyshina, O. V., Kaminski, F., Khachane, A.N., Lang, S., Linke, B., McHardy, A.C., Meyer, F., Nechitaylo, T., Puehler, A., Regenhardt, D., Rupp, O., Sabirova, J.S., Selbitshka, W., Yakimov, M.M., Timmis, K.N., Vorholter, F.-J., Weidner, S., Kaiser, O., Golyshin, P.N., 2006. Genome sequence of the ubiquitous hydrocarbon-degrading marine bacterium *Alcanivorax borkumensis*. Nat. Biotechnol. 24, 997–1004.

Sebille, E. Van, England, M.H., Froyland, G., 2012. Origin, dynamics and evolution of ocean garbage patches from observed surface drifters. Environ. Res. Lett. 7, 044040.

Seemann, T., 2014. Prokka: Rapid prokaryotic genome annotation. Bioinformatics 30, 2068–2069.

Simon, M., Grossart, H.-P., Schweitzer, B., Ploug, H., 2002. Microbial ecology of organic aggregates in aquatic ecosystems. Aquat. Microb. Ecol. 28, 175–211.

Souza, C.P., Almeida, B.C., Colwell, R.R., Rivera, I.N.G., 2011. The importance of chitin in the marine environment. Mar. Biotechnol. 13, 823–830.

Stahl, W.H., Pessen, H., 1952. The microbiological degradation of plasticizers. Appl. Microbiol. 1, 30–35.

Stanislauskienė, R., Rudenkov, M., Karvelis, L., Gasparavičiūtė, R., Meškienė, R., Časaitė, V., Meškys, R., 2011. Analysis of phthalate degradation operon from *Arthrobacter* sp . 68b. Biologija 57, 45–54.

Staples, C.A., Peterson, D.R., Parkerton, T.F., Adams, W.J., 1997. The environmental fate of phthalate esters: A literature review. Chemosphere 35, 667–749.

Stewart, E.J., 2012. Growing unculturable bacteria. J. Bacteriol. 194, 4151–4160.

Stingley, R.L., Brezna, B., Khan, A.A., Cerniglia, C.E., 2004. Novel organization of genes in a phthalate degradation operon of *Mycobacterium vanbaalenii*. Microbiology 150, 3749–3761.

Stolyar, S., Van Dien, S., Hillesland, K.L., Pinel, N., Lie, T.J., Leigh, J.A., Stahl, D.A., 2007. Metabolic modeling of a mutualistic microbial community. Mol. Syst. Biol. 3, 1–14.

Sudhakar, M., Doble, M., Murthy, P.S., Venkatesan, R., 2008. Marine microbe-mediated biodegradation of low- and high-density polyethylenes. Int. Biodeterior. Biodegradation 61, 203–213.

Sulaiman, S., Yamato, S., Kanaya, E., Kim, J.J., Koga, Y., Takano, K., Kanaya, S., 2012. Isolation of a novel cutinase homolog with polyethylene terephthalate-degrading activity from leaf-branch compost by using a metagenomic approach. Appl. Environ. Microbiol. 78, 1556–1562.

Summers, S., Henry, T., Gutierrez, T., 2018. Agglomeration of nano- and microplastic particles in seawater by autochthonous and de novo-produced sources of exopolymeric substances. Mar. Pollut. Bull. 130, 258–267.

Sung, H.R., Lee, J.M., Kim, M., Yun, B.R., Shin, K.S., 2015. Donghicola tyrosinivorans sp. Nov., A tyrosine-degrading bacterium isolated from seawater. Int. J. Syst. Evol. Microbiol. 65, 4140–4145.

Sutherland, I.W., 2001. Biofilm exopolysaccharides: A strong and sticky framework. Microbiology 147, 3–9.

Swenson, W., Arendt, J., Wilson, D.S., 2000a. Artificial selection of microbial ecosystems for 3-chloroaniline biodegradation. Environ. Microbiol. 2, 564–571.

Swenson, W., Wilson, D.S., Elias, R., 2000b. Artificial ecosystem selection. Proc. Natl. Acad. Sci. 97, 9110–9114.

Syranidou, E., Karkanorachaki, K., Amorotti, F., Avgeropoulos, A., Kolvenbach, B., Zhou, N., Fava, F., Corvini, P.F., Kalogerakis, N., 2019. Biodegradation of mixture of plastic films by tailored marine consortia. J. Hazard. Mater. 375, 33–42.

Syranidou, E., Karkanorachaki, K., Amorotti, F., Franchini, M., Repouskou, E., Kaliva, M., Vamvakaki, M., Kolvenbach, B., Fava, F., Corvini, P.F.X., Kalogerakis, N., 2017a. Biodegradation of weathered polystyrene films in seawater microcosms. Sci. Rep. 7, 1–12.

Syranidou, E., Karkanorachaki, K., Amorotti, F., Repouskou, E., Kroll, K., Kolvenbach, B., Corvini, P.F., Fava, F., Kalogerakis, N., 2017b. Development of tailored indigenous marine consortia for the degradation of naturally weathered polyethylene films. PLoS One 12, 1–21.

Takada, H., 2006. Call for pellets! International Pellet Watch Global Monitoring of POPs using beached plastic resin pellets. Mar. Pollut. Bull. 52, 1547–1548.

Tanasupawat, S., Takehana, T., Yoshida, S., Hiraga, K., Oda, K., 2016. *Ideonella sakaiensis* sp. nov., isolated from a microbial consortium that degrades PET. Int. J. Syst. Evol. Microbiol. 66, 2813–2818.

Tecon, R., Mitri, S., Ciccarese, D., Or, D., van der Meer, J.R., Johnson, D.R., 2019. Bridging the holistic-reductionist divide in microbial ecology. mSystems 4, 1–17.

Tedetti, M., Semperv, R., 2006. Penetration of ultraviolet radiation in the marine

environment . A review. Photochem. Photobiol. 82, 389–397.

Teuten, E.L., Rowland, S.J., Galloway, T.S., Thompson, R.C., 2007. Potential for plastics to transport hydrophobic contaminants. Environ. Sci. Technol. 41, 7759–7764.

Teuten, E.L., Saquing, J.M., Knappe, D.R.U., Barlaz, M.A., Jonsson, S., Bjorn, A., Rowland, S.J., Thompson, R.C., Galloway, T.S., Yamashita, R., Ochi, D., Watanuki, Y., Moore, C., Viet, P.H., Tana, T.S., Prudente, M., Boonyatumanond, R., Zakaria, M.P., Akkhavong, K., Ogata, Y., Hirai, H., Iwasa, S., Mizukawa, K., Hagino, Y., Imamura, A., Saha, M., Takada, H., 2009. Transport and release of chemicals from plastics to the environment and to wildlife. Philos. Trans. R. Soc. B Biol. Sci. 364, 2027–2045.

Thompson, R.C., Moore, C.J., vom Saal, F.S., Swan, S.H., 2009. Plastics, the environment and human health: current consensus and future trends. Phil. Trans. R. Soc. B 364, 2153–2166.

Tokiwa, Y., Calabia, B.P., Ugwu, C.U., Aiba, S., 2009. Biodegradability of plastics. Int. J. Mol. Sci. 10, 3722–3742.

Trifunovic, D., Schuchmann, K., Muller, V., 2016. Ethylene glycol metabolism in the acetogen *Acetobacterium woodii*. J. Bacteriol. 198, 1058–1065.

Tsiota, P., Karkanorachaki, K., Syranidou, E., Franchini, M., Kalogerakis, N., 2018. Microbial degradation of HDPE secondary microplastics: Preliminary results, in: Proceedings of the International Conference on Microplastic Pollution in the Mediterranean Sea. pp. 181–188.

Tsubouchi, T., Ohta, Y., Haga, T., Usui, K., Shimane, Y., Mori, K., Tanizaki, A., Adachi, A., Kobayashi, K., Yukawa, K., Takagi, E., Tame, A., Uematsu, K., Maruyama, T., Hatada, Y., 2014. *Thalassospira alkalitolerans* sp. nov. and *Thalassospira mesophila* sp. nov., isolated from a decaying bamboo sunken in the marine environment, and emended description of the genus *Thalassospira*. Int. J. Syst. Evol. Microbiol. 64, 107–115.

Turner, A., 2010. Marine pollution from antifouling paint particles. Mar. Pollut. Bull. 60, 159–171.

Turusov, V., Rakitsky, V., Tomatis, L., 2002. Dichlorodiphenyltrichloroethane (DDT): Ubiquity, persistence, and risks. Environ. Health Perspect. 110, 125–128.

Tyanova, S., Temu, T., Sinitcyn, P., Carlson, A., Hein, M.Y., Geiger, T., Mann, M., Cox, J., 2016. The Perseus computational platform for comprehensive analysis of (prote)omics data. Nat. Methods 13, 731–740.

Vamsee-Krishna, C., Phale, P.S., 2008. Bacterial degradation of phthalate isomers and their esters. Indian J. Microbiol. 48, 19–34.

Van Sebille, E., Wilcox, C., Sherman, P., Hardesty, B.D., Law, K.L., 2016. Modelling global

distribution, risk and mitigation strategies of floating plastic pollution, in: Geophysical Research Abstracts EGU General Assembly.

Van Vliet, E.D.S., Reitano, E.M., Chhabra, J.S., Bergen, J.P., Whyatt, R.M., 2011. A review of alternatives to di (2-ethylhexyl) phthalate-containing medical devices in the neonatal intensive care unit. J. Perinatol. 31, 551–560.

Vered, G., Kaplan, A., Avisar, D., Shenkar, N., 2019. Using solitary ascidians to assess microplastic and phthalate plasticizers pollution among marine biota: A case study of the Eastern Mediterranean and Red Sea. Mar. Pollut. Bull. 138, 618–625.

Volterra, V., 1926. Fluctuations in the abundance of a species considered mathematically. Nature 118, 558–560.

Wackett, L., 2015. Broad specificity microbial enzymes. Microb. Biotechnol. 8, 188–189.

Wagner, M., Scherer, C., Alvarez-muñoz, D., Brennholt, N., Bourrain, X., Buchinger, S., Fries, E., Grosbois, C., Klasmeier, J., Marti, T., Rodriguez-mozaz, S., Urbatzka, R., Vethaak, A.D., Winther-nielsen, M., Reifferscheid, G., 2014. Microplastics in freshwater ecosystems: what we know and what we need to know. Environ. Sci. Eur. 26, 1–9.

Wang, H., Zhang, X., Yan, S., Qi, Z., Yu, Y., 2012. *Huaishuia halophila* gen. nov., sp. nov., isolated from coastal seawater. Int. J. Syst. Evol. Microbiol. 62, 223–228.

Wang, W., Yang, S., Hunsinger, G.B., Pienkos, P.T., Johnson, D.K., Avignone-rossa, C., 2014. Connecting lignin-degradation pathway with pre-treatment inhibitor sensitivity of *Cupriavidus necator*. Front. Microbiol. 5, 1–10.

Wang, W., Zhong, R., Shan, D., Shao, Z., 2014. Indigenous oil-degrading bacteria in crude oil-contaminated seawater of the Yellow sea, China. Appl. Microbiol. Biotechnol. 98, 7253–7269.

Wang, Y., Tam, N.F.Y., 2019. Microbial remediation of organic pollutants, Second. ed, World Seas: An Environmental Evaluation.

Wang, Y.P., Gu, J.D., 2006a. Degradation of dimethyl isophthalate by *Viarovorax paradoxus* strain T4 isolated from deep-ocean sediment of the South China Sea. Hum. Ecol. Risk Assess. 12, 236–247.

Wang, Y.P., Gu, J.D., 2006b. Degradability of dimethyl terephthalate by *Variovorax paradoxus* T4 and *Sphingomonas yanoikuyae* DOS01 isolated from deep-ocean sediments. Ecotoxicology 15, 549–557.

Ward, J.E., Kach, D.J., 2009. Marine aggregates facilitate ingestion of nanoparticles by suspension-feeding bivalves. Mar. Environ. Res. 68, 137–42.

Webb, H., 2012. Biodegradation of poly(ethylene terephthalate) by marine bacteria, and strategies for its enhancement. Swinburne University of Technology.

Webb, H.K., Arnott, J., Crawford, R.J., Ivanova, E.P., 2013. Plastic degradation and its environmental implications with special reference to poly(ethylene terephthalate). Polymers (Basel). 5, 1–18.

Webb, H.K., Crawford, R.J., Sawabe, T., Ivanova, E.P., 2009. Poly(ethylene terephthalate) polymer surfaces as a substrate for bacterial attachment and biofilm formation. Microbes Environ. 24, 39–42.

Wei, R., Zimmermann, W., 2017. Microbial enzymes for the recycling of recalcitrant petroleum-based plastics: how far are we? Microb. Biotechnol. 10, 1308–1322.

Wei, X.-F., Linde, E., Hedenqvist, M.S., 2019. Plasticiser loss from plastic or rubber products through diffusion and evaporation. npj Mater. Degrad. 3.

Wenning, R.J., Martello, L., 2014. POPs in marine and freshwater environments, in: Environmental Forensics for Persistent Organic Pollutants. Elsevier B.V., pp. 357–390.

Wiegant, W.M., de Bont, J.A., 1980. A new route for ethylene glycol metabolism in Mycobacterium E44. J. Gen. Microbiol. 120, 325–331.

Wilkes, R., Aristilde, L., 2017. Degradation and metabolism of synthetic plastics and associated products by *Pseudomonas* spp.: Capabilities and challenges. J. Appl. Microbiol. 123, 582–593.

Williams, H.T.P., Lenton, T.M., 2007a. Artificial selection of simulated microbial ecosystems. Proc. Natl. Acad. Sci. 104, 8918–23.

Williams, H.T.P., Lenton, T.M., 2007b. Artificial ecosystem selection for evolutionary optimisation, in: Banzhaf, W., Ziegler, J., Christaller, T., Dittrich, P., Kim, J.T. (Eds.), Advances in Artificial Life. ECAL. pp. 93–102.

Woodall, L.C., Jungblut, A.D., Hopkins, K., Id, A.H., Robinson, F., Gwinnett, C., Paterson, G.L.J., 2018. Deep-sea anthropogenic macrodebris harbours rich and diverse communities of bacteria and archaea. PLoS One 1–11.

Wright, R., 2019. Marine bacteria and the plastisphere. Biol. Sci. Rev. 31, 2–5.

Wright, R.J., Gibson, M.I., Christie-Oleza, J.A., 2019. Understanding microbial community dynamics to improve optimal microbiome selection. Microbiome 7, 1–14.

Wu, X., Wu, L., Liu, Y., Zhang, P., Li, Q., Zhou, J., Hess, N.J., Hazen, T.C., Yang, W., Chakraborty, R., 2018. Microbial interactions with dissolved organic matter drive carbon dynamics and community succession. Front. Microbiol. 9, 1–12.

Wu, Y.H., Yu, P.S., Zhou, Y.D., Xu, L., Wang, C.S., Wu, M., Oren, A., Xu, X.W., 2013. *Muricauda antarctica* sp. nov., a marine member of the *Flavobacteriaceae* isolated from Antarctic seawater. Int. J. Syst. Evol. Microbiol. 63, 3451–3456.

Xie, H.J., Shi, Y.J., Zhang, J., Cui, Y., Teng, S.X., Wang, S.G., Zhao, R., 2010. Degradation of

phthalate esters (PAEs) in soil and the effects of PAEs on soilmicrocosm activity. J. Chem. Technol. Biotechnol. 85, 1108–1116.

Xu, X.W., Wu, Y.H., Zhou, Z., Wang, C.S., Zhou, Y.G., Zhang, H. Bin, Wang, Y., Wu, M., 2007. *Halomonas saccharevitans* sp. nov., *Halomonas arcis* sp. nov. and *Halomonas subterranea* sp. nov., halophilic bacteria isolated from hypersaline environments of China. Int. J. Syst. Evol. Microbiol. 57, 1619–1624.

Yang, T., Id, L.R., Jia, Y., Fan, S., Wang, Junhuan, Wang, Jiayi, Nahurira, R., Wang, H., Yan, Y., 2018. Biodegradation of di-(2-ethylhexyl) phthalate by *Rhodococcus ruber* YC-YT1 in contaminated water and soil. Int. J. Environ. Res. Public Health 15, 1–20.

Yang, Y., Liu, G., Song, W., Ye, C., Lin, H., Li, Z., Liu, W., 2019. Plastics in the marine environment are reservoirs for antibiotic and metal resistance genes. Environ. Int. 123, 79–86.

Yang, Y., Yang, J., Jiang, L., 2016. Comment on "A bacterium that degrades and assimilates poly(ethylene terephthalate)." Science (80-.). 353, 759-b.

Yoshida, S., Hiraga, K., Takehana, T., Taniguchi, I., Yanaji, H., Maeda, Y., Toyohara, K., Miyamoto, K., Kimura, Y., Oda, K., 2016a. A bacterium that degrades and assimilates poly(ethyleneterephthalate). Science (80-.). 351, 1196–1199.

Yoshida, S., Hiraga, K., Takehana, T., Taniguchi, I., Yanaji, H., Maeda, Y., Toyohara, K., Miyamoto, K., Kimura, Y., Oda, K., 2016b. Response to Comment on " A bacterium that degrades and assimilates poly(ethylene terephthalate) ." Science (80-.). 353, 759–c.

Yu, G., Smith, D.K., Zhu, H., Guan, Y., Lam, T.T., 2017. GGTREE: an R package for visualization and annotation of phylogenetic trees with their covariates and other associated data. Methods Ecol. Evol. 8, 28–36.

Yuan, S.Y., Liu, C., Liao, C.S., Chang, B. V., 2002. Occurrence and microbial degradation of phthalate esters in Taiwan river sediments. Chemosphere 49, 1295–1299.

Yue, F., Lishuang, Z., Jing, W., Ying, Z., Bangce, Y.E., 2017. Biodegradation of phthalate esters by a newly isolated *Acinetobacter* sp . Strain LMB-5 and characteristics of its esterase. Pedosphere 27, 606–615.

Zadjelovic, V., Gibson, M.I., Dorador, C., Christie-oleza, J.A., 2019. Genome of *Alcanivorax* sp. 24: A hydrocarbon degrading bacterium isolated from marine plastic debris. Mar. Genomics 1–4.

Zettler, E.R., Mincer, T.J., Amaral-Zettler, L.A., 2013. Life in the "Plastisphere": Microbial communities on plastic marine debris. Environ. Sci. Technol. 47, 7137−7146.

Zhang, R., Lai, Q., Wang, W., Li, S., Shao, Z., 2013. *Thioclava dalianensis* sp. nov., isolated from surface seawater. Int. J. Syst. Evol. Microbiol. 63, 2981–2985.

Zhang, W.P., Wang, Y., Tian, R.M., Bougouffa, S., Yang, B., Cao, H.L., Zhang, G., Wong, Y.H., Xu, W., Batang, Z., Al-suwailem, A., Zhang, X.X., Qian, P., 2014. Species sorting during biofilm assembly by artificial substrates deployed in a cold seep system. Sci. Rep. 4, 1–7.

Zhang, X.M., Elkoun, S., Ajji, A., Huneault, M.A., 2004. Oriented structure and anisotropy properties of polymer blown films: HDPE, LLDPE and LDPE. Polymer (Guildf). 45, 217–229.

Zhang, Y.-M., Sun, Y., Wang, Z.-J., Zhang, J., 2013. Degradation of terephthalic acid by a newly isolated strain of Arthrobacter sp . 0574. S. Afr. J. Sci. 109, 1–4.

Zhang, Z., Claessen, D., Rozen, D.E., 2016. Understanding microbial divisions of labor. Front. Microbiol. 7, 1–8.

Zhao, B., Wang, H., Mao, X., Li, R., Zhang, Y., Tang, S., Li, W., 2012. *Halomonas xianhensis* sp. nov., a moderately halophilic bacterium isolated from a saline soil contaminated with crude oil. Int. J. Syst. Evol. Microbiol. 62, 173–178.

Zhou, J., Ning, D., 2017. Stochastic community assembly: Does it matter in microbial ecology? Microbiol. Mol. Biol. Rev. 81, 1–32.

Appendices

Appendix 1. Understanding microbial community dynamics to improve optimal microbiome selection.

Wright *et al. Microbiome* (2019) 7:85
https://doi.org/10.1186/s40168-019-0702-x

Microbiome

RESEARCH Open Access

Understanding microbial community dynamics to improve optimal microbiome selection

Robyn J. Wright[1*], Matthew I. Gibson[2,3] and Joseph A. Christie-Oleza[1*]

Abstract

Background: Artificial selection of microbial communities that perform better at a desired process has seduced scientists for over a decade, but the method has not been systematically optimised nor the mechanisms behind its success, or failure, determined. Microbial communities are highly dynamic and, hence, go through distinct and rapid stages of community succession, but the consequent effect this may have on artificially selected communities is unknown.

Results: Using chitin as a case study, we successfully selected for microbial communities with enhanced chitinase activities but found that continuous optimisation of incubation times between selective transfers was of utmost importance. The analysis of the community composition over the entire selection process revealed fundamental aspects in microbial ecology: when incubation times between transfers were optimal, the system was dominated by *Gammaproteobacteria* (i.e. main bearers of chitinase enzymes and drivers of chitin degradation), before being succeeded by cheating, cross-feeding and grazing organisms.

Conclusions: The selection of microbiomes to enhance a desired process is widely used, though the success of artificially selecting microbial communities appears to require optimal incubation times in order to avoid the loss of the desired trait as a consequence of an inevitable community succession. A comprehensive understanding of microbial community dynamics will improve the success of future community selection studies.

Keywords: Artificial microbiome selection, Microbial communities, Microbial ecology, Polymer degradation, Chitin degradation, Ecological succession, Microbial community dynamics

Background

Evolution is able to act upon multiple levels of biological organisation [1-5]. It had previously been contested that a whole microbial community may be used as a unit of selection artificial microbiome selection and that a community may become progressively better at a selective process over successive transfers [2, 6-8]. The artificial selection of a measurable and desirable trait is thought to outperform traditional enrichment experiments, as it bypasses community bottlenecks and reduces stochasticity [8]. Artificial selection has been shown to induce statistically significant responses, in both microcosm [2, 8] and computational ecosystems [3]. While microbial communities with desirable phenotypes have been achieved, the results of these experiments have been limited and the composition of these communities has not generally been determined. The underlying mechanisms and key players in this selection have therefore not been identified, nor have the growth parameters involved (e.g. incubation time) been systematically optimised [9].

Microbial communities are known to go through distinct stages of community succession, where they may see large enrichments of different groups of organisms [10-16]. During the colonisation and degradation of the abundant marine polymer, chitin, three phases of community succession were previously observed: (1) selection of colonising organisms, (2) selection of chitin degraders and (3) chitin degraders are overtaken by cheaters [10]. Cheaters, often called cross-feeders, are organisms that

* Correspondence: R.Wright.1@warwick.ac.uk; J.Christie-Oleza@warwick.ac.uk
[1]School of Life Sciences, University of Warwick, Coventry, UK
Full list of author information is available at the end of the article

are not metabolically capable of carrying out a particular process themselves, but are able to benefit from the public goods generated by others [17-19]. For example, in the environment, it has been shown that the number of organisms capable of taking up the by-products of chitin hydrolysis is far higher than the number that encodes for chitinases [17]. Furthermore, marine microorganisms 'leak' a large diversity of organic matter which in turn may be used by the rest of the community [19, 20] enhancing microbial interdependencies [21]. It has however been previously observed that if the abundance of cheaters becomes sufficiently high, then access to the resource may even be blocked completely [22], leading to a loss of community function.

The undulations between cooperation and competition drive niche-specialisation and higher-level community organisation [23]. The structure of the microbial community has been suggested to significantly alter the observed phenotype in artificial microbiome selection experiments [9]. Community structure may be altered through changes in species' composition or interactions between organisms, ultimately leading to changes in the community phenotype. Computational models have shown that community structure, with [24] or without genetic changes [9], can be responsible for differences between the phenotypes of a community subjected to a directed selection and one that is randomly selected. Hence, the understanding of microbial community ecology suggests that controlling microbial community dynamics is important for achieving a high-functioning microbial community.

In the present study, we aimed to determine the mechanisms behind artificial microbiome selection and early microbial community succession in order to optimise the selection of a process, i.e. chitin degradation. Chitin is one of the most abundant polymers on Earth (i.e. the most abundant polymer in marine ecosystems) constituting a key component in oceanic carbon and nitrogen cycles [25]. Many microorganisms are already known to degrade chitin, and the enzymes and pathways used to do so are well characterised [26]. We found that a microbiome could be artificially evolved to achieve higher chitinase activities, but there were certain methodological caveats to this selection process. We found that the incubation time between transfers needed to be continuously optimised in order to avoid community drift and decay. Microbial community composition was evaluated, and we confirmed that, if transfer times are not continuously optimised, efficient biodegrading communities are rapidly taken over by cheaters and predators with a subsequent loss of degrading activity.

Results

The experimental setup for artificially selecting microbial communities is depicted in Fig. 1 (see the Materials and methods section for more details).

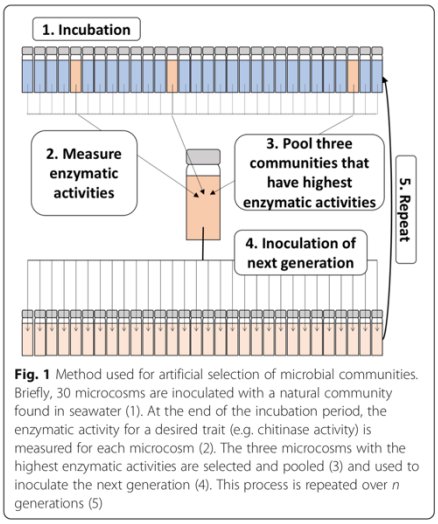

Fig. 1 Method used for artificial selection of microbial communities. Briefly, 30 microcosms are inoculated with a natural community found in seawater (1). At the end of the incubation period, the enzymatic activity for a desired trait (e.g. chitinase activity) is measured for each microcosm (2). The three microcosms with the highest enzymatic activities are selected and pooled (3) and used to inoculate the next generation (4). This process is repeated over *n* generations (5)

First artificial selection experiment: process optimisation

Our first artificial selection experiment highlighted the need to carry out each transfer when the desired trait (i.e. chitinase activity) was at its peak and not at a predefined incubation time, as done previously [2, 6, 8]. Initially, we set a standardised 9-day incubation time between transfers because this was the time it took for chitinase activity to peak in a preliminary enrichment experiment (data not shown). After 14 transfers, we did not observe a strong increase in chitinase activity (Fig. 2a and Additional file 1: Figure S1) and, intriguingly, in nine out of the 14 transfers, we observed a lower activity in the positive selection than in the randomly selected control (Fig. 2a), suggesting that a random selection of microcosms is more effective in enhancing chitinase activity than actively selecting for the best communities. To further investigate the reasons behind this low efficiency, we took regular enzymatic activity measurements in the incubation period between transfers 14 and 15 (Fig. 2b). We found that chitinase activity was peaking much earlier within the incubation, i.e. at day 4, and by the end of 9 days, the chitinase activity had dropped below the activities registered for the random selection experiment (Fig. 2b). Attending to this result, after transfer 15, we set up an additional experiment, run in parallel, where the incubation time between transfers was shortened to 4 days. Shortening the incubation time led to a selection of higher chitinase activities at transfers 16 and 17, but the progressive increase in activity had stalled by transfers 18 and 19

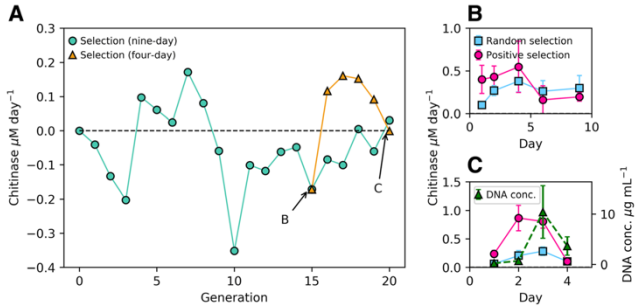

Fig. 2 Chitinase activity in artificial selection experiment 1. **a** Enzymatic activity measured over 20 generations. Each point represents the mean of the positive selection communities (n = 30) from which the mean of the randomly selected controls (n = 30) was subtracted. The black dotted line (zero) represents where chitinase activity of the positive selection is equal to that of the random selection. **b** Chitinase activity measured within the incubation period of generation 15 of the 9-day incubation. **c** Chitinase activity and DNA concentration of the positive selection measured within the incubation period of generation 20 of the 4-day incubation. Each point in panels **b** and **c** represents absolute chitinase activity measured in the positive (red) and random selection (blue). Arrows in panel **a** indicate the generations in which the regular monitoring of chitinase activity was performed, i.e. shown in panels **b** and **c**

(Fig. 2a). Chitinase activity was again measured every day within the incubation period before the final transfer, 20, and we found that the enzymatic activity was almost nine times higher on day 2 than day 4 (Fig. 2c), indicating that the optimal incubation time had again been reduced. Interestingly, using DNA as a proxy for biomass (see Additional file 1: Supplementary information and Figure S2 for more details), we observed low concentrations on day 2, i.e. when chitinase activity was at its peak, indicating a very high enzymatic activity amongst the existing microbial population (Fig. 2c). Although the chitinase activity was still high on day 3, there was also a considerable increase in biomass, suggesting a relatively less-active chitinolytic community at this time point. Both chitinase activity and biomass had dropped at day 4, presumably as a consequence of grazing (as discussed below).

While the 9-day incubation experiment gave an overall negative trend, shortening the incubation times to the chitinase maxima drastically increased the benefits of artificial community selection, i.e. initially to 4 days (generation 15, Fig. 2b) and later to 2 days (generation 20, Fig. 2c). This suggests that the selection of an efficient chitin-degrading community shortens the time required not only to reach maximum chitinase activity, but also to enter decay due to community succession.

Microbial community succession

We carried out MiSeq amplicon sequencing of the 16S and 18S rRNA genes to characterise the microbial community succession that occurred within the first selection experiment and, by this way, gain insight into the strong variability in chitinase activity observed over time. We sequenced the communities that were used as the inoculum for each of the 20 transfers, both 9- and 4-day-long experiments, as well as the community obtained from the daily monitoring of the incubation period for transfer 20. This data was processed using both Mothur [27] and DADA2 workflows [28, 29], obtaining similar results (Additional file 1: Figures S3 and S4). DADA2 results are presented here as this workflow retains greater sequence information, better identifies sequencing errors and gives higher taxonomic resolution [30]. Unique taxa are therefore amplicon sequence variants (ASVs) rather than operational taxonomic units (OTUs).

Community succession over the 4-day incubation period within transfer 20

The daily microbial community analysis over 4 days at transfer 20 showed a progressive increase in prokaryotic diversity (from 0.83 to 0.93, according to Simpsonâ€™s index of diversity) whereas a strong decrease in diversity was observed amongst the eukaryotic community (from 0.93 to 0.38; Fig. 3a). SIMPER analyses were carried out to identify those 16S and 18S rRNA gene ASVs that were contributing most to the differences over the four successive days observed in Fig. 3b. The top 5 ASVs in these analyses were responsible for 50% and 60% of the temporal variation for the 16S and 18S rRNA genes, respectively (Fig. 3c).

For the 16S rRNA gene, the most important ASVs were ASV3 (*Thalassotalea*, contributing to 16% of the community variation between the four days, p = 0.025), ASV4 (Cellvibrionaceae, 15% variation, p = 0.033), ASV5 (*Crocinitomix*, 8% variation, p = 0.033), ASV7 (*Terasakiella*, 6%

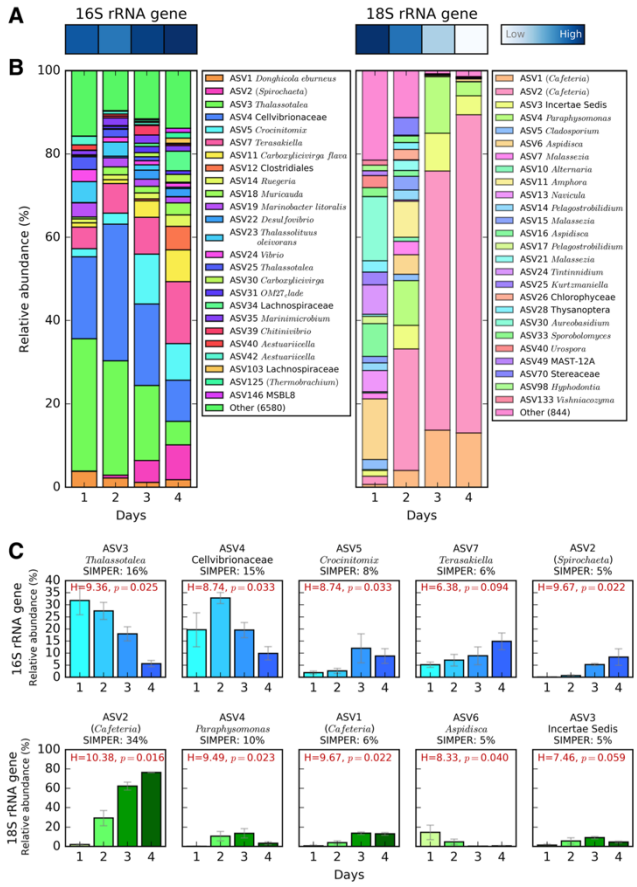

Fig. 3 Daily microbial community analysis over the 4-day incubation period within generation 20. The analysis was performed on the three communities that showed highest chitinase activity by the end of the 4 days and which would have been used to inoculate the next generation. **a** Simpson's index of diversity of the 16S (left) and 18S rRNA gene (right) amplicon analysis. The scale ranges between 0.38 (low) and 0.93 (high). **b** Community relative abundance over the 4-day incubation period. Only ASVs with abundance above 1% in at least one time point are shown. The abundance for each ASV is a mean value from the three communities. ASVs were classified to genus level using the SILVA database (v132). Names in brackets were not identifiable with the standard analysis pipeline and were identified through a BLAST search of the NCBI database. **c** Five 16S and 18S rRNA gene ASVs that contributed the most to the community variations over time according to a SIMPER analysis. The percentage of variation to which each ASV contributes is indicated. Error bars represent the standard deviations of the three communities used to inoculate the next generation

variation, p = 0.094) and ASV2 (*Spirochaeta*, 5% variation, p = 0.022) (Fig. 3c). ASVs 3 and 4 (both *Gammaproteobacteria*) represented over 50% of the prokaryotic community abundance on day 2, when chitinase activity was highest, and their abundances followed a similar pattern to the chitinase activity over 4 days (Fig. 2c), suggesting that these ASVs may be the main drivers of chitin hydrolysis. On the other hand, ASVs 7 (*Alphaproteobacteria*) and 2

(*Spirochaetes*) both showed a progressive increase over time (i.e. from a combined relative abundance of 5% on day 1 to 23% on day 4; Fig. 3c), suggesting that these ASVs could be cross-feeding organisms that benefit from the primary degradation of chitin. Interestingly, the overall 16S rRNA gene analysis also showed a strong succession over time at higher taxonomic levels (Fig. 4). While *Gammaproteobacteria* pioneered and dominated the initial colonisation and growth, presumably, via the degradation of chitin (i.e. with 73% relative abundance during the first 2 days), all other taxonomic groups became more abundant towards the end of the incubation period (e.g. *Clostridia*, *Bacteroidia* and *Alphaproteobacteria* increased from an initial relative abundance of 0.1, 2.8 and 12% on day 1 to 13.5, 22 and 21% on day 4, respectively, Fig. 4). Microbial isolates confirmed *Gammaproteobacteria* as the main contributors of chitin-biodegradation (as discussed below).

The SIMPER analysis of the 18S rRNA gene highlighted ASV2 (*Cafeteria* sp., contributing to

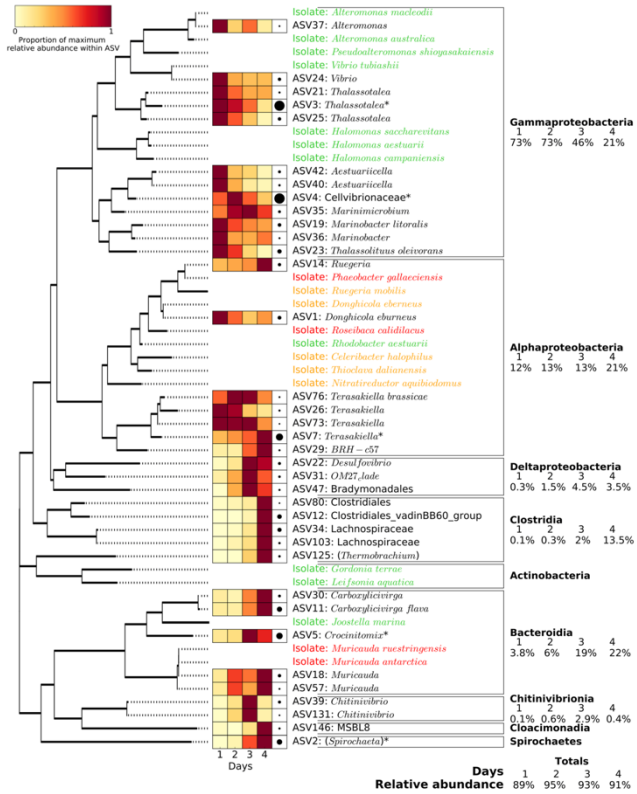

Fig. 4 Phylogenetic analysis and relative abundance of the major 16S rRNA gene ASVs (i.e. with relative abundance above 0.5% in at least one of the 4 days) and bacterial isolates obtained at the end of the artificial selection experiment. Phylogenetic grouping is represented by a mid-point-rooted maximum likelihood phylogenetic tree. The 36 ASVs represented in the figure (out of the 6605 total ASVs detected) accounted for 92% of all 16S rRNA gene relative abundance. The heatmap represents the relative abundance of each ASV over the 4 days, with darker red showing the day at which the ASV showed maximum abundance. Black circles on the right of the heatmap represent the maximum relative abundance for that ASV amongst the entire community. The 20 isolates are coloured depending on their ability to grow on chitin and the monomer, GlcNAc (green), the GlcNAc only (orange) or neither (red)

34% of the community variation between 4 days, p = 0.016), ASV4 (*Paraphysomonas*, 10% variation, p = 0.023), ASV1 (*Cafeteria* sp., 6% variation, p = 0.392), ASV6 (*Apsidica*, 5% variation, p = 0.040) and ASV3 (Incertae Sedis, 5% variation, p = 0.059) as the five main ASVs contributing to 60% of the community variation over 4 days (Fig. 3c). ASV2, which was 96% similar to the bactivorous marine flagellate *Cafeteria* sp., was by far the most striking Eukaryotic organism, showing an increase in relative abundance from 2% on day 1 up to over 76% on day 4 (Fig. 3b, c). As observed in prokaryotes, eukaryotic phylogenetic groups also showed a large variation between the beginning and the end of the incubation period, mainly due to the increase of *Bicosoecophyceae* over time (i.e. from 2.6 to 89% relative abundance driven by both ASV1 and ASV2, Additional file 1: Figure S5).

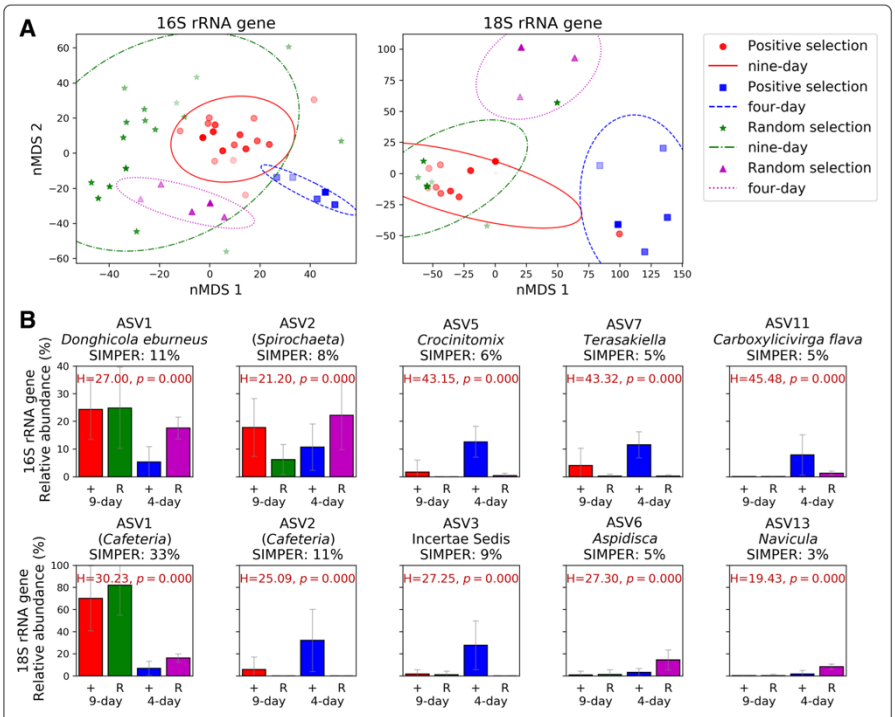

Fig. 5 Microbial community variation over the entire artificial selection experiment. **a** nMDS plot showing Bray-Curtis distance of 16S (left) and 18S rRNA gene communities (right). Distance between the community composition obtained from 9-day (red circles) and 4-day incubations (blue squares) of the positive selection, and 9-day (green stars) and 4-day incubations (purple triangles) of the random controls are shown. The marker colour intensity correlates to the generation number, where progressive darker colours represent later generations. Each point represents the mean of the three communities selected from one generation used to inoculate the following one, for the positive selection. Random communities were pooled before sequencing. Ellipses show the mean plus the standard deviation of each group of samples. Stress values are 0.175 for the 16S rRNA gene and 0.063 for the 18S rRNA gene. **b** Five 16S (top panel) and 18S rRNA gene ASVs (bottom panel) that contributed the most towards community variations between the 9-day (generations 0â€“20) and 4-day (generations 16â€“20) positive (+) and random (R) selections according to SIMPER analyses. The percentage of variation to which each ASV contributes is indicated. ASVs were classified to the species level with the standard analysis pipeline using the SILVA database (v132) where possible. Names in brackets were not identifiable and were identified through a BLAST search of the NCBI database. Relative abundances and error bars shown are the mean and standard deviations of all generations within that treatment

Community succession over the entire artificial selection experiment

We analysed the 16S and 18S rRNA gene community composition (Fig. 5, Additional file 1: Figure S6) at each transfer in order to determine the effect that positive or random selection of communities had across the 20 transfers, both for the 9-day incubation experiment (i.e. transfers 0 to 20) and shortened 4-day incubation experiment (i.e. transfers 16 to 20). Most interestingly, the overall community variability across all transfers (16S and 18S rRNA gene nMDS analysis, Fig. 5a) showed that only the positive selection of the shortened 4-day incubations differentiated the community from the random selection, which was confirmed by a PerMANOVA test using Bray-Curtis distance (16S rRNA gene $p = 0.001$, 18S rRNA gene $p = 0.002$, Additional file 1: Table S2), while the 9-day selection mostly clustered with the random control communities. This is a clear explanation as to why the 9-day incubation time was not allowing a progressive selection of a community with better chitinase activities than those obtained randomly and, only when the time was shortened, did we observe an effect of the positive selection over the random selection.

SIMPER analyses were carried out to determine the ASVs that most strongly contributed to the differences between groups (i.e. positive versus random selections and 9-day versus 4-day incubation times, Fig. 5b). For the 16S rRNA gene, the top 5 ASVs identified by the SIMPER analysis contributed to 35% of the community variation, while for the 18S rRNA gene, they accounted for 61% (Fig. 5b). The 16S rRNA gene ASVs 5, 7 and 11 (*Crocinitomix*, *Terasakiella* and *Carboxylicivirga flava*, respectively) presented a much higher abundance in the 4-day-positive selection than in any other selection (13%, 11% and 8%, respectively), suggesting that these species were the major contributors to the differentiation of these communities, as seen in Fig. 5a. As observed above for the 4-day incubation analysis, *Cafeteria* sp. (18S rRNA gene ASV1 and ASV2, both 96% similar) was again the most conspicuous eukaryotic organism. ASV2 was more abundant in the positive 4-day selection (32% of the relative abundance), while ASV1 was highest in the three other selections (70% and 82% in the positive and random 9-day selection, respectively, and 16% in the random 4-day selection; Fig. 5b).

Chitinase gene copies in artificially assembled metagenomes

Artificially assembled metagenomes, generated by PICRUSt [31] from the 16S rRNA gene amplicon sequences, were used to search for enzymes involved in chitin degradation: KEGG orthologs K01183 for chitinase, K01207 and K12373 for chitobiosidase, K01452 for chitin deacetylase and K00884, K01443, K18676 and K02564 for the conversion of GlcNAc to fructose-6 phosphate (Additional file 1: Figure S7 and Table S3) [32-34]. As expected from the measured chitinase activities, the shortened 4-day incubation experiment showed over 30 times more chitinase (K01183) gene copies than the 9-day incubation experiment (i.e. an average of 0.66 copies per bacterium were observed in the 4-day incubation experiment while only 0.025 copies per bacterium were observed over the same transfers in the 9-day experiment). Also, from the daily analysis of transfer 20, the chitinase activity was positively correlated with the normalised chitinase gene copy number ($r^2 = 0.57$), with a peak in chitinase activity *and* chitinase gene copies on day 2 (i.e. over one chitinase gene copy per bacterium). The most striking result from this analysis was the strong bias of taxonomic groups that contributed to the chitinase and chitin deacetylase genes; chitinase genes were mainly detected in *Gammaproteobacteria* and some *Bacteroidia*, whereas the chitin deacetylase genes were almost exclusively present in *Alphaproteobacteria*. It is worth highlighting that the chitosanase gene (K01233), the enzyme required to hydrolyse the product from chitin deacetylation, chitosan, was not detected in any of the artificial metagenomes. Chitobiosidases (K01207 and K12373) and enzymes involved in the conversion of GlcNAc to fructose-6 phosphate (K00884, K01443, K18676 and K02564) were more widespread. Nevertheless, this data needs to be taken with caution as these were not real metagenomes.

Isolation and identification of chitin degraders

Bacterial isolates were obtained from the end of the artificial selection experiments to confirm the ability of the identified groups to degrade chitin. From the 50 isolates obtained, 20 were unique according to their 16S rRNA gene sequences. From these, 18 showed at least 98% similarity with one or more of the MiSeq ASVs (Additional file 1: Table S4) although, unfortunately, none belonged to the most abundant ASVs detected during the community analysis. The ability for chitin and GlcNAc degradation by each one of the isolates was assessed. We found that 16 of these isolates could grow using GlcNAc as the sole carbon source, but only 11 of these strains could grow on chitin (Fig. 4). The four remaining bacteria from the 20 isolated could not grow using chitin or GlcNAc. Most interestingly, all isolates from the class *Gammaproteobacteria* ($n = 7$) were capable of chitin degradation whereas only a smaller subset of isolates had this phenotype in other abundant taxonomic groups, such as *Bacteroidia* (1 out of 3) or *Alphaproteobacteria* (1 out of 8, Fig. 4).

We confirmed that both a cheater (i.e. isolate able to grow on GlcNAc but not chitin; *Donghicola eburneus*, *Alphaproteobacteria*) and a cross-feeder (i.e. isolate not capable of growth with GlcNAc or chitin; *Phaeobacter*

gallaeciensis, *Alphaproteobacteria*) were only able to grow with chitin in the presence of a chitin-degrading isolate (*Pseudoalteromonas shioyasakaiensis*, *Gammaproteobacteria*; Additional file 1: Figure S8). As expected, while no growth was observed in the absence of the chitin degrader, both the cheater and the cross-feeder grew over two orders of magnitude more when co-cultured with the degrader (Additional file 1: Figure S8).

Second artificial selection experiment: implementing an improved selection process

A second selection experiment showed an extremely rapid boost in chitinase activity, demonstrating that implementing an optimised incubation time between transfers largely enhances the selection of a desired trait. For this experiment, chitinase activity was measured daily until a peak in chitinase activity was observed. The communities with the highest chitinase activity on this day were used to transfer to the next set of microcosms. By implementing this improved technique, we measured chitinase activity of almost 90 μM day^{-1} in only 7 transfers (Fig. 6 and Additional file 1: Figure S9), when the maximum activity achieved in the first experiment was 0.9 μM day^{-1} (Fig. 2c). While the different culture conditions between both experiments may have exacerbated the differences (i.e. the first artificial selection was carried out in 22 mL vials, with intermittent shaking and incubated at 23 °C, and the second artificial selection was carried out in 2% mL 96-well plates, with constant shaking and incubated at 30 °C), the fact that the randomly selected control from the second artificial selection experiment reached similar chitinase activity levels to those observed in the first experiment (i.e. ~ 0.08 μM day^{-1}, Additional file 1: Figure S9) suggests the culture conditions were not the underlying reason behind the strong increase in chitinase activity observed during the second experiment where the conditions were optimised.

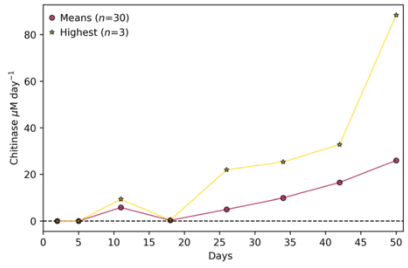

Fig. 6 Chitinase activity of artificial selection experiment 2. The graph shows the mean chitinase activity of the positive selection, from which the mean of the random selection was subtracted. The means of all communities within the generation (n = 30; red) and those of only the three communities that were pooled for the inoculum of the next generation (yellow) are shown

Discussion

Artificial selection of microbial communities is, in principle, a powerful and attractive technique which has surprisingly been used in only a limited number of studies to date [2, 6, 8], possibly due to the lack of success as a consequence of poor process optimisation. Here, using chitin degradation as a case study and a detailed analysis of the community succession, we show that artificial selection of microbial communities can be greatly improved by controlling the incubation times between transfers. We believe that the rapid succession of microbial community structure means transfers need to be done at the peak of the selected phenotypic activity (e.g. chitinase activity) or these get swiftly replaced by less efficient communities of cross-feeding microorganisms (i.e. â€˜cheatersâ€™ and grazers). Previous studies that have artificially selected microbial communities for a particular phenotype did not report optimisation of the incubation time between transfers [2, 6, 8] which, in our hands, would have resulted in a negative selection (Fig. 2). In agreement with our results, Penn and Harvey [9] suggested that the observed phenotype in artificial ecosystem selection experiments could be significantly affected by interactions between different species and therefore microbial community structure.

A comprehensive understanding of microbial ecology helps to explain the importance of the timing during transfers. Datta et al. [10] observed three distinct stages of community structure during the colonisation of chitin particles: (a) attachment, (b) selection and (c) succession. Each phase was characterised by having relatively higher abundances of organisms that were (a) good at attaching to chitin particles, (b) good at degrading chitin particles and (c) not able to degrade chitin, but able to benefit from others that could, i.e. cheaters and cross-feeders [17, 18, 22, 35]. During our first experiment, as communities became better and faster at degrading chitin, we were measuring the chitinase activity when the communities were in the succession rather than in the selection stage and, by that point, the active chitinolytic community had decayed and was dominated by a cross-feeding community (Figs. 3 and 4). Hence, it was only when selecting at phenotypic time optima when chitinase activity improved and the overall community differentiated from the random control communities (Figs. 5 and 6). Due to the stochasticity of complex microbial communities, this time optima is difficult to predict and continuous phenotypic monitoring is required. It is also interesting to note the selection of the grazer *Cafeteria* sp. (90% of the

eukaryotic community), a genus of bactivorous marine flagellates that are commonly associated with marine detritus [36]. The predator-prey dynamics postulated by Lotka, Volterra's equations would also support the need to shorten transfer times to favour the prey's growth, i.e. chitinolytic bacteria [37, 38]. We note, however, that there may be a lower limit to optimal transfer times (possibly around 2, 3 days, Fig. 2c) as sufficient time has to be given for slower growing marine taxa [39] to (i) develop a biofilm [40], (ii) initiate the hydrolysis of the polymer to access the sugars and (iii) allow the generation of sufficient biomass to overcome the dilution between transfers.

Interestingly, a strong successional pattern was observed at a higher taxonomic level. While *Gammaproteobacteria* dominated during the initial stages when chitinase activity was at its peak (accounting for over 70% of the prokaryotic community), other groups increased in abundance during the later stages (i.e. *Alphaproteobacteria*, *Bacteroidia* and *Clostridia*), similarly to the pattern previously observed by Datta et al. [10] and Enke et al. [22, 35]. The fact that *Gammaproteobacteria* are major contributors to chitin degradation is not new [41-46]. All *Gammaproteobacteria* isolates obtained from the end of the experiments were able to grow using chitin as the only source of carbon and energy (Fig. 4) confirming that this class is likely responsible for most of the chitinase activity observed. On the other hand, *Alphaproteobacteria*, the numerically dominant class of heterotrophic bacteria in surface oceans [47, 48], follow a cross-feeding and/or cheating life-strategy as five out of eight *Alphaproteobacterial* isolates could only use *N*-acetyl-D-glucosamine (GlcNAc) and only one could use chitin (Additional file 1: Table S4). The dependence of cheaters and cross-feeders on the presence of a chitin-degrader was confirmed with co-cultures (Additional file 1: Figure S8) and agreed with the results generated by others [22].

The PICRUSt metagenome analysis (Additional file 1: Figure S7) further confirmed that almost all chitinase gene copies were encoded by *Gammaproteobacteria* (i.e. 90%; almost one gene copy encoded per bacterium) and, to a lesser extent, by some *Bacteroidia*. Chitin is made up of molecules of GlcNAc linked by (1,4)-Î²-glycosidic bonds, and it has previously been found that initial degradation of chitin takes place predominantly by (i) chitinases which depolymerise the (1,4)-Î²-glycosidic bonds either at the ends or in the middle of chains, or (ii) chitobiosidase enzymes which also hydrolyse (1,4)-Î²-glycosidic bonds but only at the ends of chitin chains. Genes for the intracellular enzymes involved in GlcNAc utilisation (i.e. the transformation of GlcNAc to fructose-6-phosphate) were much more widespread amongst different taxonomic groups, highlighting the broader distribution of cross-feeding or cheating organisms which can benefit from the extracellular depolymerisation of chitin which generates freely available GlcNAc to the community. Alternative degradation of chitin may also occur by deacetylation and deamination of the GlcNAc amino sugar, transforming chitin into chitosan and cellulose, respectively, after which they can be depolymerised by a range of other enzymes (e.g. chitosanases or cellulases) [26, 49, 50]. While *Alphaproteobacteria* did not contribute to chitinase enzymes, they *did* potentially encode for most of the chitin deacetylases in the system, although no chitosanases were detected.

Chitinolytic organisms have previously been found to make up between 0.1 and almost 6% of prokaryotic organisms in aquatic ecosystems [17, 51], while over a third of the organisms in these habitats can utilise only the products of chitin hydrolysis (i.e. GlcNAc) [17, 52-54]. With *Gammaproteobacteria* being primarily responsible for the degradation of chitin here, the success of the artificial selection for an enhanced chitinolytic community was possibly achieved by the selective enrichment of this group between the beginning (5% of the prokaryotic community, within the expected range of *Gammaproteobacteria,* found within natural environments) [17, 51] and end of the experiment (75% of the community).

Finally, chitin degradation is a task that single microorganisms can perform efficiently, but other more laborious phenotypic traits are rarely carried out entirely by a single microorganism in nature. It is now well documented that a distribution of labour is favoured in natural microbial communities [55-59]. The detrimental effects of community dynamics and drift described here could be overcome by synthetically assembled microbial communities, preventing the system from moving away from the high-performing desired community. Nevertheless, this still requires a comprehensive understanding of the community structure and the necessity to select and isolate the microbes of interest.

Conclusions

Here, we have proven the validity of artificially selecting a natural microbial community to better degrade chitin, but have highlighted the caveats for achieving this goal, which require a better understanding of the ecology of the system. We found that continuous optimisation of incubation times is essential in order to successfully implement this process, as optimal communities rapidly decay due to their replacement by cheaters and cross-feeders, as well as the increase of potential predators such as grazers and, although not tested here, viruses. Hence, future artificial selection experiments should adjust transfer incubation times to activity maxima to successfully evolve enhanced community phenotypes and, eventually, allow the enrichment and isolation of microbes of interest.

Materials and methods

Microbial inoculum

The microbial community used as an inoculum was obtained from bulk marine debris collected during boat tows from both Plymouth Sound (Devon, UK; June 2016) and Portaferry (Northern Ireland, UK; August 2016).

Chitinase activity measurements

Chitinase activity was measured as the liberation of the fluorescent molecule 4-methylumbelliferyl (MUF) from three chitinase substrates (MUF-*N*-acetyl-β-D-glucosaminide, MUF-β-D-*N*,*N*'-diacetylchitobioside and MUF-β-D-*N*,*N*',*N*''-triacetylchitotrioside; Sigma Aldrich, UK), following the previously described method [42, 60, 61] (Additional file 1: Supplementary information). Standards curves were obtained using chitinase from *Streptomyces griseus* (Sigma Aldrich, UK) dissolved in sterile phosphate-buffered saline solution (pH 7.4; 0.137 M) with a highest concentration of 0.1 UmL^{-1} (activity equivalent to 144 μM day^{-1}). Samples were diluted prior to measurement if they were expected to be above this range.

Artificial selection

The process for artificial selection is depicted in Fig. 1. Briefly, 30 individual microcosms per treatment and generation were incubated in the dark under the conditions described below. At the end of each incubation period, the three microcosms with the highest chitinase activities (or three random microcosms in the case of the control) were pooled and used as the inoculum for the next generation of microcosms (n = 30). This was repeated across multiple transfers. Two artificial selection experiments were performed, the first to optimise the process and the second to implement optimal conditions and achieve a high-performing chitinolytic microbial community.

First artificial selection experiment

Incubations were carried out at 23 °C in 22 mL glass vials (Sigma Aldrich), each containing 20 mL of autoclaved seawater (collected from outside Plymouth Sound, Devon, UK; June 2016) supplemented with NaH_2PO_4, F/2 trace metals [62] (Additional file 1: Supplementary information) and 100 mg of chitin powder (from shrimp shells; Sigma Aldrich) as the sole source of carbon and nitrogen. Generation 0 was started with 200 μL of microbial inoculum. The efficiency of the selection process was assessed by comparing a 'positive selection' (where the three communities with highest activity were pooled and 200 μL was used to inoculate each one of the 30 microcosms of the next generation) against a 'random selection' (where three communities were chosen at random, using a random number generator within the Python module Random, to inoculate the following generation) to give a control against uncontrollable environmental variation [63]. Each treatment was repeated across 20 generations with incubation times of 9 days. In parallel, treatments where incubation times were shortened to 4 days were set up after generation 15. Samples were taken from each community and stored in 20% glycerol at , 80 °C for further microbial isolation, and pellets from 1.5 ml of culture were collected by centrifugation (14,000 x *g* for 5 min) and stored at ,-20 °C for final DNA extraction and community analysis.

Second artificial selection experiment

A second selection experiment was set up implementing optimal transfer incubation times. Microcosms were incubated in 2 mL 96-well plates (ABgene™, ThermoFisher Scientific) covered by Corning® Breathable Sealing Tapes to stop evaporation and contamination while allowing gas exchange. Each well contained 1.9 mL of a custom mineral media containing $MgSO_4$, $CaCl_2$, KH_2PO_4, K_2HPO_4, 0.52 M NaCl and artificial seawater trace metals (Additional file 1: Supplementary information), supplemented with 10 mg of chitin powder. The microbial inoculum was 100 μL (i.e. initial inoculum and transfer between generations). Chitinase activity was measured daily. Transfer between generations was carried out just after the peak of chitinase activity had occurred, calculated as the mean chitinase activity across the 30 microcosms of the positive selection treatment. Plates were incubated in the dark at 30°C with constant shaking (150rpm). Eight days was the maximum incubation time allowed to reach maximum chitinase activity due to volume constraints. Pellets from 1.5 mL were collected by centrifugation (14,000 x *g* for 5 min) and stored at -20°C for final DNA extraction

DNA extraction and amplicon sequencing

DNA was extracted using the DNeasy Plant Mini Kit (Qiagen) protocol, with modifications as follows (adapted from [64]): 300 μL 1x TAE buffer was used to resuspend cell pellets and these were added to ~ 0.4 g of sterile 0.1 mm BioSpec Zirconia/Silica Beads in 2 mL screw cap microtubes (VWR international). Bead beating was carried out for 2 x 45 s and 1 x 30 s at 30 Hz using a Qiagen Tissue Lyser. Cell lysates were then processed in accordance with the manufacturer's instructions, with an extra centrifugation step to ensure all liquid was removed (1 min, 13,000 x *g*) directly before elution of samples. A Qubit® HS DNA kit (Life Technologies Corporation) was used for DNA quantification after which they were diluted to equalise the concentrations across samples. A Q5® Hot Start High-Fidelity 2X Master Mix (New England Biolabs® Inc.) was used to amplify the 16S rRNA gene v4-5 regions using primers 515F-Y and 926R [65], and the 18S rRNA gene v8, 9 regions using primers V8F and 1510R [66] (Additional file 1: Supplementary information). PCR products were purified using AmpliClean

Magnetic Beads (NimaGen, The Netherlands). Index PCR was carried out using Illumina Nextera Index Kit v2 adapters. Samples were normalised using a SequelPrep™ Normalisation Plate Kit (ThermoFisher Scientific). Samples were pooled and 2 x 300 bp paired-end sequencing was carried out using the MiSeq system with v3 reagent kit. Negative DNA extraction controls and library preparation negative controls as well as chitin-only positive controls were processed and sequenced alongside samples.

Microbial community structure determination

Two different workflows were used to analyse the sequencing data: DADA2 [28, 29] and Mothur [27]. DADA2 delivers better taxonomic resolution than other methods (e.g. Mothur) as it retains unique sequences and calculates sequencing error rates rather than clustering to 97% similarity [30]. The resultant taxonomic units are referred to as amplicon sequence variants (ASVs) rather than operational taxonomic units (OTUs from Mothur). For the DADA2 analysis, sequencing data were processed following the DADA2 (version 1.8.0) pipeline [28]. Briefly, the data were filtered, i.e. adapter, barcode and primer clipped, and the ends of sequences with high numbers of errors were trimmed. The amplicons were denoised based on a model of the sequencing errors and paired-end sequences were merged. Only sequences between 368, 379 for the 16S rRNA gene and 300, 340 for the 18S rRNA gene were kept and chimaeras were removed. The resulting ASVs were classified using the SILVA reference database (v132) [67]. For the Mothur analysis [27], sequencing data were filtered, i.e. adapter, barcode and primer clipped, sequence length permitted was 450 bp for the 16S rRNA gene and 400 bp for the 18S rRNA gene, maximum number of ambiguous bases per sequence = 4 and maximum number of homopolymers per sequence = 8. Taxonomy assignment was performed using the SILVA reference database (Wang classification, v128) [67] and operational taxonomic units (OTUs) set at 97% similarity. For both processing workflows, chloroplasts, mitochondria and Mammalia were removed from the 16S rRNA gene and 18S rRNA gene datasets; eukaryotes were removed from the 16S rRNA gene dataset; and bacteria and archaea were removed from the 18S rRNA gene dataset. The average number of reads per sample was approximately 12,500 for the 16S rRNA gene and 20,000 (Mothur) or 34,000 (DADA2) for the 18S rRNA gene. Samples with less than 1000 total reads were excluded from downstream analyses. Although most analyses were carried out using relative abundance, each sample was subsampled at random to normalise the number of reads per sample, and the resulting average coverage was 92% (Mothur) or 94% (DADA2) for the 16S rRNA gene and 99% (Mothur and DADA2) for the 18S rRNA gene.

Microbial isolation and characterisation

Microbes were isolated from the final transfer of positive selection experiments by plating serial dilutions on Marine Broth 2216 (BD Difco™) and mineral medium plates (i.e. custom medium, Additional file 1: Supplementary information) supplemented with 0.1% *N*-acetyl-D-glucosamine (GlcNAc) and 1.5% agar. Colonies were re-streaked on fresh agar plates until pure isolates were obtained. The identification of isolates was carried out by sequencing the partial 16S rRNA gene (GATC BioTech, Germany) using primers 27F and 1492R [68] (Additional file 1: Supplementary information).

Isolates were grown in custom mineral medium supplemented with either 0.1% chitin or 0.1% GlcNAc (*w*/*v*), as sources of carbon and nitrogen, to test for chitinase activity and chitin assimilation, respectively. Growth was monitored over 14 days by measuring (i) chitinase activity (as described above), (ii) optical density at 600 nm and (iii) protein content (following the manufacturer's instructions; QuantiPro™ BCA Assay Kit, Sigma Aldrich, UK). Isolates were also tested on custom mineral medium agar plates made with the addition of 0.1% chitin and 0.8% agarose. Plates were incubated at 30°C for 21 days to allow the formation of halos indicative of chitinase activity.

Co-cultures were performed using isolates *Pseudoalteromonas shioyasakaiensis* (chitin degrader), *Donghicola eburneus* (cheater, capable of growth on GlcNAc but not chitin) and *Phaeobacter gallaeciensis* (cross-feeder, not capable of growth on either chitin or GlcNAc). Combinations of these strains were grown in 25 cm^2 tissue culture flasks with 25 mL custom mineral media (Additional file 1: Table S1) supplemented with 0.1% (*w*/*v*) of chitin. Cultures were incubated at 30 °C with shaking at 200 rpm for 3 days. Pellets from 1.5 ml of culture on days 0 and 3 were collected by centrifugation (14,000 x *g* for 5 min) and stored at , -20°C for DNA extraction, as above. Specific primers were designed for each of the isolates (see Additional file 1: Supplementary methods and materials), and qPCR was performed (Applied Biosystems 7500 Fast Real-Time PCR system) using 1 μL template DNA following the manufacturer's instructions for the GoTaq® qPCR Master Mix (Promega). Final primer concentrations were 0.5, 0.9 and 0.9 M, for the degrader, cheater and cross-feeder, respectively. Results were normalised to standard curves that used DNA extracted from pure cultures.

Statistical analyses

All analyses of chitinase activity and most MiSeq data analyses were carried out using custom Python scripts (Python versions 2.7.10 and 3.6.6) using the modules colorsys, csv, heapq, matplotlib, numpy, os, pandas, random, scipy, scikit-bio, sklearn [69] and statsmodels. SIMPER analyses and plotting of phylogenetic trees were

performed in R (R version 3.3.3) [70] using the following packages: ape [71], dplyr, ggplot2, gplots, ggtree [72], lme4, phangorn [73], plotly, tidyr, vegan [74] and phyloseq [75]. The top 5 ASVs identified in each SIMPER analyses were classified to their closest relative using a BLAST search of the GenBank database. Hypothetical community functions were obtained using PICRUSt in QIIME1 [31, 76] by mapping ASVs to the Greengenes database [77] (v13.5) at the default 97% similarity threshold. The PICRUSt analysis includes almost 35% of all ASVs, accounting for a mean relative abundance of 53%, 68% and 81% for the positive selection 9-day, 4-day and daily analyses, respectively. The Nearest Sequenced Taxon Index (NSTI) obtained for each of the taxonomic groups is available in Additional file 1: Table S3 (a full summary for each sample can be found on GitHub https://github.com/R-Wright-1/ChitinActivity). The three groups with the highest relative abundance, *Gammaproteobacteria*, *Alphaproteobacteria* and *Bacteroidia* (i.e. 29.3%, 26.4% and 16.6%, respectively) showed NSTI values of 0.07, 0.09 and 0.18, respectively. Sequences used for phylogenetic trees were aligned using the SILVA Incremental Alignment (www.arb-silva.de) [78] and midpoint rooted maximum likelihood trees were constructed using QIIME1 [76]. All scripts can be found at https://github.com/R-Wright-1/ChitinActivity. All sequences have been deposited in the NCBI Short Read Archive (SRA) database under Bioproject PRJNA499076. qPCR data was analysed using custom Python scripts.

Additional file

Additional file 1: Supplementary information and supplementary materials and method: **Tables S1**, **S4** and **Figures S1**, **S9**. (DOCX 1240 kb)

Acknowledgements
MiSeq amplicon sequencing was carried out by the University of Warwick Genomics Facility. We also thank Etienne Low-Decarie, for introducing us to the concept of microbial community artificial selection; Danielle Green, for collecting seawater from Portaferry, Sally Hilton, Michaela Mausz; the Warwick Genomics Facility for amplicon sequencing help and advice and Vinko Zadjelovic, Gabriel Erni Cassola, Audam Chhun; and the rest of the Christie-Oleza group, for insightful discussions and advice throughout the project. We thank SÃ©verine Rangama and Rui Abreu Pereira for help with the qPCR.

Authors' contributions
RW and JCO designed the study. RW performed all the experiments with guidance from JCO and MIG. RW wrote the first draft of the manuscript, and all authors contributed substantially to revisions. All authors read and approved the final manuscript.

Funding
Robyn Wright was supported by a Midlands Integrative Biosciences Training Partnership PhD scholarship via grant BB/M01116X/1, Joseph Christie-Oleza by National Environment Research Council Independent Research Fellowship NE/K009044/1 and Matthew Gibson by European Research Council grant 638631.

Availability of data and materials
All sequences have been deposited in the NCBI Short Read Archive (SRA) database under Bioproject PRJNA499076. All additional data and script files used for analysis can be found at https://github.com/R-Wright-1/ChitinActivity. Data will be uploaded to a data repository if this manuscript is accepted.

Ethics approval and consent to participate
Not applicable.

Consent for publication
Not applicable.

Competing interests
The authors declare that they have no competing interests.

Author details
[1]School of Life Sciences, University of Warwick, Coventry, UK. [2]Department of Chemistry, University of Warwick, Coventry, UK. [3]Medical School, University of Warwick, Coventry, UK.

Received: 1 February 2019 Accepted: 21 May 2019
Published online: 03 June 2019

References
1. Johnson CR, Boerlijst MC. Selection at the level of the community: the importance of spatial structures. Trends Ecol Evol. 2002;17:83, 90.
2. Swenson W, Wilson DS, Elias R. Artificial ecosystem selection. Proc Natl Acad Sci. 2000;97:9110, 4.
3. Williams HTP, Lenton TM. Artificial selection of simulated microbial ecosystems. Proc Natl Acad Sci. 2007;104:8918, 23.
4. Goodnight CJ. Multilevel selection: the evolution of cooperation in non-kin groups. Popul Ecol. 2005;47:3, 12.
5. Goodnight CJ. Heritability at the ecosystem level. Proc Natl Acad Sci. 2000; 97:9365, 6.
6. Swenson W, Arendt J, Wilson DS. Artificial selection of microbial ecosystems for 3-chloroaniline biodegradation. Environ Microbiol. 2000;2:564, 71.
7. Williams HTP, Lenton TM. Artificial ecosystem selection for evolutionary optimisation. In: Banzhaf W, Ziegler J, Christaller T, Dittrich P, Kim JT, editors. Adv Artif Life ECAL; 2007. p. 93, 102.
8. Blouin M, Karimi B, Mathieu J, Lerch TZ. Levels and limits in artificial selection of communities. Ecol Lett. 2015;18:1040–8.
9. Penn AS, Harvey I. The Role of Non-Genetic Change in the Heritability, Variation and Response to Selection of Artificially Selected Ecosystems.In Proceedings of the ninth international conference on artificial life. MIT Press. pp. 352–7.
10. Datta MS, Sliwerska E, Gore J, Polz MF, Cordero OX. Microbial interactions lead to rapid micro-scale successions on model marine particles. Nat Commun. 2016;7:1–7.
11. Dang H, Lovell CR. Bacterial primary colonization and early succession on surfaces in marine waters as determined by amplified rRNA gene restriction analysis and sequence analysis of 16S rRNA genes. Appl Environ Microbiol. 2000;66:467, 75.
12. Ortiz-Álvarez R, Fierer N, de los Ríos A, Casamayor EO., Barberán A. Consistent changes in the taxonomic structure and functional attributes of bacterial communities during primary succession. ISME J. 2018;12:1658, 67.
13. Kiørboe T, Tang K, Grossart H, Ploug H. Dynamics of microbial communities on marine snow aggregates: colonization, growth, detachment, and grazing mortality of attached bacteria. Appl Environ Microbiol. 2003;69:3036, 47.
14. Simon M, Grossart H-P, Schweitzer B, Ploug H. Microbial ecology of organic aggregates in aquatic ecosystems. Aquat Microb Ecol. 2002;28:175, 211.
15. Kiørboe T, Grossart HP, Ploug H, Tang K. Mechanisms and rates of colonisation of sinking aggregates. Appl Environ Microbiol. 2002;68:3996, 4006.
16. Wu X, Wu L, Liu Y, Zhang P, Li Q, Zhou J, et al. Microbial interactions with dissolved organic matter drive carbon dynamics and community succession. Front Microbiol. 2018;9:1–12.
17. Beier S, Bertilsson S. Uncoupling of chitinase activity and uptake of hydrolysis products in freshwater bacterioplankton. Limnol Ocean. 2011;56: 1179, 88.
18. Keyhani NO, Roseman S. Physiological aspects of chitin catabolism in marine bacteria. Biochim Biophys Acta 1473. 1999;1473:108, 22.

19. Cordero OX, Ventouras L, Delong EF, Polz MF. Public good dynamics drive evolution of iron acquisition strategies in natural bacterioplankton populations. Proc Natl Acad Sci. 2012;109:20059, 64.
20. Christie-Oleza JA, Sousoni D, Lloyd M, Armengaud J, Scanlan DJ. Nutrient recycling facilitates long-term stability of marine microbial phototroph-heterotroph interactions. Nat Microbiol. 2017;2:1–10.
21. Morris JJ, Lenski RE, Zinser ER. The Black Queen Hypothesis: evolution of dependencies through adaptive gene loss. MBio. 2012;3:1–9.
22. Enke TN, Datta MS, Schwartzman J, Cermak J, Schmitz D, Barrere J, et al. Modular assembly of polysaccharide-degrading marine microbial communities. Curr Biol. 2019;29:1–8.
23. Dang H, Lovell CR. Microbial surface colonization and biofilm development in marine environments. Microbiol Mol Biol Rev. 2016;80: 91-138.
24. Penn A. Modelling Artificial Ecosystem Selection: A Preliminary Investigation. In: Banzhaf W, Ziegler J, Christaller T, Dittrich P, Kim JT. (eds) Advances in Artificial Life. ECAL 2003. Lecture Notes in Computer Science. vol 2801. Berlin: Springer; 2003.
25. Souza CP, Almeida BC, Colwell RR, Rivera ING. The importance of chitin in the marine environment. Mar Biotechnol. 2011;13:823, 30.
26. Beier S, Bertilsson S. Bacterial chitin degradation-mechanisms and ecophysiological strategies. Front Microbiol. 2013;4:1–12.
27. Schloss PD, Westcott SL, Ryabin T, Hall JR, Hartmann M, Hollister EB, et al. Introducing mothur: open-source, platform-independent, community-supported software for describing and comparing microbial communities. Appl Environ Microbiol. 2009;75:7537, 41.
28. Callahan BJ, Sankaran K, Fukuyama JA, McMurdie PJ, Holmes SP. Bioconductor workflow for microbiome data analysis: from raw reads to community analyses. F1000Research. 2016;5:1492.
29. Callahan BJ, McMurdie PJ, Rosen MJ, Han AW, Johnson AJA, Holmes SP. DADA2: High-resolution sample inference from Illumina amplicon data. Nat Methods. 2016;13:581–3.
30. Hugerth LW, Andersson AF. Analysing microbial community composition through amplicon sequencing: from sampling to hypothesis testing. Front Microbiol. 2017;8:1–22.
31. Langille MGI, Zaneveld J, Caporaso JG, McDonald D, Knights D, Reyes JA, et al. Predictive functional profiling of microbial communities using 16S rRNA marker gene sequences. Nat Biotechnol. 2013;31:1814, 21.
32. Kanehisa M, Goto SKEGG. Kyoto Encyclopedia of Genes and Genomes. Nucleic Acids Res. 2000;28:27, 30.
33. Kanehisa M, Furumichi M, Tanabe M, Sato Y, Morishima K. KEGG: new perspectives on genomes, pathways, diseases and drugs. Nucleic Acids Res. 2017;45:D353, 61.
34. Kanehisa M, Sato Y, Kawashima M, Furumichi M, Tanabe M. KEGG as a reference resource for gene and protein annotation. Nucleic Acids Res. 2016;44:D457, 62.
35. Enke TN, Leventhal GE, Metzger M, Saavedra JT, Cordero OX. Microscale ecology regulates particulate organic matter turnover in model marine microbial communities. Nat Commun. 2018;9:1–8.
36. Patterson D, Steinberg G, Nygaard K, Steinberg G. Heterotrophic flagellates and other protists associated with oceanic detritus throughout the water column in the mid north atlantic. J Mar Biol Assoc UK. 1993;73:67, 95.
37. Volterra V. Fluctuations in the abundance of a species considered mathematically. Nature. 1926;118:558, 60.
38. Lotka AJ. Elements of physical biology. Sci Prog Twent Century. 1926; 21:341–3.
39. Joint I, MÃ¼hling M, Querellou J. Culturing marine bacteria, an essential prerequisite for biodiscovery. Microb Biotechnol. 2010;3:564, 75.
40. Sutherland IW. Biofilm exopolysaccharides: a strong and sticky framework. Microbiology. 2001;147:3–9.
41. Das SN, Sarma PVSRN, Neeraja C, Malati N, Podile AR. Members of Gammaproteobacteria and Bacilli represent the culturable diversity of chitinolytic bacteria in chitin-enriched soils. World J Microbiol Biotechnol. 2010;26:1875, 81.
42. Leclerc GR, Buchan A, Maurer J, Moran MA, Hollibaugh JT. Comparison of chitinolytic enzymes from an alkaline, hypersaline lake and an estuary. Environ Microbiol. 2007;9:197, 205.
43. Kielak AM, Cretoiu MS, Semenov AV, SÃ¸rensen SJ, Van Elsas JD. Bacterial chitinolytic communities respond to chitin and pH alteration in soil. Appl Environ Microbiol. 2013;79:263, 72.
44. Fontanez KM, Eppley JM, Samo TJ, Karl DM, DeLong EF. Microbial community structure and function on sinking particles in the North Pacific Subtropical Gyre. Front Microbiol. 2015;6:1–14.
45. Aunkham A, Zahn M, Kesireddy A, Pothula KR, Schulte A, BaslÃ© A, et al. Structural basis for chitin acquisition by marine Vibrio species. Nat Commun. 2018;9:1, 13.
46. Giubergia S, Phippen C, Nielsen KF, Gram L. Growth on chitin impacts the transcriptome and metabolite profiles of antibiotic-producing *Vibrio coralliilyticus* S2052 and *Photobacterium galatheae* S2753. mSystems. 2017;2:1, 12.
47. Morris RM, RappÃ© MS, Connon SA, Vergin KL, Siebold WA, Carlson CA, et al. SAR11 clade dominates ocean surface bacterioplankton communities. Nature. 2002;420:806, 10.
48. Billerbeck S, Wemheuer B, Voget S, Poehlein A, Giebel HA, Brinkhoff T, et al. Biogeography and environmental genomics of the Roseobacter-affiliated pelagic CHAB-I-5 lineage. Nat Microbiol. 2016;1:1, 8.
49. Beygmoradi A, Homaei A. Marine chitinolytic enzymes, a biotechnological treasure hidden in the ocean? Appl Microbiol Biotechnol. 2018;102(23): 9937–48.
50. Patil RS, Ghormade V, Deshpande MV. Chitinolytic enzymes: an exploration. Enzyme Microb Technol. 2000;26:473, 83.
51. Cottrell MT, Moore JA, David L, Kirchman DL. Chitinases from uncultured marine microorganisms. Appl Environ Microbiol. 1999;65:2553, 7.
52. Eckert EM, Baumgartner M, Huber IM, Pernthaler J. Grazing resistant freshwater bacteria profit from chitin and cell-wall-derived organic carbon. Environ Microbiol. 2013;15:2019, 30.
53. Nedoma J, Vrba J, Hejzlar J, Å imek K, StraÅ¡krabovÃ¡ V. N-acetylglucosamine dynamics in freshwater environments: concentration of amino sugars, extracellular enzyme activities, and microbial uptake. Limnol Oceanogr. 1994;39:1088, 100.
54. Riemann L, Azam F. Widespread *N*-acetyl-D-glucosamine uptake among pelagic marine bacteria and its ecological implications. Appl Environ Microbiol. 2002;68:5554, 62.
55. Ponomarova O, Patil KR. Metabolic interactions in microbial communities: untangling the Gordian knot. Curr Opin Microbiol. 2015;27:37, 44.
56. Zhang Z, Claessen D, Rozen DE. Understanding microbial divisions of labor. Front Microbiol. 2016;7:1, 8.
57. Cavaliere M, Feng S, Soyer O, Jiminez J. Cooperation in microbial communities and their biotechnological applications. Environ Microbiol. 2017;19:2949, 63.
58. Delgado-Baquerizo M, Eldridge DJ, Ochoa V, Gozalo B, Singh BK, Maestre FT. Soil microbial communities drive the resistance of ecosystem multifunctionality to global change in drylands across the globe. Ecol Lett. 2017;20:1295, 305.
59. Hug LA, Co R. It Takes a village: microbial communities thrive through interactions and metabolic handoffs. mSystems. 2018;3:e00152, 17.
60. Hood MA. Comparison of four methods for measuring chitinase activity and the application of the 4-MUF assay in aquatic environments. J Microbiol Methods. 1991;13:151, 60.
61. Köllner KE, Carstens D, Keller E, Vazquez F, Schubert CJ, Zeyer J, et al. Bacterial chitin hydrolysis in two lakes with contrasting trophic statuses. Appl Environ Microbiol. 2012;78:695, 704.
62. Guillard RRL, Ryther JH. Studies of marine planktonic diatoms: *I. cyclotella*, *Nana hustedt*, and *Detonula confervacea* (cleve) gran. Can J Microbiol. 1962;8:229, 39.
63. Day MD, Beck D, Foster JA. Microbial communities as experimental units. Bioscience. 2011;61:398, 406.
64. Bryant JA, Clemente TM, Viviani DA, Fong AA, Thomas KA, Kemp P, et al. Diversity and activity of communities inhabiting plastic debris in the North Pacific Gyre. mSystems. 2016;1:e00024, 16.
65. Parada AE, Needham DM, Fuhrman JA. Every base matters: assessing small subunit rRNA primers for marine microbiomes with mock communities, time series and global field samples. Environ Microbiol. 2016;18:1403, 14.
66. Bradley IM, Pinto AJ, Guest JS. Design and evaluation of Illumina MiSeq-compatible, 18S rRNA gene-specific primers for improved characterization of mixed phototrophic communities. Appl Environ Microbiol. 2016;82:5878, 91.
67. Quast C, Pruesse E, Yilmaz P, Gerken J, Schweer T, Glo FO, et al. The SILVA ribosomal RNA gene database project: improved data processing and web-based tools. Nucleic Acids Res. 2013;41:590, 6.
68. Lane DJ. 16S/23S rRNA sequencing. In: Stackebrandt E, Goodfellow M, editors. Nucleic Acid Tech Bact Syst; 1991. p. 115, 75.

69. Pedregosa F, Weiss R, Brucher M. Scikit-learn: machine learning in Python. J Mach Learn Res. 2011;12:2825, 30.
70. R Development Core Team. R: A language and environment for statistical computing. Vienna: R Foundation for Statistical Computing; 2008. http://www.R-project.org.
71. Paradis E, Claude J, Strimmer K. APE: analyses of phylogenetics and evolution in R language. Bioinformatics. 2004;20:289, 90.
72. Yu G, Smith DK, Zhu H, Guan Y, Lam TT. GGTREE: an R package for visualization and annotation of phylogenetic trees with their covariates and other associated data. Methods Ecol Evol. 2017;8:28, 36.
73. Schliep KP. phangorn: phylogenetic analysis in R. Bioinformatics. 2011; 27:592, 3.
74. Dixon P. VEGAN, a package of R functions for community ecology. J Veg Sci. 2003;14:927, 30.
75. McMurdie PJ, Holmes S. phyloseq: An R Package for Reproducible Interactive Analysis and Graphics of Microbiome Census Data. PLoS ONE. 2013;8(4): e61217. https://doi.org/10.1371/journal.pone.0061217.
76. Caporaso JG, Kuczynski J, Stombaugh J, Bittinger K, Bushman FD, Costello EK, et al. QIIME allows analysis of high-throughput community sequencing data. Nat Methods. 2010;7:335, 6.
77. Desantis TZ, Hugenholtz P, Larsen N, Rojas M, Brodie EL, Keller K, et al. Greengenes, a chimera-checked 16S rRNA gene database and workbench compatible with ARB. Appl Environ Microbiol. 2006;72:5069, 72.
78. Pruesse E, Peplies J, Glöckner FO. SINA: accurate high-throughput multiple sequence alignment of ribosomal RNA genes. Bioinformatics. 2012;28:1823, 9.

Publisher's Note

Appendix 2. Proteins identified through genomic analysis of *Thioclava* sp. BHET1 as potentially involved with PET, BHET and TPA degradation.

Genome position	Prokka annotation	Assigned by	Enzyme	Substrate	Product	In cellular proteome	In exo-proteome
1741	Thermostable monoacylglycerol lipase	HMM	Lipase/esterase	PET	MHET/TPA/ BHET	+	-
0051	S-formylglutathione hydrolase					+	-
3993	Hypothetical protein					-	-
2746	Arylesterase					-	-
4046	Non-heme chloroperoxidase					-	-
6534	Non-heme chloroperoxidase					-	-
1504	Hypothetical protein	CDS	Poly(3-hydroxybutyrate) depolymerase	BHET	TPA/EG	+	-
2867	Terephthalate 1,2-dioxygenase, terminal oxygenase component subunit alpha 2	Prokka	Terephthalate dioxygenase	TPA	1,6-dihydroxycyclohexa-2,4-diene-dicarboxylate	-	-
2868	Terephthalate 1,2-dioxygenase, terminal oxygenase component subunit beta 1					-	-
2870	Terephthalate 1,2-dioxygenase, reductase component 1					-	-
2869	1,2-dihydroxy-3,5-cyclohexadiene-1,4-dicarboxylate dehydrogenase	Prokka	1,2- dihydroxy-3,5-cyclohexadiene-1,4-dicarboxylate dehydrogenase	1,6-dihydroxycyclohexa-2,4-diene-dicarboxylate	Protocatechuate	-	-
1143	Anthranilate 1,2-dioxygenase large subunit	BLAST with *Ideonella sakaiensis* gene	TPA dioxygenase	TPA	1,6-dihydroxycyclohexa-2,4-diene-dicarboxylate	+	-
2475	Anthranilate 1,2-dioxygenase large subunit					+	-
1142	Biphenyl 2,3-dioxygenase subunit beta					+	-

Genome position	Prokka annotation	Assigned by	Enzyme	Substrate	Product	In cellular proteome	In exo-proteome
1379	Ferredoxin--NADP reductase					+	-
1576	1,2-phenylacetyl-CoA epoxidase, subunit E					+	-
2474	3-ketosteroid-9-alpha-monooxygenase, ferredoxin reductase component					+	-
2045	4-hydroxythreonine-4-phosphate dehydrogenase	BLAST with *Ideonella sakaiensis* gene	1,2- dihydroxy-3,5-cyclohexadiene-1,4-dicarboxylate dehydrogenase	1,6-dihydroxycyclohexa-2,4-diene-dicarboxylate	Protocatechuate	+	-
1124	Protocatechuate 3,4-dioxygenase alpha chain	KOALA	Protocatechuate 3,4-dioxygenase, alpha subunit	Protocatechuate	β-carboxy muconate	-	-
1125	Protocatechuate 3,4-dioxygenase beta chain		Protocatechuate 3,4-dioxygenase, beta subunit			+	-
1816		Prokka					
1817	Catechol 1,2-dioxygenase	BLAST with Ideonella gene	Protocatechuate 3,4-dioxygenase			+	+
1123	3-carboxy-cis,cis-muconate cycloisomerase		3-carboxy-*cis, cis*-muconate cycloisomerase	β-carboxy muconate	γ-carboxy muconolactone	-	-
1126	hypothetical protein		4-carboxy muconolactone decarboxymase	γ-carboxy muconolactone	3-oxoadipate-enol-lactone	-	-
2472	3-oxoadipate enol-lactonase 2		3-oxoadipate-enol-lactonase	3-oxoadipate-enol-lactone	3-oxoadipate	+	-
6956	3-oxoadipate enol-lactonase 2	KOALA				-	-
1109	3-oxoadipate CoA-transferase subunit B					-	-
1110	3-oxoadipate CoA-transferase subunit A		3-oxoadipate-CoA-transferase	3-oxoadipate	3-oxoadipyl-CoA	-	-
1108	Beta-ketoadipyl-CoA thiolase					-	-

Genome position	Prokka annotation	Assigned by	Enzyme	Substrate	Product	In cellular proteome	In exo-proteome
1195	Sorbitol dehydrogenase	KOALA	Alcohol dehydrogenase	Ethylene glycol	Acetaldehyde	+	-
0999	Acetaldehyde dehydrogenase 2		Acetaldehyde dehydrogenase	Acetaldehyde	Acetyl-CoA/Ethanol	+	-
0884	Alcohol dehydrogenase		Alcohol dehydrogenase	Ethanol	Acetaldehyde	+	-

Appendix 3. Proteins identified through genomic analysis of *Bacillus* sp. BHET1 as potentially involved with PET, BHET and TPA degradation.

Genome position	Prokka annotation	Assigned by	Enzyme	Substrate	Product	In cellular proteome	In exo-proteome
2434	Di-peptidyl peptidase 5	HMM	PETase	PET	MHET/TPA/BHET	-	-
2574	2-succinyl-6-hydroxy-2,4-cyclohexadiene-1- carboxylate synthase	HMM				-	-
3830	Thermostable monoacylglycerol lipase	HMM				-	-
3456	2-hydroxy-6-oxo-6-phenylhexa-2,4-dienoate hydrolase	HMM				-	
0634	3-hydroxyanthranilate 3,4-dioxygenase	EC 1.13.11.-	HAAO; 3-hydroxyanthranilate 3,4-dioxygenase [EC:1.13.11.6]	Protocatechuate	Hydroxyquinol	-	-
1620	Tryptophan 2,3-dioxygenase		TDO2; tryptophan 2,3-dioxygenase [EC:1.13.11.11]			+	-
2731	4-hydroxyphenylpyruvate dioxygenase		HPD; 4-hydroxyphenylpyruvate dioxygenase [EC:1.13.11.27]			+	-
2735	Homogentisate 1,2-dioxygenase		HGD; homogentisate 1,2-dioxygenase [EC:1.13.11.5]			+	-
3328	Catechol-2,3-dioxygenase		catE; catechol 2,3-dioxygenase [EC:1.13.11.2]			-	-
0149	Cytochrome c biogenesis protein CcsB	KOALA	resB; cytochrome c biogenesis protein			+	-
0150	Cytochrome c biogenesis protein CcsA	Prokka	-			+	-
0213	Cytochrome b6-f complex iron-sulphur subunit	KOALA	MQCRA; menaquinol-cytochrome c reductase iron-sulphur subunit [EC:1.10.2.-]			+	-
0214	Menaquinol-cytochrome c reductase cytochrome b subunit		MQCRB; menaquinol-cytochrome c reductase cytochrome b subunit			+	-

0215	Cytochrome c-551	MQCRC; menaquinol-cytochrome c reductase cytochrome b/c subunit	+	-
0258	Cytochrome c oxidase subunit 2	coxB; cytochrome c oxidase subunit II [EC:1.9.3.1]	+	-
1044	Putative monooxygenase	ncd2; nitronate monooxygenase [EC:1.13.12.16]	+	-
1495	Cytochrome c oxidase subunit 4B	coxD; cytochrome c oxidase subunit IV [EC:1.9.3.1]	+	-
1496	Cytochrome c oxidase subunit 3	coxC; cytochrome c oxidase subunit III [EC:1.9.3.1]	+	-
1497	Cytochrome c oxidase subunit 1	coxA; cytochrome c oxidase subunit I [EC:1.9.3.1]	+	+
1498	Cytochrome c oxidase subunit 2	coxB; cytochrome c oxidase subunit II [EC:1.9.3.1]	+	+
1535	Putative cytochrome bd menaquinol oxidase subunit I	cydA; cytochrome bd ubiquinol oxidase subunit I [EC:7.1.1.7]	+	-
2081	Cytochrome c-550	cccA; cytochrome c550	+	-
2649	Heme-degrading monooxygenase HmoA	K21481	+	-

Appendix 4. Screening of bacterial isolates ability to grow using plasticizers as a sole carbon source.

Number	Information				Ability to grow with [2]						Used for further analysis
	Isolated from [1]	Isolated on plates of [1]	Colony description		DBP	DEHP	DINP	DIDP	ATBC	TOTM	
			Colour	Size (mm)							
1	DBP	MM+DBP	Cream	3	+	+	+	w	-	w	
2	DBP	MM+DBP	Yellow	2	w	w	-	-	-	w	
3	DBP	MB	Peach	3	s	s	s	s	s	w	
4	DBP	MB	Yellow	3	w	w	w	w	-	w	
5	DBP	MM+DBP	Cream	1	-	s	-	-	-	w	
6	DINP	MM+DINP	Peach/yellow	3	-	s	-	-	-	s	
7	DINP	MM+DINP	Peach	2	-	s	s	-	-	w	
8	DINP	MB	Cream	3-4	+	w	+	+	-	+	DINP8
9	DINP	MM+DINP	White	2	-	-	s	-	s	s	
10	DINP	MB	Peach/brown	2	w	w	w	-	-	w	
11	DINP	MB	Peach	Joined	w	-	+	-	-	w	
12	DIDP	MM+DIDP	White	Uneven, 4	s	s	-	s	s	s	
13	DIDP	MB	Orange	3	w	s	w	-	-	s	
14	DIDP	MB	Cream	Joined, 3	+	+	+	+	-	+	DIDP14
15	DIDP	MB	Pink	2	w	+	+	+	s	+	DIDP15
16	DIDP	MM+DIDP	White	Fungus-like, 10	w	-	w	-	-	w	
17	TOTM	MB	Pink	2	+	w	-	-	-	+	
18	TOTM	MB	White	2	w	-	+	-	s	+	
19	TOTM	MB	White	2	+	+	+	+	-	+	
20	TOTM	MM+TOTM	White	Fungus-like, 10	-	s	s	-	-	s	
21	DEHP	MB	Orange	3	s	s	-	-	-	+	
22	DEHP	MB	Cream	1-2	+	+	+	+	s	+	
23	DEHP	MB	Cream	3	+	+	+	+	s	+	DEHP23
24	DEHP	MB	Pink	2	+	+	+	+	s	+	
25	DEHP	MM+DEHP	White	Uneven, 4	-	-	-	-	-	s	
26	DEHP	MM+DEHP	Yellow	Joined	s	s	s	-	-	s	

27	DEHP	MB	Peach/orange	Joined	-	-	w	-	w	w	
28	ATBC	MM+ATBC	White	2	+	+	+	+	s	+	ATBC28
29	ATBC	MB	Cream	3	+	+	+	+	w	+	ATBC29
30	ATBC	MM+ATBC	Yellow	2	w	w	w	w	w	w	
31	ATBC	MB	White	Fungus-like, 10	-	s	s	s	w	-	
32	BHET	MM+BHET	Cream	2	w	w	w	w	w	w	TOTM32
33	BHET	MM+BHET	Cream	2	s	s	w	s	-	s	
34	BHET	MM+BHET	Yellow with brown centre	5	w	+	w	+	-	+	BHET34
35	DEHP	MM+DEHP	White	3	w	-	-	-	-	w	
36	DBP	MM+DBP	White	2	-	s	s	s	s	s	
37	DBP	MM+DBP	White	2	s	-	-	-	s	s	
38	DBP	MM+DBP	White	2	-	-	-	-	s	s	
39	DEHP	MM+DEHP	Cream	Joined, 3	-	-	-	-	s	s	
40	ATBC	MM+ATBC	Cream/yellow	1	w	-	-	-	+	s	ATBC40
41	TOTM	MM+TOTM	Cream	1	w	-	-	-	w	-	
42	DBP	MM+DBP	White	1	+	+	+	+	w	+	DBP42

[1] Plasticizer enrichment culture that the isolate came from.

[2] + (green) indicates growth on a substrate, +++ (green) indicates strong growth, - (red) indicates no growth, w (orange) indicates weak growth and s (red) indicates that there was evidence that a surfactant was produced, but no growth was obvious.

Appendix 5. Proteins identified through genomic analysis of *Halomonas* sp. ATBC28 as potentially involved with plasticizer degradation.

Genome position	Prokka annotation	Assigned by	Enzyme	Substrate	Product	In cellular proteome	In exo-proteome
0629	Toluene-4-sulphonate monooxygenase system iron-sulphur subunit TsaM1	Local BLAST	Phthalate 4,5-dioxygenase	Phthalate	Phthalate-4,5-cis-dihydrodiol	-	-
0630	Phthalate 4,5-dioxygenase oxygenase reductase subunit		Phthalate 4,5-dioxygenase	Phthalate-4,5-cis-dihydrodiol	4,5-Dihydroxyphthalate	-	-
0632	Protocatechuate 3,4-dioxygenase alpha chain	KOALA	Protocatechuate 3,4-dioxygenase alpha subunit	3,4-dihydroxy benzoate	β-carboxy muconate	-	-
0633	Protocatechuate 3,4-dioxygenase beta chain		Protocatechuate 3,4-dioxygenase beta subunit			+	-
0639	3-carboxy-*cis,cis*-muconate cycloisomerase		3-carboxy-*cis,cis*-muconate cycloisomerase	β-carboxy muconate	γ-carboxy muconolactone	+	-
0635	3-oxoadipate enol-lactonase 2		4-carboxymuconolactone decarboxylase	γ-carboxy muconolactone	3-oxoadipate-enol-lactone	-	-
0638	3-oxoadipate CoA-transferase subunit A	CDS	Glutaconate CoA-transferase subunit A	3-oxoadipate	3-oxoadipyl-CoA	+	+
0636	Beta-ketoadipyl-CoA thiolase	Prokka	Acetyl-CoA acyltransferase	3-oxoadipyl-CoA	Succinyl-CoA	-	+
1239	Alcohol dehydrogenase	KOALA	Alcohol dehydrogenase	Alcohol	Aldehyde	+	+
1238	Long-chain-aldehyde dehydrogenase		Aldehyde dehydrogenase	Aldehyde	Carboxylic acid	+	+
1456	Long-chain-fatty-acid--CoA ligase		Fatty-acid-CoA ligase	Carboxylic acid/fatty acid	Fatty acyl-CoA	+	+
1457	3-hydroxybutyryl-CoA dehydrogenase		Acyl-CoA dehydrogenase	Fatty acyl-CoA	Trans-enoyl-CoA	+	+
1458	Short-chain-enoyl-CoA hydratase		Enoyl-CoA hydratase	Trans-enoyl-CoA	B-hydroxyacyl-CoA	+	+
1455	3-methylmercaptopropionyl-CoA dehydrogenase		Acyl-CoA dehydrogenase	B-hydroxyacyl-CoA	B-ketoacyl-CoA	+	+

0688	Beta-ketoadipyl-CoA thiolase		Acyl-CoA acetyltransferase	B-ketoacyl-CoA	Acetyl-CoA + carboxylic/fatty acid	+	+
4867	3-[(3aS,4S,7aS)-7a-methyl-1,5-dioxo-octahydro-1H-inden-4-yl]propanoyl:CoA ligase	KOALA	Fatty-acid-CoA ligase	Carboxylic acid/fatty acid	Fatty acyl-CoA	+	+
4872	Acyl-CoA dehydrogenase		Acyl-CoA dehydrogenase	Fatty acyl-CoA	Trans-enoyl-CoA	+	+
4870	putative enoyl-CoA hydratase echA8		Enoyl-CoA hydratase	Trans-enoyl-CoA	B-hydroxyacyl-CoA	+	+
4879	Acyl-CoA dehydrogenase	Prokka	Acyl-CoA dehydrogenase	B-hydroxyacyl-CoA	B-ketoacyl-CoA	+	+
4908	3-ketoacyl-CoA thiolase	KOALA	Acyl-CoA acetyltransferase	B-ketoacyl-CoA	Acetyl-CoA + carboxylic/fatty acid	+	+
0264	Sialic acid-binding periplasmic protein SiaP					+	+
2103	Na(+)/H(+) antiporter NhaD					+	-
2757	Protein SphX					+	+
3181	Maltose/maltodextrin import ATP-binding protein MalK					+	-
0243	sn-glycerol-3-phosphate-binding periplasmic protein UgpB					+	+
3177	putative ABC transporter-binding protein	Prokka	Transporter			+	+
1992	sn-glycerol-3-phosphate-binding periplasmic protein UgpB					+	+
3176	Sucrose porin					+	+
1142	Cation/acetate symporter ActP					+	-
0269	Solute-binding protein					+	+
0485	Putative amino-acid ABC transporter-binding protein YhdW					+	+
0923	Solute-binding protein					+	+

1865	Leucine-, isoleucine-, valine-, threonine- and alanine-binding protein					+	+
4470	Ferric aerobactin receptor					+	+
2195	Hypothetical protein					+	+
0212	Hypothetical protein					+	-
4176	Ferrichrome outer membrane transporter/phage receptor					+	+
1500	Outer membrane protein TolC					+	+
2643	Outer membrane efflux protein BepC					+	+
1225	C4-dicarboxylate-binding periplasmic protein DctP					+	+
3348	Putative lipoprotein YiaD	Prokka	Surfactant			+	+
4375	Esterase EstB	Prokka	Esterase	DBP/DEHP/MBP/ MEHP/ATBC/TBC/ DBC/MBC	MBP/MEHP/PA/ PA/TBC/DBC/ MBC/Citrate	-	+

Appendix 6. Proteins identified through genomic analysis of *Mycobacterium* sp. DBP42 as potentially involved with plasticizer degradation.

Genome position	Prokka annotation	Assigned by	Enzyme	Substrate	Product	In cellular proteome	In exo-proteome
3203	Pectin degradation repressor protein KdgR	KOALA	Transcriptional regulator			+	-
3202	Biphenyl 2,3-dioxygenase subunit alpha	KOALA	Phthalate 3,4-dioxygenase alpha subunit	Phthalate	Phthalate-3,4-cis-dihydrodiol	+	-
3201	Biphenyl 2,3-dioxygenase subunit beta		Phthalate 3,4-dioxygenase beta subunit	Phthalate-3,4-cis-dihydrodiol	3,4-dihydroxy phthalate	+	-
3196	Hypothetical protein	Local BLAST	3,4-dihydroxyphthalate decarboxylase	3,4-dihydroxy phthalate	3,4-dihydroxy benzoate	+	-
3206	Protocatechuate 3,4-dioxygenase alpha chain	KOALA	Protocatechuate 3,4-dioxygenase alpha subunit	3,4-dihydroxy benzoate	β-carboxy muconate	+	-
3205	Protocatechuate 3,4-dioxygenase beta chain		Protocatechuate 3,4-dioxygenase beta subunit			+	-
3207	3-carboxy-*cis,cis*-muconate cycloisomerase		3-carboxy-*cis,cis*-muconate cycloisomerase	β-carboxy muconate	γ-carboxy muconolactone	+	-
3208	3-oxoadipate enol-lactonase 2		4-carboxymuconolactone decarboxylase/ 3-oxoadipate enol-lactonase	γ-carboxy muconolactone	3-oxoadipate-enol-lactone/ 3-oxoadipate	+	+
3209	3-oxoadipate CoA-transferase subunit A		3-oxoadipate CoA-transferase alpha subunit	3-oxoadipate	3-oxoadipyl-CoA	+	-
3210	3-oxoadipate CoA-transferase subunit B		3-oxoadipate CoA-transferase beta subunit			+	-
1282	Dihydrolipoyllysine-residue acetyltransferase component of pyruvate dehydrogenase complex		2-oxoglutarate dehydrogenase	3-oxoadipyl-CoA	Acetyl-CoA	+	-
4463	Beta-ketoadipyl-CoA thiolase		2-oxoglutarate dehydrogenase	3-oxoadipyl-CoA	Succinyl-CoA	+	-

0019	putative cutinase		Cutinase	Dibutyl phthalate	Phthalate + butanol	+	-
3195	S-(hydroxymethyl)mycothiol dehydrogenase	KOALA	S-(hydroxymethyl)mycothiol dehydrogenase	Butan-1-ol	Butanal	+	-
5697	Succinate semialdehyde dehydrogenase [NAD(P)+] Sad		Succinate semialdehyde dehydrogenase [NAD(P)+] Sad	Butanal	Butyrate	+	-
1663	Long-chain-fatty-acid--CoA ligase		Fatty-acid CoA ligase	Butyrate	Butanoyl-CoA	+	-
4430	putative acyl-CoA dehydrogenase fadE25		Acyl-CoA dehydrogenase	Butanoyl-CoA	Crotonoyl-CoA	+	-
4433	Putative acyl-CoA dehydrogenase FadE17	CDS				+	-
4432	1,4-dihydroxy-2-naphthoyl-CoA synthase		Enoyl-CoA hydratase	Crotonoyl-CoA	Acetoacetyl-CoA	+	+
4474	2,3-dehydroadipyl-CoA hydratase	KOALA				+	-
4463	Beta-ketoadipyl-CoA thiolase		2-oxoglutarate dehydrogenase	Acetoacetyl-CoA	Acetyl-CoA	+	-
5572	Nitrilotriacetate monooxygenase component A	CDS	Monooxygenase	Ethyl hexanol	Alcohol	+	-
5608	putative oxidoreductase		putative oxidoreductase	Alcohol	Aldehyde	+	-
5607	hypothetical protein		Aldehyde dehydrogenase	Aldehyde	Carboxylic acid	-	-
5611	Long-chain-fatty-acid--CoA ligase	KOALA	Long-chain-fatty-acid--CoA ligase	Carboxylic acid	Carboxylic acid-CoA	+	-
5609	Acyl-CoA dehydrogenase		Fatty-acid-CoA dehydrogenase	Carboxylic acid-CoA	Crotonoyl-CoA	-	-
5610	2,3-dehydroadipyl-CoA hydratase		2,3-dehydroadipyl-CoA hydratase	Crotonoyl-CoA	Acetoacetyl-CoA	+	-
5613	Cinnamoyl-CoA:phenyllactate CoA-transferase	CDS	Cinnamoyl-CoA:phenyllactate CoA-transferase	Acetoacetyl-CoA	Acetyl-CoA + Carboxylic acid	+	-
1268	Carboxylesterase B		Alpha/beta hydrolase fold	Acetyl tributyl citrate	Tributyl citrate	+	+
0724	4,5:9,10-diseco-3-hydroxy-5,9,17-trioxoandrosta-1(10),2-diene-4-oate hydrolase	CDS	Hydrolase	Tributyl citrate	1,3-dibutyl citrate/ 2-(2-butoxy-2-oxoethyl)-2-hydroxysuccinate	+	-
1749	3-isopropylmalate dehydratase small subunit	KOALA	3-isopropylmalate dehydratase/Aconitase hydratase	Citrate	Isocitrate	+	-

5755	Isocitrate lyase 1		Isocitrate lyase 1	Isocitrate	Glyoxylate + Succinate	+	+
5706	DNA protection during starvation protein	Prokka	DNA protection during starvation			+	-
2974	Hypothetical protein	CDS	Potential antigen			+	-
3075	Hypothetical protein	CDS	Stress protein			+	-

Appendix 7. Summary of compounds detected through targeted (T) and untargeted (UT) metabolomic analyses of *Mycobacterium* sp. DBP42 and *Halomonas* sp. ATBC28 culture supernatants when grown with phthalate, DBP, DEHP or ATBC as sole carbon sources.

Compound and formula	Detection in *Mycobacterium* sp. DBP42 treatments [1]				Detection in *Halomonas* sp. ATBC28 treatments [1]			
	Phthalate [2]	DBP [2]	DEHP [2]	ATBC [3]	Phthalate [2]	DBP [2]	DEHP [2]	ATBC [3]
Monobutyl phthalate ($C_{12}H_{14}O_4$)		UT (8.04)				UT (7.91)		
Phthalate ($C_8H_6O_4$)	UT (3.25)	T	UT (0.47)		UT (3.89)	UT (0.41)	UT (0.25)	
Phthalic anhydride ($C_8H_4O_3$)	UT (3.26)	UT (7.65)	UT (0.68)		UT (3.81)	UT (6.30)	UT (0.09)	
Butyl benzoate ($C_{11}H_{14}O_2$)		UT (8.16)				UT (8.56)		
3,4-dihydroxy phthalate ($C_8H_6O_6$)		T						
3,4-dihydroxy benzoate (protocatechuate; $C_7H_6O_4$)		T						
β-carboxy muconate / γ-carboxy muconolactone ($C_7H_6O_6$)		T						
3-oxoadipate-enol-lactone ($C_6H_6O_4$)		T						
3-oxoadipate ($C_6H_8O_5$)		T						
Acetyl dibutyl citrate ($C_{16}H_{26}O_8$)								UT (7.37)
Dibutyl citrate ($C_{14}H_{22}O_6$)				T, UT (11.64)				UT (2.78)
Monobutyl citrate ($C_{10}H_{16}O_7$)				T, UT (6.39)				UT (-8.11)
Citrate ($C_6H_8O_7$)				T				

[1] Green indicates that the compound was confidently detected in that treatment while red indicates that the compound was detected, but not in significantly higher quantities than in other conditions.
[2] Numbers in brackets indicate $\log_2$ fold change in detection between the DBP and ATBC treatments.
[3] Numbers in brackets indicate $\log_2$ fold change in detection between the ATBC and DBP treatments.